Fabrication and loading of microcontainers for oral drug delivery

Petersen, Ritika Singh

Publication date:
2015

Document Version
Publisher's PDF, also known as Version of record

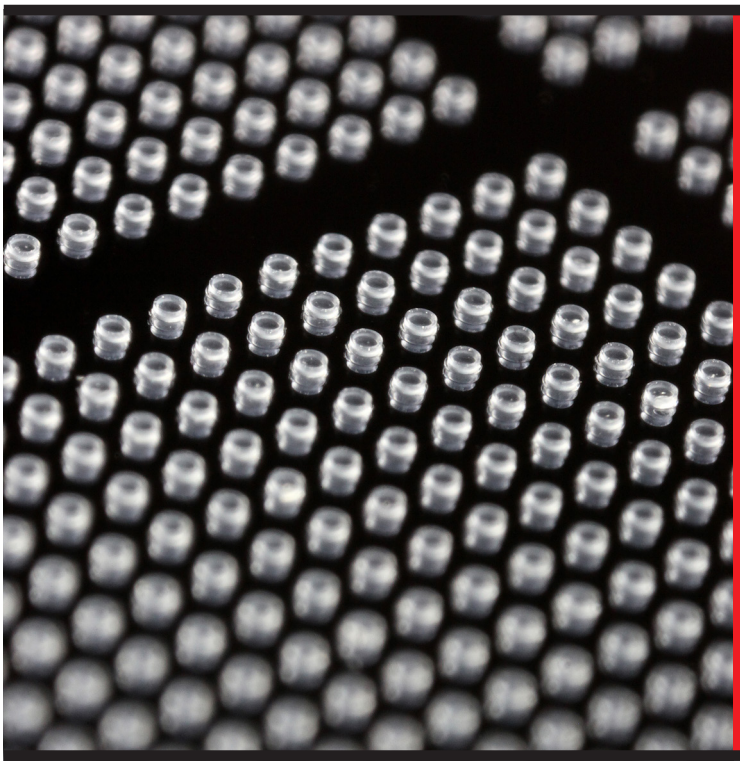

Fabrication and loading of micro-containers for oral drug delivery

Ritika Singh Petersen
PhD Thesis September 2015

DTU Nanotech
Department of Micro- and Nanotechnology

Danmarks Tekniske Universitet

Fabrication and loading of microcontainers for oral drug delivery

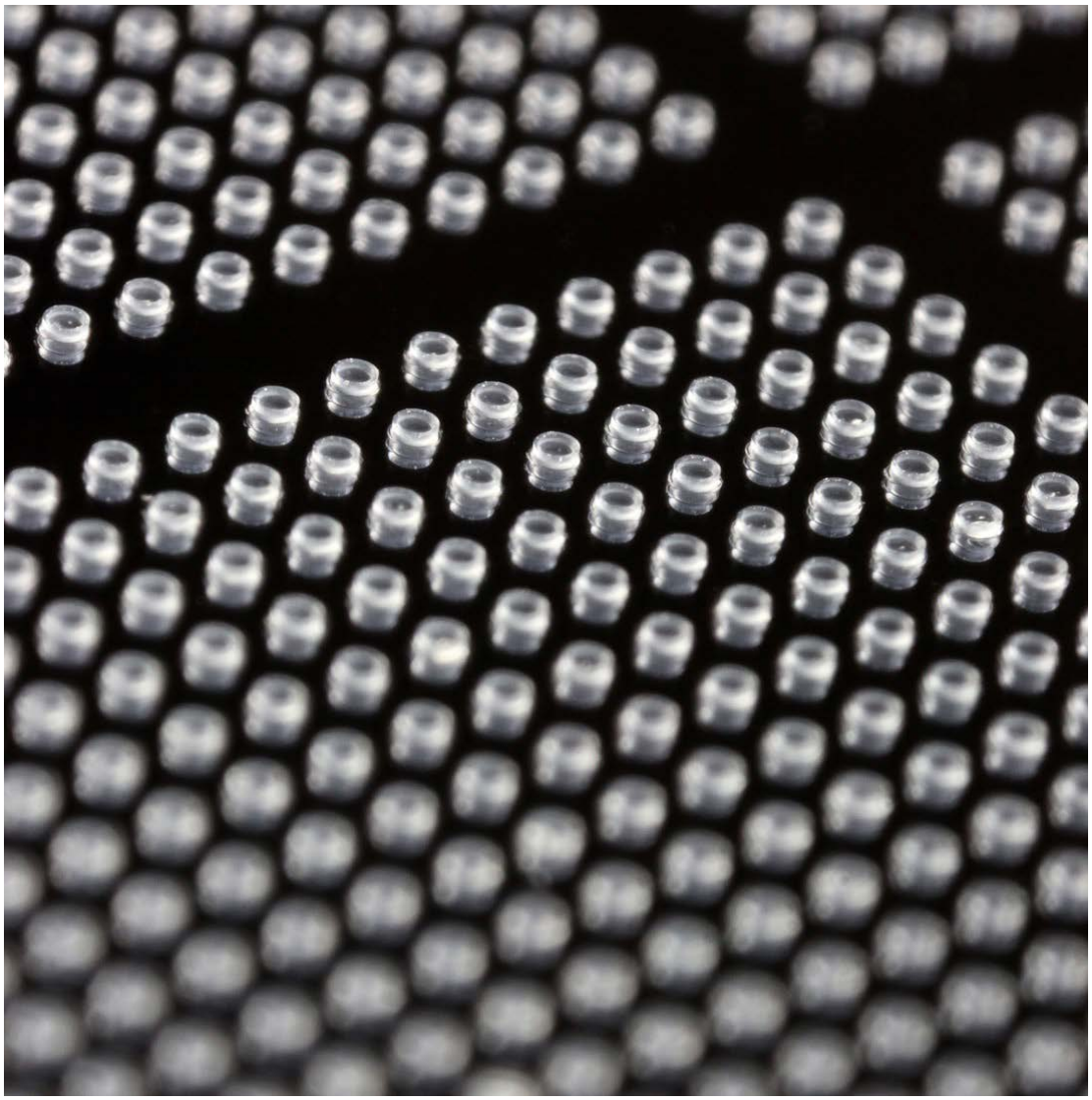

Ritika Singh Petersen

PhD Thesis, 23rd September 2015

Preface

This Ph.D. thesis is written as a partial fulfillment of the requirements for obtaining the Ph.D degree at the Technical University of Denmark (DTU). The Ph.D. project is carried out at the Department of Micro- and Nanotechnology (DTU Nanotech) during the period from 15th of September 2012 to the 14th of September 2015. This Ph.D. project is part of NAMEC, a VKR Center of Excellence which has been financed by the Villum Kann Rasmussen foundation and IDUN, Centre of Excellence for Intelligent oral Drug delivery Using Nano and microfabricated containers which is financed by The Danish National Research Foundation.

This Ph.D project was supervised by:
Main supervisor: Professor Anja Boisen
Co-supervisor: Senior Researcher Stephan Sylvest Keller

I would like to express my sincere gratitude to Anja Boisen. She has always been a role model for me: for someone I have great respect, admiration as well as comradeship, a perfect blend that is hard to find in a supervisor. This thesis would be incomplete without thanking Stephan Sylvest Keller. Stephan has complemented me during my PhD in a true manner. I would also like to thank Ole Hansen with whom I had some great discussions on clean room processing and publication issues. I would like to thank my officemates, Rasmus for being very encouraging, Rikke for her caring attitude (and a lot more ☺) and Kuldeep for long discussions on everything Indian. I extend my gratitude to Sanjukta for all the help regarding polymers, Tomas for the help regarding Raman, and Line Hagner for the help in KU Pharma. And many thanks to the whole Nanoprobes group. They have made coming to DTU and doing science really a lot of fun. I will also like to thank all my co-authors for their support. I am grateful to Danchip staff especially Conny, Berit, Chantal and Claus and DTU Nanotech administration. DTU Nanotech admin is one of the most amazing administration staffs I have ever come across.

Finally, none of my efforts matter if I don't thank my family especially my two elder brothers, Nityanand Singh and Paritosh Kr. Singh and my husband Dirch Hjorth Petersen for being the pillars of my life. My brothers made it possible for me to come out of India to pursue higher education. And my husband supported me to keep my mind sound even in the biggest chaos of life. He is a complete package: he is my companion, my best friend, my consultant on the matters of life, and above all my soulmate.

Ritika Singh Petersen
September 23, 2015, DTU Nanotech
Technical University of Denmark

List of Publications

Paper I

Hot embossing and mechanical punching of biodegradable microcontainers for oral drug delivery. / Petersen, R. S.; Mahshid, R.; Andersen, N. K.; Keller, S. S.; Hansen, H. N.; Boisen, A. In: Microelectronic Engineering, Vol. 133, 2015, p. 104–109.

Paper II

Fabrication of a Ni stamp with high aspect ratio, two-leveled, cylindrical microstructures using dry etching and electroplating. / Petersen, R. S.; Keller, S. S.; Hansen, O.; Boisen, A. In: Journal of Micromechanics and Microengineering, Vol. 25, 2015, 055021.

Paper III

Hot punching of high-aspect-ratio 3D polymeric microstructures for drug delivery. / Petersen, R. S.; Keller, S. S.; Boisen, A. In: Lab-on-a-chip, 2015.

Paper IV

Fabrication and loading of biopolymer microcontainers for oral drug delivery using hot punching./ Petersen, R. S.; Borre, M. T.; Keller, S. S.; Boisen, A. In: Microtas2015 proceedings (accepted)

Paper V

Hot punching of drug-polymer matrices to load drug delivery micro-reservoirs./ Petersen, R. S.; Keller, S. S.; Boisen, A.

Patent

Method for manufacturing carrier containing e.g. proteins for human during oral drug delivery operation for food and drug administration application in pharmaceutical industry, involves providing active ingredient to core layer. / Nagstrup, J.; Petersen, R. S.; Keller, S. S.; Boisen, A. UYDA Nonstandard, WO2015028670A2, Published in 2015.

My Contribution to the Papers

Paper I

I performed all the experiments for the hot embossing and mechanical punching of the polymer films. The punching tool was fabricated by the authors, Rasoul Mahshid and Nis. K. Andersen. I was involved in the fabrication process of the punching tool where I gave inputs for the design and the set-up. I conducted the characterizations of the punching tool and the punched polymer. I took part in evaluation of the results and had a major contribution in writing the manuscript.

Paper II

I planned and executed the fabrication of Ni stamp in cleanroom. I performed the profilometry and microscopy measurements of the Si master, Ni stamp and polymer microstructures. I took part in evaluation of the results and wrote the complete manuscript.

Paper III

I planned and executed all the experiments. I had a major contribution in evaluation of the results and writing the manuscript.

Paper IV

I participated in planning of the experiments. The bachelor student, Mads T. Borre, whom I was supervising performed the experiments. I participated in discussion of the results, and wrote the complete manuscript.

Paper V

I planned and executed all the experiments. I had a major contribution in evaluation of the results and writing the manuscript.

Patent

I planned and performed all the experiments related to hot punching. I participated in discussion of the results and had minor contribution in writing the manuscript.

Abstract

Oral drug delivery is considered as the most patient compliant delivery route. However, it faces many obstacles, especially due to the ever-increasing number of drugs that are poorly soluble and barely absorbed in the gastro-intestinal tract. Moreover, drugs can degrade in the harsh acidic environment of stomach before they reach the intestine. These issues lead to reduced bioavailability of active ingredients. To combat that novel oral drug delivery systems have been developed. Some of these systems that have gained significant interest in this field are reservoir based drug delivery microdevices. These microreservoir based-systems have dimension ranging from 10 μm to 500 μm. Additional functionalities are added to control the site and profile of drug release through mucoadhesive layers, asymmetric geometry and unidirectional drug release. Most of these devices have been fabricated using microfabrication methods with materials such as Si and photoresists. However, there is a need to shift from these materials towards biocompatible and biodegradable polymers such as poly-l-lactic acid (PLLA) or poly-e-caprolactone (PCL). Hot embossing is one of the most viable and matured methods to fabricate microstructures in such biopolymers. However, hot embossing is unable to produce discrete 3D microdevices due to the inherent problem of a residual layer that connects all the microdevices to each other. Therefore, hot punching which is combination of hot embossing and mechanical punching has been developed in this project. This process utilizes a stamp in connection with the ability to apply heat and pressure to transfer the stamp pattern to a film. Processes have been optimized for fabrication of nickel stamps with two layered, high aspect ratio microstructures. Bosch deep reactive ion etching of Silicon producing sloped sidewalls required for stamp production has been developed. The sloped sidewalls ensure a successful separation of stamp and film after patterning. High aspect ratio, 3D, discrete microcontainers in PLLA and PCL are fabricated using hot punching. High throughput and replication fidelity is achieved. Characterization of spin coating of drug-polymer films is thoroughly performed using microscopy, profilometry, differential scanning calorimetry, Raman spectroscopy, X-ray diffraction and microdissolution release tests. These films are applied for loading of microcontainers. Furosemide which is an important loop diuretic drug with low solubility and permeability is used as a model drug and embedded in a PCL matrix. The crystallinity of the drug is tailored by the process parameters of spin coating. Release profiles ranging from rapid burst release to sustained zero-order release are obtained by tuning spin coating. The hot punching technique is then applied for loading of microcontainers with the spin coated drug-polymer matrix. It has been demonstrated that hot punching is a fast, parallel, single step process that can load containers with high yield. Furthermore, the drug-polymer matrix loaded in the containers is characterized using the above mentioned techniques. Finally, zero-order sustained release of furosemide drug from microcontainers is successfully demonstrated.

Danske Resumé

Lægemidler til oral administration betragtes som den mest patientvenlige lægemiddelform. Orale lægemidler møder dog mange forhindringer, især det stadigt stigende antal lægemidler, som er dårligt opløselige og knap absorberes i mave-tarmkanalen. Desuden kan lægemidler nedbrydes i det barske sure miljø i maven, før de når tarmen. Disse problemer fører til nedsat biotilgængelighed af aktive lægemiddelstoffer. For at tackle dette er en ny kategori af orale lægemiddeladministrationssystemer blevet udviklet. Nogle af de systemer, der har fået stor interesse i dette område, er administrationssystemer baseret på mikrobeholdere. Disse mikrobeholdersystemer har dimension på 10 μm til 500 μm. Yderligere funktionalitet er tilføjet for at styre lokalitet og profil af medikamentfrigivelse ved slimhindeklæbende lag, asymmetrisk geometri og retningsbestemt medikamentfrigivelse. De fleste af denne type systemer er blevet fremstillet ved hjælp mikrofabrikationsmetoder med materialer som silicium og fotoresist, men der er behov for at skifte fra disse materialer mod biokompatible og bionedbrydelige polymerer såsom poly-L-mælkesyre (PLLA) eller poly-e-caprolactone (PCL). Hot Embossing er en af de mest gængse metoder til fremstilling af mikrostrukturer i sådanne biopolymerer. Men Hot Embossing ikke er i stand til at producere adskilte 3D mikrostrukturer da et tilbageværende sammenhændende lag vil forbinde alle strukturer med hinanden. Derfor er en metode, Hot Punching, som kombinerer Hot Embossing med en mekanisk udskæring, blevet udviklet i dette projekt. Denne proces overfører et mønster fra et stempel til en film ved hjælp af varme og tryk. En proces er blevet optimeret til fremstilling af nikkel stempler med mikrostrukturer i to niveauer og højt dimensionsforhold. En Bosch proces (dyb reaktiv ionætsning) i silicium er blevet udviklet til at producerer skrå sidevægge, der er nødvendige til stempel fabrikation. De skrå sidevægge sikrer en vellykket adskillelse af stempel og film efter Hot Punching processen, som er blevet brugt til at fremstille mikrobeholdere i PLLA og PCL med højt dimensionsforhold. Massefabrikation og korrekt reproduktion af 3D mikrobeholdere er blevet demonstreret. Karakterisering af spin-coating af lægemiddel-polymerfilm er grundigt udført under anvendelse af mikroskopi, profilometri, differentialscanningskalometri, Raman spektroskopi, røntgendiffraktion og mikroopløsning lægemiddelfrisættelsestest. Disse film anvendes senere til at dosere lægemiddel i mikrobeholderne. Furosemid, der er et vigtigt slyngediuretikum lægemiddel med lav opløselighed og permeabilitet, indlejres i en PCL-matrix og anvendes som modelsystem. Krystalliniteten af lægemidlet er bestemt af procesparametrene for spin-coating. Medikamentfrigivelsesprofiler som spænder fra straks frigivelse til langvarig zero-order frigivelse opnås ved at justere spin-coating processen. Hot Punching teknikken bruges derefter igen, men nu til at fylde mikrobeholderne med den spin-coatede lægemiddel-polymer-matrix. Det er blevet vist, at Hot Punching metoden er en hurtig og parallel 1-trins proces, der med høj reproducerbarhed kan fylde mikrobeholderne. Lægemiddel-polymer-matricen som er fyldt i mikrobeholderne er karakteriseret med de ovennævnte teknikker. Endeligt er zero-order langtidsfrigivelse af lægemiddel fra mikrobeholdere demonstreret.

Table of Contents

Abbreviations

µg, mg, g, kg: Microgram, milligram, gram, kilogram,
nm, µm, mm, cm, m: Nanometer, micrometer, millimeter, centimeter, meter
sec, min(s), hr(s): Seconds, minute(s), hour(s)
pl, nl, µl, ml,: Picoliter, nanoliter, microliter, milliliter,
mJ: MilliJoule
mN, N: MilliNewton, Newton
Pa, MPa: Pascal, MegaPascal
°C: Celcius
KV: KiloVolts
mW: MilliWatts
rpm: Rotations per minute

wt: Weight
T_g: Glass Transition Temperature
T_m: Melting Point
Tc: Crystallization Temperature
M_w: Molecular weight

Ni: Nickel
Si: Silicon
Au: Gold
WC: Tungsten Carbide
CO_2: Carbon diOxide

PLLA: Poly-L-Lactic Acid
PCL: Poly-ε-CaproLactone
PLGA: Poly(Lactic-co-Glycolic Acid)
PLA: Poly Lactic Acid
PDMS: Poly-Di-MethylSiloxane
PMMA: Poly-Metha-MethylAcrylate
PAA: Poly Acrylic Acid
PVA: Poly Vinyl Alcohol
PEG: Polyethylene Glycol
PVP: PolyVinylPyrrolidone
PE: PolyEthylene
PS: PolyStyrene
FC: FluoroCarbon
F: Furosemide
PCL-F: PolyCaproLactone-Furosemide

PEGDMA: Poly(Ethylene Glycol) DiMethAcrylate
PFPE: PerFluoroPolyEther

WHO: World Health Organization
FDA: US Food and Drug administration
BCS: Biopharmaceutics Classification System
API: Active Pharmaceutical Ingredient
GI: Gastro-intestinal

DSC: Differential Scanning Calorimetry
SEM: Scanning Electron Microscopy
XRPD/XRD: X-Ray Powder Diffraction/ X-Ray Diffraction
HPLC: High-Performance Liquid Chromatography
CCD: Charge-Coupled Device

PRINT: Polymer Replication In Non-wetting Template
MIMIC: MIcroMolding In Capillary
SAMIM: Solvent-Assisted MIcroMolding
CFL: Capillary Force Lithography
µDISS: MicroDissolution
µContact: MicroContact
µTransfer: MicroTransfer
LIGA: Lithography, Electroplating, and Molding
DEEMO: Dry etching, Electroplating and Molding

DRIE: Deep Reactive Ion Etching
RIE: Reactive Ion Etching
UV: UltraViolet
UVO: UltraViolet/Ozone
MEMS: MicroElectroMechanical Systems
AOE: Advanced Oxide Etch
MVD: Molecular Vapor Deposition.
HAR: High-Aspect-Ratio
3D: 3-Dimensional

MM: Material Multiplier
UTS: Ultimate Tensile Strength
SD: Standard Deviations

CHAPTER 1
INTRODUCTION AND LITERATURE REVIEW

CHAPTER 1
INTRODUCTION AND LITERATURE REVIEW

1.1. Motivation

Oral route is the most preferred drug delivery route as it has highest patient compliance and it does not require health care professionals for drug administration [1]. However, pharmaceutical industry is facing many challenges in administering drug orally due to the intrinsic physio-chemical properties of the drugs. Between the oral ingestion and the final effect of the active pharmaceutical ingredients (APIs), there are numerous barriers which the active compound must overcome before being absorbed by the cells. The first line of attack is from the biological metabolism [2]. Typically an API encounters enzymatic degradation, hydrolysis and chemical deactivation in the acidic gastric environment [3]. When the drug reaches the small intestine, many of the newly developed drug compounds exhibit a poor solubility in the intestinal fluid, and slow dissolution compared to a relatively rapid peristaltic flow in the upper intestine. Finally, drug molecules generally show low permeation through the intestinal mucosa. Thus, during its transit in the system, the API is potentially lost or degraded, thereby, reducing the bioavailability of the therapeutic agent significantly [2, 4]. Consequently, frequent drug administrations are needed in order to maintain an efficient therapeutic effect. This in turn leads to higher risk of side-effects.

To combat these issues of oral drug delivery, various forms of drug delivery systems have been developed ranging from drug-polymer micro/nanospheres to implantable chips [5, 6]. Some of the systems that have gained significant interest recently are reservoir based microdevices. Different functionalities like mucoadhesion and pH-triggered release can be integrated in these micro-reservoirs [7, 8]. Thus, the drug filled in the reservoirs can be protected from degradation in the stomach while at the same time its release can be controlled by the added features. A mucoadhesive layer can help the reservoirs to adhere to the intestinal mucosa and a pH sensitive layer can allow unidirectional release leading to less wastage, fewer side-effects and higher bioavailability of the drug [9-11]. Such reservoir based devices can be fabricated as micrometer sized containers. These devices have been fabricated using conventional Si microtechnology like photolithography and reactive ion etching [12, 13] in materials such as Si and various photoresists like SU-8 and poly(methyl methacrylate) (PMMA) [9, 12, 13]. However, there is a need to move towards more biocompatible and biodegradable polymers such as poly-l-lactic acid (PLLA), poly-ε-caprolactone (PCL) or poly lactic-co-glycolic acid (PLGA) [14]. In order to fabricate devices in such polymers, polymer technologies like micro/nanoimprinting, soft lithography, and 3D printing are required [15-17]. Hot embossing is one of the most viable solutions to fabricate micro/nanostructures in polymer in a replicable manner with high throughput [18, 19]. However, unlike injection molding and 3D printing, this processing technique is unable to fabricate discrete 3D structures. This is due to the inherent residual layer left after the embossing process connecting the micro/nanostructures to each other [20]. Generally, to remove this residual layer, RIE or laser machining is used. Unfortunately, both of these techniques produce complex etch residues and are time consuming [21, 22]. For the application of oral drug delivery, such techniques can potentially render the polymer non-biodegradable and might also damage the drug if it has been already loaded

in the microdevice. In order to use biopolymers as the fabrication material for next-generation oral drug delivery devices, new fabrication methods need to be developed. Thus in this thesis, hot punching as a novel technique to not only fabricate microcontainers for reservoir based oral drug delivery but also to load these microcontainers in a high throughput, drug-benign manner has been developed.

This chapter aims at providing the background and motivation for the work presented in this thesis. The report starts with a brief explanation of the microdevice that we planned to fabricate in this project in section 1.2. Then a discussion of the state of the art reservoir-based microdevices for oral drug delivery is given in section 1.3. The various techniques for the fabrication of drug delivery devices including microelectromechanical systems (MEMS) technology and soft lithography are described briefly. Focusing on hot embossing, various tools that have been developed to address the inherent challenge of removing residual layer are provided. After that a brief discussion on the fabrication of high aspect ratio multilayer Ni stamps for hot embossing polymer films is presented. Then spin coating as one of the processes for producing drug-polymer films is described. Finally the daunting task of loading of the microcontainers with the drug is examined. Section 1.4 provides the project funding and framework. The objective of this Ph.D. project is presented in section 1.5 and the thesis structure is outlined in section 1.6.

1.2 Drug delivery device concept

Currently, many drug delivery systems based on micro/nano particles are developed. These particles can be mass produced; however, precise control of the size, surface properties and shape of such particles has been a challenge. Thus in this project we set out to fabricate microcontainers with controlled size of reservoirs that can be loaded with drug in a precise manner. The ideal device (Fig.1.1) has the following features:

1. The container is fabricated in biocompatible and biodegradable polymers like PLLA, PCL, PLGA earlier approved by the US Food and Drug Administration (FDA) for applications in drug delivery to prevent the accumulation of harmful residues in the human body.
2. The container is loaded efficiently with drug in different forms like powder, liquid or embedded in a polymer matrix potentially allowing control of the release profile.
3. The size of a single container is a few hundred microns for it to be small enough to have adequate contact with the intestinal wall but large enough to avoid endocytosis [23].
4. The geometry of the container is disc-like so that a higher surface area is in contact with the intestinal lining. This provides a better adhesion of microcontainer to the intestinal wall so that the container is more stable in the harsh flow conditions that can dislodge it and disrupt the drug release [23].
5. The drug release is unidirectional, preferably controlled by a biodegradable or pH-sensitive membrane. This membrane along with the container protects the drug during its transit through the GI system. Thus, the site where drug is released is controlled passively using the layer.
6. Functional coatings like mucoadhesive layers are added to increase the adhesion of containers to the intestinal wall, allowing better bioavailability of the drug.

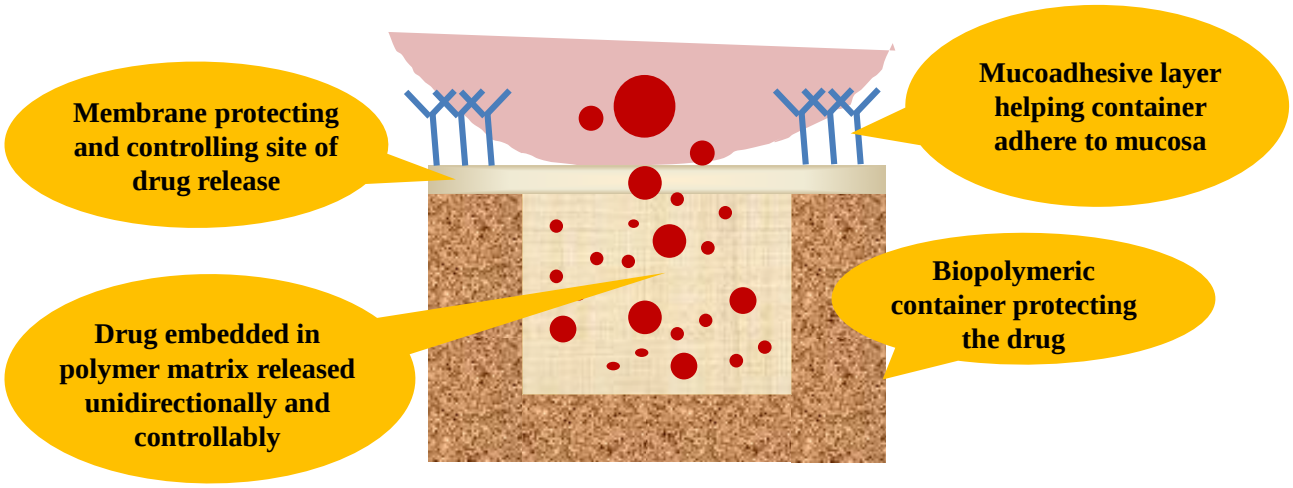

Fig.1.1 Basic concepts and features of the microcontainers for oral drug delivery.

In the realization of this concept it is worth noting, that very likely a large number of microcontainers is required per dose. Therefore, the requirement for high throughput fabrication methods is an important aspect.

1.3 Review of existing research

1.3.1. Microfabricated reservoir based drug delivery devices

In order to fabricate devices as the one mentioned above, the technology applied should give precise control over the size, shape and morphology of the microdevices. This helps in reducing polydispersity, improving drug encapsulation and achieving uniform drug dosage among the devices. MEMS technology is mature enough to provide such precise control on the fabrication parameters and dimensions. Based on this, the first single and multi- reservoirs based devices have been fabricated in Si and photoresist using MEMS technology. The first concept of such a device was mentioned by Martin and Grove *et al.* in 2001 [24]. After that, many active and passive devices have been fabricated based on this idea [5, 6, 25]. The Desai group has worked exhaustively in this area and has acquired significant expertise in fabrication and characterization of reservoir based drug delivery systems. Their first devices were microwells fabricated in Si using photolithography and reactive ion etching [12]. The structures had a height of 2 µm, a reservoir depth of 1 µm and a width of 50-150 µm (Fig.1.2.A). Further, bioadhesion features were added to these devices by modifying their surfaces and attaching lectin. It was proven through in vitro tests on CaCo-2 cells that the adhesion of these devices was improved. Later, various single and multiple reservoir based devices have been produced in photoresists like SU-8 and PMMA [26, 27]. Multiple reservoirs have been successfully filled with three different types of drugs. Using microtransfer molding, devices in PLGA and gelatin (Fig.1.2.B) have also been fabricated though these structures are connected to each other by a residual film [23]. Hansford *et al.* has developed a process that combines discontinuous dewetting of resin on a poly-di-methylsiloxane (PDMS) mold and microtransfer molding to avoid the formation of residual layers (Fig.1.2.C). They have successfully fabricated particulate microstructures such as a) single and b) multiple reservoirs, c) capsulelike microstructures, and d) foldable microstructures in poly(ethylene glycol) dimethacrylate (PEGDMA) and PLGA polymer [28]. They have also performed the loading of drug in such

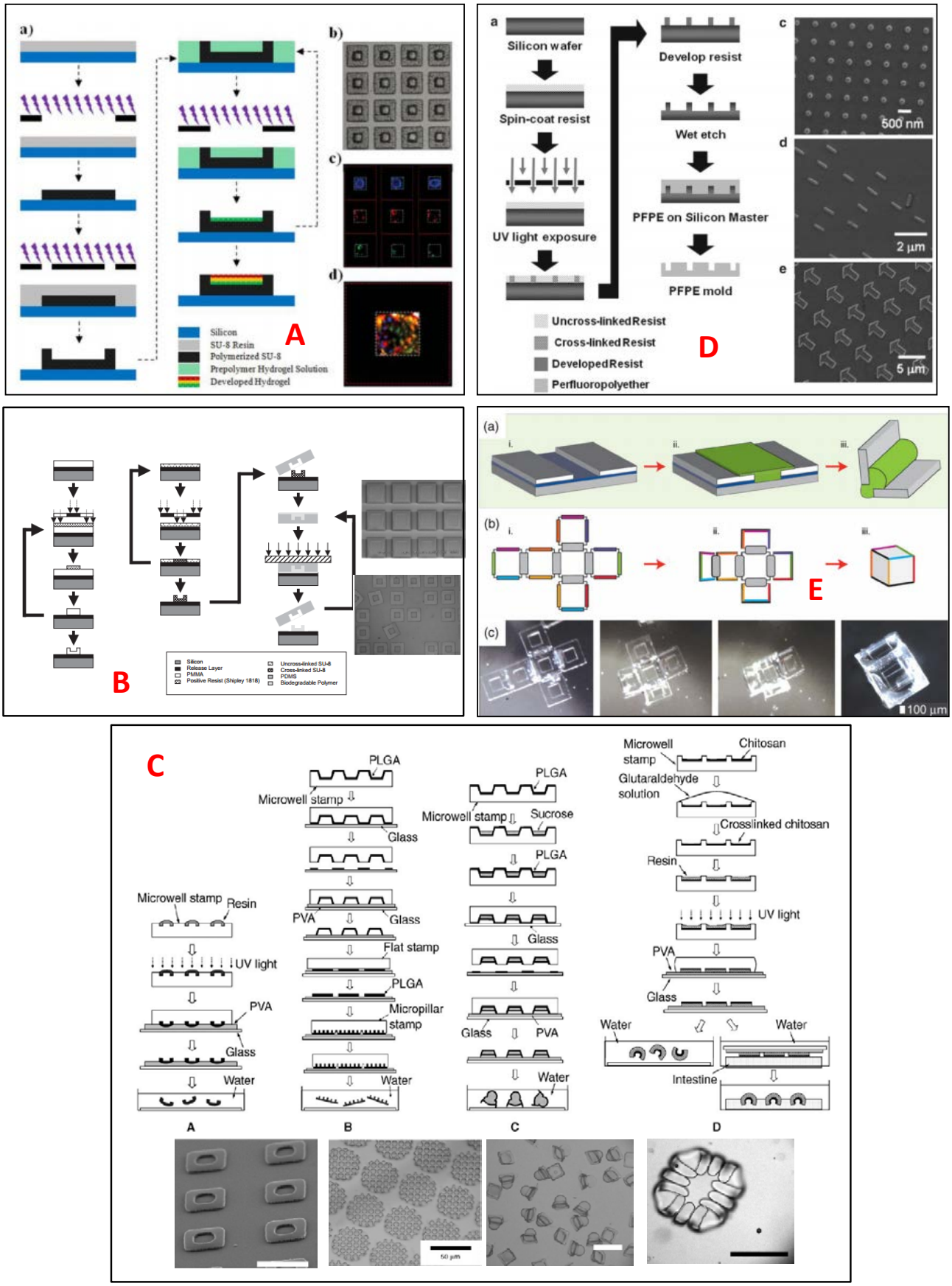

Fig.1.2.A. Fabrication and loading of SU-8 microcontainers using photolithography [26], B. Fabrication of SU-8 and

PMMA microcontainers using photolithography and etching, fabrication of PLGA microcontainers using molding [23], C. Discontinous dewetting and microtransfer printing applied to form various single and multiple reservoirs-based microstructures, micrococapsules and foldable hydrogels [28], D. PRINT technique for the fabrication of micro/nanostructures [26], and E. 3D microcontainers fabricated using self-folding of patterned SU-8 with PCL hinges [35].

microstructures with high yield using the same techniques. The DeSimone group has developed a versatile fabrication process called particle replication in non-wetting template (PRINT) that can be used to fabricate a range of polymeric micro/ nanostructures of different shapes, sizes and materials (Fig.1.2.D).The backbone of the PRINT process is a non-wetting template fabricated in fluorinated perfluoropolyether (PFPE) elastomer [29, 30]. It is a photo-curable resin with extremely low surface energy (8–10 dyne/cm^2), high gas permeability, high elastic recovery, good mechanical strength and high chemical and solvent resistance. The PRINT process is in principle microcontact molding except that the PDMS mold is replaced by a PFPE mold. This mold with low surface energy allows the capillary filling of the cavities without any residual layer in between. The pre-polymer is later solidified by UV light or thermal heating. Applying PRINT, particles for drug delivery with sizes ranging from 200 nm to 7 μm have been fabricated in different materials such as poly(ethylene glycol) (PEG), Poly(L-lactic acid) (PLLA) and PLGA and tested in vitro and in vivo [31-33]. The Gracias group has developed different self-folding 3D microcarriers for drug delivery [34]. The fabrication process is a combination of planar lithographic techniques and hinge-based self-folding driven by surface tension. These devices are generally prepared by deposition of one or more layers of polymer solution on a flat substrate, micropatterning with the desired geometry and release by dissolution of an underlying sacrificial layer. Azam and coworkers have successfully encapsulated beads, chemicals, mammalian cells and bacteria in 3D microcontainers fabricated by the heat-driven self-folding of SU-8 planar structures with PCL hinges (Fig.1.2.E) [35]. To summarize, these are some of the MEMS technology and soft lithography processes that have been used in fabricating oral drug delivery devices. Other soft lithography techniques like micromolding in capillaries (MIMIC), solvent-assisted micromolding (SAMIM), microcontact printing and capillary force lithography (CFL) have been used to produce tissue engineering scaffolds [36-38].

1.3.2 Hot embossing of discrete 3D microstructures

One of the most commonly used processes applied in the fabrication of polymer microstructure is hot embossing. Hot embossing is remarkably versatile in terms of the materials, shapes and sizes

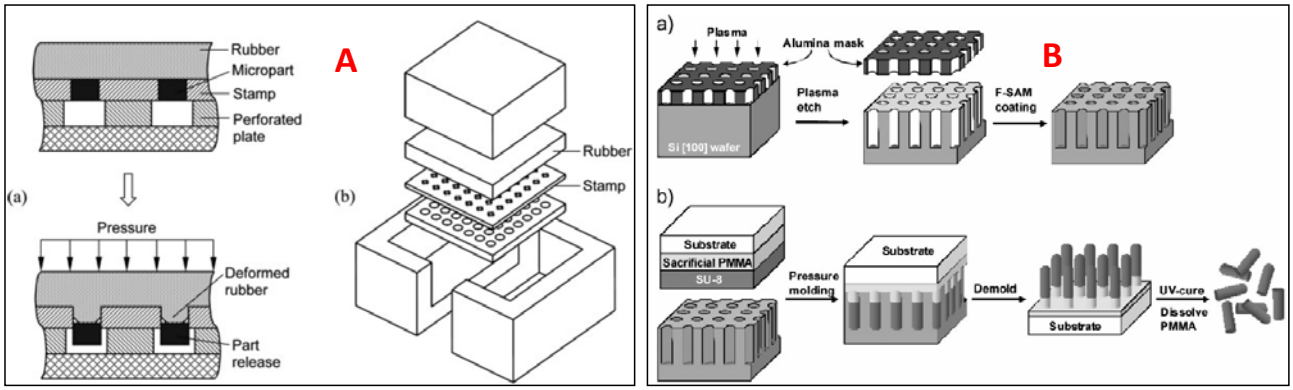

Fig.1.3.A. Basic principle and ejection setup for rubber-assisted ejection for fabrication of 3D discrete microparts [44], B. bilayer embossing to fabricate SU-8 nanorods on PMMA sacrificial layer [45].

that can be embossed in a fast, replicable manner with high yield. Unlike soft lithography, this technique can produce high aspect ratio microstructures, as high as 1:12 [39]. Compared to PDMS molds used in soft lithography, hot embossing uses hard stamps made in Ni, steel or Cu that can be applied for hundreds of runs without any significant damage [40-42]. However, fabricating discrete 3D microdevices using hot embossing has been a challenge due to the presence of an inherent residual layer connecting the structures. Traditionally, the residual layer has been removed by RIE and laser machining. However, since these methods leave unwanted complex residues, their use is undesirable for devices applied in drug delivery. Other unhazardous methods of removing the residual layer have been developed. Kuduva-Raman-Thanumoorthy *et al.* describe a punching process after hot embossing to produce discrete three-dimensional (3D) structures using a special set up as shown in Fig.1.3.A [43]. Heckele *et al.* introduced bilayer embossing with a device layer on a sacrificial layer. However, this process requires precise control of the penetration depth of the stamp in the sacrificial layer and careful selection of the device and sacrificial layers in order to avoid delamination as shown in Fig.1.3.B [44, 45]. In this project hot punching technique has been developed for fabrication of high aspect ratio 3D microcontainers.

1.3.3 Stamp fabrication

In order to fabricate microcontainers in polymer films, a reliable stamp made in hard materials like Ni, Cu, steel etc. needs to be prepared. Among the most frequently used stamp materials, Ni is very robust and can easily be electroplated on a master template to create complex three dimensional structures at high resolution. Another advantage of a Ni stamp is that it can be used for mass production in roll-to-roll processing [46]. Ni stamps can be fabricated with two well-known processes: LIGA (Lithography, Electroplating, and Molding) [47] or DEEMO (Dry etching,

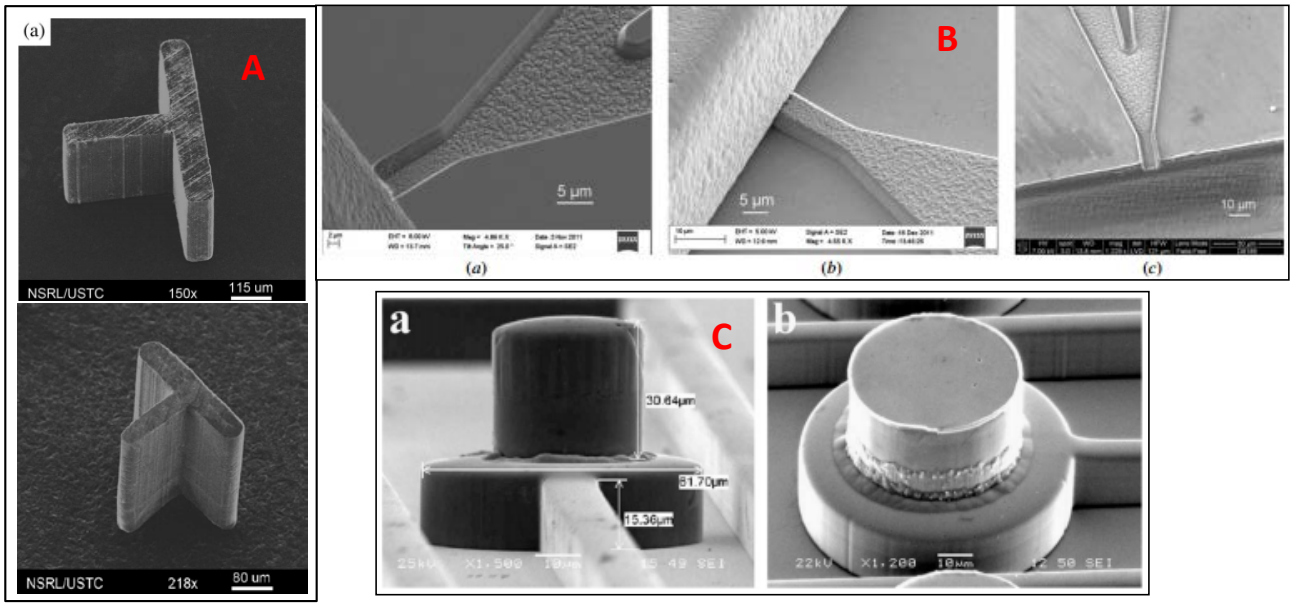

Fig.1.4.A. Fabrication of Ni stamp with high aspect ratio structures: (upper) aspect ratio of 8.25 achieved using Ni stamp and (lower) aspect ratio of 16.5 achieved by using Ni-PTFE stamp [50], B. two-leveled Ni stamp for the fabrication of microfluidic polymer systems [51], and C. two-level cylindrical Ni stamp for the fabrication of blind via hole application on PWB [52].

electroplating and molding) [48]. In both processes, a master is first fabricated either in photoresist by lithography or in Si by lithography and dry etching. Subsequently, Ni is electroplated and the master is removed. This electroplated Ni structure is used for embossing in polymers. The availability of photoresists like SU-8 that allow definition of high aspect ratio structures with very smooth surfaces without use of expensive X-ray synchrotron lithography makes LIGA a viable option for the preparation of Ni stamps. However, it is very difficult to completely remove the SU-8 master from the electroplated Ni stamp in particular in narrow trenches and the resulting increased surface roughness might affect the hot embossing process [49]. Guo *et al*. have been able to emboss single level structures with a minimal width of 40 µm and an aspect ratio of 8 using a Ni stamp prepared with the LIGA process as illustrated in Fig.1.4.A [50]. In this project, a Ni stamp with two-leveled cylindrical microstructures with vertical dimensions > 80 µm and an aspect ratio of 8 has been fabricated using a modified and optimized DEEMO process. Tanzi *et al.* have fabricated two leveled microdevices with rectangular features using the DEEMO process as shown in Fig.1.4.B [51]. Park *et al.* presented the fabrication of a two-leveled Ni stamp with cylindrical features as shown in Fig.1.4.C [52]. In both cases, the aspect ratio of the microstructures is only around 2.

1.3.4 Polymer film preparation

Throughout the research, one process that is common to most of the fabrication techniques is spin coating. Spin coating has been used for depositing photoresists and for obtaining polymer films and drug-polymer matrices. In this project furosemide as a model drug has been loaded in both biopolymer microcontainers fabricated using hot punching and SU-8 microcontainers fabricated using photolithography. To fill the drug, it is first embedded in a polymer (PCL) matrix. This is achieved by first preparing a drug-polymer solution and spin coating it to obtain the required thickness [53]. In the past, drug-polymer films have been fabricated by compression molding (Fig.1.5.b), lamination, roll milling (Fig.1.5.c) and extrusion [54-56]. Most of these techniques either require complicated instrumentation or high temperatures that can damage the active ingredients in a drug. More benign methods like drop casting (Fig.1.5.a) and spin coating (Fig.1.5.b) are available [53]. Between these two processes, spin coating gives more precise control on the thicknesses of the films. Spin coating leads to fast solvent evaporation during the film formation. This is beneficial for stabilizing the drug in amorphous form in the amorphous part of its polymer matrix [57]. Due to the aforementioned advantages, spin coating is applied for making patches for buccal, sublingual, transdermal and oral drug delivery systems [58-61]. However, there is a lack of literature on tuning the process parameters of spin coating to modify the crystallinity and morphology of drug-polymer film. In Konno *et al* and Kellner *et al.* the effect of sample preparation in terms of drug to polymer ratio and use of different polymer matrices on the crystallinity and morphology of drug in spin coated drug-polymer film has been described [57,62]. In this project, tailoring of the crystallinity and thereby the release of drug by modifying the spin coating parameters has been explored.

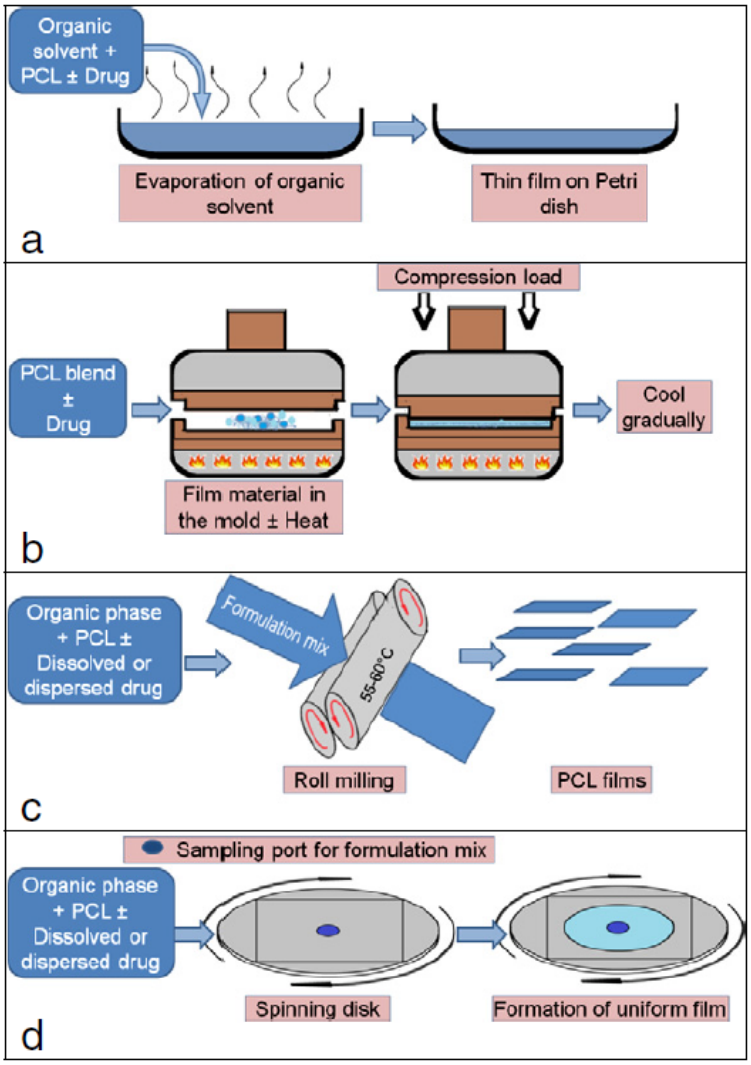

Fig.1.5 Various techniques like a) solution casting, b) compression molding, c) roll milling, and d) spin casting/coating, for producing thin PCL films [53].

1.3.5 Loading of drug into microreservoirs

The important requirements for the loading of drug in microreservoirs are: a) the process should be a high throughput scalable process that preferably leads to low waste of expensive drugs and b) the active ingredients of drug should remain intact during the loading process. The Desai group has successfully filled microreservoirs using photolithography in a controlled manner [26]. This technique is high throughput but the drug is susceptible to irreversible damage during the UV radiation exposure (Fig.1.6.A). Another technique is a drop-on-demand process of inkjet printing [63]. This process does not affect the therapeutic ingredients but is slow and serial (Fig.1.6.B). There are also other issues afflicting inkjet printing like clogging of the ink jet nozzle and the inability to print with high molecular weight polymers. In Nielsen *et al* screen printing has been developed as a technique to load furosemide in powder form in microcontainers (Fig.1.6.C). The process is simple and high throughput, but reproducibility and precise control of the drug dosage in containers are challenging [64]. In Marizza *et al*. the hydrophobic drug ketoprofen is loaded in hydrophilic PVP matrix by first ink jet printing the containers with polymer and then loading the

polymer with drug using supercritical CO_2 (Fig.1.6.B). This process provides high reproducibility and good control on the dosage by tuning the impregnation parameters such as the impregnation pressure [65]. However, so far this process suffers from low throughput. It is also challenging for loading of drug into microdevices manufactured in biopolymers as these devices themselves might get dissolved in supercritical CO_2 thereby losing their structural integrity. Other approaches involving capillary action in nanowire-coated oral microdevices (Fig.1.6.D)[66] and wet microcontact printing have also been developed (Fig.1.6.E) [67].

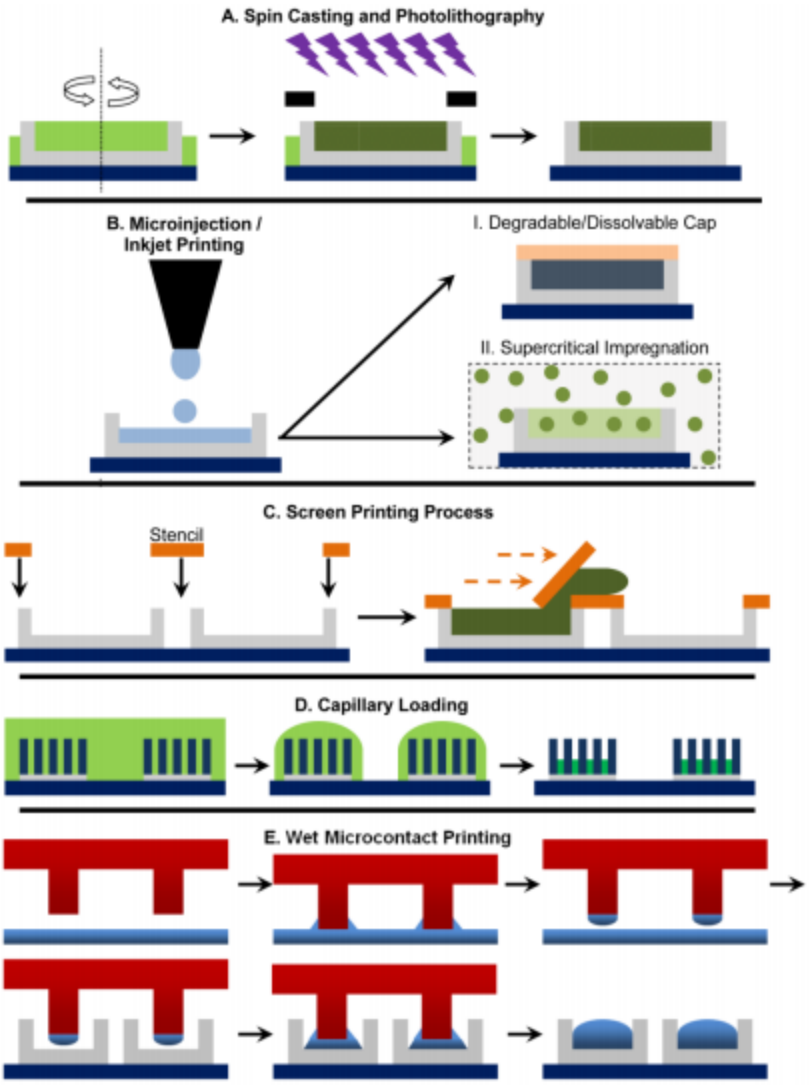

Fig.1.6. Different techniques for loading of drug in microreservoirs: A. crosslinking proteins using photolithography in microreservoirs, B. Inkjet printing to first fill the containers with polymer and then use of supercritical CO^2 to fill the drug in the polymer matrix, C. screen printing of the drug powder on the microcontainers using a stencil, D. applying capillary forces to microscopically confine the drug on nano-wires, and E. microcontact printing of a drug laden PDMS stamp into the cavities of the microdevices [2].

The summary of the introduction section is given in Table 1.

Table 1: Summary of the introduction section

Process	***Fabrication techniques in literature***	***Pros and Cons***
Fabrication of micro-reservoir based devices	1. Standard MEMS techniques like RIE and Photolithography	Good for MEMS materials like Si and photoresists, not for biopolymer based fabrication.
	2. µTransfer molding	Good for biopolymer based device fabrication but the problem of residual layer persists.
	3. µTransfer molding using discontinuous dewetting	Fabrication of biopolymer based devices without residual layer
	4. Self-folding based on surface tension	So far stable structures have been fabricated in SU-8 and not in biopolymers
	5. PRINT	Fabrication of biopolymer based devices of various sizes, shapes and materials, really versatile, scalable process.
Hot embossing for fabrication of 3D discrete microstructures	1. ejection set up	Good for producing simple structures but cannot produce complicated 3D structures plus a special ejection set up is required.
	2. bilayer embossing	Good for producing 3D structures, scalable and fast process but not truly versatile. The polymer materials for the bilayer need to be selected based on certain requirements.
Fabrication of Ni stamp	LIGA	Very versatile and widely used to fabricate different shapes and sizes of stamps using SU-8 as the master mold. However, after electroplating of Ni, removal of SU-8 especially for HAR structures is very difficult.
	DEEMO	As versatile as LIGA, Si etching after Ni electroplating is relatively easy. However, optimization of Bosch process to achieve smooth sidewalls can be challenging.
Preparation of polymer-drug films for patches	Spin casting	Simple process without any need for special tools, no waste of material but good control on film thickness is challenging, especially for thin films.
	Spin coating	Simple process with minimal need on instrumentation, precise control on film thickness can be achieved but leads to waste of material.
	Other high-temperature procedures like compression molding, roll-milling and lamination.	Good control on the film thickness can be achieved but complex instrumentation is required. High temperature can be detrimental to the API in the film
Loading of drug in	1. Spin coating and photolithography	Precise control on the dosage but potentially detrimental to the drug. Also it is a costly and

microreservoirs		laborious process with a lot of material waste
	2. Microinjection	Precise control on the dosage, benign to the drug and less wastage of material. It is slow serial process. It can be scaled up using parallel printers.
	3. Inkjet printing and supercritical CO_2	Precise control on the dosage, benign to the drug and less waste of material. It is a slow serial process that is difficult to be scaled up. It is unsuitable for loading of reservoirs made in biopolymers that potentially dissolve in supercritical CO_2
	4. Screen printing	Simple and quick process, good for filling drug in powder form, which means higher dosage per microdevice, however precise control on dosage is difficult to achieve. Also leads to waste of drug.
	5. Capillary loading	Simple and quick but applicable for certain dimensions.
	6. µContact printing	Simple and quick, needs alignment of drug coated stamp into reservoirs.

1.4 Project funding and framework

The PhD study is carried out as part of a larger consortium, NAnoMEChanical sensors and actuators, fundamentals and new directions (NAMEC) - a VKR Centre of Excellence, working on micro systems for oral drug delivery among other technologies such as sensors. The work presented here is in continuation of the work performed earlier by Johan Nagstrup, PhD (2009-12) who was also funded by NAMEC. The last part of the PhD is funded by Danmarks Grundforskningsfonds og Villum Fondens Center for Intelligent Drug Delivery and Sensing Using Microcontainers and Nanomechanics (IDUN). The main collaborators for the oral drug delivery project consist of members from the Department of Micro and Nanotechnology (DTU Nanotech), at the Technical University of Denmark and pharmacists from the Department of Pharmaceutics and Analytical Chemistry at the University of Copenhagen (KU Farma). The fabrication and loading of the microcontainers, addition of different functionalities like mucoadhesion etc, characterization of the drug loaded in microcontainers is carried out in DTU Nanotech. The new drug formulations and some of the fundamental research on drug and animal testing are performed in KU Farma. The cleanroom fabrication is performed in the state-of-the-art facilities of Danchip.

1.5. Aim of the PhD

The overall aim of this project is to fabricate and load reservoir-based oral drug delivery microsystems in biopolymers. This section lists the goals set forth at the beginning of the PhD. The goals are based on the vision and the device described in section 1.2.

• Develop fabrication methods for micro structuring of biodegradable polymers, preferably the ones that can be scaled up for mass production.

• Fabrication of microcontainers in biodegradable polymers.

• Loading of the microcontainers with drug.

1.6 Thesis outline

This section presents an overview of the chapters in the thesis and a short summary of the content of each chapter. The thesis is divided into eight chapters plus appendices. The appendices include MATLAB codes, some additional SEM micrographs and other supporting documents. The first chapter of the thesis is on the introduction and motivation of the research and the past and current research done in the field in the form of literature review. It is followed by a materials and methods chapter. After that, five chapters covering five different topics of i) spin coating, ii) fabrication of stamp and hot embossing, iii) punching which includes both mechanical punching and hot punching, and iv) drug release from microcontainers are presented. These chapters are followed by conclusion and outlook and the last chapter comprises of the publications and manuscripts finished during the course of this PhD. Thus the chapters are as follows:

Chapter 2. This chapter focuses on the materials and methods used in the thesis:
a) The thermal and crystallographic properties, surface modifications and general applications of SU-8, PLLA, PCL, poly acrylic acid (PAA), PDMS polymers and furosemide (F) drug are described.
b) Characterization tools that are used throughout the research are presented. These include: optical and electron microscopy, profilometry, X-ray diffraction, differential scanning calorimetry (DSC), Raman microscopy and microdiss. Process parameters and a brief theory regarding these tools are given.

Chapter 3. Here, relevant theories on spin coating that relies on, among others, centrifugal forces and solvent evaporation are presented. A small section on the spin coating technique including preparation of solutions and optimization of spin coating has been described. Finally based on the theory, the spin curves have been evaluated.

Chapter 4. In this chapter, first a brief description of the two deep reactive ion etching (DRIE) processes: continuous DRIE and Bosch, used in the project is given. After that theory on the hot embossing process including effect of parameters derived by solving parallel plate squeeze flow theory and discussion of demolding issues of stamp have been presented. This discussion forms the basis for the stamp design so that the demolding forces are minimized and good replication yield is achieved. Further, a small section on the process flow of fabrication of Ni stamp is provided. This is followed by the optimization results obtained for the fabrication of Ni stamp by applying the two DRIE processes described earlier. Finally, results obtained for embossing of PLLA film by Ni stamp are discussed.

Chapter 5. This chapter is named as punching as it includes both the mechanical punching and hot punching of polymer films. The basic idea behind using mechanical punching for the fabrication of microcontainers is presented. This forms the initial inspiration for the development of hot punching process which is a combination of hot embossing and mechanical punching processes. The fundamental concepts of hot punching as applied for fabrication and loading of microcontainers are presented. After this, a small section on the process flows of mechanical punching and hot punching

are illustrated. The chapter ends with the results obtained by applying hot punching for the fabrication and loading of microcontainers.

Chapter 6. In this chapter, the fundamental theories of Fick's law and power law that are used to describe drug release from various systems have been provided. This is followed by a short derivation of release profile of drug embedded in polymer matrix loaded in microcontainers. Finally, the measured drug release from microcontainers is evaluated.

Chapter 7. Conclusion and outlook

Chapter 8. Published papers, proceeding, manuscripts and filed patent.

CHAPTER 2
MATERIALS AND CHARACTERIZATION METHODS

CHAPTER 2
MATERIALS AND CHARACTERIZATION METHODS

2.1 Materials

This section gives a brief overview of the key photoresists and polymers used in the project. For each material, there is a short introduction, a description of its applications with particular focus on drug delivery, a summary of some of the relevant properties and finally an outlook on its use in the presented research.

2.1.1 SU-8

SU-8 is an epoxy based (Fig.2.1.A), negative, near UV photoresist (SU-8 2075, Microchem, USA). It has been used for fabrication of remarkable microstructures with aspect ratio as high as 20 [68]. The photoresist can be spin coated to thicknesses >200 μm. Over the years, SU-8 processing has been established due to its vast application as lift off resist, for fabrication of stamps for molding, as master for LIGA process and for actual microdevices [69, 70]. As a microdevice, SU-8 micro/nanostructures have been applied in tissue engineering, microfluidics, drug delivery systems, and mechanical systems such as microgrippers and microvalves. Apart from its ease of fabrication and ability to produce high aspect ratio structures, the main properties that have led to its widespread use, are its good chemical, thermal and mechanical stability. For the applications in bio-related fields, it has been shown that SU-8 is biocompatible and that it potentially could be used in implantable devices [71]. However, SU-8 is not biodegradable and that limits its applicability in oral drug delivery systems. Nonetheless, for the oral drug delivery devices described in section 1.2, it is an ideal prototype material which can be easily structured using photolithography and utilized for moving forward in the research on loading and characterization of drug polymer matrices in microcontainers. On certain occasions, surface modification of SU-8 is required. This is achieved by exposing the containers in ultra-violet/ozone (UVO) for at least 20 minutes or oxygen plasma for 5-10 minutes [72, 73]. This increases the surface energy of SU-8 from approx.26 mN/m to79 mN/m just after the treatment [73].

2.1.2 Poly-di-methylsiloxane (PDMS)

PDMS is a widely used silicon-based organic polymer. It is generally sold as a prepolymer along with a curing agent. The PDMS bought as Sylgard 184 (Dow Corning) is used by mixing prepolymer and curing agent in 10:1 ratio. The mixture is degassed and cured after spin coating or film casting with UV light or thermally [74]. PDMS can be dispensed on a master with complex high aspect ratio micro- and nano-sized features. If left for few hours the polymer can completely conform to the surface because of its good rheological properties in the uncured state, forming a perfect replicate of the master. Typically, the cured PDMS is then separated from the master and can itself be used as a mold for casting of other polymers. Easy processing and handling, flexibility and low cost have been the main factors for the success of PDMS as a mold for soft lithography processes like micromolding in capillaries (MIMIC), solvent-assisted micromolding (SAMIM), microcontact printing and capillary force lithography (CFL), pioneered by the Whitesides group [36-38]. The properties that promote PDMS as a good material for microfluidics and Bio-MEMS

are that it is inert, nontoxic, and biocompatible [71, 75]. However, PDMS is not biodegradable and this constrains its application in drug delivery system. Its gas permeability and transparency are an advantage for cell culturing to supply light and oxygen for their growth [76]. However, its high absorption of hydrophobic small molecules makes the use of PDMS devices for drug discovery problematic. Its high absorption of organic solvents only allows aqueous chemistry in microfluidic PDMS channels which is also limited because the water diffuses into it with time [76, 77]. Moreover, the application of PDMS as material for micromolding stamps is also limited due to its deformability. The high compressibility (2 N/mm^2) of PDMS causes shallow relief features of a stamp to deform or collapse [77, 78]. Many of these stamps are damaged after few cycles of molding. These challenges have led to the development of modified PDMS materials like h-PDMS, fluorinated-PDMS or photo-patternable PDMS [79-81]. An alternative to PDMS is perfluoropolyether (PFPE) developed by Rolland and DeSimone. While PFPE is a more chemically, thermally and mechanically stable elastomer, it retains the high gas permeability, flexibility and easy processing properties of PDMS. This material is used in the polymer replication in non-wetting template (PRINT) process for the fabrication of discrete 3D micro and nanostructures [77, 29]. However, it is relatively expensive and it is still not stable enough for long runs of molding when compared to stamps made in Ni and steel.

In this research PDMS has been used as an elastic deformable layer below PLLA and PCL polymer films during hot punching of the polymers [82]. For hot punching purposes, the hydrophobic PDMS surface properties have often been modified by oxygen plasma treatments. In the plasma, the surface becomes more hydrophilic due to the rapid substitution of -C bonds with -O bonds [83]. Another technique is exposure to ultraviolet/ozone UVO which increases the hydrophilicity of the PDMS surface by inducing the formation of –OH bonds (Fig.2.1.B) [84]. The PDMS surface energy changes from 19 mJ/m^2 to72 mJ/m^2 just after such UVO and plasma exposures [84]. However, the surface properties after plasma activation are not stable and PDMS recovers its hydrophobicity due to the migration of uncrosslinked PDMS to the surface [85]. This recovery is a limitation for a lot of applications like bonding of films or glass to PDMS in microfluidics. Here, it has been used to our advantage because the hydrophobic recovery facilitates the harvesting of PLLA microcontainers for drug delivery.

2.1.3. Poly acrylic acid (PAA)

PAA is a water soluble polymer of high molecular weight acrylic acid (CH_2=$CHCO_2H$, Fig.2.1.C) [86]. It has been widely used for disposable packaging and in the pharmaceutical industry as thickening, emulsifying and suspension agent [87]. Recently, it has gained popularity in drug delivery systems due to its application in hydrogel formation [88]. PAA can be mixed with a plethora of other polymers like PEG, chitosan or poly-vinyl pyrrolidone (PVP) to provide characteristics such as mucoadhesion or pH sensitivity to the drug delivery microdevices [89-91].

In this project, PAA has been loaded in the microcontainers to demonstrate the loading of hydrophilic drug matrices. Furthermore, PAA films have been used as a sacrificial layer for release of both SU-8 and PLLA microcontainers [82]. The side chains of the PAA polymer contain (Na^+)– carboxylate groups. PAA is easily spin coated and its solubility properties can be altered by

reversible ion-exchange from water-soluble (Na^+ counterion) to water-insoluble (Ca^{2+} counterion) forms [92]. The acidic nature of PAA leads to the crosslinking of SU-8 during its processing [93]. Addition of OH^- ions by mixing sodium hydroxide (NaOH) in the PAA aqueous solution can increase the pH of PAA. This allows for the use of PAA as a sacrificial layer for SU-8 processing. PAA has a surface energy of around 72mJ/m^2 when it is in aqueous solution [94]. This property is important when the polymer is loaded in microcontainers and also when it is used as bonding layer for PLLA microcontainers. PAA has a T_g of around 106 °C [95]. This is to be noted for the optimization of thermal bonding of PLLA microcontainers in this project as the best bonding is achieved around this T_g. PAA with M_w 90000 is bought from Sigma Aldrich as 35% wt. aqueous solution.

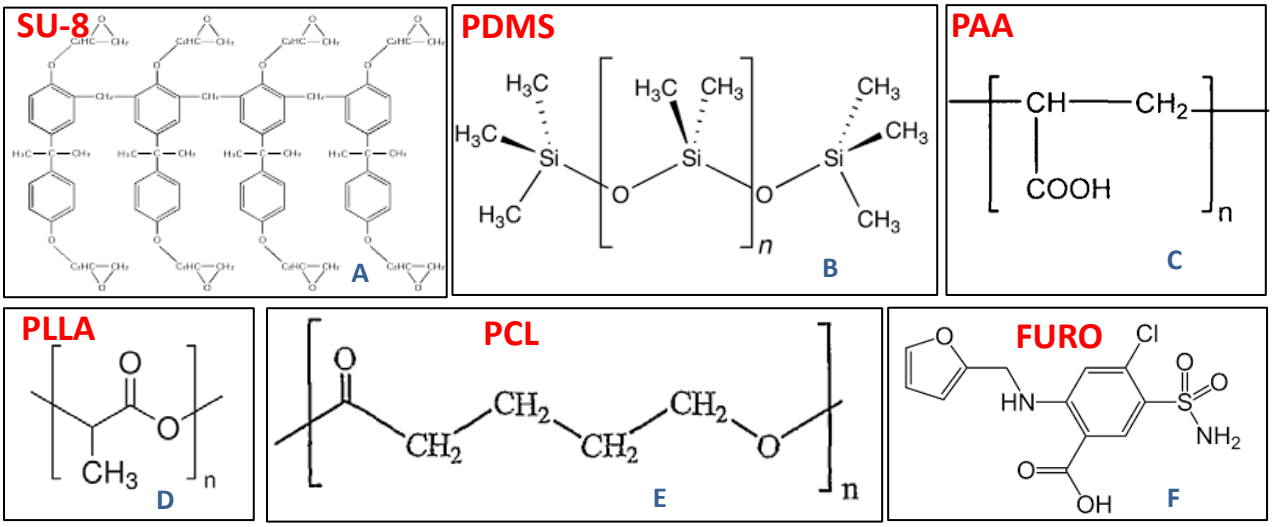

Fig. 2.1 Structural formulas of A. SU-8: the 8 epoxy groups from where the name SU-*8* is derived, B. PDMS: the silicone groups at the surface get converted to silanol groups (-OH) in place of methyl groups (-CH_3) after oxygen plasma exposure, C. PAA with acrylic acid chain consisting of carboxylic group (-COOH) attached to vinyl functional group (−CH=CH_2), D. PLLA with the chiral lactic acid that in different arrangements, gives PLGA, PDLA etc., E. PCL prepared by the ring opening polymerization of ε-caprolactone, F. Furosemide with fixed anthranilic acid moiety, flexible furan ring and sulfonamide group that give rise to its polymorphs.

2.1.4 Poly-L-Lactic Acid (PLLA)

There is significant interest in biopolymers such as Poly lactic acid (PLA) for biological and pharmaceutical applications. PLA is biocompatible and biodegradable aliphatic polyester and can be acquired from plant based sources such as corn starch and sugarcane [96]. It is a thermoplastic, high-strength, and high-modulus polymer. It has a wide range of applications including food packaging, tissue engineering, and even plastic surgery [96]. PLA can be processed by injection molding, blow molding, thermoforming, extrusion and more recently 3D printing [97-99].

There are several different forms of PLA due to the chiral nature of lactic acid ($CH_3CH(OH)CO_2H$) [96, 97]. The polymer that has been applied in this research is Poly-l-lactic acid (PLLA) which is a result of the polymerization of L-lactide. The thermal properties of this polymer are $T_g \approx 55$ °C and $T_m \approx 175$ °C, depending on the molecular weight and synthesis parameters [96]. PLLA films can be obtained with various methods such as extrusion, drop casting and spin coating [100]. To prepare

the solution for spin coating, PLLA can be dissolved in organic solvents like chlorinated solvents (dichloromethane, chloroform), benzene, acetonitrile, and others [96]. The crystallinity of a polymer like PLLA can increase during its thermal processing. This increases its glass transition temperature and lowers the degradation rate. For drug delivery applications this in turn might affect the drug release [96, 97]. The glass transition temperature and degradation rate of PLA polymers has been studied in the NAMEC consortium by Sanjukta Bose [101]. For example, enzymatic degradation of PDLLA has been studied by measuring the resonance frequencies of coated microcantilever sensors before and after the degradation. PLLA is hydrophobic in nature but with the exposure to oxygen plasma or UVO, its surface properties can be modified [102, 103]. The surface energy changes from 30mJ /m^2 to around 64 mJ/m^2 just after the exposure [104, 103]. In this research the properties of PLLA have been explored to fabricate microcontainers and load these with drug. PLLA with M_w = 120000 and density around 1.2-1.4 g/cm^3 has been bought from Sigma Aldrich.

2.1.5 Poly-ε-caprolactone (PCL)

Just like PLA, PCL is a thermoplastic aliphatic ester that is biocompatible and biodegradable [105]. Hence, it is widely used in tissue engineering as stents and scaffolds and in drug delivery systems as drug-polymer micro/nano particles as well as buccal, transdermal and sublingual patches [53]. PCL can be dissolved in organic solvents and is hydrophobic. The main differences between PCL and PLA are: i) PCL is a synthetic polymer synthesized by the ring opening polymerisation of ε-caprolactone group; ii) PCL has a very slow degradation rate; and iii) T_g = -60 °C and T_m= 60 °C, which implies that it is in a rubbery and semi-crystalline state at room temperature. The low T_g indicates good rheological and viscoelastic properties for easy manufacturing and moldability into complex shapes [105]. Low degradation rates make it apt for slow sustained drug release. PCL is a polymer that can be easily combined with other polymers such as PEG or polystyrene (PS) to tailor the drug release or increase its degradation rate [105]. In this research, PCL with Mw = 100000 is bought from Sigma Aldrich. The density of PCL is 1.145g/cm^3.

2.1.6 Furosemide (F)

Furosemide is the model drug used in this research. It is an anthranilic acid derivative marketed as Lasix. As the name suggests this drug “lasts” for “six” hrs, that is, it remains effective for 6 hrs in the human system. It is a fast and strong loop diuretic that acts on the ascending loop of Henle in kidney [106]. Furosemide allows removal of unwanted water and salt from the body through urine. Thus it is used for the treatment of edema, hypertension and congestive heart failure. It has been on the WHO’s List of Essential Medicine [107].

Even though furosemide is such an important drug there are many challenges for its optimal bioavailability in the body. According to the Biopharmaceutics classification system (BCS), furosemide is a class IV drug with very poor water solubility and intestinal permeability [106,107]. The strong hydrogen bonds present in the drug render it poorly soluble but allow hydrolysis in aqueous solutions. Another challenge with furosemide is its high susceptibility to storage and manufacturing conditions. Besides hydrolysis, furosemide is prone to photochemical degradation and thermal degradation [108]. This drug suffers from side effects due to high diuresis peak and high drug absorption variability when it is administered as conventional burst-release tablets and

capsules. High diuresis peak can lead to weakness, fatigue and hyperglycemia in patients. Besides, furosemide needs frequent administration which leads to low patient compliance [109].

Furosemide exists as various crystalline polymorphs, solvates and amorphous forms. This is due to the high conformational flexibility of the Furan ring and sulfonamide group around the fixed anthranilic acid moiety [110]. The most stable form of furosemide is its crystalline polymorph form I. When an amorphous form of furosemide stabilizes into crystalline form, it generally takes this polymorph form [110, 111]. It is well known that amorphous solid forms, due to the lack of the three-dimensional long range order of molecular packing which exists in their crystalline counterparts, dissolve faster than crystalline forms. This leads to increase in the solubility, dissolution rate and therefore bioavailability of the drug [112]. However, since furosemide degrades at the melting point it is difficult to produce amorphous furosemide by heating and quench cooling as it is done for many other drugs [109]. Nielsen et al, produced amorphous furosemide salt and acid by spray drying of crystalline furosemide dissolved in methanol [113]. However, the amorphous form is highly unstable. In this research furosemide is embedded in PCL polymer. Furosemide dissolves in acetone which has been used to make its solution for spin coating. Thus a homogenous solution consisting of 2 g of furosemide, 8 g of PCL, 40 ml of acetone and 20 ml of DCM is prepared for spin coating PCL-F film. This drug-polymer film is either used as a patch or is loaded in SU-8 and PLLA microcontainers.

The summary of the materials section is given in Table 2.1.

Table. 2.1. Summary of the various materials that are used in the work

Material	**Relevant properties**	**Application in this research**
SU-8	1. negative photoresist with well-established fabrication process 2. inherently hydrophobic behavior 3. possibility of achieving higher surface energy by UVO or oxygen plasma exposure 4. good thermal, chemical and mechanical stability.	Prototype material for fabrication for microcontainers and addition of functionalities
PDMS	1. thin conformal rubbery films possible 2. inherently hydrophobic behavior that can be modified by UVO or oxygen plasma exposure 3. hydrophobic recovery 4. viscoelastic behavior.	Elastic layer deposited on Si substrate for punching of PCL, PCL-F and PLLA films for the fabrication and loading of microcontainers
PAA	1. water soluble polymer 2. thin layers possible by spin coating of aqueous solution 3. high surface energy and thus, high adhesion 4. application as hydrogel carrier for drugs.	Sacrificial layer on which microcontainers are bonded, hydrophilic polymer matrix loaded in containers
PLLA	1. biocompatible and biodegradable 2. thermoplastic with T_g = 60 °C and T_m = 150 °C 3. easy processing and ability to make thin films by spin coating 4. hydrophobic behavior but surface properties can be	Main material for the fabrication of biopolymer microcontainers

	modified using UVO or oxygen plasma.	
PCL	1. biocompatible and biodegradable 2. thermoplastic with T_g = -60 °C and T_m = 60 °C 3. easy processing and ability to make thin films by spin coating 4. inherent hydrophobic behavior	Material for polymer matrix in which furosemide is embedded, also used for fabrication of biopolymer microcontainers
FUROS-EMIDE	1. poor solubility and permeability 2. dissolves in acetone	Model Class IV drug

2.2. Characterization methods

This section briefly introduces the various characterization methods used throughout the research. Three different types of characterization are described here: i) structural and topographical characterization which includes microscopy and profilometry techniques, ii) solid state characterization including XRD, Raman and DSC, and iii) drug release studies performed using microdissolution.

2.2.1. Scanning electron microscopy (SEM)

SEM is a versatile instrument used for structural and morphological characterization. Electron microscopy was developed to surpass the resolution limits of optical microscopy. The resolution limit d_r due to the diffraction of radiation is given by:

$$d_r = \frac{\lambda}{2n \sin\theta} \tag{2.1}$$

where, λ = wavelength of the radiation, n = refractive index of the medium between the lens and the object, θ = half angle formed by the lens at the object. The denominator of the equation ($n\ sin\theta$) is

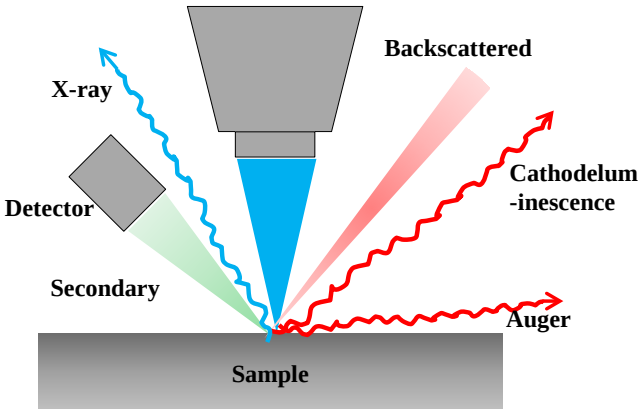

Fig.2.2 Concept of SEM: The electron beam travels through electromagnetic fields and lenses, which focus the beam down toward the sample. Once the beam hits the sample, electrons and X-rays are ejected from the sample, and collected by detectors.

also called numerical aperture [114]. Since the wavelength of an electron is thousand times lower than that of visible light, electron microscopes provide much higher resolution than optical microscopes. SEM works on the principle of recording the scattering of the secondary electrons produced by the incident primary electrons from the surface of the specimen. Thus when the primary electrons are raster scanned, the secondary electrons are generated in the same raster

scanned manner [115]. These electrons are collected by photodetectors to obtain a SEM micrograph (Fig.2.2). There are other types of signals that could be collected like back scattering electrons or characteristic X-rays. In this research, two kinds of imaging modes are used: high vacuum and variable pressure secondary electron modes [115, 116]. High vacuum mode was used for samples sputtered with Au before imaging, Si masters and Ni stamps while variable pressure mode was used for all the polymeric samples to avoid unwanted charging of these non-conducting materials. The samples are characterized either using SEM Zeiss Supra 40 VP in variable pressure mode at 8 kV operating voltage and 13 Pa pressure or using SEM JEOL JSM 5500LV in high vacuum mode at 15 kV operating voltage.

2.2.2. Profilometry

Two types of profilometers are used in order to acquire topographical measurements: A stylus profiler and a confocal profiler. Both instruments can measure a wide range of step heights from few nanometers to several millimeters. In the stylus profilometer the stylus is in contact with the sample during the scan, and the height movement of the stylus is registered by

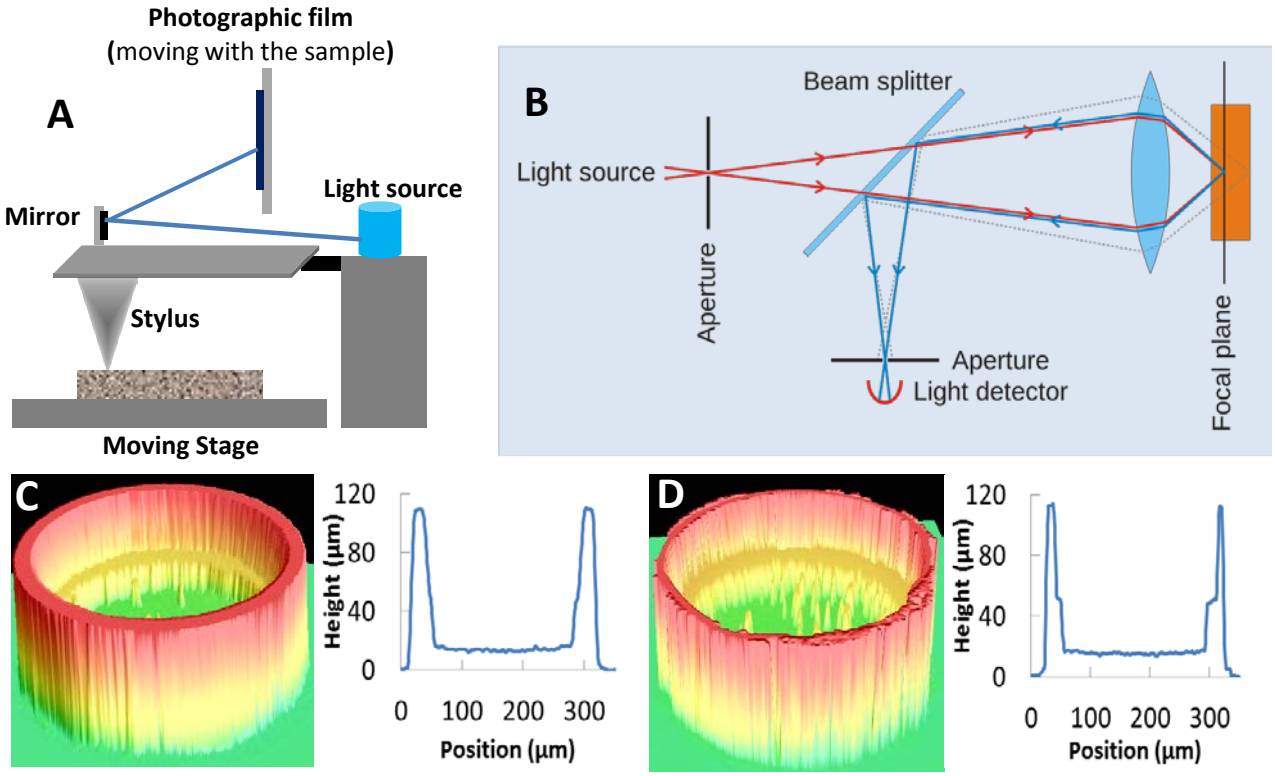

Fig.2.3 Profilometry: A. stylus profiler used to measure thickness of polymer films, B. optical profiler used for dimensional measurements of microstructures; Optical profiler measurements of individual microcontainers with 20 µm (C) and 10 µm (D) wall thicknesses [82].

a sensor, giving the height profile measurement (Fig.2.3.A) [117]. This measurement technique is applied for measuring the thicknesses of various spin coated films. The films are scratched by a scalpel to expose the substrate and then height measurements are performed at low stylus force of 3 mg using a Dektak XTA instrument.

For the measurement of microstructures such as the ones on Si masters, Ni stamps and the PLLA microcontainers, Sensofar PLU confocal profilometer is operated. This is a non-contact measurement and better suited for high aspect ratio features. In the confocal profiler, the sample is scanned vertically in steps so that every point on the surface passes through the focus of the objective lens. A very small aperture is placed in front of the detector to admit light from a single point as it passes through the focus (Fig.2.3.B) [118]. In-plane raster scanning is required in order to build up the confocal image at each vertical step. Since PLLA and PCL samples are almost transparent, it is difficult to get 100% signal. However, with some optimization the information obtained with the confocal profiler is sufficient to measure the height profiles. In Fig.2.3.C and D, the measurements of PLLA microcontainers with different wall thicknesses of 20µm and 10µm taken by optical profiler are demonstrated.

2.2.3. X-ray diffraction (XRD)

X-ray diffraction is based on Bragg's law which is

$$n\lambda = 2d \sin\theta \tag{2.2}$$

where λ = De Broglie wavelength of the incident wave, n = positive integer, θ = angle of the incident wave and d = spacing of the planes in a crystal lattice. Thus, Bragg's law describes the

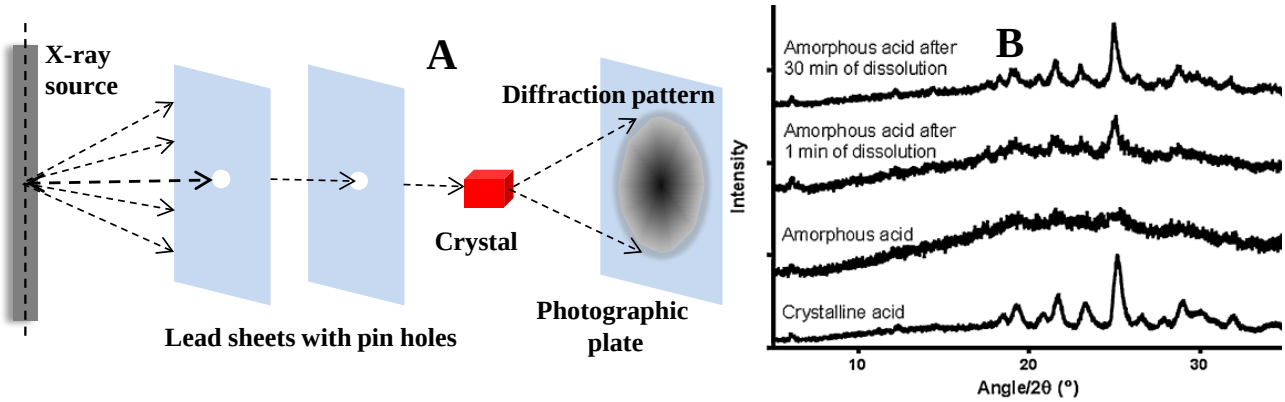

Fig.2.4.A. Schematic of a typical XRD experiment, and B. An example of XRD of furosemide from Line *et al.* -XRD of amorphous acid form compacts after 1min and 30 min of dissolution at pH 6.5 in a µDiss profiler. The diffractograms for crystalline and amorphous furosemide acid starting material are shown as references [113].

relationship between the wavelength of the electromagnetic radiation, the diffraction angle and the lattice spacing in a crystalline sample. In a XRD, when the Bragg condition is satisfied, constructive interference is produced due to the interaction between the monochromatic X-ray beam and a crystalline sample. The diffracted X-rays are then detected and the recorded signals processed. By scanning the sample for a range of 2θ angles, all the possible diffraction directions of the lattice are attained (Fig. 2.4.A). Hence X-ray diffraction can be used to study 3D crystalline structure and crystal lattice properties but it is not possible to perform analysis of chemical structures. XRD is a non-destructive method that allows small sample size [119].

In this research XRD is mainly used for the characterization of furosemide (F) drug and PCL polymer. For the crystalline furosemide distinct sharp XRD peaks are recorded. Compared to that amorphous polymers show no peaks but only a broad halo (Fig. 2.4.B) [113]. All XRD analysis are performed using an X'Pert PRO X-ray diffractometer (PANalytical, Almelo, The Netherlands; MPD

PW3040/60 XRD; Cu KR anode; λ = 1.541 Å; 45 kV; 40 mA). A starting angle of 5° 2θ and an end angle of 35° 2θ are employed for the scans. A scan speed of 0.6565° 2θ/min and a step size of 0.01313° 2θ are selected. Data are collected using the X'Pert Data Collector software (PANalytical B.V.).

2.2.4. Raman spectroscopy

Raman spectroscopy provides information about molecular vibrations for sample identification and quantification. It can be used to study solid, liquid and gaseous samples. This spectroscopic technique is based on inelastic scattering of monochromatic laser light, when it interacts with a sample. The frequency of incident photons changes when they are absorbed by the sample and then reemitted. The frequency of this reemitted photons is shifted up or down in comparison to the original monochromatic frequency, which leads to the Raman Effect. This shift provides information about vibrational, rotational and other low frequency transitions in molecules (Fig. 2.5.A) [120]. Similar to XRD, Raman spectroscopy is also a non-destructive characterization method that allows working with small sample size. Raman spectroscopy is applied in pharmaceutical research to identify the APIs and the polymorphic forms of a drug (Fig. 2.5.B and C). The different polymorphic forms of the same molecule have different properties that influence the bioavailability of the drug [121]. In this paper, PCL-F processed with different parameters and loaded in microcontainers is characterized using Raman spectroscopy. Raman spectra are collected with a DXR Raman microscope (Thermo Scientific, Germany) equipped with a frequency-stabilized single mode diode laser (780 nm). The laser power is set to 24 mW at the sample position (center of the container) and the estimated resolution is 2.4 – 4.4 cm^{-1}. An exposure time of 30 sec and averaging of three scans are used.

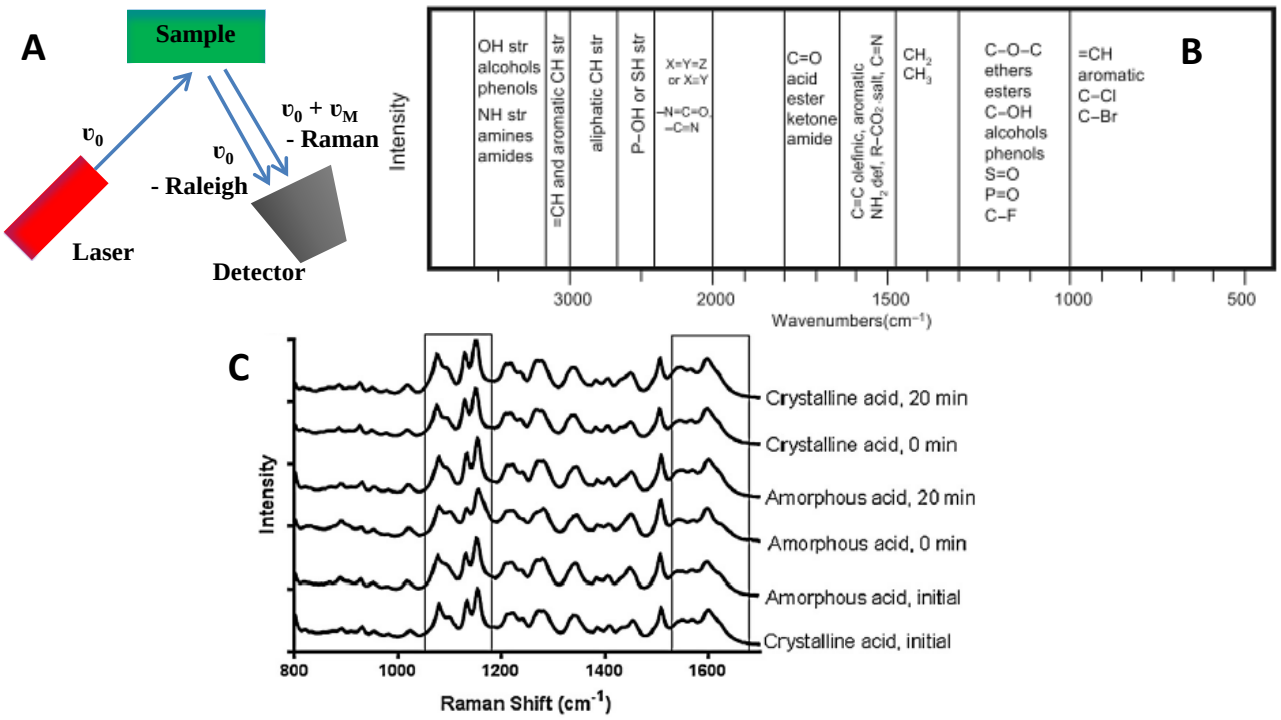

Fig. 2.5.A. Schematic of Raman spectroscopy, B. Illustration of wavenumbers characteristic of important functional groups [121], and C. An example of measurement of APIs using Raman spectroscopy from Line *et al.* showing Raman

spectra of amorphous and crystalline furosemide acid compacts during dissolution at pH 6.5. Boxes highlight spectral regions where differences can be observed during dissolution of the amorphous acid form [113].

2.2.5. Digital Scanning Calorimetry (DSC)

DSC is an important thermoanalytical technique that analyses the heat flow related to material transitions as a function of time and temperature. It basically measures the energy necessary to keep the sample and the reference at the same temperature when both of them are subjected to an identical temperature gradient (Fig. 2.6.A.). For an exothermic transition (such as crystallization) heat is released from the sample while for an endothermic transition (such as melting) more heat is to be supplied to the sample with respect to the reference. Glass transition is observed as an endothermic shift in the baseline (heat flow signal) due to an increase in the specific heat capacity of the polymer. Generally glass transition temperature (T_g) is determined from the center point of the heat flow change (Fig. 2.6.B.) [122].In this project DSC has been used to study the thermal behavior of PCL-F matrix. DSC is performed in a Perkin-Elmer DSC 4 fitted with a 3600 Thermal Analysis Data Station. Sample sizes are 10mg where the pure PCL and PCL-F solutions of same concentration are pipetted in aluminium pan. The solvent is allowed to evaporate overnight. The samples are hermetically sealed in the pans (Perkin-Elmer kit No. 219-0062) and scanned at 2 °C/min over the range -80 °C to 225°C.

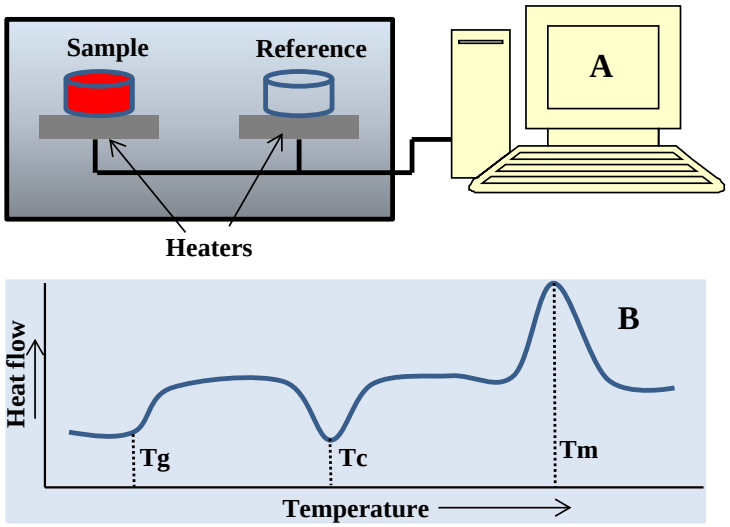

Fig.2.6.A. Schematic of differential scanning calorimetry system (DSC), B. Typical DSC plot including T_g transition and crystallization and melting peaks.

2.2.6. Microdissolution and drug release studies

Dissolution testing is an essential tool for evaluating the performance of a drug in vitro. In this method, the drug release from delivery systems is characterized by recording the evolution of the drug concentration in a liquid with optical probes [123]. It is an important determinant of the in vivo performance and also essential for quality control purposes. However, it can be difficult to predict oral bioavailability based on in vitro dissolution as the processes occurring in the GI-tract are very complex and, therefore, difficult to mimic precisely. Nevertheless, dissolution tests remain important and can provide at least indications towards the in vivo performance [124].

The traditional methods of dissolution measurements involve manual or automatic sampling from the dissolution vessel and measuring the concentration using UV spectrophotometer or high-performance liquid chromatography (HPLC) [125]. This process is laborious and expensive. The use of fiber optic technology for dissolution measurements allows continuous in situ analysis of the drug concentration with more data points and without any need for sample withdrawal and preparation for analysis. The dissolution experiments described in this thesis are performed with a µDiss profiler (pION Inc, Woburn, MA). A µDiss profiler is a miniaturized dissolution apparatus with thermostated channels using in situ fiber optic UV probes immersed in 2-20 mL of dissolution media. The probe is rod shaped with a mirror at one end, two optical fibers connected to the other end, and a window with well-defined spacing between the mirror and the fibers. UV light emitted from the optical fiber travels through the dissolution media through the window between probe and mirror, where it is reflected back to a second optical fiber. On the path through the media the light is scattered by the analyte molecules. This signal is then detected by photodetectors or CCDs resulting in real time measurements of UV absorption [125, 126]. This technique eliminates potential errors in sample preparation and also wastage of sample. The tool is low-maintenance and running the tests is straightforward [127]. However, care must be taken to avoid passage or trapping of bubbles, excipients, or undissolved particles at the probe detection window that can interfere with the signals [128]. Fig.2.7.A shows the set-up of a µDiss profiler containing 6 channels and the schematic of one probe. Fig.2.7.B provides an example of typical microdissolution measurement from Lu *et al.* In the µDiss profiler dissolution studies in this project, 10 mL of phosphate buffer (pH = 7.4) are utilized. A rotation speed of 100 rpm and a temperature of 37 °C are applied during the experiments.

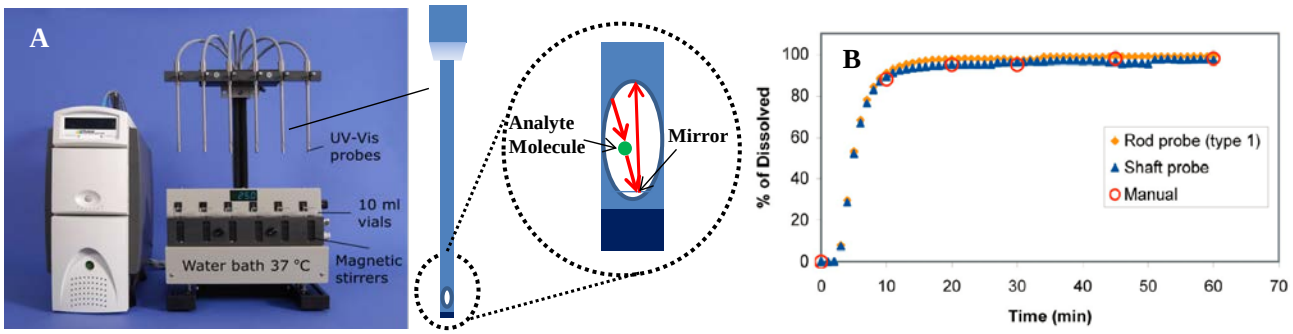

Fig.2.7.A Photograph of the set-up of a µDiss profiler containing 6 channels and the schematic of one probe alongwith the closeup, B. An example of dissolution measurement from Lu *et al.* showing dissolution profiles of an immediate-release capsule formulation comparing use of shaft probes and rod probes with use of manual sampling and HPLC finish [125].

CHAPTER 3
SPIN COATING

CHAPTER 3
SPIN COATING

As mentioned in the introduction section, spin coating has developed as a viable method of fabricating polymer films with controlled thicknesses. In this project, spin coating has been used at numerous occasions: from spin coating of photoresists in cleanroom to spin coating of polymer solutions in fumehood. One of the most important applications of spin coating presented in this thesis is the fabrication of drug-polymer matrices as drug delivery patches and as films for loading into microcontainers using hot punching. Hence, in this section, a brief overview of spin coating process is provided. This is followed by the method of spin coating of polymer solutions applied in the research. Finally, some results on spin coating are presented. Detailed information on drug-polymer patches and drug-polymer loading is provided in chapter 5 on punching and in papers IV-VII of chapter 8.

3.1 Theory of spin coating

In spin coating, a solution (polymer or photoresist dissolved in a solvent) is applied to a horizontal disc which is either static or rotating at low angular velocity. To get the desired thickness of the film, after dispensing the solution, the disc is then rotated at high angular velocity. The adhesive force at the liquid-solid interface and the centrifugal force lead to shearing of the liquid. There is radial flow of the liquid where the polymer liquid solution is ejected from the disc. This results in the formation of highly controlled and reproducible thin polymer film. Fig.3.1 shows the spin coating process.

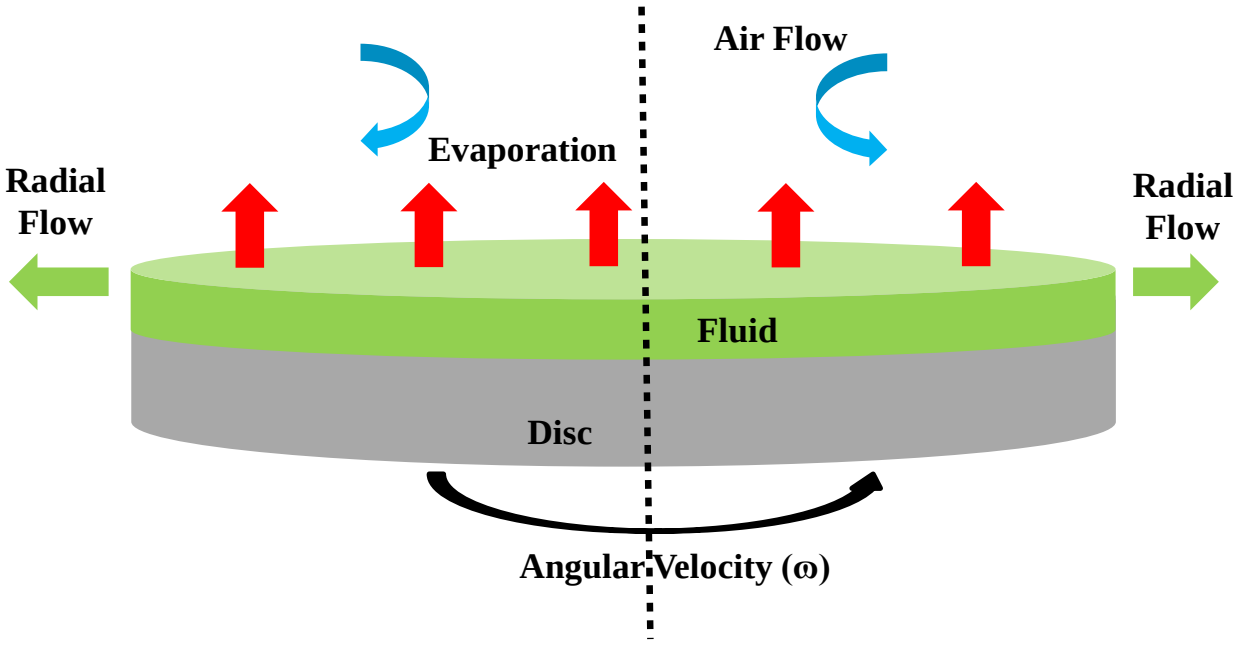

Fig.3.1 Schematic of spin coating process.

In order to model spin coating process, Emslie, Bonner, and Peck [128] made the following assumptions:

1. The fluid that is spin coated is a Newtonian fluid with a linear relationship between viscous stress and strain rate.

2. Non slip condition is present at the fluid-solid interface. This implies that the adhesive force of the fluid to the solid substrate is higher than the cohesive force present in the fluid. Therefore, the fluid velocity (v) is zero ($v = 0$) at the surface of the disc.
3. The rotating disc is assumed to be an infinite plane. This is reasonable considering that the thicknesses of the spin coated films that are in nanometers to micrometers range while the substrates generally are Si wafers with diameters of 2-12 inches.
4. Other forces such as gravitational forces or Coriolis forces are neglected.

Using cylindrical polar co-ordinates (r, θ, z) with origin at the center of rotation, z perpendicular to the plane, and the axes r and θ rotating with the plane with angular velocity ω, the viscous and centrifugal forces per unit volume are described by the following equation:

$$-\eta\left(\frac{\partial^2 v}{\partial^2 z}\right) = \rho\omega^2 r \tag{3.1}$$

where, η = absolute viscosity, ρ = fluid density, and v = velocity in the direction of r
The following flow and velocity boundary conditions are assumed: i) $v = 0$ at the surface of the disc ($z = 0$) and ii) $dv/dz = 0$ at the free surface of the liquid ($z = h$) since at the free surface, there is no shearing force. Applying the boundary conditions, continuity equation and using few integrations, the film thickness $h(t)$ at any time t is given by [128]:

$$h = \frac{h_0}{\sqrt{1 + 4Kh_0^2 t}} \tag{3.2}$$

where, h_0 is the thickness at $t = 0$ and

$$K = \frac{\rho\omega^2}{3\eta} \tag{3.3}$$

From equations 3.2 and 3.3, it can be derived that

$$h\ \alpha \sqrt{\frac{\eta}{\omega^2 t}} \tag{3.4}$$

From equation 3.4, it can be inferred that when the fluid is more viscous, or is rotated at slower speed or for short duration, a thick film is produced. However, equation 3.2 is only valid for the early stage of fluid thinning. In the later stage, after the ejection of the fluid at high speeds, thinning of the polymer film due to evaporation of the solvents becomes significant and influences the outcome of the spin coating process. Meyerhofer introduced evaporation during spin coating process [129]. He approximated that the height of the fluid h could be written as sum of the solid content (S) and the solvent (L) present in spin coated fluid, that is,

$$h = S + L \tag{3.5}$$

This implies that the concentration of solids $C(t)$ can be written as

$$C(t) = \frac{S}{(S + L)} \tag{3.6}$$

By applying continuity equation, it can be obtained that the change in the solid height as the function of time is:

$$\frac{dS}{dt} = -C(t)\frac{2\omega^2 h^3}{3\vartheta} \tag{3.7}$$

where ϑ is the kinetic viscosity ($= \eta/\rho$). Since it is the solvent that evaporates, the change in liquid height should include the evaporation term as:

$$\frac{dL}{dt} = -[1 - C(t)]\frac{2\omega^2 h^3}{3\vartheta} - e \tag{3.8}$$

where, e = evaporation rate of solvent. With various additional assumptions and describing the viscosities of the solutions as the power law function of the solute concentration, the final height achieved is calculated as [130]:

$$h_f = \left\{\frac{3C_0^3 \eta_0 e}{2(1 - C_0)\omega^2}\right\}^{1/3} \tag{3.9}$$

where C_0 and η_0 are the initial concentration and kinetic viscosity of the fluid, respectively. Thus from Equation (3.9), it can be inferred that:

$$h \propto \omega^{-2/3} \tag{3.10}$$

This dependence is accurate for the spin coating of high viscosity fluid films or at low rotational speeds for short spin times.

To summarize, in this section, some fundamental analytical calculations for the spin coating process are described. It can be observed that a basic analysis as presented here can provide an understanding of such a complex process. For simple cases, these equations can allow predicting the final film thickness exclusively based on process parameters and material properties.

3.2 Method of spin coating of polymer solutions

For spin coating, first a homogenous polymer solution is prepared. 10 %wt. 15 %wt. and 20 %wt. PLLA solutions are dissolved in DCM. 14.7 %wt. solution consisting of 2 g of FURO, 8 g of PCL, 40 ml of acetone and 20 ml of DCM is also prepared. All the solutions are heated to a temperature of 50 ºC on a hot plate for about 24 hrs to ensure complete dissolution of the polymer and the formation of a homogeneous, transparent solution. During heating the solutions are constantly stirred with a magnetic stirrer. In order to avoid evaporation of DCM and acetone, paraffin films are used to seal the lids of the bottles. The solutions are cooled to room temperature before spin-coating. All the polymer film samples studied in this project are spin coated using a WS-650 spin coater (Laurell Technologies Corporation, Pennsylvania, United States). Clean Si wafers without any pretreatment or coated with PDMS are used as carrier substrates for the experiments. The wafers are clamped to the chuck of the spin coater using vacuum. During spin coating, the chuck is accelerated in 1 sec to the final spin speed. The spin coating process is started immediately after dispensing of the solution because the solvents used in the experiments such as acetone and DCM are very fast evaporating.

3.3 Results and discussion on spin coating of polymer solutions

For the fabrication of the microcontainers a PLLA thickness of several 10s of µm is required. Similar requirements exist for the thickness of the PCL-F films for container loading. To predict the thickness using spin coating, spin curves showing the film thickness as a function of the spin speed are prepared experimentally. For this purpose, solutions of different concentrations are spin coated either on Si substrates or on PDMS coated Si substrates. The thickness of the film (h_f) is measured using a stylus profilometer and the values are fitted with a least square fit using

$$h_f = A\omega^{-2/3} + B \tag{3.11}$$

where, A and B are the fitting coefficients. The value of coefficient B represents the deviation of the final thickness from the -2/3 dependence on the angular velocity ω, as per the equation 3.9 of theory section. Thus, higher the value of B, greater is the deviation. The matlab script for the fitting is included in Appendix 1.

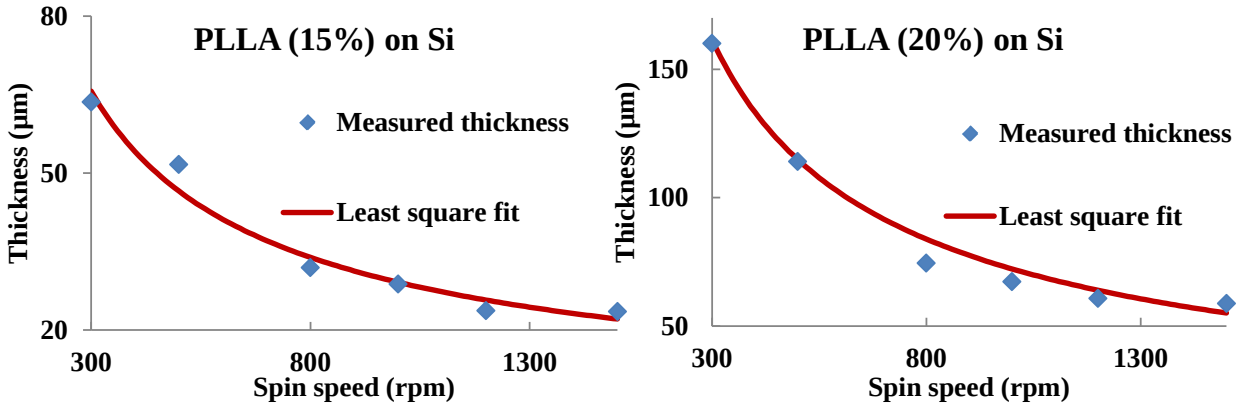

Fig.3.2 Measured and fitted thicknesses of PLLA films when PLLA solutions of 15%wt. concentration (left) and 20%wt. concentration (right) are spin coated on Si wafers.

As can be seen in the Fig.3.2 and Table.3.1, when the PLLA solution (15% wt. and 20% wt. PLLA dissolved in DCM) is directly spin coated on Si wafers, the dependence of the final film thickness h_f on the angular velocity ω is very close to -2/3 similar to equation 3.9, where the rate of evaporation plays a significant role. Since DCM evaporates really fast due to its low boiling point, it can be inferred that evaporation has to be considered in spin coating of PLLA solution even at low velocity of 500 rpm. However, when the same PLLA solution is spun on PDMS, this dependence gets changed (Fig.3.2). It could be due to the absorption of solvent DCM by PDMS layer that leads to faster removal of solvent from the solution, thereby leading to a thicker layer. When a PLLA solution with lower initial concentration (10% wt.) and hence lower initial viscosity is spin coated, higher deviation from -2/3 dependence on ω is observed (Appendix 2). Nevertheless, keeping these parameters and dependencies in mind, reproducible film thicknesses have been achieved throughout the research.

Table. 3.1 represents the values of coefficients A and B derived after fitting of measured and calculated values.

PLLA solution	Coefficiant A	Coefficient B
PLLA 15% on Si	2.9660e+03	-0.5287
PLLA 20% on Si	7.2527e+03	-3.0049
PLLA 15% on PDMS	3.1237e+03	26.3207

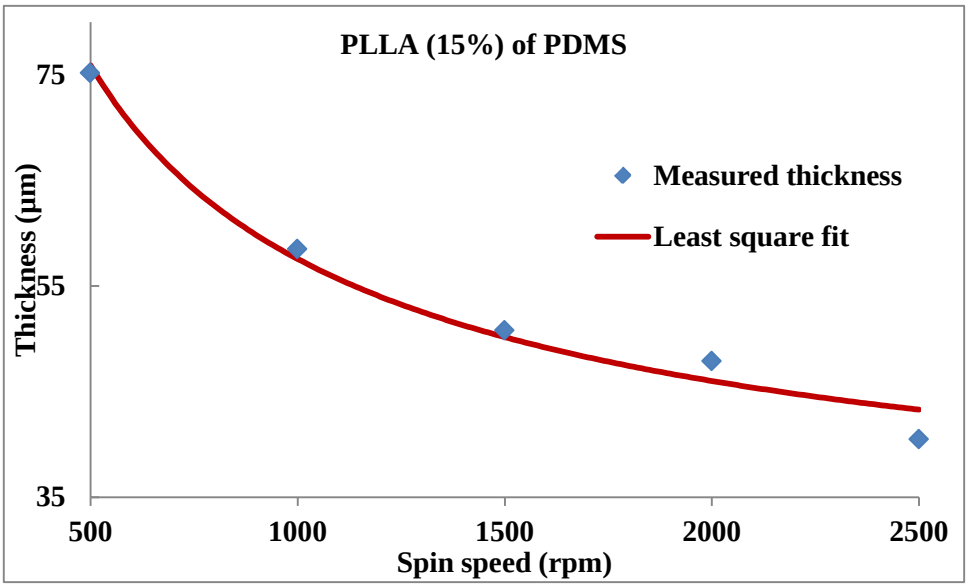

Fig.3.3 Measured and fitted thicknesses of PLLA films when PLLA solutions of 15%wt. concentration is spin coated on PDMS deposited Si wafers.

In this research, spin coating is also applied for the fabrication of drug delivery patches. The spin coating parameters such as spin speed, the annealing temperature and time, and the rate of cooling of annealed films have been investigated to achieve control on the crystallinity of drug in these patches. It has been demonstrated that the drug crystallinity and hence drug release can be controlled by tailoring the spin coating parameters.

CHAPTER 4
FABRICATION OF STAMP AND HOT EMBOSSING

CHAPTER 4

FABRICATION OF STAMP AND HOT EMBOSSING

In this chapter, first, the key process steps of hot embossing are explained. The influence of initial thickness of the polymer film, the temperature applied and the stamp design on the embossing process are discussed. The section on demolding describes the necessity of fabricating a robust stamp with required features of smooth surfaces and sidewalls and positive profiles of the protrusions, in order to decrease the demolding forces. After that, DRIE is introduced as a method of fabrication of Si master for electroplating of Ni. Two types of deep reactive etching processes are used in the project: i) continuous DRIE process and ii) multiplexed Bosch DRIE process. Later, a short summary of the process flow for the fabrication of Ni stamp is provided. Then in the results section, DRIE optimization for the preparation of the Si master is discussed. Finally, the hot embossing of the Ni stamp in PLLA is briefly described. The complete process flow for the fabrication of Ni stamp followed by hot embossing is described in paper II of chapter 8.

4.1. Theory

4.1.1 Introduction to hot embossing

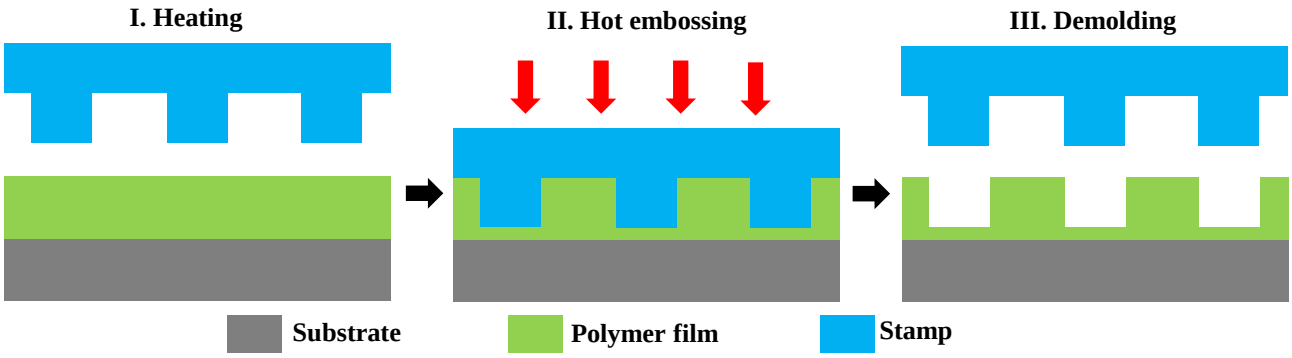

Fig.4.1 Hot embossing of a polymer film by a mold for fabricating micro/nano patterns.

Hot embossing is a viable solution for fabricating micro/nanopatterns in polymer films. The relatively expensive step of the process is fabrication of stamp/mold which is done only once. Applying this stamp, identical structures can be mass produced reproducibly. In hot embossing process, first a polymer is heated, then a mold is pressed in it and after the polymer is cooled down, the mold is seperated from the polymer producing micro/nano patterns in the polymer as shown in Fig.4.1 [131].

In detail [132], hot embossing process is divided into four major steps as depicted in Fig.4.2:
1. Heating of the embossing plates to the desired temperature above T_g of the thermoplastic polymer. This temperature should be high enough to allow the complete filling of the cavities but low enough to not alter the sample properties or lead to excess thermal stress caused by different thermal expansion of the mold and the polymer.
2. Embossing of the mold in the polymer sample while applying pressure. This pressure should be high enough to allow complete filling of the cavities in a reasonable time but low enough to not alter the sample properties or to lead to mold damages.

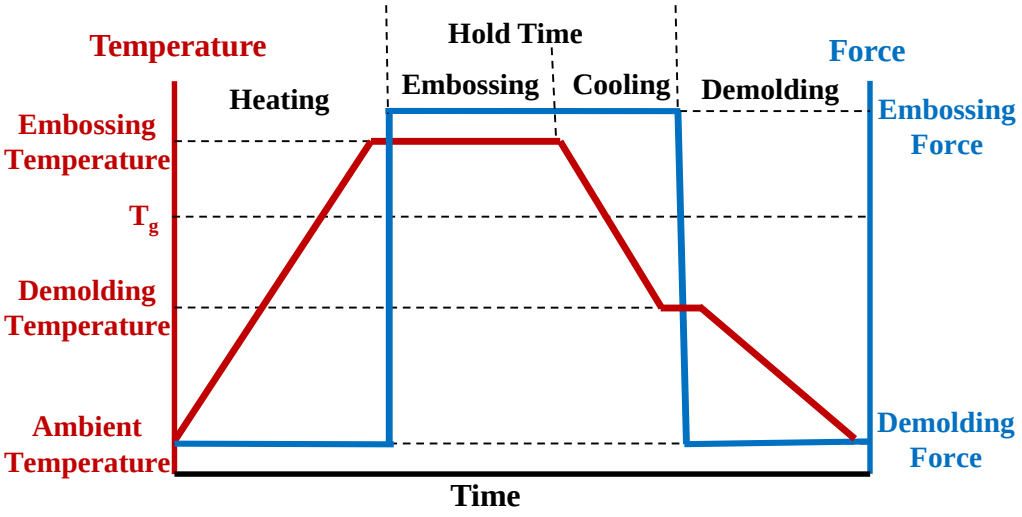

Fig.4.2 Typical behavior of the process parameters, force and molding temperature, in a hot embossing cycle

3. Cooling down of the embossing plates below the T_g of the polymer sample, while maintaining the pressure.

4. Demolding of the mold from the sample performed below the T_g of the polymer sample but preferably above the room temperature. The optimal demolding temperature resulting in the lowest demolding forces is found experimentally.

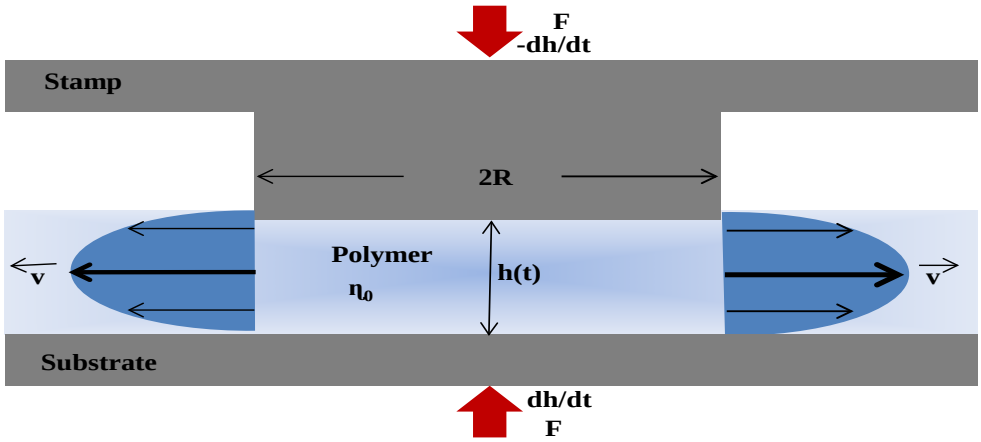

Fig.4.3 Squeeze flow in geometry similar to that encountered in hot embossing.

Hot embossing can be represented by the simple model of squeeze flow of Newtonian fluids [131, 132]. In this model, the sample substrate is stationary while the mold with protrusions of radius R and height h_f, moves vertically with the speed of dh/dt. This small vertical displacement leads to large lateral flow (v) of the polymer. The polymer is spin coated to have an initial thickness, h_0. Applying continuity, conversation of momentum for an incompressible liquid and Stefan equation, which gives the steady state solution of an incompressible, viscous fluid of viscosity η_0 between two parallel discs separated by a distance $h(t)$ (Fig.4.3), the force F can be expressed as [131-133]:

$$F = \frac{3\pi R^4 \eta_0}{2h(t)^3}\frac{dh}{dt} \tag{4.1}$$

$$\frac{1}{h(t)^2} = \frac{1}{h_0^2} + \frac{4F}{3\pi\eta_0 R^4} t \tag{4.2}$$

This model is rather simple and does not consider the more complex aspects of the process such as i) non-newtonian flow with a non-uniform shear velocity distribution, and ii) shear thinning, characterized by a decrease in the viscosity with increasing shear rate at high temperatures. However, this simple model can give many qualitative insights in the hot embossing process especially the effect of mold design, rough estimates of required temperature and pressure. etc. [131, 132]. Some of the rules for optimization of the hot embossing process that can be inferred from equations 4.1 and 4.2 are:

i) *Effect of initial film thickness*: From equation 4.2, it can be inferred that if the initial thickness of the film is high, then the embossing process time is lowered. This is because when the film is thick, the polymer can flow in the central plane of the film with less resistance from boundary friction. However, for a thick film, a thick residual layer is obtained after the demolding process.

ii) *Effect of* e*mbossing temperature*: From equation 4.2, it can be inferred that the low viscosity of the polymer can potentially lead to short embossing times. When the polymer is subjected to heat, the viscosity decreases. Therefore, the higher the molding temperature is, the lower is the viscosity and the shorter is the time required to fill the cavities. However, in some cases high molding temperature might not reduce the total processing time since it might require more time to heat the embossing plates and cool them down below the T_g of the polymer.

iii) *Effect of mold geometry*: From equation 4.1, $F \propto R^4$, which implies that if the protrusions on the stamp are very large, large forces would be needed to fill the cavities.

iv) *Residual layer*: In equation 4.1, $F \propto h^{-3}$, this means that as $h(t) \rightarrow 0$, the force required becomes extremely large. This in turn means that it is practically impossible to remove the residual layer completely.

4.1.2 Demolding and stamp design considerations

The first step in the hot embossing process is the fabrication of stamp. A robust, well-designed stamp with smooth sidewalls and surfaces is of utmost importance in embossing. As mentioned in section 4.1.1, the stamp protrusions should not be too wide to avoid large lateral polymer flow and unacceptable long processing times. Moreover, the stamp cavities and protrusions should be distributed homogeneously over the entire stamp to reduce variations in the filling of cavities and the thickness of the remaining residual layer [131]. The stamp should have smooth surfaces and sidewalls to minimize frictional forces between stamp and polymer. There should not be any undercuts or overhanging structures that can result in the interlocking of polymer and stamp. The stamp should preferably have positive sidewalls, again to reduce interlocking. Typically, an anti-adhesion layer is deposited on the stamp to reduce the adhesion between the stamp and the molded polymer. The above mentioned features of a stamp help in minimizing the demolding forces to produce a defect-free molded structure with good replication fidelity and high yield. Another aspect that can be considered during stamp fabrication is the stamp material itself. If possible, the stamp material can be chosen such that the difference between the thermal coefficient of expansion for stamp and polymer materials can be reduced. This in turn reduces the formation of large compressive stresses during cooling [134]. Therefore, stamps fabricated in polymers such as PDMS

or perfluoropolyether (PFPE) can be beneficial in avoiding the fracture or deformation of molded parts [134, 135]. However, these stamps are not very durable and in long term, can be very costly. Hence, in next few sections, DRIE which is one of the most important processes in the fabrication of stamps in hard materials like Si and Ni is presented.

4.1.3 Deep reactive ion etching technology (DRIE)

DRIE is a standard anisotropic Si etching technology [136, 137]. A DRIE system consists of low frequency inductively coupled plasma (ICP) electronics, load lock, carousel wafer loading unit and a process chamber. The plasma is generated by an inductive coil assembly coupled at 13.56 MHz via the matching unit, in an aluminum chamber. A high density plasma is produced that can provide high etch rates with negligible substrate damage. The bottom platen electrode, on which the sample wafer is placed, is independently biased at 13.56 MHz. Process gas is introduced in the chamber through a small inlet near the upper electrode assembly. The wafer platen is maintained at a desired temperature using a chiller. Plasma is produced by the oscillating electric field of the upper coil by ionizing the gas molecules in the chamber. The electrons are accelerated in this field. Some of these electrons are lost to the chamber walls while some of them accumulate on the lower platen. Since the plasma is mainly positive consisting of positive ions stripped of their electrons, a high potential difference is achieved between the positive plasma and the negative platen. Hence, the ions start accelerating and bombarding the sample placed on the lower platen. The ions collide with the sample and some of them remove material from the sample by physical sputtering due to their high kinetic energy. Other ions react with the sample producing volatile by-products, thereby etching it chemically. The schematic of the physical and vertically directed chemical etching in a DRIE chamber is illustrated in Fig.4.4.

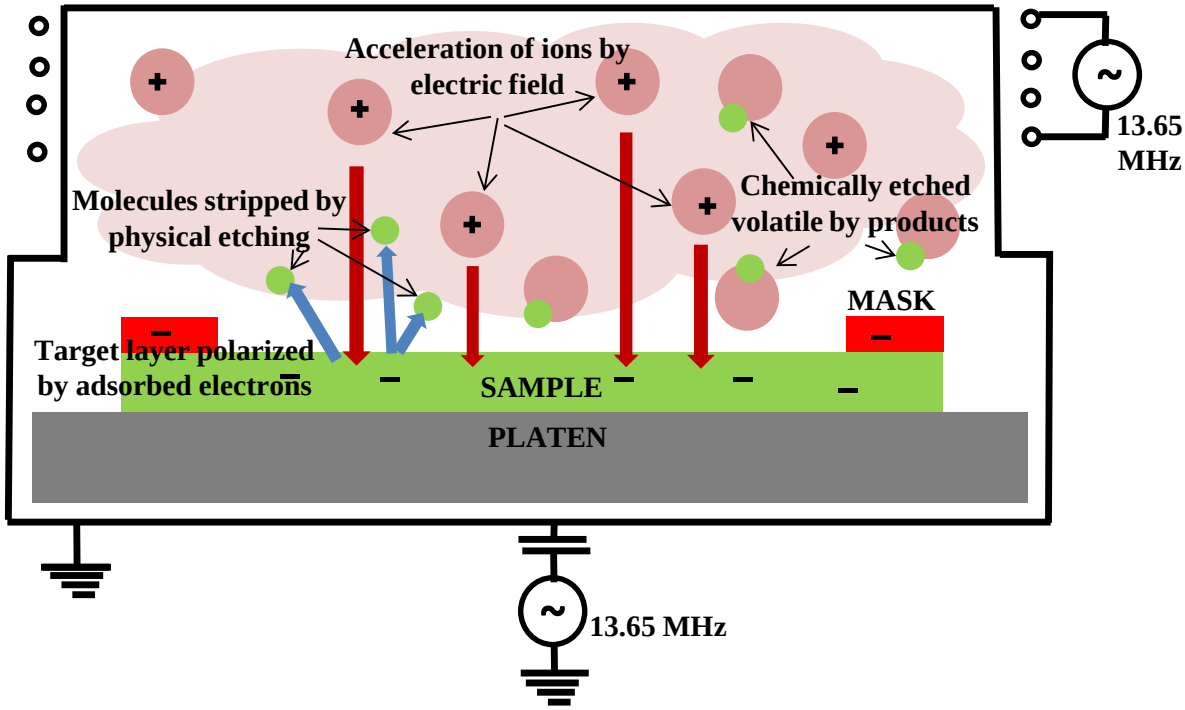

Fig.4.4 Schematic of the physical and vertically directed chemical etching in a DRIE chamber.

DRIE is a complex process that can be tailored by many process parameters such as the type of gases, gas flow ratios, platen power, coil power or chamber pressure. DRIE is able to produce high-aspect-ratio (HAR) features in Si for fabrication of vias for interconnects, for MEMS applications and for DEEMO (dry etching, electroplating and molding) to produce Si masters for electroplating Ni molds. DRIE is based on two processes either happening simultaneously or sequentially: i) ionic bombardment to etch the exposed surface, and ii) sidewall passivation by an inhibitor preventing lateral sidewall etching. With the control of the etching and passivation processes, deep vertical trenches can be fabricated. There are different types of DRIE processes. The three most commonly used approaches are: i) cryogenic continuous process [138], ii) continuous process at room temperature [139], and the most commonly used of all iii) Bosch time multiplexed process [138]. In this project, continuous process at near room temperatures (10 °C) and Bosch process are explored.

4.1.3.1 Continuous DRIE process

In the continuous DRIE process, SF_6 and O_2 are injected into the chamber. Fluorine, SF_x and O radicals are produces in the plasma and diffuse towards the substrate. Fluorine reacts with Si spontaneously to produce volatile SiF_x molecules. SiF_4 is the main by-product of such exothermal chemical reaction that desorbs from the Si surface. At the same time, O radicals can interact with the SiF_x to deposit a protective layer of siliconoxyhalide ($Si_xO_yF_z$) passivation layer on the sidewalls to avoid lateral etching. At the trench bottom, Si is etched by the incident ion bombardment. The addition of O_2 (<5%) to the SF_6 gas flow initially significantly increases the F-radical concentration in the plasma. However, after a certain O_2 partial pressure is reached, the F-radical concentration starts decreasing due to dilution. Consequently, the Si etch rate increases initially due to a higher F-radical density and then in the later stages decreases because of the growing $Si_xO_yF_z$ film and F-radical dilution [139]. If a cavity is etched with a process where the etching is reduced and passivation is increased controllably, one can expect to obtain a positive profile of the sidewalls. Related to the above discussion, it can be inferred that the ratio of O_2 gas flow to the total gas flow SF_6+O_2 can be used to control the sidewall angle in the trenches [140]. However, it is a challenge to control the passivation in this continuous process and maintain the balance between lateral and vertical etch rates. Table 4.1 shows the effect of increase in certain etching parameters on the continuous DRIE process features such as undercut, etch rate, slope and roughness.

Table 4.1 Effect of increase in etching parameters on the continuous DRIE process [139]

	Undercut	Etch rate	Slope	Bowing	Roughness
O_2 flow	–	~	++	–	++
Platen bias	++	++	–	+	–
Pressure	+	~	–	–	+
Temperature	++	~	~	++	–

++: increase,
–: decrease,
+: slight increase,
~: almost constant.

4.1.3.2 Multiplexed Bosch DRIE process

The second process that is explored is the multiplexed Bosch process. In this process generally SF_6 and C_4H_8 gases are used for short durations in a sequential manner of etch and passivation cycles. In the etch cycle, SF_6 reacts with Si to form volatile SiF_x gas, thereby, chemically etching Si. In the passivation cycle C_4F_8 is introduced in the chamber to deposit a thin polymeric passivation layer (C_xF_y) obtained through the adsorption of C and CF_x radicals during ion bombardment. This passivation layer is removed from the horizontal surfaces in the subsequent etch cycle through ion bombardment with fluorine radicals. However, the sidewall passivation remains intact, leading to overall anisotropic etch of Si [141]. These alternating cycles create periodic structures on the sidewalls called scallops (Fig. 4.5). Optimal etching can be achieved by the control of etch and passivation cycles times and other process variables that control gas species fluxes in the chamber, summarized in Table 4.2.

Table 4.2 List of important process parameters that affect etching of Si during DRIE [142]

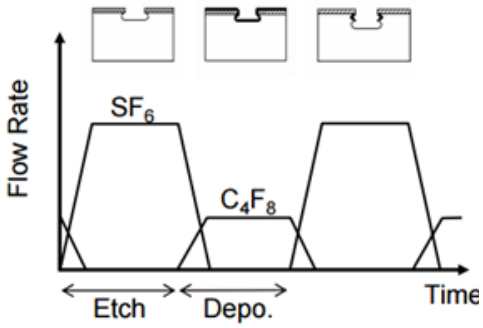

Reactants Supply	Plasma Power Conditions	Etch/Passivation Adjustment
• SF_6 flow rate • C_4F_8 flow rates	• Electrode power during etching • Coil power • Electrode power during passivation • APC positions	• Etching cycle • Passivation cycle

Fig. 4.5 Graph showing the gas flow cycles during plasma etching. Note the overlaps caused by the finite time response of the mass flow controllers [ref].

In order to control the sidewall profile during the fabrication of the Si master for electroplating of the Ni stamp, there are some parameters that can be varied as shown in Table 4.3. In this project sidewalls with a positive slope are achieved by controlling etch and passivation cycles time ratios.

Table 4.3 Summary of process trends [143]

Trends for Controlling process results	Etch rate	Profile (↑ negative) (↓ positive)	Selectivity	Grass	Breakdown	Sidewall Roughness
Etch gas increase	↑↑	↑↑	↑	↓	↑	↑
Deposition gas increase	↓↔	↔	↑	↑	↓↔	↓
Etch:Dep time ratio increase	↑	↑	↑↔	↓	↑↔	↑
Pressure increase	↑↑	↑	↑	↓↔	↑	↑
Deposition Coil Power increase	↓↔	↓↔	↑↔	↑	↓↔	↓
Etch Coil Power increase	↑	↑	↑	↓	↑	↑

4.2 Methods

In this section the basic stamp design with the description of the unit feature is provided. After that, a short summary of the process flow for the fabrication of the Si master, electroplating of the Ni stamp and hot embossing in the PLLA film using the Ni stamp is presented.

4.2.1. Stamp design

The stamp contains 16 square arrays with 20 x 20 individual stamp units. Each stamp unit corresponds to one microcontainer and thus the stamp design enables fabrication of 6400 devices in a single embossing run. Fig.4.6 shows an individual stamp unit. It consists of two parts, an inner disc and an outer ring structure and there are three important parameters: 1) The diameter of the inner disk, which translates into the microcontainer reservoir, 2) the space between the inner disc and the outer ring that corresponds to the wall of the container and 3) the width of the outer ring structure, which transforms into the separation trench between the microcontainer and the surrounding polymer film.

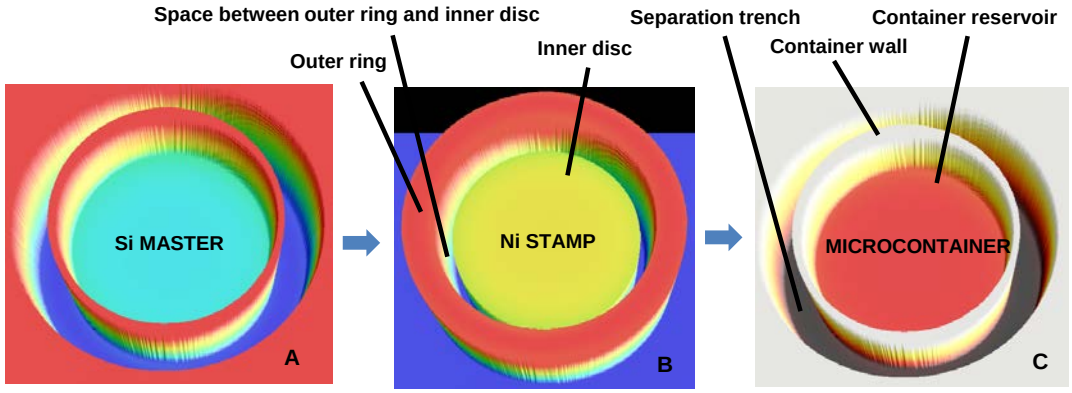

Fig.4.6 Various features of the stamp and microcontainers and subsequent translation of the Si master (A) into a Ni stamp (B) and then further into biopolymer microcontainers (C) with the inner reservoir, walls around it and the separation trench between the container and the surrounding polymer film

4.2.2. Fabrication of Si master, Ni stamp and hot embossing of PLLA films

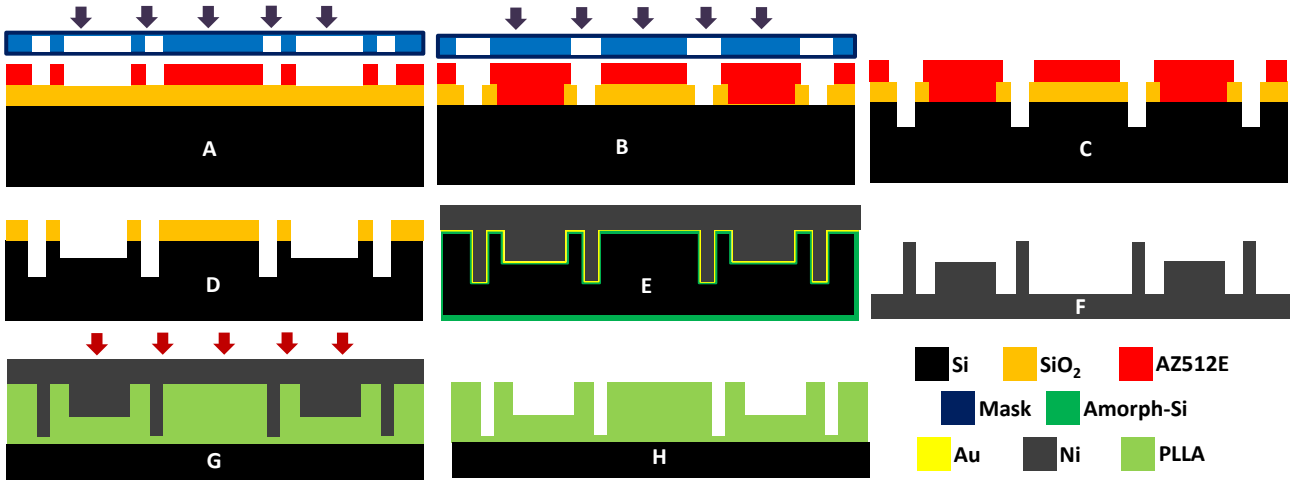

Fig.4.7 Process flow for the fabrication of Si master, Ni stamp and polymer replica A. Exposure of AZ5214E photoresist spin coated on a thermally oxidized Si wafer, using base mask and development, B. Exposure of second layer of AZ5214E spin coated after oxide etch with AOE, using separation mask and development, C. First DRIE etch, D. Second DRIE etch after AZ5214E stripping, E. Au deposition on amorphous-Si coated Si master and Ni electroplating, F. Wet KOH Si etch to release the Ni stamp and

deposition of fluorocarbon using MVD, G. Embossing of Ni stamp in spin coated PLLA film, H. Demolding to finish replication of microcontainers in PLLA.

The complete process flow for the fabrication of the Si master and the electroplating of the Ni stamp is described in paper II. The process can be summarized as two steps of lithography performed using two different masks followed by two steps of deep reactive ion etching. The first mask is called base mask as it defines the base of the containers after the first RIE and the second mask is called separation mask as it defines the separation distance. The process starts with the spin coating of photoresist on a thermally oxidized Si wafer followed by the exposure of AZ5214E photoresist using the first base mask and development (Fig.4.7.A).After that the pattern is transferred to silicon dioxide using advanced oxide etching (AOE). Then the first AZ5214E resist layer is stripped. Subsequently, spin coating of second AZ5214E photoresist layer, exposure of AZ5214E using separation mask and development are carried out (Fig.4.7.B). Later, the first Bosch DRIE etch is performed (Fig.4.7.C). The resist is stripped and the patterned oxide layer is exposed. This oxide layer becomes the etch mask for the second DRIE etch. After the second etch, the Si master is fabricated (Fig.4.7.D). A new sacrificial oxide layer is grown and subsequently etched to obtain smoother sidewalls. Once the sidewalls are smooth enough, a sacrificial layer of amorphous Si is deposited. A Au seed layer is sputtered on the Si master and Ni is electroplated (Fig.4.7.E). Si is wet etched in KOH to release the Ni stamp (Fig.4.7.F). Fluorocarbon (FC) is then coated on this stamp using molecular vapor deposition (MVD). The stamp is then embossed in spin coated PLLA film (Fig.4.7.G) and demolding is performed resulting in the replication of the microcontainers in PLLA (Fig.4.7.H).

4.3. Results and discussion

This section illustrates some of the results obtained during the optimization of DRIE process for the fabrication of Ni stamp. The first part of this section describes the details of the unsuccessful attempts of application of the continuous DRIE process for fabricating the Si master. The second part briefly summarizes the successful attempt of the application of the Bosch process for the fabrication of the Si master and the Ni stamp. Finally, a short discussion on the hot embossing of PLLA films is presented.

4.3.1 Fabrication of Si master with continuous DRIE process

A continuous DRIE etch at 10 °C was initially chosen to fabricate HAR structures in Si. The process parameters used are summarized in Table 4.4.

Table 4.4 Continuous DRIE process parameters used in the SPTS Pegasus DRIE tool. The process is run at 10°C

Gas Flow	Pressure	Coil Power	Platen Power
SF6/O2/Ar = 180/160/100 sccm	246 → 91 mT	2800 W	170 → 215 W

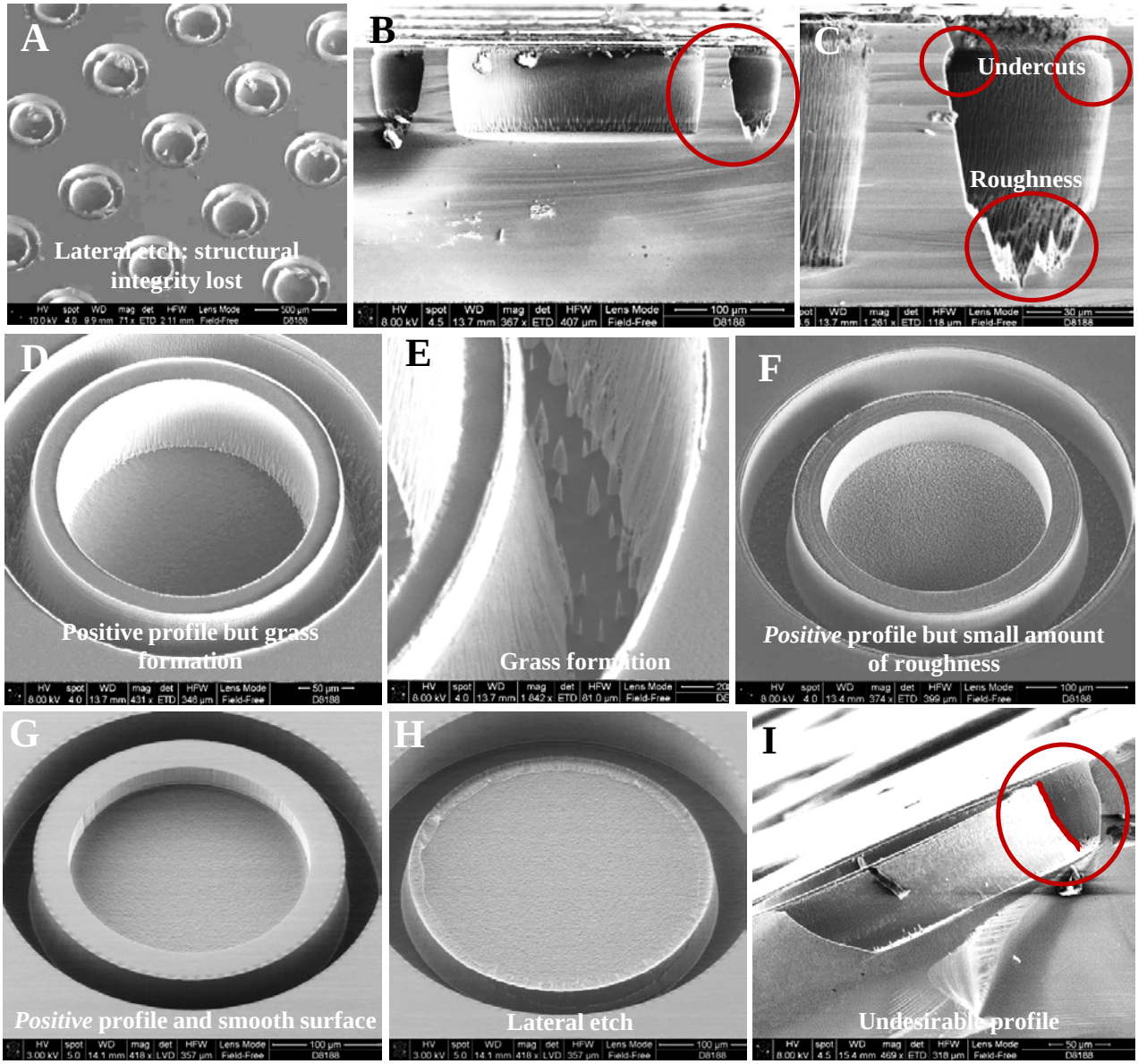

Fig.4.8. Summary of application of continuous DRIE for the fabrication of Si master for Ni electroplating.

Based on the information in Table 4.4, the process is run with variable pressure in an attempt to achieve sidewalls with a positive slope. At the start of the process, the pressure is as high as machine tolerances allow at 230 mTorr and is then linearly decreased to 90 mTorr for the duration of the process. The coil power is kept constant at 2800 W while the platen power is increased linearly from 170-215 W. The three gases that are allowed in the chamber are SF_6, O_2 and Ar. As discussed above in section 4.1.3.1, SF_6 is the main etch gas. O_2 gas initially promotes the etching by increasing the concentration of F radicals. At a later stage O2 contributes to the formation of a passivation layer while Ar ions are basically used for physical bombardment. When gas flows are used as described in Table 4.3.1, 10 µm wide walls on the wafer lose their structural integrity due to high lateral etch (Fig.4.8.A). Besides, high surface roughness and undercuts are observed (Fig. 4.8.B and C). Therefore, the ratio of O_2 to SF_6 is modified to achieve the desired sidewall profile. In the next few experiments, the SF_6 gas flow is lowered to 100 sccm while maintaining the oxygen

flow at 160 sccm. With this process, structural integrity is preserved, however, very high surface roughness is observed at sidewalls and the bottom of the trenches (Fig. 4.8.D). Thus to avoid excessive lateral etching and excessive surface roughness, the SF_6 flow is increased to 120 sccm and the O_2 flow is lowered to 90 sccm. With this process the roughness is reduced and the structural integrity is improved, but some lateral etch can still be observed (Fig. 4.8.E and F). To remove the remaining roughness, an isotropic Si wet etch is performed. This produces smoother surfaces (Fig. 4.8.G), however the already thinned down 10 µm walls are completely lost (Fig. 4.8.H). Moreover the cross section micrograph shows that the profile is not as desired after the two DRIE cycles for 2-leveled microcontainer structures (Fig. 4.8.I). Hence, the continuous DRIE etch is disregarded and a more standardized process with improved control of the outcome is desired.

4.3.2 Fabrication of Si master with Bosch DRIE process

Finally, a standard Bosch process is chosen and optimized. Some of the standard processes developed by the manufacturers of the equipment at DTU Danchip are available to the users. The most suitable method called *Process D* is chosen for the initial experiments (Table.4.5). Without

Table 4.5 Standard *Process D* parameters developed by the manufacturers of STS Pegasus DRIE tool

Process D recipe

Main etch (D->E)	**Etch**	**Dep**
Gas flow (sccm)	SF_6 275 O_2 5	C_4F_8 150
Cycle time (secs)	2.4	2.0
Pressure (mtorr)	26	20
Coil power (W)	2500	2000
Platen power (W)	35	0
Cycles	110 (process time 08:04)	
Common	Temperature 0 degs, HBC 10 torr, Long funnel, with baffle & 100 mm spacers	

further optimization the process results in formation of tall grass-like structures (Fig.4.9.A). To reduce the grass formation, the duration of the etch cycle is increased to 4 sec. Nagarajan *et al.* suggested that if the Bosch process is combined with an isotropic etch, positive sidewall profiles can be produced [144]. Thus, after the Bosch process run, an isotropic etch is performed. This not only fails to give completely smooth sidewalls but also results in the loss of structural integrity of 10 µm wide walls (Fig.4.9.B and C). Due to the unpredictable nature of Si isotropic etch and hence less control on the process, it is completely avoided in future experiments. After many experiments on Si test structures, the optimized parameters for process D are obtained. The detailed description of the process optimization is available in paper II of chapter 8. Structurally intact HAR microstructures with minimal undercut and low surface roughness can be obtained by the combination of the optimized Bosch process and multiple oxide layer growth and etching steps (Fig.4.9.D). After the optimization of Bosch process several other Si masters with HAR structures have successfully been fabricated (Fig. 4.9.I and J).

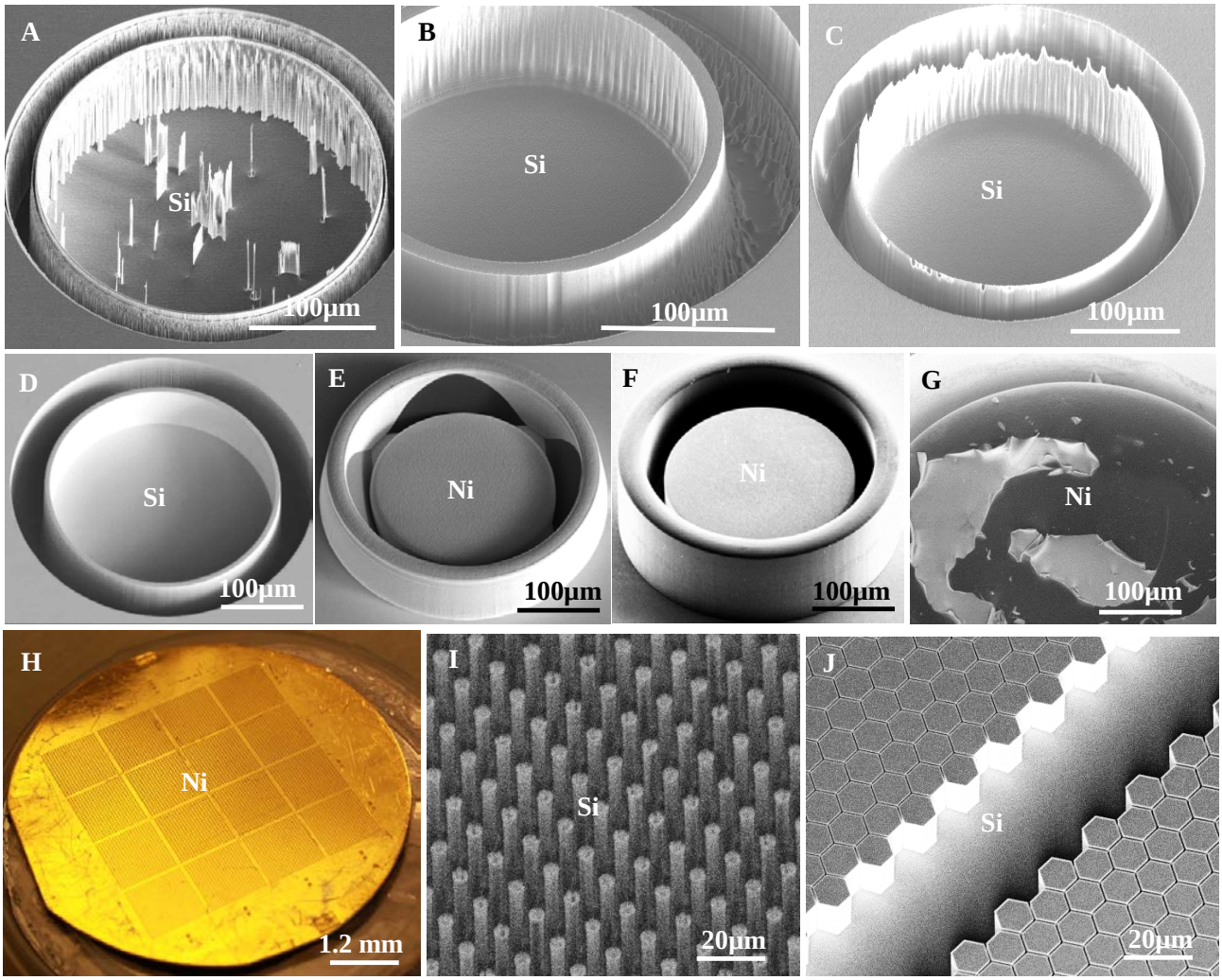

Fig. 4.9 SEM micrograph of: A. Fabrication of Si master using standard *process D*, B. Fabrication of Si master using standard *process D* plus isotropic etch, C. Laterally etched walls of Si master after isotropic etch, D. Successful fabrication of Si master, E. <111> etch stop during KOH etching of Si master, F. Unit feature on the successfully fabricated Ni stamp with smooth walls and surfaces and positive profile, G. Peeling of NiV seed layer after cleaning of stamp in DCM; H. Photograph of successfully fabricated Ni stamp; SEM micrograph of: I. Pillars and J. Hexagonal structures etched in Si using the optimized process.

4.3.3 Ni stamp fabrication

Here, the Ni stamp fabrication is briefly described. Details on the fabrication process are included in paper II of chapter 8. First, the Si master is coated with Au and applied as mold for Ni electroplating. After electroplating, is the Si is etched using KOH. However, during this process the etching stops at the <111> Si plane producing distinct features on the four sides of the Ni stamp features (Fig.4.9.E).To avoid this, amorphous Si is deposited on the Si master before coating with Au for electroplating. With this sacrificial amorphous Si layer, all the Si is removed in the KOH. Hence, a robust two-leveled HAR Ni stamp is produced with all the required properties for embossing such as smooth surfaces and sidewalls, slightly positive sidewall profile and negligible undercuts (Fig.4.9.F and H). All these features reduce the frictional forces during demolding of the stamp. A fluorocarbon anti-stiction coating is deposited on the Ni stamps to lower the adhesion forces. It is worth mentioning here that for some stamps NiV has been used as the seed layer for Ni

electroplating. For this material there is a high risk of oxidation, leading to defects in the stamp. Moreover, if strong organic solvents like DCM are used for cleaning the stamp after embossing, it is observed that the NiV layer peels off (Fig.4.9.G). Hence, a Cr/Au layer is recommended as seed layer for Ni electroplating. The transition to NiV was initially made due to the assumption that the FC antistiction layer deposited in MVD is not able to attach to Au. It was realized that this assumption was irrelevant as the topmost layer exposed in the Ni stamp is not Au but Cr.

4.3.4. Hot embossing of PLLA films

The Ni stamp fabricated as described above is used to emboss the PLLA film at 90 °C for 15 min at a pressure of 1.9 MPa. The demolding is performed at 50 °C. A long process time of 15 minutes is chosen because the embossing temperature is only 30 °C above the T_g of PLLA. This implies that the viscosity of PLLA is relatively high, the polymer fluid flow is slow and hence longer time is needed to completely fill the cavities of the mold. However, the relatively low embossing temperature of 90 °C and a demolding temperature of 50 °C are well suited for reducing the thermal stress developed due to the difference in contraction of Ni and polymer during cooling. Thus the combination of the robust Ni stamp with a smooth surface, the anti-stiction layer and the small difference between embossing/demolding temperatures leads to low frictional forces, low adhesion forces and low thermal stress, overall resulting in low demolding forces. This enables fabrication of HAR (>9) structures with good replication fidelity and yield. Details on the embossing process are included in paper II of chapter 8.

CHAPTER 5
PUNCHING

CHAPTER 5
PUNCHING

In this chapter, the concepts of punching as a method for the fabrication and loading of microcontainers are introduced. The chapter includes a short description of mechanical punching which has been the first attempt of obtaining 3D discrete microcontainers. The idea behind this process is to fabricate reservoirs in a polymer film using hot embossing. Then the reservoirs can be filled with drug powder. After that different polymer layers such as pH-sensitive Eudragit layers can be deposited using spray coating like pH-sensitive Eudragit layer. Finally, the filled polymer reservoirs with the functional coatings are punched out using a single step mechanical punching process. This process served as inspiration for the development of the hot punching process which is a combination of hot embossing and mechanical punching. The basic concepts of hot punching that are applied for the fabrication and loading of microcontainers are explained in this chapter, both from a theoretical perspective and with an overview of the experimental results. Mechanical punching is described in detail in paper I, the hot punching in paper III, and the loading in paper IV, V and VII of chapter 8.

5.1. Theory

In this section, some theoretical aspects of mechanical punching and hot punching for the fabrication and loading of microcontainers are presented. The total force that is to be applied during the mechanical punching of polymer film is described. The expression for the required polymer film thickness for disruption of the residual layer during hot punching is derived. Furthermore, the combined effect of work of adhesion and total contact area between the punched polymer and the mold, on the likelihood of punched polymer to get attached to the mold or remain on its substrate is explained.

5.1.1 Mechanical Punching

Mechanical punching is generally used to produce holes in metallic sheets. In punching, the sheet is positioned between the punch and the die. The punch moves downward and plunges into the die. The edges of the punch and the die move past each other in parallel, thereby cutting the sheet (Fig.5.1). Thus, the punching process has three phases: i) when the punch touches the sheet, the sheet is deformed, ii) then the punch penetrates the sheet and the sample is cut, and finally iii) the shear stress within the material is high enough to fracture the sheet along the contour of the cut. The cut-out piece of the sheet is ejected downwards using a plunger [145]

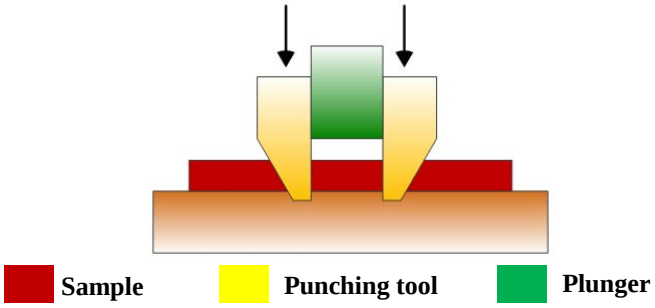

Fig.5.1 Schematic of mechanical punching of polymer as applied in this project.

The total punching force F is given by [146]:

$$F = L * t_s * UTS * MM \quad (5.1)$$

L = Punch perimeter = $2\pi R$, R being the radius of the punching tool, t_s = thickness of the sheet, UTS = ultimate tensile strength of the sheet to be punched, MM = material multiplier for the sheet material which generally ranges from 0.5 for soft Al to 1.4 for hard steel [146].

5.1.2 Hot Punching

Hot punching is a combination of hot embossing and mechanical punching. Hot punching proceeds in three phases: i) the stamp achieves conformal contact with the substrate spatially confining the polymer to be punched, ii) the polymer is cut by the highest protrusion on the stamp, and finally iii) the tensile stress within the polymer becomes high enough to rupture the film along the contour of the cut. Similar to hot embossing, the polymer to be punched is heated above T_g to facilitate flow of the material.

The most important difference between hot embossing and hot punching is that hot punching leads to penetration/disruption of the residual layer which is almost impossible to achieve in hot embossing. This is obtained by allowing the stamp to form complete conformal contact with the substrate on which the polymer film is spin coated. This conformal contact is obtained in two ways: i) with a deformable stamp such as a stamp fabricated in PDMS or other soft polymer (Fig.5.2.A) [36-38] or ii) with a deformable substrate (Fig.5.2.B) [147]. One way to obtain a deformable substrate is deposition of an elastic layer such as PDMS on a Si wafer before spin coating of the polymer to be punched.

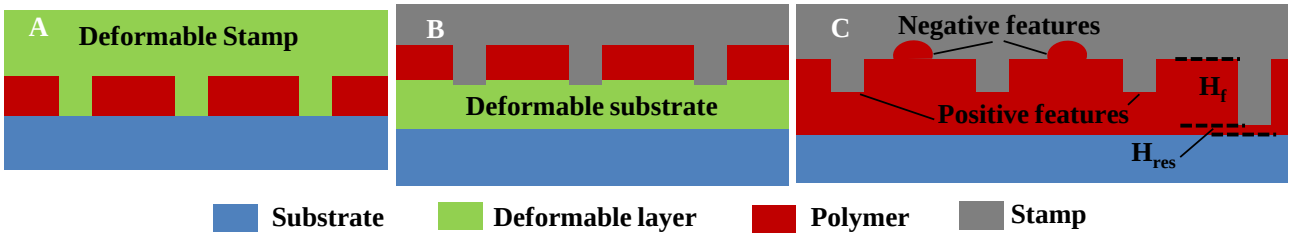

Fig.5.2 Conformal contact obtained by: A. a deformable stamp or B. a deformable substrate. C. Calculation of required polymer thickness to completely fill effective volume (V_{fill}) during the hot embossing process. H_f is the distance between the most elevated structure of the mold, and the mold baseline. The rectangles are positive structures while the semicircles are negative structure. H_{res} is the residual layer remaining after embossing.

5.1.3 Calculation of required polymer film thickness

In hot embossing, the total amount of polymer volume (V_{fill}) that is required to fill the cavities in the stamp can be calculated assuming that the volume of the polymer is constant [131]. Fig.5.2.C is the pictorial representation of a typical stamp. If the highest elevated feature on the stamp has a height, H_f, the total surface area to be filled on the stamp is A, the volume of a negative feature is V_{neg} and the volume of a positive feature is V_{pos}.

$$V_{fill} = AH_f + \sum V_{neg} - \sum V_{pos} \quad (5.2)$$

If the volume of the residual layer with thickness H_{res} is taken into account, then the volume V_0 of the initial polymer layer is:

$$V_0 = AH_{res} + V_{fill} \quad (5.3)$$

This implies that the initial thickness, H_o of the polymer that has to be spin coated to achieve complete filling of the mold is:

$$H_0 = H_{res} + \frac{V_{fill}}{A} \tag{5.4}$$

In hot punching, the thickness of the residual layer is assumed to be H_{res} = 0. This means that H_0 can be derived by the total volume of the cavities. To be able to successfully disrupt the residual layer, the thickness of the spin coated film should be slightly lower than H_0. In that case polymer fluid can be completely confined in cavities of the mold and the highest protrusions of the stamp can achieve conformal contact with the substrate below the polymer.

5.1.4. Adhesion during demolding

Once the hot punching is performed and the polymer microstructures are punched out of the surrounding polymer film, two situations can occur during demolding: i) the punched polymer remains inside the mold, or ii) the polymer stays on the underlying substrate. This behavior of the punched polymer is dictated by the work of adhesion of polymer and mold compared to the work of adhesion of polymer and substrate [148]. The work of adhesion is described as the increase of Gibbs free energy per unit area when an interface is formed between two individual surfaces. This work of adhesion is the reversible of the work per unit area required to separate two surfaces that adhere to each other [149]. The work of adhesion is basically due to the attractive Van der Waals forces [149]. If the total contact surface area between polymer and mold is A_{pm} and the work of adhesion at the polymer-mold interface is W_{pm}, then the total adhesion energy between the polymer and mold is $A_{pm}W_{pm}$. W_{pm} can be calculated by the Young-Dupré equation [150]:

$$W_{pm} = \gamma_p + \gamma_m - \gamma_{pm} \tag{5.5}$$

where γ_p and γ_m are the surface energies of polymer and mold, respectively, and γ_{pm} is the interfacial energy between the polymer and mold generally described with the unit mJ/m^2. The interfacial energy γ_{pm} is approximately

$$\gamma_{pm} = \left(\gamma_p^{1/2} - \gamma_m^{1/2}\right)^2 \tag{5.6}$$

Similarly, the total adhesion energy between the polymer and the substrate is the product of total contact surface area of polymer to substrate, A_{ps} and the work of adhesion between the polymer-substrate interface, W_{ps} where

$$W_{ps} = \gamma_p + \gamma_s - \gamma_{ps} \tag{5.7}$$

Where γ_p and γ_s are the surface energies of polymer and substrate, respectively, and γ_{ps} is the interfacial energy between the polymer and substrate which can be calculated from γ_p and γ_s as in equation 5.6. When

$$A_{ps}W_{ps} > A_{pm}W_{pm} \tag{5.8}$$

The punched out microstructures are obtained as 3D discrete structures on the substrate. Otherwise, the punched out structures remain in the mold. This criterion has been used for the fabrication and loading of microcontainers in this research. From equation 5.8, it could be inferred that the process outcome can be modified by changing either the work of adhesion (W_{pm} and W_{ps}) or the contact surface areas (A_{pm} and A_{ps}). The work of adhesion for various surfaces is lowered by depositing antistiction coatings with low surface energy such as a fluorocarbon layer [151]. The adhesion can

also be increased through an increase in the surface energy by surface treatment in UVO/oxygen plasma [72-74].The contact surface area can be modified by controlling the filling of the mold cavity volume e.g. by reducing the initial thickness of the polymer. For example, during the fabrication of microcontainers, the thickness of polymer is chosen so that the cavities defining the walls of the container are completely filled. However the deeper cavities defining the distance between two microcontainers are not completely filled. This reduces the total contact area between the polymer and the mold, thereby helping the polymer to remain on its substrate (*process A* of paper III in chapter 8).Though it is more difficult and costly, and the contact surface area can also be modified by changing the aspect ratios of the protrusions of the mold. The higher is the aspect ratio of the protrusions on the mold, the higher is the tendency of the punched polymer to remain in the mold cavities [152].

5.2 Methods

In this section, the process flows for mechanical punching and hot punching are briefly described. In this project, hot punching has been applied in two ways: i) for the fabrication of arrays of discrete 3D microstructures such as microcontainers in various materials, and ii) for the loading of reservoir-based microstructures for oral drug delivery with various kinds of polymer matrices. The detailed process descriptions can be found in paper I of chapter 8 for mechanical punching, paper III and IV for hot punching and paper V and VII for drug loading.

5.2.1 Mechanical Punching

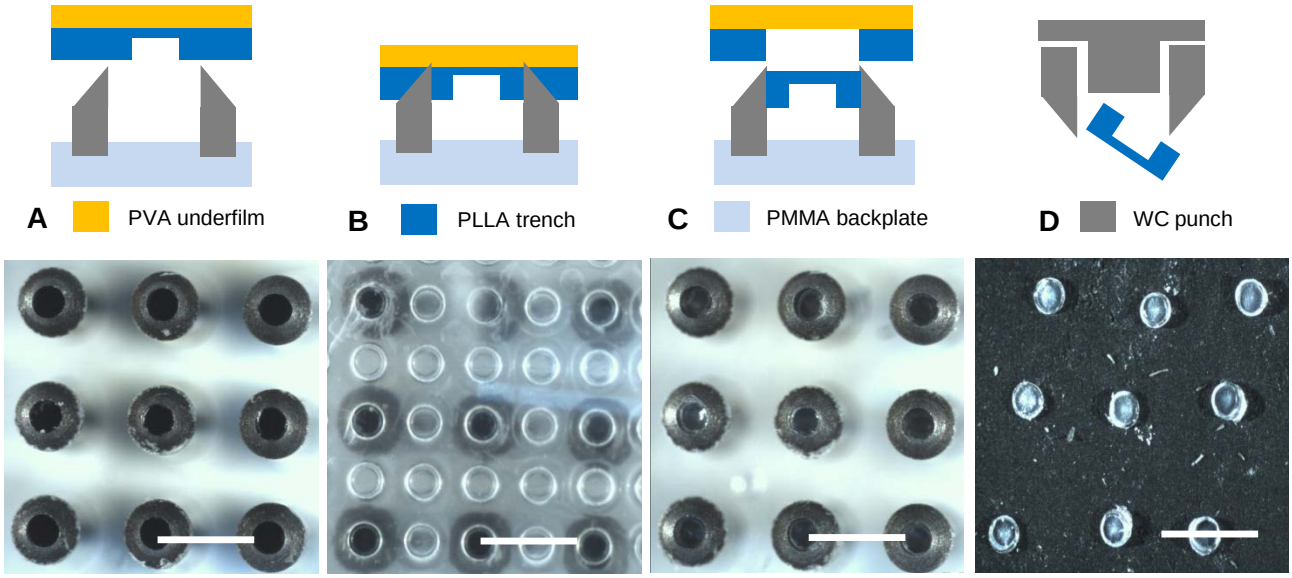

Fig.5.3 Mechanical punching process flow and corresponding optical images: A. Array of 3x3 punches, B. Alignment of PLLA trenches with punches array, C. Punching of PLLA film, D. Released microcontainers. (Scale bar: 1mm)

In this process a Si stamp is used for the fabrication of reservoirs in PLLA films. Afterwards a microreservoir on these films is aligned to a mechanical punch and the area around the reservoir is punched to give 3D discrete microcontainer. The process of producing reservoirs in the film starts with the fabrication of Si stamp. The stamp is obtained by using DRIE and photolithography. A thin fluorocarbon (FC) film is deposited on top of the Si stamp by plasma polymerization. The Si stamp

is embossed in a spin coated PLLA film at 90 ºC with a pressure of 1.9MPa for 15mins. The hot plates of the embossing equipment are then cooled down to 50 ºC, the PLLA sample and Si stamp are demolded, and a PLLA film with reservoirs is obtained. To punch this film, it is first peeled from the Si carrier wafer and mounted on a PMMA backplate with a soft polyvinyl alcohol (PVA) underlayer (Fig.5.3.A). Then, an array of 3X3 punches is aligned using the optical microscope (Fig.5.3.B). A fixed weight is placed on the stack to punch out the containers. After the weight is removed the punched parts are retained in the punching tool leaving behind through-holes in the PLLA film (Fig.5.3.C). The stuck polymer microparts are pushed out using a thin wire with a diameter of 200 µm (Fig.5.3.D). Finally, 3D discrete microcontainers are obtained.

5.2.2 Hot Punching for the fabrication of microcontainers

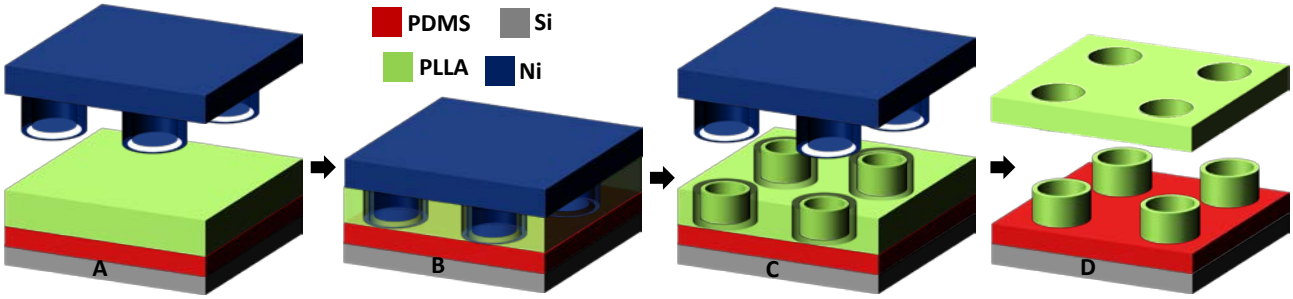

Fig.5.4 *Process A* - Hot punching process to fabricate microcontainers on PDMS layer: A. Spin coated PLLA film on ozone treated hydrophilic PDMS layer; B. Hot embossing leading to punching of PLLA containers from the surrounding film; C. Demolding of the stamp leaving the punched microcontainers on the PDMS layer along with the surrounding polymer film; D. Hydrophobic recovery of PDMS layer, PLLA containers ready to be collected after peeling of interconnecting film.

The process starts with the spin coating of a PLLA device layer on an elastic PDMS layer (Fig.5.4.A). After that, the device layer is embossed by a robust Ni stamp and at the same time punched due to the presence of the underlying elastic layer (Fig.5.4.B). Once the punching process is finished the microcontainers are separated from the rest of the PLLA film. Depending on the surface pretreatment of PDMS before deposition of the PLLA layer, these microstructures either remain on the underlying PDMS layer (Fig.5.4.C) or get attached to the Ni stamp. When the PLLA microcontainers remain on PDMS layer after demolding, the process is named as *Process A*. In this process once the PDMS layer recovers its hydrophobicity, it is possible to mechanically peel the interconnecting PLLA film from the PDMS, while the PLLA containers remain attached (Fig.5.4.D). When the microcontainers get attached to the stamp, they are then transferred to a sacrificial layer such as water soluble PAA layer by thermal bonding and this process is named as *Process B*. Process A and B are described in detail in paper III of chapter 8. Process B is mainly used for the fabrication of microcontainers for drug loading in the next section.

5.2.3 Hot Punching for the loading of microcontainers

In this project, two types of polymer matrices: i) hydrophobic (PCL) and ii) hydrophilic (PAA) are loaded in SU-8 and PLLA microcontainers. PCL and PAA are chosen in order to demonstrate that different drugs can be mixed in solution with either hydrophobic or hydrophilic polymers and can

be loaded in containers as drug-polymer matrices. PCL represents the hydrophobic polymers applied for sustained release of drug. PAA represents the hydrophilic polymers used as either hydrogels or to increase the solubility of drug.

SU-8 and PLLA microcontainers are fabricated using photolithography (Appendix 5) and hot punching (process B, paper III), respectively. Based on the thermal stability and relative deformability of the microcontainer materials, two different approaches are chosen to fill them. For microcontainers fabricated in non-deformable thermosetting materials such as SU-8 photoresist, the polymer matrix layer is spin coated on an elastic PDMS layer. On the other hand, for the microcontainers fabricated in deformable thermoplastic materials such as PLLA or PCL, the polymer matrix is spin coated directly on Si.

In order to fill the SU-8 microcontainers with PCL, PCL solution is spin coated on PDMS layer deposited on Si (Fig.5.5.A). Then, the spin coated PCL film is punched using the SU-8 microcontainers as a mold. This is achieved at a temperature of 65 ºC and a pressure of 1 bar applied for 30 min to both the upper and lower plates of the embossing tool. This temperature is above the melting temperature of PCL, which fills the SU-8 container at this stage (Fig.5.5.B). The hot plates are cooled down to 35 ºC and the SU-8 containers are demolded. The punched PCL is detached from the remaining PCL film and remains confined in the SU-8 container, thus filling them (Fig.5.5.C). To load PAA in SU-8 microcontainers, SU-8 containers and PDMS surfaces are modified in ozone for 20 min to increase their surface energies. Rest of the process is kept the same as loading of PCL.

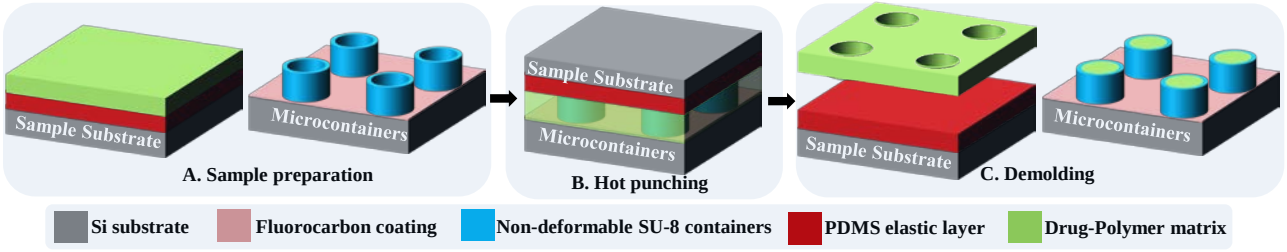

Fig.5.5 Loading of SU-8 microcontainers: A. Spin coating PCL solution on PDMS deposited Si substrate, B. Hot punching of the PCL film by SU-8 microcontainer mold, C. Demolding and loading of microocntainers

Similar processes are conducted for loading of PCL and PAA polymer matrices in PLLA microcontainers, except that in this case the elastic PDMS layer below the polymer matrix film is not applied. The loading of PCL and PAA in PLLA containers is performed at 75 ºC and 60 ºC, respectively, applied only on the plate of the embossing tool with which PCL and PAA substrates are in contact, with a lower pressure of < 0.5 bar.

5.3 Results and discussion

This section provides analytical values derived using the theory in section 5.1.1-5.1.4 and the fabrication results for the different processes involving punching. In section 5.3.1, the force required for mechanical punching is calculated. As discussed in the theory section 5.1.2-5.1.4, hot punching is possible when either the stamp or the substrate is elastically deformable to allow conformal contact. Furthermore, the initial thickness of the polymer has to be below the thickness required to fill the cavities in the stamp assuming that no residual layer is left. Finally, based on the

surface contact areas and the interfacial adhesions of the polymer to the mold and to the substrate, the structures punched out either remain on the underlying layer or adhere to the stamp. In the following sections, these different aspects of hot punching are discussed and successful fabrication of microcontainers is demonstrated. Afterwards, it is shown that the conditions for the attachment of the punched out polymer films to the microcontainers are fulfilled and successful loading of SU-8 and PLLA microcontainers with hydrophobic PCL and hydrophilic PAA is achieved.

5.3.1 Mechanical Punching

The punching tool used for mechanical punching has a diameter of 350 µm. Based on the equation 5.1 in the section 5.1.1, the punching forces required to punch out 350 µm diameter circular features from a PLLA polymer film of 50 µm thickness is estimated. The ultimate tensile strength of PLLA polymer is UTS ≈ 50 MPa [96]. The material multiplier is chosen as MM = 0.3 which is the same as the one for a soft Al sheet [146]. With these values a punching force of F = 0.825 N is obtained. The total punching force for 3X3 (=9) punches is 9*(0.825) = 7.425 N. Thus when a weight of 1 kg (F = 9.8N) is applied on the tungsten carbide (WC) punches fabricated in this project, the PLLA film should be punched out. At the same time, such a force should be small enough to prevent damage to the punching tool. In paper I of chapter 8 it is shown that this force is sufficient to successfully punch the PLLA films for fabrication of microcontainers.

5.3.2 Hot Punching for the fabrication of microcontainers

5.3.2.1 Calculation of required polymer film thickness

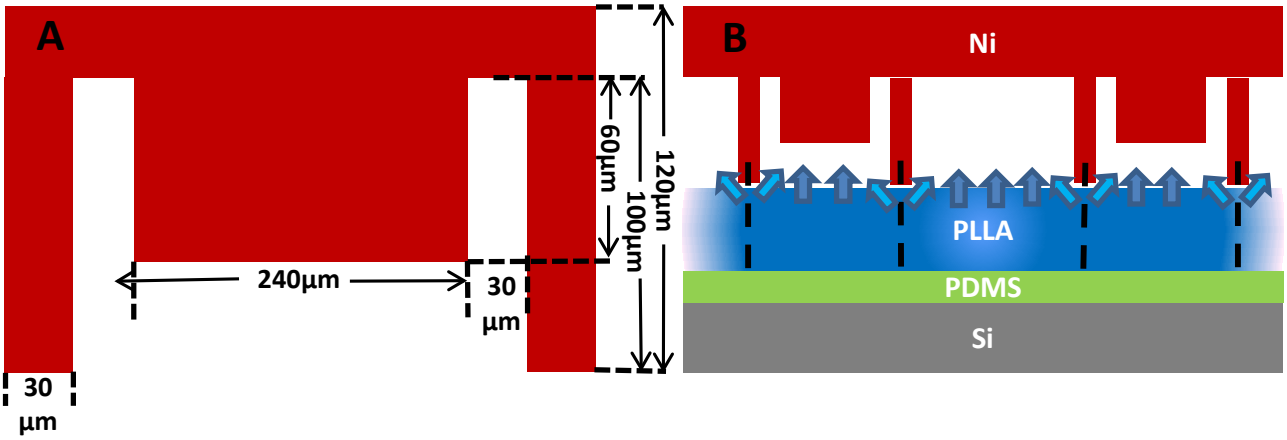

Fig.5.6 A. Different dimensions of the unit feature on Ni stamp. B. The protrusions and cavities on the Ni stamp.

In order to fabricate PLLA microcontainers using hot punching, Ni stamp is created with the wall thickness 30 µm and reservoir height of 60 µm across the wafer. Few stamps produced later have reservoir height of 73 µm to increase total drug loading. Fig.5.6.A above shows the different dimensions of a unit feature on the Ni stamp. Fig.5.6.B gives the overview of the protrusions and the cavities of a unit feature on stamp with center to center distance between two containers being 640 µm. Thus the thickness of the polymer required to completely fill the container without residual layer formation (H_{res} = 0) using equation 5.4 is:

$$H_0 \approx 100 \left\{1 - \frac{\pi}{4}\left(\frac{240^2 + 360^2 - 300^2}{640^2}\right)\right\} \tag{5.9}$$

From equation 5.9, H_0 is calculated to be around 81 µm. Therefore, hot punching with the Ni stamp is performed in spin coated PLLA layer of around 80 µm thickness. Moreover, in order to achieve conformal contact between the Ni stamp and PLLA substrate, a flexible PDMS layer is deposited on Si and then PLLA solution is spin coated on it.

5.3.2.2 Adhesion during demolding

In order to fabricate microcontainers that stay on the underlying PDMS layer after demolding (*process A*, paper III) it is necessary that the adhesion of the punched out PLLA polymer with PDMS layer is higher than the adhesion of PLLA with Ni stamp. While if the microcontainers need to be transferred to another sacrificial layer (*process B*, paper III), it is desirable that the containers stick to the Ni stamp so that the containers attached to the stamp, could be bonded to the sacrificial layer. Thus, for *process A*, according to the equation 5.8, either W_{ps} needs to be increased by exposing PDMS under UVO for 30 minutes or W_{pm} needs to be decreased by coating the Ni stamp with a FC layer in the MVD [151]. Table 5.1. summarizes the values of various surface energies reproduced from different references and interfacial energies and total adhesion energy calculated using equations 5.5-5.7. The calculations for contact surface areas A_{pm} and A_{ps} can be found in the matlab codes in Appendix 1.

Table. 5.1. Different surface energies used and calculated works of adhesion and total adhesion energies

Substrate	Surface energy of			Work of adhesion between		Total adhesion energy between		Result
	PLLA polymer (γ_p)	flurocarbon deposited Ni stamp (γ_m)	substrate(γ_s)	PLLA and Ni stamp (W_{pm})	PLLA and substrate (W_{ps})	stamp and PLLA ($W_{pm}A_{pm}$)	substrate and PLLA ($W_{ps}A_{ps}$)	
UVO treated PDMS	30 mJ/m^2 [104]	6 mJ/m^2 [151]	72 mJ/m^2 [84]	26.92 mJ /m^2	92.95 mJ /m^2	4.97 *10^{-6} mJ	9.47*10^{-6} mJ	microcontainers stay on UVO treated PDMS
Untreated PDMS	30 mJ/m^2	6 mJ/m^2	18 mJ/m^2 [84]	26.92 mJ /m^2	46.5 mJ /m^2	4.97 *10^{-6} mJ	4.73 *10^{-6} mJ	microcontainers stick to Ni stamp
PAA	30 mJ/m^2	6 mJ/m^2	72 mJ/m^2 [94]	26.92 mJ /m^2	92.95 mJ /m^2	4.97 *10^{-6} mJ	9.47*10^{-6} mJ	microcontainers attched to Ni stamp bond to PAA layer

[84, 94, 104, 151] references for surface energy values

When the stamp is completely filled then the total adhesion energy between the stamp and PLLA ($W_{pm}A_{pm}$) is less than the total adhesion energy between the PLLA and ozone treated PDMS substrate ($W_{ps}A_{ps}$). Hence the PLLA microcontainers stick to the underlying PDMS layer.

For the *process B* in paper III, the PDMS layer is not exposed to UVO. As can be seen in table 5.1, $W_{ps}A_{ps}$ is less than $W_{pm}A_{pm}$ in this case. Hence, the punched out containers stick to the Ni stamp. However, when this stamp with the containers is bonded to a water soluble PAA layer with high surface energy, the containers can be transferred to this sacrificial layer. Thermal bonding has been optimized for *process B*, where the best result is obtained when the PAA layer is freshly spin coated or PAA-PEG aqueous solution is used. Further optimization can be done by spin coating these high surface energy sacrificial layers on a flexible film. It is expected that such a flexible film will allow improved conformal contact between sacrificial layer and containers during bonding. For example, microcontainers attached to the Ni stamp have been quite successfully bonded to acrylate based pressure sensitive tapes (Appendix 3). Fig.5.7.A shows >95% yield for punching of containers where the interconnecting polymer layer with through holes is shown. Fig.5.7.B and C shows >95% yield of microcontainers lying in an array on the PDMS film after hot punching with process A. These containers can be further processed such as loaded with drug powder by screen printing and covered with a pH-sensitive layer before PDMS recovers its hydrophobicity [64]. After the processing and once PDMS recovers its hydrophobicity completely, the containers can be easily scraped off the substrate for further testing.

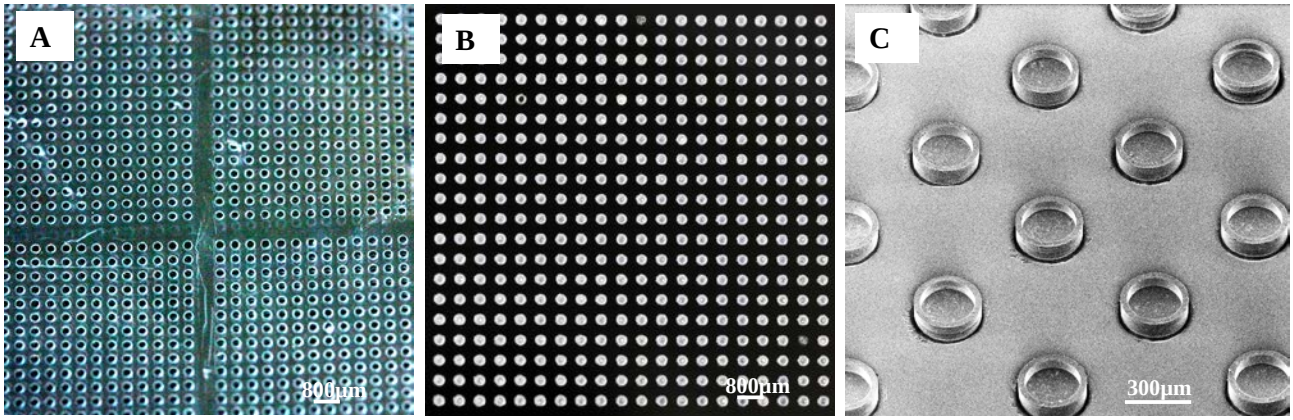

Fig.5.7.A. photograph of the interconnecting polymer layer with through holes after hot punching of PLLA film, B. photograph of and C. SEM micrograph of microcontainers lying in an array on the PDMS film after hot punching.

5.3.3 Hot Punching for the loading of microcontainers

The main concept behind using hot punching for loading of drug into microcontainers is that microcontainers themselves can be applied as a stamp to punch a spin-coated drug-polymer film. In order to successfully load the microcontainers, it is required that the punched out polymer matrix remains attached to this container stamp after demolding. In order to punch the polymer films, as described earlier, conformal contact of the microcontainers and the polymer matrix substrate is necessary. At the same time, in order to ensure that the punched polymer is transferred to the containers, the total adhesion energy between the container material and the polymer matrix should be higher than the total adhesion energy between the polymer matrix and the substrate below.

The calculation of the initial thickness of the polymer film required for conformal contact of container mold with the polymer substrate and the total adhesion energy between the SU-8 and PLLA microcontainer molds and PCL polymer are similar to the ones discussed above for the hot punching process and will not be repeated here. These calculations have been performed in detail in paper V of chapter 8. In this paper, furosemide (F) and PCL drug-polymer (PCL-F) matrix have been successfully loaded in PLLA and SU-8 microcontainers with high yield and high throughput. The table from the paper is reproduced here depicting the dimensions of SU-8 and PLLA microcontainers. Using the values shown in the table, the initial thickness of the polymer film derived for the loading of SU-8 microcontainers is 48.4 µm and for the loading of PLLA microcontainers is 69.9 µm. The discussion in this section mainly focuses on the loading of SU-8 and PLLA microcontainers with hydrophilic PAA polymer. Additionally a few details on the successful loading of microcontainers with PCL-F polymer are illustrated.

Table.5.2. Dimensions of SU-8 and PLLA microcontainers

Cont-ainer	Depth of inner reservoir, H_1 (µm)	Diameter of inner reservoir, D_1 (µm)	Total height of container, H_2 (µm)	Outer diameter of container, D_2 (µm)	Center to center distance between containers, L (µm)
SU-8	70	200	100	300	450
PLLA	73	240	100	300	640

5.3.3.1 Loading of SU-8 microcontainers

Table.5.3 Calculated work of adhesion and the total adhesion from the surface energies reproduced from references.

Microcontainers	Substrate	Surface energy of			Work of adhesion between		Total adhesion energy between		Result
		PAA polymer (γ_p)	microcontainer (γ_m)	substrate(γ_s)	PAA and microcontainer(W_{pm})	PAA and substrate (W_{ps})	PAA and microcontainer(W_{pm})	PAA and substrate (W_{ps})	
SU-8	treated PDMS	72 mJ/m^2 [94]	79 mJ/m^2 [73]	72 mJ/m^2 [84]	151 mJ /m^2	144 mJ /m^2	11.67*10^{-6} mJ	10.18*10^{-6} mJ	PAA stays in PLLA containers
PLLA	Si	72 mJ/m^2	63.6 mJ/m^2 [103]	60 mJ/m^2†	135.34 mJ /m^2	92.95 mJ /m^2	13.6*10^{-6} mJ	13.2*10^{-6} mJ	PAA stays in PLLA containers

[73, 84, 94, 103] references for surface energy values.

† The values of surface energy of Si vary significantly in literature based on its surface conditions like presence of native oxide, surface roughness and cleanliness. The values found in literature range from 30 mJ/m^2 to 90 mJ/m^2 [153, 154], so an average value of 60 mJ/m^2 has been chosen for calculations here. Contact angle measurements need to be performed to obtain Si surface energy.

Since hard baked SU-8 is relatively non-deformable, polymer-drug film is deposited on PDMS to obtain a deformable substrate required for conformal contact during hot punching. In order to load a hydrophilic polymer like PAA, the surface energies of SU-8 microcontainers and underlying PDMS layer are altered by exposure to UVO for 15-20 minutes. With this treatment, the surface energy of PDMS layer is increased to improve PAA wetting which is essential for the spin coating of PAA on PDMS. The surface energy of SU-8 is increased to improve adhesion of PAA to the SU-8 walls and promote filling of the microcontainers. Table.5.3 summarizes the work of adhesion and the total adhesion calculated based on the surface energies reproduced from references. It can be seen from the table that given the surface conditions described here, the total adhesion energy between PAA and SU-8 microcontainers ($W_{pm}A_{pm}$) is more than the total adhesion energy between PAA and PDMS substrate ($W_{ps}A_{ps}$). Thus, PAA polymer should have a higher tendency to remain confined in the SU-8 microcontainers, thereby filling them. Fig. 5.8 shows a SEM micrograph of an empty SU-8 microcontainer (A), and of PCL loaded (B) and PAA (C) loaded SU-8 microcontainers.

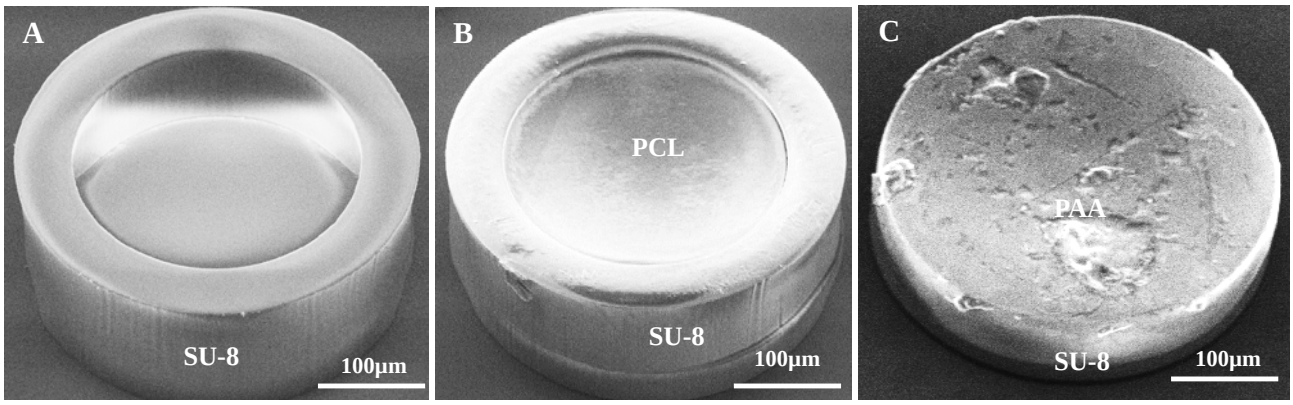

Fig. 5.8.A.show the SEM micrograph of an empty SU-8 microcontainer, B. PCL loaded, and C. PAA loaded SU-8 microcontainer.

5.3.3.2 Loading of PLLA microcontainers

Since PLLA is a relatively deformable polymer, the substrate is not required to be flexible. Thus for the loading of PLLA microcontainers, the polymers to be filled are not spin coated on a PDMS layer, but directly on Si substrate. PLLA microcontainers are deformed during punching (Fig.5.9.A) when both the polymer film to be punched and PLLA microcontainers are heated to above 60 °C because the T_g of PLLA is somewhere between 50-60 °C [96].Therefore, only the plate with which the polymer sample is in contact is heated in the embossing tool, while the plate with which the microcontainers are in contact is kept at room temperature. Besides, no additional pressure is applied apart from the pressure required to bring the microcontainer mold and the polymer sample in contact. This helps in keeping the PLLA microcontainers intact while filling them. When the PLLA containers that are fabricated by *process A* are loaded with polymer, detachment from the underlying PDMS layer and attachment to the PCL film as shown in Fig.5.9.B is observed. Therefore, microcontainers fabricated by *process B* lying on a sacrificial layer, are more suitable for this type of filling (Fig.5.10.A).

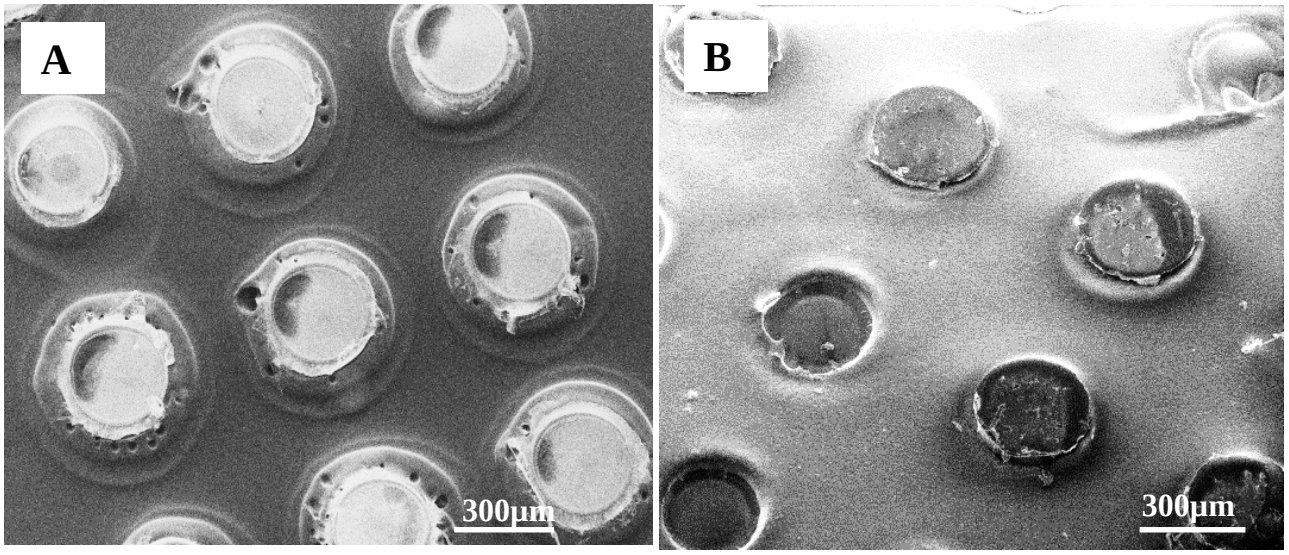

Fig.5.9 SEM micrographs of A. Deformed PLLA microcontainers during the loading of PCL, and B. Containers fabricated using *process A* getting detached from substrate and attached to PCL film being punched.

Similar to the loading of SU-8 microcontainers with PAA as described in section 5.3.3.1, PLLA microcontainers (Fig.5.10.A) are treated with UVO for 15 minutes to increase the surface energy. From Table 5.2, since $W_{pm}A_{pm} > W_{ps}A_{ps}$, after the hot punching process, the punched PCL fills the PLLA microcontainers as shown in Fig.5.10.B. In Fig.5.10.C.successful loading with PAA has been achieved.

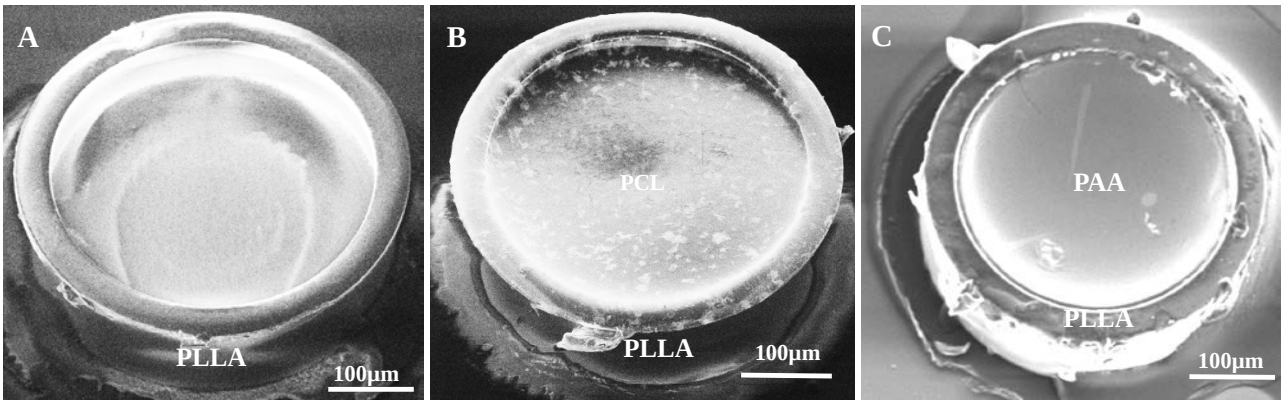

Fig.5.10 SEM micrographs of A. Empty PLLA microcontainer, B. PCL loaded and C. PAA loaded PLLA microcontainer.

Complete filling of the containers is essential as incomplete filling leads to reduced A_{pm} which in turn will result in lower adhesion of polymer to mold. If that occurs, the punched polymer will stay on the substrate after demolding as shown for PCL (Fig.5.11.A) and PAA (Fig.5.11.B). Incomplete filling and/or non-uniform polymer film thickness can also lead to dewetting and formation of voids in punched and loaded polymers as illustrated in Fig.5.11.C [152, 155].

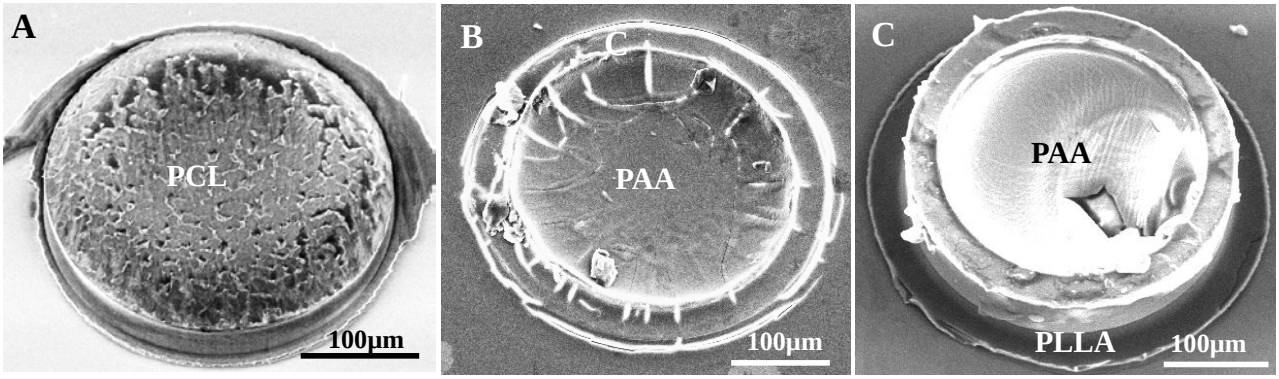

Fig.5.11 SEM micrographs of A. PCL and B. PAA punched polymer that remain on their respective substrates after demolding due to incomplete filling; C. Incomplete filling also leads to voids in loaded polymers.

It should be noted from the discussion on the total adhesion energy dictating the adhesion of punched polymers to its substrate or the mold during demolding, that it does not take into account other mechanisms-in-action. These mechanisms comprise of, but are not limited to, frictional forces at the sidewalls, thermal stresses and interlocking at the stamp undercuts. etc. Some of these mechanisms are neglected assuming that the stamp has significantly smooth walls, no undercuts and positively sloped protrusions. Moreover, after the disruption of residual layer, these mechanisms actually have tendency to keep the punched polymer in the mold. The more difficult part is to minimize this tendency as required for the fabrication of microcontainers using hot punching.

So far there has not been any discussion about the influence of the air that is present when the stamp and the sample are brought into contact on the outcome of the hot punching process. When PAA is filled in microcontainers, additional water vapor, evaporated from the PAA aqueous solution, is present. During the molding process, due to the high pressure applied on the mold and sample, this air is probably compressed to a fraction of its initial volume in the cavity. Some of this compressed air might diffuse into the polymers. During demolding the expansion of the trapped air might promote separation of the stamp and the molded structures. Thus it is speculated that for fabricating microcontainers, the experiments should be performed without any vacuum while for loading the microcontainers with drug-polymer matrix, it would be more beneficial to conduct experiments in a vacuum chamber.

CHAPTER 6
DRUG RELEASE

CHAPTER 6
DRUG RELEASE

This chapter goes through the basic theory behind drug release in a media. Fick's laws and power law of diffusion that form the basics of drug release have been described. Based on the theory, an expression for drug release from SU-8 microcontainer has been derived. The experimental values of the drug release from the microcontainers are fitted for the power law and it is demonstrated that the release is first-order non-Fickian release.

6.1 Theory of drug release

Dissolution is the measurement of the rate of how fast a solid drug dissolves in a liquid medium. When a drug is dissolved in a medium, two things happen sequentially: i) the molecules at the surface of the drug particle dissolve and saturate diffusion layer and ii) slowly the dissolved particle then diffuse out of the diffusion layer. This second process is the rate limiting process in dissolution [156]. According to Fick's first law of diffusion, molar flux due to diffusion is proportional to concentration gradient [156, 157].

$$J = -D\frac{dc}{dx} \tag{6.1}$$

Where *D* is the diffusion coefficient or diffusivity, *c* is the concentration and *x* is the distance. The negative sign in equation 6.1 depicts that diffusion occurs from higher concentration to lower concentration. Fick's first law applies to steady state systems, where concentration is constant. Applying, Fick's first law and mass conservation, Fick's second law that predicts how diffusion causes the concentration to change with time, is derived [167]:

$$\frac{dc}{dt} = D\left(\frac{\partial^2 c}{\partial x^2} + \frac{\partial^2 c}{\partial y^2} + \frac{\partial^2 c}{\partial z^2}\right) \tag{6.2}$$

where x, y, z are the three spatial Cartesian coordinates. When the following assumptions are made, equation 6.2 can be solved for thin film systems: i) Diffusional mass transport is release-rate limiting, ii) Diffusion coefficient is constant, iii) There is a perfect sink condition in the release medium during the entire dissolution, iv) There is no significant swelling and erosion during dissolution, v) Mass transfer resistance on the surface of the system is negligible as the system is stirred, (vi) The device geometry is that of a thin film with negligible edge effects, and vii) The size of the drug particles is much smaller than the thickness of the film [157]. Using these assumptions and applying boundary conditions, for a monolithic plane sheet, Ficks second law is solved to give [157,158]

$$\frac{M_t}{M_\infty} = 1 - \frac{8}{\pi^2}\sum_{n=0}^{\infty}\frac{exp[-D(2n+1)^2\pi^2 t/L^2]}{(2n+1)^2} \tag{6.3}$$

Early time, when $0 \leq \frac{M_t}{M_\infty} \leq 0.6$

$$\frac{M_t}{M_\infty} = 4\left(\frac{Dt}{\pi L^2}\right)^{1/2} \tag{6.4}$$

Late time, when $0.4 \leq \frac{M_t}{M_\infty} \leq 1.0$

$$\frac{M_t}{M_\infty} = 1 - \frac{8}{\pi^2}exp\left(-\frac{\pi^2 Dt}{L^2}\right) \tag{6.5}$$

Here, M_t and M_∞ are cumulative amount of drug released at time t and ∞, respectively, and L is the thickness of the monolithic sheet. Thus from equation 6.4 it can be inferred that the drug release is proportional to square root of time ($\sqrt{t}$) during the initial phase of dissolution.

There is also a power law which can be used to describe various forms of dissolution profiles. This power law which was first identified by Alfrey [159] and later developed by Peppas [160] is used frequently to describe not only Fickian diffusion but also non-Fickian diffusion and is given as:

$$\frac{M_t}{M_\infty} = kt^n \tag{6.6}$$

where, k is a constant incorporating structural and geometric characteristics of the system, and n is the release exponent, which is indicative of the mechanism of diffusion:

i) When n < 1/2, then it is pseudo-Fickian release like one-dimensional radial drug release from cylinder or sphere.

ii) When n = 1/2, then the diffusion is classical/Fickian as given by drug release from a slab where initial drug concentration>>drug solubility.

iii) When 1/2 < n < 1, then the diffusion is anomalous or subdiffusion like drug release from swelling of polymer matrix.

iv) When n = 1, it is case II diffusion that is predominant for drug release from reservoir systems with constant activity source.

v) When n>1, it is superdiffusion or supercase II which happens for drug released from cold drawn strained polymers [161-163].

It can be inferred that equation 6.3-6.5 are special cases of this general power law.

6.2. Furosemide release from PCL matrix loaded in SU-8 microcontainers

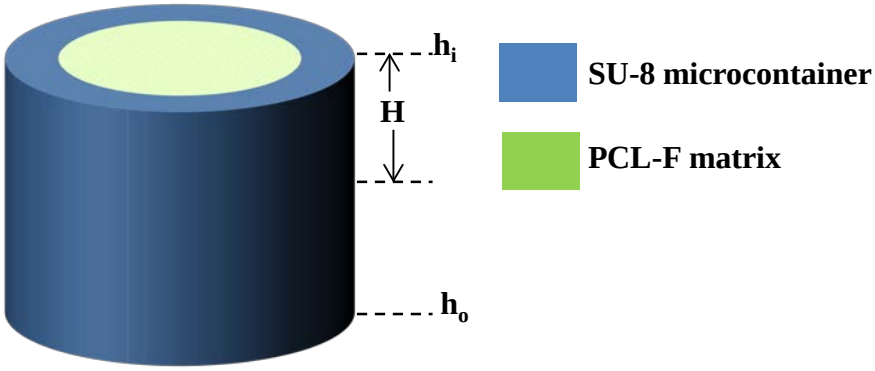

Fig.6.1 Diagram of the drug dissolved from polymer matrix loaded in microcontainer: h_i is the initial dispersed height of drug, h_o is the total depth of the reservoir, and H is the distance to the interface between the dissolved and dispersed regions at any time t.

In the following analysis, drug release from SU-8 microcontainers is studied taking into account all the assumptions afore mentioned in the theory section for Fickian diffusion. It is assumed that the drug release from PCL matrix is mainly diffusion based since PCL has very slow degradation rate. It doesn't swell or erode in the given time duration of drug release (5 hrs).

The drug release starts from the top of the microcontainer and proceeds through the depth of the cylindrical reservoir structure (Fig.6.1). Taking h_i as the initial dispersed height of drug, h_o as the total depth of the reservoir, *r* as the radius of the reservoir, *J* as the diffusion flux, *C(h)* as the drug concentration (mg/ml) within the matrix at the height *h*, C_s as drug solubility in the release media which is equal to the concentration of drug at the interface between the dissolved and dispersed (undissolved) regions in the container reservoir, *Q(t)* as the drug released (mg) from the container at time *t*, *M(t)* is the drug remaining in the container at time *t* and *D* is the diffusion coefficient of drug.

At steady state,

$$J\pi r^2 = \frac{dQ}{dt} \tag{6.7}$$

Applying Fick's law,

$$J = D\frac{dc}{dh} \tag{6.8}$$

Using Equation 6.7 and 6.8, integrating from h_i to any height *H* and applying boundary conditions as, $C(H) = C_s$ and $C(h_i) = 0$, we obtain,

$$\frac{dQ}{dt} = \frac{\pi r^2 D C_s}{H - h_i} \tag{6.9}$$

Drug in the reservoir at time $t = 0$,

$$M_0 = \pi r^2 h_0 C_0 \tag{6.10}$$

Similarly, drug in the reservoir at time *t*,

$$M(t) = \pi r^2 H C_0 \tag{6.11}$$

So the total amount of drug released is

$$Q(t) = M_0 - M(t) = \pi r^2 C_0 (h_0 - H) \tag{6.12}$$

Differentiating Equation 6.12 with respect to *t*,

$$\frac{dQ}{dt} = \pi r^2 C_0 \frac{dH}{dt} \tag{6.13}$$

Equating, 6.9 and 6.13 and integrating the equation from time = 0 to *t* and putting $h_i = 0$,

$$H = \sqrt{\frac{D C_s t}{C_0}} \tag{6.14}$$

From 6.9 and 6.14, it can be inferred that *dQ/dt* is proportional to $1/\sqrt{t}$, which implies if *Q(t)* is integrated over time, it is proportional to $\sqrt{t}$. This represents the early time Fickian release from a monolithic slab with no edge effects as described in theory section of drug release. However, when the furosemide release profile from PCL matrix loaded in SU-8 microcontainers is measured after 14 days of storage using microdiss, the profile of drug released is observed to be linear after the small initial burst release as shown in Fig. 6.2. This indicates that the drug release follows zero-order Case II diffusion [163]. To understand this unexpected behavior, drug distribution in the PCL matrix is investigated using Raman spectroscopy and it is found out that the overall amount of the drug increases with the depth of the microcontainer. This non-uniform drug distribution is because of the drug migration to the surface of the spin coated PCL-F film during the drying and storage

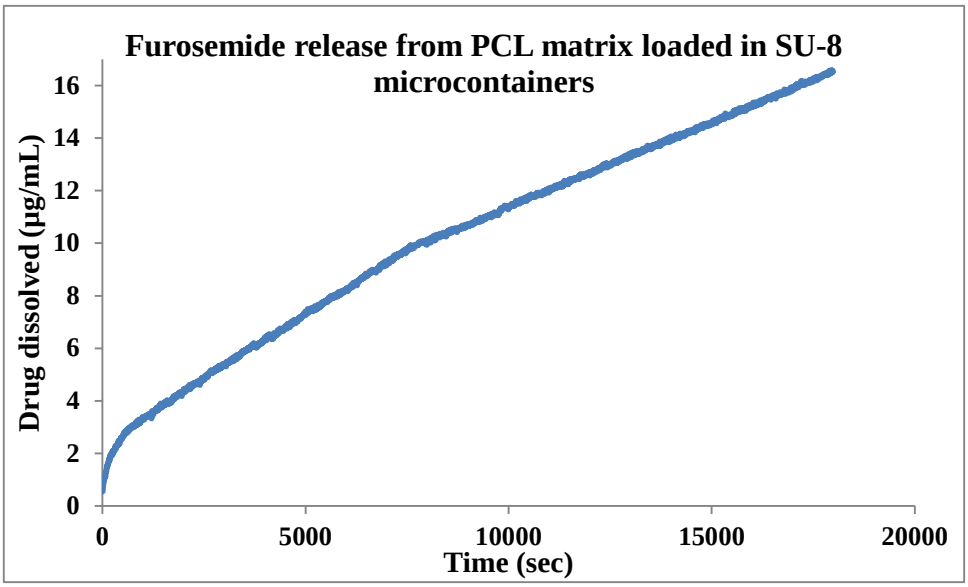

Fig.6.2 Zero-order furosemide release from PCL matrix loaded in the SU-8 containers

stages [164]. Further, when hot punching is performed where the polymer flow is similar to that in hot embossing, the furosemide-rich surface fills the reservoir cavity first followed by the furosemide-deficient lower surfaces [165]. This non-uniform drug distribution ensures that the slowing down of the drug release due to increase in the diffusion barrier is compensated by the increase in drug release due to surplus amount of drug lying in the reservoir. This compensation leads to an overall zero-order release of furosemide from PCL matrix loaded in the SU-8 containers.

CHAPTER 7
CONCLUSION AND OUTLOOK

CHAPTER 7
CONCLUSION AND OUTLOOK

7.1 Conclusion

At the beginning of this project, we set forth the goal of fabricating and loading biopolymer microcontainers for oral drug delivery applications. To our delight, we made many significant advances in the direction of achieving this goal. Fig.7.1 shows some of the major successes obtained in last three years while completing this PhD, which are also described in the publications presented in chapter 8 of this thesis.

The first successful attempt of fabricating 3D discrete microcontainers has been obtained by applying mechanical punching. The fabrication of punches for mechanical punching of poly-l-lactic acid (PLLA) polymer films with reservoirs is successfully achieved (Fig.7.1.A). Using these punches, 3D microcontainers in PLLA are fabricated reproducibly (Fig.7.1.B and C). Taking inspiration from the success of mechanical punching, hot punching process as a combination of hot embossing and mechanical punching processes, has been developed. In order to fabricate high-aspect-ratio (HAR) complicated structures like microcontainers in polymers by hot punching, a robust Ni stamp is fabricated. The Ni stamp is fabricated by electroplating Ni on a Si master (Fig.7.1.D). The Ni stamp produced after the optimization of deep reactive ion etching (DRIE) and electroplating processes possesses all the features of a good-quality stamp for hot embossing (Fig.7.1.E). These features are: i) smooth sidewalls and surfaces, ii) slightly positive profiles of the protrusions, and iii) no undercuts and overhanging structures. Using this stamp, the HAR microcontainer features (aspect ratio > 9) are replicated in PLLA film with significantly high yield, reproducibility and replicability (Fig.7.1.F). The process flow for the fabrication of Ni stamp has been developed to such an extent that many other micro/nanostructures are obtained later on without any difficulty or further process optimization.

The Ni stamp is also applied for hot punching of PLLA film to fabricate discrete 3D PLLA microcontainers. Two kinds of hot punching processes (*process A* and *process B*) have been developed where microcontainers have been obtained either on the underlying PDMS layer ((Fig.7.1.G) or on a sacrificial layer that can be dissolved later on (Fig.7.1.H and I). For both the processes, high yield and good replication fidelity are achieved. Hot punching is not just limited to the fabrication of microcontainers. It can be easily be used for the fabrication of other kinds of 3D microstructures. Some of the highlights of hot punching process for fabrication of individual microstructures are:

i) The residual layer obtained in hot embossing is penetrated during a single hot punching processing step without formation of residues and without need of additional equipment compared to similar attempts using reactive ion etching or laser machining techniques.

ii) The process allows fast fabrication of large high aspect ratio microstructures on wafer-scale.

iii) The punched out microstructures are obtained at well-defined positions on a handling substrate, which facilitates further processing such as drug loading and functional layer deposition.

iv) The process is scalable and very versatile where the targeted microstructures can be of different shapes, sizes and thermoplastic materials.

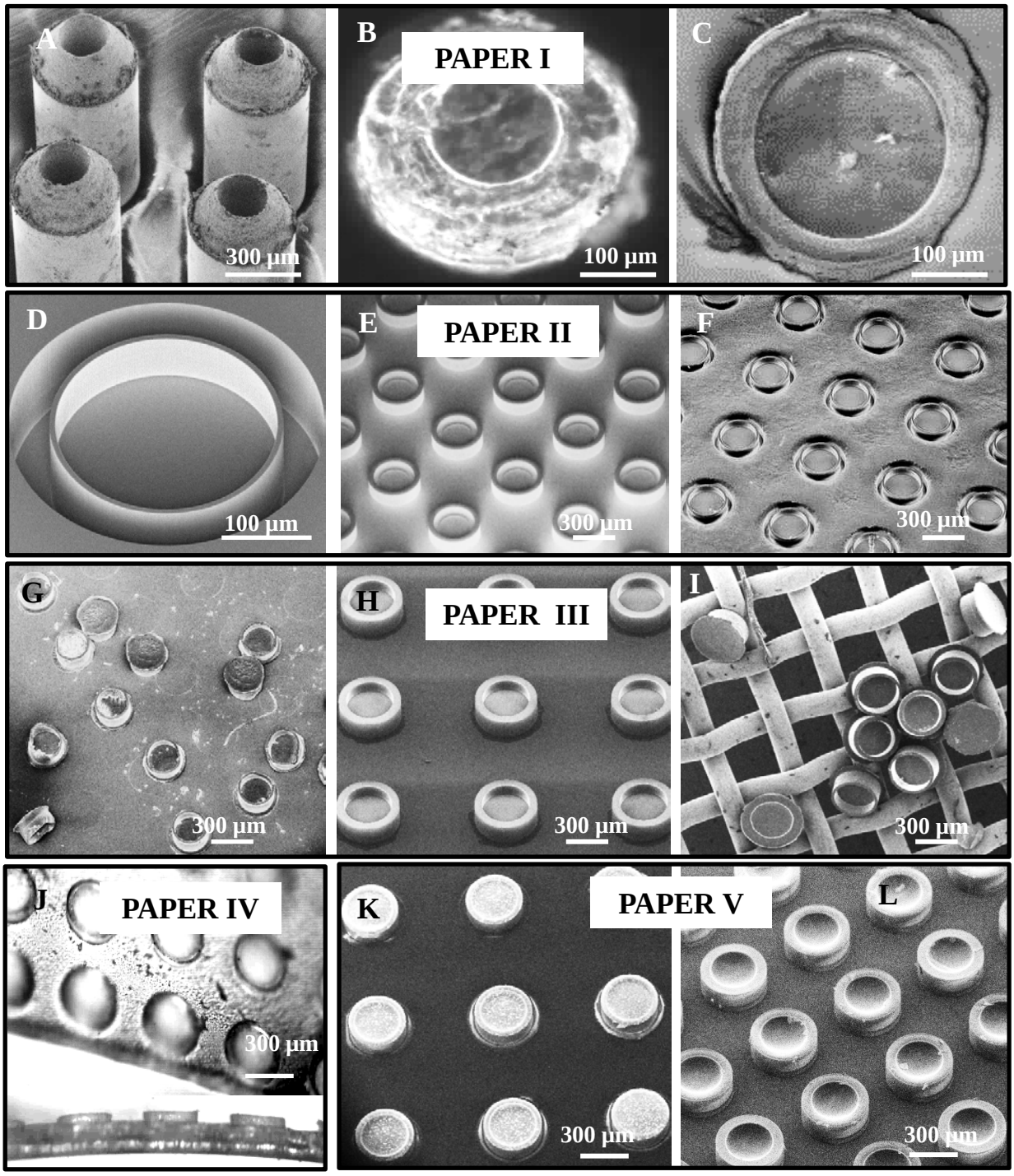
A
300 µm
B
PAPER I
100 µm
C
100 µm
D
100 µm
E
PAPER II
300 µm
F
300 µm
G
300 µm
H
PAPER III
300 µm
I
300 µm
J
PAPER IV
300 µm
K
PAPER V
300 µm
L
300 µm

Fig.7.1.A. SEM micrograph of tungsten carbide punches, B. Optical image and C. SEM micrograph of punched PLLA polymer with reservoir in the center; SEM micrographs of D. Si master with 10 μm wall, E. Ni stamp fabricated by optimized process parameters, F. PLLA polymer with microcontainer features embossed by Ni stamp, G. PLLA microcontainer on PDMS film fabricated by hot punching, H. PLLA microcontainer on water soluble sacrificial layer fabricated by hot punching, I. Microcontainers filtered through a mesh after the dissolution of sacrificial layer; J. Optical image and K. SEM micrograph of PLLA containers loaded with PCL-F matrix, L. SEM micrograph of SU-8 containers loaded with PCL-F matrix.

To add to the versatility of hot punching process, loading of microcontainers is also performed by applying hot punching. Both PLLA (Fig.7.1.J and K) and SU-8 microcontainers (Fig.7.1.L) are successfully loaded with PCL and PAA polymer matrices in which drug can be embedded. Thus hot punching emerges as a fast process of loading drug in microreservoirs based drug delivery devices including, but not limited to microcontainers. Some of the highlights of hot punching process for loading are:

i) It is a versatile process that can be used to fill different combinations of drug and polymer;
ii) Apart from the sample preparation, the process is a single-step, parallel process with high throughput.
iii) It doesn't require any special printing or alignment tools; neither the process needs to be performed in cleanroom or under high vacuum, making it a simple process that can be scaled up.
iv) Other advantages are that it is comparatively benign towards the drug, it can be used for high-aspect ratio filling and in principle the leftover drug-polymer can be reused in making fresh batch of solution.

In addition to the above mentioned fabrication-based advantages, it is also found that hot punching can help in the zero-order release of furosemide (F) drug from the poly-ε-caprolactone (PCL) matrix loaded in SU-8 microcontainers (Fig.7.1.M). This zero-order release is attributed to the non-uniform drug distribution in the matrix which in turn results from the polymer flow during the hot punching process.

Finally, the technique of spin coating has been demonstrated as a simple yet effective way of tailoring drug release kinetics from spin coated PCL-F patches. By changing the thicknesses (Fig.7.1.N), annealing temperature and time and cooling rate, the crystallinity of the drug has been modified systematically. These modifications in the drug crystallinity as well as the stresses built up in the patches during spin coating process are shown to affect the drug release kinetics. Thus by tailoring the spin coating process parameters, drug release from patches can be tailored.

7.2 Outlook

Before starting to look into the future, it would be appropriate to enumerate some of the preliminary experiments that have been carried out recently and have shown promising results. One of these experiments is on micropatches, which is the core design described in the patent in chapter 8. The idea behind these patches is to use hot punching to cut multiple layers of polymer films for drug delivery applications. These layers can contain different functionalities like pH-sensitivenesss, mucoadhesion etc. along with a drug layer and a protective polymer layer. During hot punching, the

material properties of the outermost protective layer could be tuned such that this layer can rise up in the mold faster than the other underlying layers, thereby, creating a shell-like structure. Another method could be to first punch different functional and drug layers and then spray coat the final protective layer on top of these punched out micropatches. The micropatch design is simple, low cost and easy to fabricate. Besides, it is potentially very versatile where different drug layers or barrier layers can be chosen to tune drug release. It has immense potential to be upscaled via roll-to-roll processing. Fig.7.2 shows some encouraging results from preliminary work done in this direction. Fig.7.2.A demonstrates the punching of PCL-F matrix on plasticized Eudragit L-100 film. This film can be easily handled and once ingested can dissolve in intestine dispersing the microstructures in the system. Fig.7.2.B shows the patches created in PLLA layer while Fig.7.2.C shows the first attempt carried out to obtain microcontainers in a roll-to-roll machine using the Ni shims fabricated in this project. The roll-to-roll processing is carried out by Maria Matschuk from InMold Biosystems. The first experiment is conducted on polypropylene (PP) polymer sheet and soon the test would be carried out on biopolymer sheets.

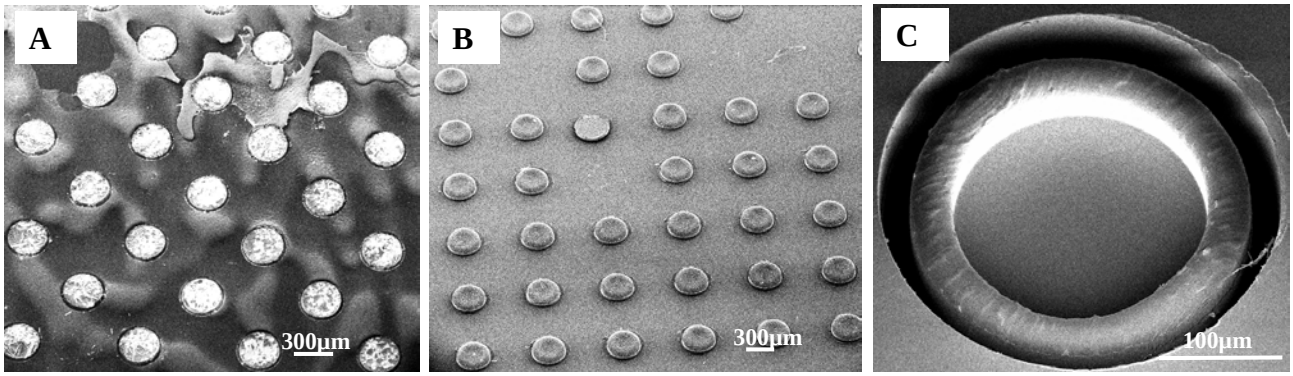

Fig.7.2 SEM micrographs of: A.Punched PCL-F matrix on plasticized Eudragit L-100 film, B. patches created in PLLA layer, C. Microcontainers fabricated by roll-to-roll processing in PP.

Thus, based on the significant advances made in the last 3 years and some of encouraging results obtained on the abovementioned preliminary concepts, the next step would be to develop the hot punching process for fabrication of microcontainers and micropatches to an extent that it can be scaled up. This would require deeper understanding of hot embossing, demolding forces and surface adhesion concepts. After that, further optimization of various processes would be required. We also hope that the processes developed in this research project can be combined with other techniques developed in the group. Combination of processes like fabrication of robust stamps and hot punching with other techniques like supercritical CO_2, spray coating of pH-sensitive layers etc. would enable us to fabricate a complete system as we envisioned in the beginning of this research. Finally we would carry out further in-vivo and in-vitro experiments on the devices that have already been fabricated and on the devices can be potentially fabricated with the above mentioned add-ons. And who knows, one day these microdevices might alleviate the pain of many people.

CHAPTER 8
PUBLICATIONS

PAPER I

Hot embossing and mechanical punching of biodegradable microcontainers for oral drug delivery

Microelectronic Engineering 133 (2015) 104–109

Contents lists available at ScienceDirect

Microelectronic Engineering

journal homepage: www.elsevier.com/locate/mee

Hot embossing and mechanical punching of biodegradable microcontainers for oral drug delivery

Ritika Singh Petersen [a,*], Rasoul Mahshid [b], Nis Korsgaard Andersen [a], Stephan Sylvest Keller [a], Hans Nørgaard Hansen [b], Anja Boisen [a]

[a] Department of Micro- and Nanotechnology, Technical University of Denmark, Building 345E, DK-2800 Kongens Lyngby, Denmark
[b] Department of Mechanical Engineering, Technical University of Denmark, Building 427A, DK-2800 Kongens Lyngby, Denmark

ARTICLE INFO

Article history:
Received 22 August 2014
Received in revised form 1 November 2014
Accepted 13 November 2014
Available online 21 November 2014

Keywords:
Hot embossing
Mechanical punching
Biodegradable polymer
Drug delivery
Microcontainers

ABSTRACT

A process has been developed to fabricate discrete three-dimensional microcontainers for oral drug delivery application in Poly-L-Lactic Acid (PLLA) polymer. The method combines hot embossing for the definition of holes in a PLLA film and mechanical punching to penetrate the polymer layer around the holes, after filling them with drug. Here, we demonstrate the fabrication of microcontainers with a diameter of 340 μm and a height of 50 μm. The process is temperature benign so that the compositional integrity of the drug is preserved. It also provides a good flexibility for creating different sizes and shapes of microcontainers. Finally, the process is compatible with roll-to-roll processing that could lead to low cost high volume production.

1. Introduction

Recently, drug delivery micro devices in the form of microneedles, micropatches or microreservoirs have been developed, using Microelectromechanical systems (MEMS) fabrication techniques like photolithography and reactive ion etching (RIE) [1–4]. These fabrication methods give good control on the size and structure of drug delivery devices. Such devices can be easily fabricated and multiple functionalities can be added to improve the administration efficiency [5]. Microcontainers are one such type of innovative oral drug delivery devices where holes are defined and loaded with drug [6]. The container surface can be further modified by covalent binding of bioadhesive lectins [7]. The bioadhesive targeting allows the containers to stick to the intestinal walls for unidirectional release of the drug.

Ainslie and Desai developed microcontainers in classical microfabrication materials such as Si and SU-8 [6]. However, there is a need to move toward biocompatible and biodegradable polymers for drug delivery applications [8]. Using biocompatible polymers for fabrication of micro devices minimizes the hazardous effects on the human body due to their presence [9]. Using biodegradable polymers also reduces the risk related to their accumulation in the gastrointestinal tract [10]. However, this shift in materials requires a shift in fabrication techniques from standard MEMS processing to polymer processing techniques like hot embossing.

Hot embossing has been successfully used in the past to define microreservoirs in biodegradable polymers [11]. The process gives a good control over the size of the microstructures and has been applied on various polymers approved by the US Food and Drug Administration (FDA) such as Poly-L-Lactic Acid (PLLA) and Polycaprolactone (PCL). However, the technique faces the inherent challenge of the presence of a residual layer that connects all the microstructures to each other. This limits the use of hot embossing for the fabrication of discrete three-dimensional (3D) microcontainers. This residual layer could be removed by RIE [12] but etching in plasma can lead to formation of complex bi-products and affect the overall structure. Laser cutting is an emerging technology that could be used to get rid of the residual layer but it also generates residues and local heating [13].

In this paper, we present a unique way of fabricating discrete 3D microcontainers in Poly-L-Lactic Acid (PLLA) biopolymer for potential application in oral drug delivery. PLLA is processed into microcontainers using the combination of hot embossing and mechanical punching as illustrated in Fig. 1. First holes are defined in the PLLA film by hot embossing (Fig. 1A). The holes can be loaded with drug using inkjet printing [14], powder distribution [15] or other techniques available (Fig. 1B). The PLLA film is peeled from the substrate and placed on a Poly Vinyl Alcohol (PVA) foil that provides a soft padding for PLLA. This stack is then punched

* Corresponding author.
E-mail address: risi@nanotech.dtu.dk (R.S. Petersen).

http://dx.doi.org/10.1016/j.mee.2014.11.009
0167-9317/

and the 3D microcontainers are released from the punching tool (Fig. 1C). The mechanical punching technique described in the paper is based on the approach of biopsy punches, which are commonly used in medical tests for sampling of soft tissues [16,17]. Only a few researchers have tried microscale processing of polymers using cold forging or mechanical punching techniques. Traditionally, after the punching of polymer tapes and metal foils, the punched material is discarded as waste, while the remaining film with the holes is kept as the final product [18]. This is to our knowledge the first time that a fabrication technique has been proposed, where the final product is the punched 3D microcontainer and the film with the holes is discarded as waste.

Since the containers are loaded with drugs for oral drug delivery, this process offers several advantages over established MEMS fabrication processes. Firstly, mechanical punching is a temperature benign and dry process without any need of heating the sample or immersion in any kind of solvents or acids. This implies that once the drug is loaded in the holes, it will not be degraded or prematurely released during further processing. Secondly, polymer and drug are not exposed to any UV radiation that might change their properties. Thirdly, it is a residue free process, where unlike in RIE or laser cutting techniques no complex bi-products are created that could be hazardous when ingested. Finally, it is a simple and versatile process that can be easily adapted to different film thicknesses and materials.

2. Materials and methods

2.1. Materials

For the experiments, PLLA 2003D grade is purchased from Natureworks (Minnetonka, Minnesota), with Mw = 126000 Da, determined by size exclusion chromatography measurements. Dichloromethane (DCM) (anhydrous >99.8%) is supplied by Sigma Aldrich (Copenhagen, Denmark). PLLA pellets are dissolved in DCM (15 %wt) while stirring at room temperature for 24 h to obtain a viscous solution for spin coating. PVA foil is purchased from BEIL GmbH, Moderne Orthopädie (Peine, Germany). Silicon wafers (4-inch ⟨100⟩ n-type) are supplied by Okmetic (Vantaa, Finland). The chromium mask is designed using L-Edit from Tanner EDA (Monrovia, CA, USA) and supplied by DeltaMask B.V. (GJ Enschede, The Netherlands). 2.5 mm thick PMMA plates are bought from Nordiskplast (Randers, Denmark). Standard tungsten carbide (WC) tubes are used to fabricate mechanical punching tools. These tubes are found commercially as electrodes for micro EDM machining. To minimize the effect of stock variability, mechanical punches are fabricated from the same stock of the material. The original WC tube has an outer and inner diameter of 800 μm and 360 μm, respectively.

2.2. Stamp fabrication and hot embossing

In order to perform hot embossing, a Si stamp is fabricated. This is done using standard photolithography and reactive ion etching (RIE) as shown in Fig. 2. The Si wafer is spin coated with 1.5 μm of AZ5214E positive photoresist (Fig. 2A). The resist film is pre baked at 90 °C for 90 s and then exposed in a UV aligner (Karl Süss, Germany) with a dose of 70 mJ/cm^2 in hard contact mode (Fig. 2B). After development for 70 s, a short descum process with oxygen is run in a plasma asher (model 300 Plasma Processor, TePla, Germany) to remove any residues left behind. Next, the Si is etched in a deep reactive ion etch chamber (STS Pegasus ASE, UK) to define the pillars of the Si stamp (Fig. 2C). Finally the photoresist is stripped and a 140 nm thin fluorocarbon film is deposited on top of the Si stamp by plasma polymerization [19] (Fig. 2D).

PLLA solution (15 %wt) is spin coated on a second Si substrate at 1500 rpm at an acceleration of 1000 rpm/min for 1 min to obtain a film thickness of 50 ± 10 μm. The PLLA film is left for 3 h at ambient temperature to let the solvent evaporate. Then the stamp is embossed into the PLLA at 90 °C with a pressure of 1.9 MPa for 15 min (Fig. 2E). The hot plates of the embossing equipment are cooled down to 60 °C and the PLLA sample and the Si stamp are demolded (Fig. 2F).

2.3. Mechanical punching

2.3.1. Punching tool fabrication

The process used to produce the punching tool is wire electrical discharge grinding (WEDG). In 1985, Masuzawa et al. introduced this technology for manufacturing of different kinds of shapes such as punches, needle shaped parts or electron emitters with high accuracy and good repeatability [20]. The principle behind WEDG is based on electrical discharge machining (EDM) where a rotating electrode is machined by using an unwinding wire electrode. The machine used in the paper is a commercial μ-EDM SARIX machine (Sant'Antonino, Switzerland) and the punching tool is manufactured from the hollow electrode of the machine. The electrode material is tungsten carbide (WC) which possesses high strength and is readily available. The μ-EDM machine consists of a xy table with a spindle that provides the rotation of the electrode and the movement in *z* direction. The movements in *xyz* directions are controlled by an encoder with 1 μm resolution and a dressing wire unit unwinds the wire electrode. The schematic of the machine is shown in Fig. 3A.

The tip of the punching tool should be conical in order to penetrate the substrate smoothly with low force and to achieve a good surface quality for the containers. The geometry of the tool before and after μ-WEDG process is shown in Fig. 3B. The process parameters of μ-WEDG machining influence the geometrical accuracy

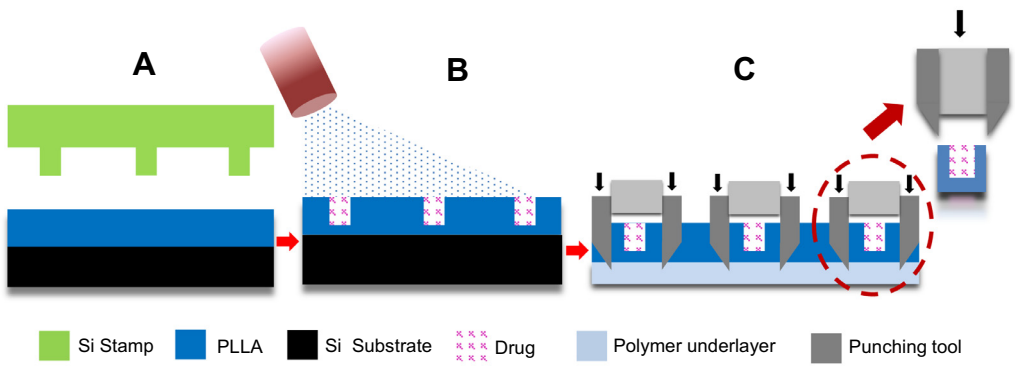

Fig. 1. (A) Formation of holes in PLLA film by hot embossing of Si stamp with pillars, (B) loading of holes with drug, (C) formation of oral drug delivery microcontainers by mechanical punching of the drug loaded polymer holes.

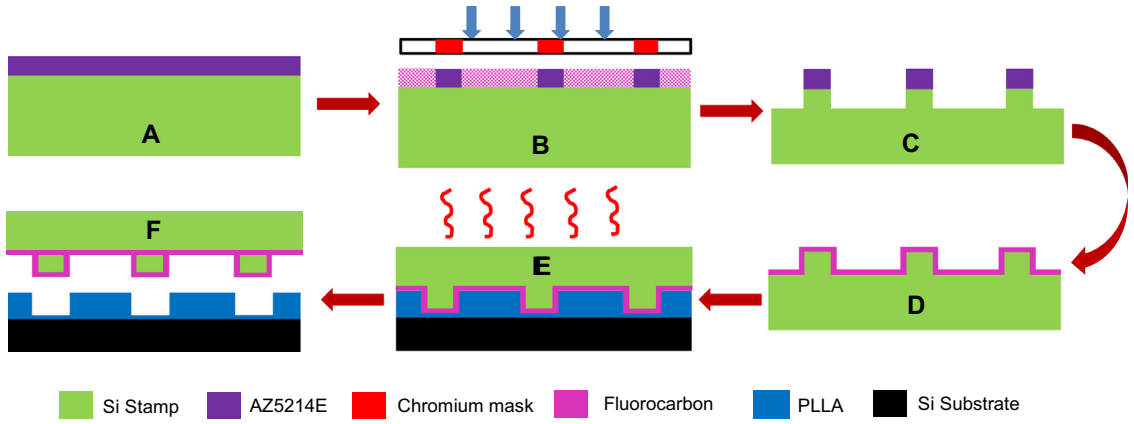

Fig. 2. Fabrication of Si stamp: (A) spin coating of AZ5214E, (B) exposure of AZ5214E, (C) dry etching of Si, (D) resist stripping and fluorocarbon deposition; fabrication of holes: (E) hot embossing of spin coated PLLA layer, (F) demolding.

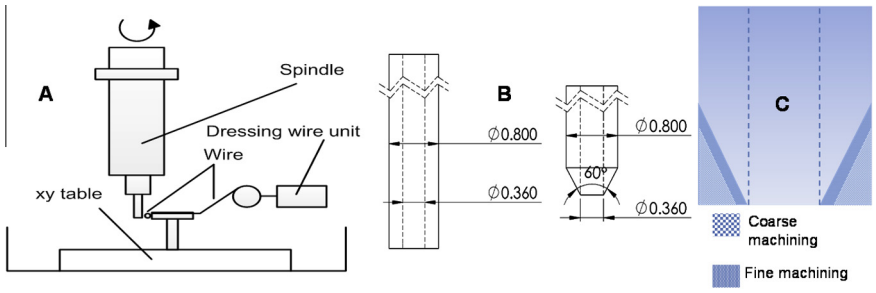

Fig. 3. Formation of punches in WC by μ-WEDG: (A) schematic of μ-WEDG machining, (B) geometry of electrode before and after μ-WEDG process, (C) coarse and fine electrode machining.

and surface quality of the punches to a great extent [21], as well as the fabrication time. The small contact area between wire and rotating electrode leads to low dressing rates and a long manufacturing process. With the fine parameter set of the machine it takes approximately 2 h to fabricate one mechanical punch. In order to increase the efficiency of the process, the electrode is fabricated by coarse machining and fine finishing as shown in Fig. 3C. With this multi-step dressing strategy, the process time is reduced from 2 h to 10 min without compromising the surface quality of the tip of the needle.

After the punches are fabricated, a 3 × 3 array of through-holes is milled in a 2.5 mm thick PMMA plate. The diameter of these through-holes is 800 μm corresponding to the outer diameter of the punches with a center to center distance of 1.2 mm. This distance is twice the center to center distance of the embossed holes. The punches are fitted in these through-holes in the PMMA plate for the punching into polymer films.

2.3.2. Mechanical punching process

First the embossed PLLA layer is delaminated from the Si substrate by immersion in water. After drying, this freestanding layer is fixed to a PMMA backplate using adhesive tape. A soft polymer layer of PVA is placed between the PLLA and PMMA layer. Then, an array of 3 × 3 punches is placed on a microscope stage with the backlight on (Fig. 4A). Next, the stack of PLLA, PVA and PMMA is placed on top of the punches array and aligned using the optical microscope (Fig. 4B). Finally, the optics of the microscope are moved and a weight of 1 kg is placed on the stack to punch out the containers. After removal of the weight, the punched parts are retained in the punching tools leaving behind holes in the PLLA film (Fig. 4C). The stuck polymer microparts can be collected by applying mechanical pressure from the other side either by a wire plunger with a diameter less than the diameter of the hole of the punching tool or by air flow. In our experiments, we use an optical fiber with the diameter of 200 μm to push out the array of 3 × 3 containers (Fig. 4D).

3. Results and discussion

3.1. Hot embossing

Fig. 5A show the fabricated Si stamp and Fig. 5B the successful replication of the Si stamp in the PLLA polymer film using the hot embossing process. The measured dimensions of the stamp and the embossed holes along with the standard deviation are given in Table 1. The height measurements are done by optical and stylus profilometers and the diameters are measured with an optical microscope. The depth of the final holes is around 32 μm, which is lower than the height of the stamp pillars. These measurements together with the non-planar top surface of the PLLA layer in Fig. 5B indicate that the stamp structures are not completely pressed into the polymer film during the hot embossing process.

Furthermore, the demolding is performed at 60 °C, which is close to the glass transition temperature T_g of PLLA [22]. When the polymer is demolded from the Si stamp, there is parasitic recovery of the elastic polymer, lowering the actual depth of the trenches [23]. When the embossing is done at higher temperature of 120 °C followed by demolding at room temperature as described in previous work [11] pattern replication is improved but the Si stamp breaks within 1–2 runs due to higher stress built up during the cooling stage [24]. With lower embossing temperature (90 °C) and higher demolding temperature (60 °C) the stress is reduced

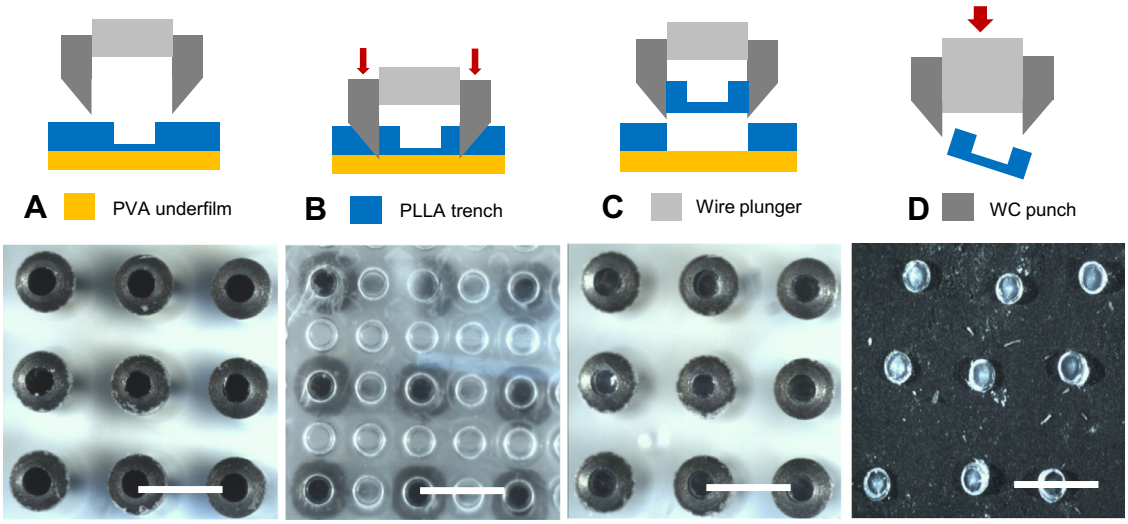

Fig. 4. Mechanical punching process flow and corresponding optical images: (A) array of 3 × 3 punches, (B) alignment of PLLA holes with punches array, (C) punching of PLLA film, (D) released microcontainers (scale bar: 1 mm).

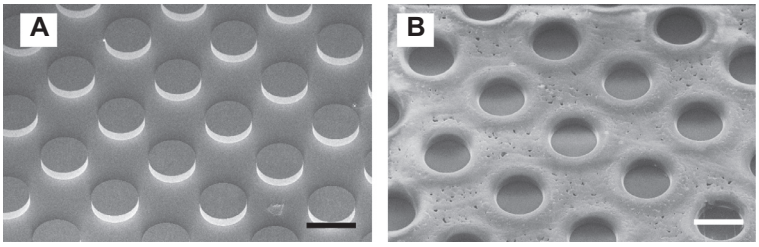

Fig. 5. SEM micrographs of: (A) Si stamp with pillars, (B) PLLA layer with embossed holes (scale bar: 300 μm).

Table 1
Measurement of dimensions of Si stamp pillars and PLLA holes along with the standard deviations in measurements. The diameters were measured using optical microscope and the heights were measured using profilometer.

Measured Parameters	Dimension (μm)
Si stamp pillars diameter	290 ± 3
Si stamp pillars height	44 ± 4
PLLA holes diameter	260 ± 9
PLLA holes depth	32 ± 4
PLLA film thickness	50 ± 10

and demolding facilitated. With this the stamp lasted for at least 8 runs with the tradeoff of slightly affected pattern replication in the PLLA film.

3.2. Mechanical punching

The functionality of the device depends on the punching accuracy due to the fact that the containers need to be preserved for drug delivery. Here, both the fabrication of the punching tool and the punching process itself have to be considered. Fig. 6A depicts four representative punches fabricated by the optimized μ-WEDG process. Several tests are run to verify the repeatability of the fabrication of the punching tool using the μ-WEDG process and the inner and outer diameters of the punches are measured with an optical microscope.

In order for the punching process to be operational, it is assumed that a lateral accuracy of ±20 μm is required. To check the dimensional reproducibility of the punching process, PLLA films with a thickness of 50 μm without any patterns are punched using the punching tools resulting in circular polymer microparts as the one shown in Fig. 6B. The punched polymer microparts are

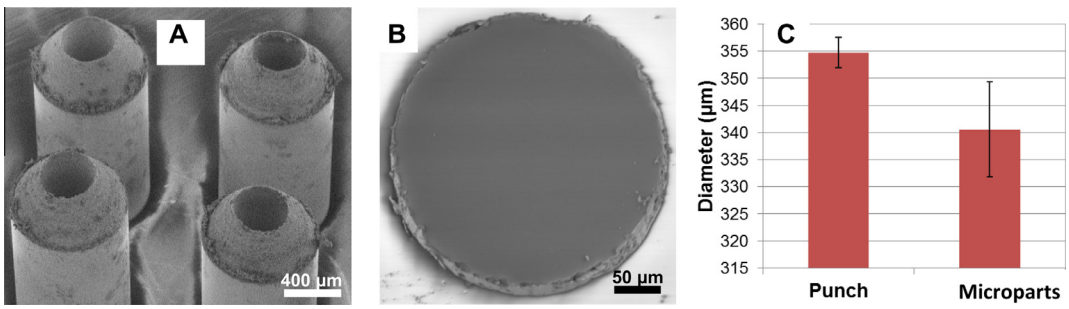

Fig. 6. (A) SEM micrograph 2 × 2 punches array, (B) SEM micrograph of punched polymer, (C) accuracy of punching process.

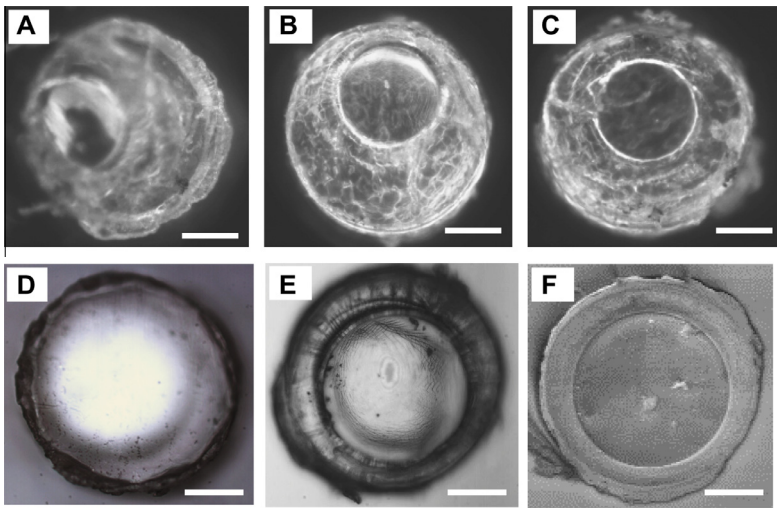

Fig. 7. Alignment of tool to180 μm holes and corresponding optical images: (A) misalignment, (B) off-centered poor alignment, and (C) good alignment, (D) optical image of thin walls of a punched 300 μm hole; fabrication of 3D microcontainer with hole of 260 μm diameter: (E) optical image, and (F) SEM micrograph of microcontainer (scale bar: 100 μm).

observed in a microscope and the diameter of the polymer is analyzed. Fig. 6C shows the results of the characterization of punching tool and punched polymer parts. The measured diameter of the punching tool is 355 ± 3 μm while it is 341 ± 9 μm for the polymer microparts. The results indicate that the process for punching tool fabrication is very repeatable. Furthermore, the total diameter of PLLA that is punched out by the tool is only 15 μm lower than the actual tool dimension, which is considered as an excellent result for punching of soft materials. We have also successfully punched out polymer films with thicknesses of up to 150 μm. The punches have shown good robustness and have lasted for hundreds of punching operations without any structural damage.

For the mechanical punching of the microcontainers, some initial tests are made on holes with diameters of 180 μm and 300 μm. Tool alignment is done for both types of holes and then containers are punched out (Fig. 7A–D). 180 μm diameter holes allowed for more alignment inaccuracy but resulted in too small volume of container. 300 μm diameter holes are difficult to align and failed to give good container walls. When the diameter of the hole is chosen to be 260 μm, enough area is available to align the tool with an inner diameter of 340 μm. With these dimensions, a thick and stable container wall with a width of around 40–50 μm can be achieved. Fig. 7E and F show successful fabrication of 3D microcontainers using hot embossing and mechanical punching.

4. Conclusions

We have successfully fabricated a Si stamp with pillars using the standard Si manufacturing techniques of photolithography and RIE. Then we have demonstrated the fabrication of microholes in biodegradable PLLA polymer films using a hot embossing process. This process can be further optimized to get better replication of the stamp dimensions in the polymer. For the fabrication of 3D microcontainers, a mechanical punching process based on the concept of biopsy punches has been successfully applied. For this purpose, mechanical punches have been produced in a repeatable manner in a robust WC material. Replication of the punch on polymer film during the punching process has been verified. Finally, keeping in mind alignment tolerances of the punch, fabrication of discrete 3D microcontainers in PLLA has been accomplished.

Hence, we have shown that the biopolymer microcontainers can be fabricated by applying hot embossing and mechanical punching. This combination of the two processes can be extended to other kinds of shapes, sizes and polymers. It is a simple technique for fabrication of discrete microparts with higher tolerances. The process has capability to be upscaled for roll-to-roll production. To develop this, an improved design of the mechanical punches and better alignment techniques are needed. Once the process is optimized, the microholes in the polymer can be loaded with drug and punched out to obtain an oral drug delivery device.

Acknowledgements

The authors acknowledge financial support by NAMEC Villum Kann Rasmussen Centre of Excellence and excellent cleanroom support from DTU Danchip, Denmark.

References

[1] Sebastien Henry, Devin V. McAllister, Mark G. Allen, Mark R. Prausnitz, J. Pharm. Sci. 87 (8) (1998) 922–925.
[2] Cynthia L. Stevenson, John T. Santini Jr., Robert Langer, Adv. Drug Deliv. Rev. 64 (14) (2012) 1590–1602.
[3] Shilpa Sant, Sarah L. Tao, Omar Z. Fisher, Qiaobing Xu, Nicholas A. Peppas, Ali Khademhosseini, Adv. Drug Deliv. Rev. 64 (6) (2012) 496–507.
[4] Rebecca S. Shawgo, Amy C. Richards Grayson, Yamen Li, Michael J. Cima, Curr. Opin. Solid State Mater. Sci. 6 (4) (2002) 329–334.
[5] Hariharasudhan D. Chirra, Ling Shao, Natalie Ciaccio, Cade B. Fox, Jennifer M. Wade, Averil Ma, Tejal A. Desai, Adv. Healthcare Mater. (2014).
[6] Kristy M. Ainslie, Tejal A. Desai, Lab Chip 8 (11) (2008) 1864–1878.
[7] Kristy M. Ainslie, Rachel D. Lowe, Tristan T. Beaudette, Lamar Petty, Eric M. Bachelder, Tejal A. Desai, Small 5 (24) (2009) 2857–2863.
[8] Ying Zhang, Hon Fai Chan, Kam W. Leong, Adv. Drug Deliv. Rev. 65 (1) (2013) 104–120.
[9] Lisa Brannon-Peppas, Int. J. Pharm. 116 (1) (1995) 1–9.
[10] Omathanu Pillai, Ramesh Panchagnula, Curr. Opin. Chem. Biol. 5 (4) (2001) 447–451.
[11] Johan Nagstrup, Stephan Keller, Kristoffer Almdal, Anja Boisen, Microelectron. Eng. 88 (8) (2011) 2342–2344.
[12] Stephen J. Pearton, David P. Norton, Plasma Processes Polym. 2 (1) (2005) 16–37.
[13] Jamal Y. Sheikh-Ahmad, Machining of Polymer Composites, Springer, New York, 2009. 300–302.
[14] Paolo Marizza, Stephan S. Keller, Anette Müllertz, Anja Boisen, J. Control. Release 173 (2014) 1–9.
[15] Line Hagner Nielsen, Stephan Sylvest Keller, Keith C. Gordon, Anja Boisen, Thomas Rades, Anette Müllertz, Eur. J. Pharm. Biopharm. 81 (2) (2012) 418–425.
[16] Howard F. Polley, William H. Bickel, Ann. Rheum. Dis. 10 (3) (1951) 277.
[17] Lynlee L. Lin, Tarl W. Prow, Anthony P. Raphael, Robert L. Harrold III, Clare A. Primiero, Alexander B. Ansaldo, H. Peter Soyer, Microbiopsy engineered for minimally invasive and suture-free sub-millimetre skin sampling, F1000Research 2 (2013).
[18] Xuelin Zhu, Tianhong Cui, J. Micromech. Microeng. 21 (4) (2011) 045032.

[19] Stephan Keller, Daniel Haefliger, Anja Boisen, J. Vac. Sci. Technol. B 25 (6) (2007) 1903–1908.
[20] T. Masuzawa, M. Fujino, K. Kobayashi, T. Suzuki, N. Kinoshita, CIRP Ann. Manuf. Technol. 34 (1) (1985) 431–434.
[21] E. Uhlmann, M. Röhner, M. Langmack, Chapter 3 – Micro-EDM. Micromanufacturing Engineering and Technology, William Andrew Publishing, Boston, 2010. p. 39–58.
[22] L.-T. Lim, R. Auras, M. Rubino, Prog. Polym. Sci. 33 (8) (2008) 820–852.
[23] Dirckx Matthew, Taylor H., Hardt D., High-temperature de-molding for cycle time reduction in hot embossing, in: Antec-conference Proceedings, vol. 5, (2007) 2926.
[24] Sunggook Park, Zhichao Song, Lance Brumfield, Alborz Amirsadeghi, Jaejong Lee, Appl. Phys. A 97 (2) (2009) 395–402.

PAPER II

Fabrication of a Ni stamp with high aspect ratio, two-leveled, cylindrical microstructures using dry etching and electroplating

Fabrication of Ni stamp with high aspect ratio, two-leveled, cylindrical microstructures using dry etching and electroplating

2015 J. Micromech. Microeng. 25 055021

(http://iopscience.iop.org/0960-1317/25/5/055021)

IOP Publishing Journal of Micromechanics and Microengineering

J. Micromech. Microeng. **25** (2015) 055021 (11pp) doi:10.1088/0960-1317/25/5/055021

Fabrication of Ni stamp with high aspect ratio, two-leveled, cylindrical microstructures using dry etching and electroplating

Ritika Singh Petersen[1], Stephan Sylvest Keller[1], Ole Hansen[2] and Anja Boisen[1]

[1] DTU Nanotech, Department of Micro- and Nanotechnology, Technical University of Denmark, Building 345E, DK-2800 Kongens Lyngby, Denmark
[2] CINF-Center for Individual Nanoparticle Functionality, Technical University of Denmark, Building 345E, DK-2800 Kongens Lyngby, Denmark

E-mail: risi@nanotech.dtu.dk

Received 14 December 2014, revised 17 February 2015
Accepted for publication 18 February 2015
Published 17 April 2015

Abstract

We describe a process for the fabrication of a Ni stamp that is applied to the microstructuring of polymers by hot embossing. The target devices are microcontainers that have a potential application in oral drug delivery. Each container is a 3D, cylindrical, high aspect ratio microstructure obtained by defining a reservoir and a separating trench with different depths of 85 and 125 μm, respectively, in a single embossing step. The fabrication of the required two leveled stamp is done using a modified DEEMO (dry etching, electroplating and molding) process. Dry etching using the Bosch process and electroplating are optimized to obtain a stamp with smooth stamp surfaces and a positive sidewall profile. Using this stamp, hot embossing is performed successfully with excellent yield and high replication fidelity.

Keywords: nickel stamp, Bosch process, electroplating, hot embossing, microcontainers

(Some figures may appear in colour only in the online journal)

1. Introduction

Concurrent with the development of new NEMS and MEMS techniques, the use of nano- and microstructures and devices for biomedical and pharmaceutical applications has proliferated. The devices were fabricated in standard silicon based materials or photosensitive polymers but recently the focus has changed to biocompatible polymers [1]. For low cost and high throughput processing of polymers, hot embossing has emerged as a viable fabrication method [2]. In order to define devices in polymers using the hot embossing technique, a microfabricated stamp is required. To achieve a reliable, high fidelity embossing, a high quality stamp must be used and the embossing parameters have to be optimized with respect to critical parameters in the application.

The target device in this work is a microcontainer based drug delivery device that has the potential to increase the bioavailability of drugs when taken orally [3]. Such a microcontainer is a two-leveled structure consisting of a cylindrical container bottom and a ring-shaped container wall defining the size of the inner reservoir [4]. Recently, we have for the first time demonstrated the embossing of microcontainers in the biodegradable and biocompatible polymer, poly-L-lactic acid (PLLA) using SU-8 stamps, but alas SU-8 stamps are not robust enough to last more than a few embossing runs [5]. For other applications, new methods for the preparation of stamps in more stable materials like steel, copper or nickel have been developed [6–8]. Among the most frequently used stamp materials, Ni is very robust and can be easily electroplated on a master template to create complex

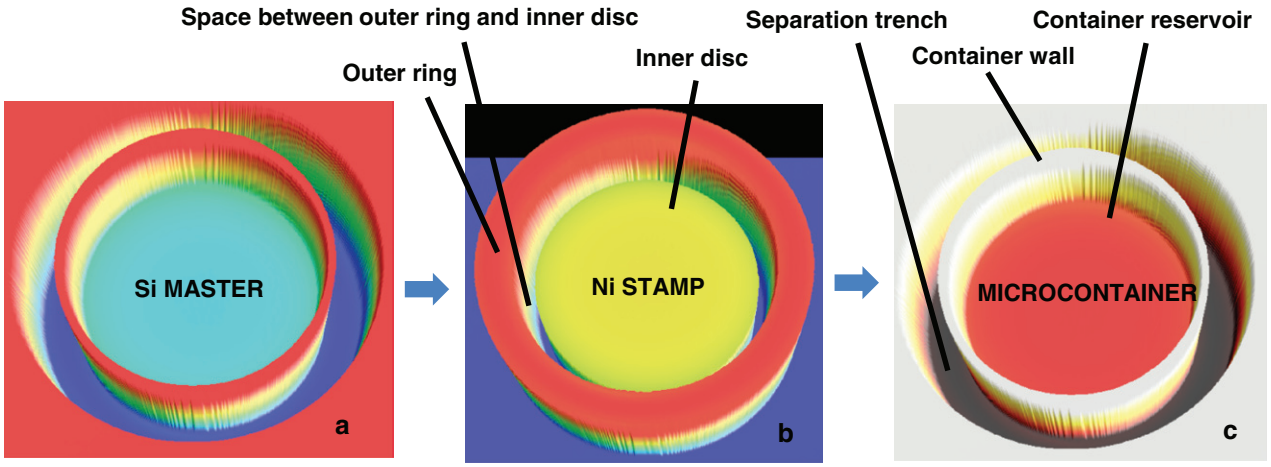

Figure 1. Various features of the stamp and microcontainers and subsequent translation of the Si master (*a*) into a Ni stamp (*b*) and then further into biopolymer microcontainers (*c*) with the inner reservoir, walls around it and the separation trench between the container and the surrounding polymer film.

3D structures at high resolution [9]. Another advantage of a Ni stamp is that it can be used for mass production in roll-to-roll processing [10].

Ni stamps can be fabricated with two well-known processes: LIGA (lithography, electroplating, and molding) [9] or DEEMO (dry etching, electroplating and molding) [11]. In both processes, a master is first fabricated either in photoresist by lithography or in Si by lithography and dry etching. Subsequently, the Ni is electroplated and the master is removed. This electroplated Ni structure is used for embossing in polymers. The availability of photoresists like SU-8 that allow the definition of high aspect ratio structures with very smooth surfaces without the use of expensive x-ray synchrotron lithography makes LIGA a viable option for the preparation of Ni stamps [9]. However, it is very difficult to completely remove the SU-8 master from the electroplated Ni stamp, particularly in narrow trenches, and the resulting increased surface roughness might affect the hot embossing process [12]. Guo *et al* have been able to emboss single level structures with a minimal width of 40 μm and an aspect ratio of eight using a Ni stamp prepared with the LIGA process [13].

In this work a microcontainer fabrication process based on DEEMO has been developed. The concept is illustrated in figure 1, which also defines the terms used throughout the paper. More specifically, we describe in detail the process that was developed for the fabrication of Ni stamps with two-leveled cylindrical microstructures using DEEMO. Tanzi *et al* have fabricated two leveled microdevices with rectangular features using the DEEMO process [14]. Park *et al* presented the fabrication of a two-leveled Ni stamp with cylindrical features [15]. In both cases, the aspect ratio of the microstructures is only around two. Here we show, to the best of our knowledge, for the first time the fabrication of a Ni stamp with two-leveled cylindrical microstructures with vertical dimensions $> 80\,\mu$m and aspect ratio > 8 using an optimized DEEMO process.

In order to obtain a good polymer replication of the stamp, the demolding forces have to be minimized to avoid

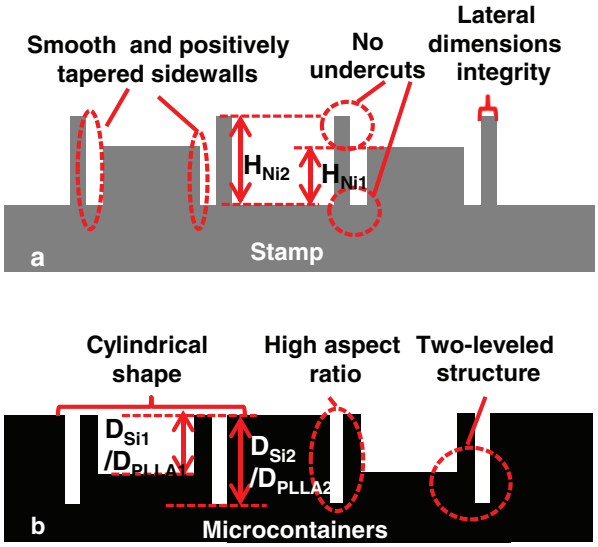

Figure 2. Design considerations and critical dimensions for fabrication of the Ni stamp (*a*) and corresponding microcontainer patterns in Si master or PLLA film (*b*). The two critical dimensions are: the reservoir depth in Si master (D_{Si1}) and PLLA (D_{PLLA1}) or the corresponding inner circle height on the stamp (H_{Ni1}), and the separation trench depth in Si master (D_{Si2}) and PLLA (D_{PLLA2}) or the corresponding height of the outer ring on the stamp (H_{Ni2}).

damage to the replica during stamp removal. This poses a number of requirements for the fabrication of the Ni stamp (figure 2(*a*)): (*a*) the stamp must have very smooth sidewalls to minimize the frictional forces between the polymer structures and the Ni stamp; (*b*) the sidewalls of the stamp should preferably have a positive taper in order to minimize the interlocking forces; (*c*) there should not be any undercut at the top of the features to avoid mechanical interlocking [16].

Due to the high aspect ratio trenches and the depth dimensions of the microstructures (figure 2(*b*)), photolithography, deep reactive ion etching (DRIE) and Si etching after electroplating has to be optimized. Additional challenges that

the design requirements pose during the fabrication process are: (1) the two-leveled geometry poses misalignment and masking issues, (2) the deep circular geometry of the inner reservoir causes problems during the etching of the Si master to release the Ni stamp, and (3) the thin vertical walls of the Si master require minimization of the lateral etch to prevent loss of structural integrity. In order to meet the design requirements of the Ni stamp, the DRIE process for Si was optimized and microstructures with the high aspect ratio of eight could be obtained. Finally, Ni was electroplated to obtain stamps with the required features, smooth surfaces and sidewalls with a positive slope. The Ni stamp was used to emboss microcontainers in PLLA films, and high fidelity replication of the stamp was demonstrated with a process yield of 100%.

2. Methods

2.1. Stamp design

The stamp contains 16 square arrays with 20 × 20 individual stamp units. Each stamp unit corresponds to one microcontainer and thus the stamp design enables the fabrication of 6400 devices in a single embossing run. Figure 1(*b*) shows an individual stamp unit. It consists of two parts, an inner disc and an outer ring structure and there are three important parameters (figures 1(*a*)–(*c*)): (1) The diameter of the inner disk, which translates into the microcontainer reservoir, (2) the space between the inner disc and the outer ring that corresponds to the wall of the container and (3) the width of the outer ring structure, which transforms into the separation trench between the microcontainer and the surrounding polymer film. The inner diameter of the outer ring structure corresponding to the final diameter of the microcontainers is kept constant at 300 μm. To achieve containers with different wall thicknesses of 10, 20, 30, and 40 μm the diameter of the inner disc is varied from 220, over 240, 260, to 280 μm. Furthermore, the width of the outer ring structure is varied from 20, over 30, 40, to 50 μm. The design variations are chosen to evaluate how thin the sidewalls can be made before losing their mechanical stability. These values for the container dimensions have been chosen based on the previous work done [4, 17] and the constraints imposed by the aspect ratio that can be produced in the polymer using a hot embossing process. The PLLA microcontainer with a wall thickness of 10 μm and a reservoir depth of 80 μm possesses a similar volume for a drug as the SU-8 microcontainer discussed in Marizza *et al* and Nielsen *et al* [4, 17].

2.2. Stamp fabrication and hot embossing

The complete process flow is illustrated in figure 3, which includes fabrication of the Si master, stamp, and polymer replica. First a 1 μm thick SiO_2 film is grown on a four-inch (1 0 0) Si wafer using wet thermal oxidation at 1100 °C for 2 h 40 min (figure 3(*a*)). This SiO_2 thickness is required for the oxide layer to act as a mask in the later Si dry etch process. Positive photoresist AZ5214E (1.5 μm thick) is spin coated on a HMDS treated wafer at 4000 rpm and prebaked at 90 °C for 90 s on a hotplate. The AZ5214E is patterned on the oxide layer using a first photolithographic mask. This first mask (base mask) is a dark field glass mask with chrome everywhere except the inner disc and the outer ring. This mask fully defines the lateral geometry of the microstructure. The resist is exposed with a UV dose of 49 mJ cm^{-2} and then developed for 60 s in AZ351B developer (figure 3(*b*)). A short oxygen plasma descum process (O_2 = 200 sccm, N_2 = 70 sccm, at 300 W for 3 min) is run to remove residues of photoresist from the developed areas. The pattern is then transferred into the oxide using a dry etch recipe (figure 3(*c*)) in an STS advanced oxide etcher (AOE). The parameters used in the recipe are as follows: coil power = 1300 W, platen power = 200 W, platen temperature = 0 °C, He flow rate = 174 sccm, C_4F_8 flow rate = 5 sccm, H_2 flow rate = 4 sccm, and pressure = 4 mTorr. After the dry oxide etch, a 1 min dip of the wafers in buffered HF (bHF) is used to remove residues of oxide left in the etched areas. Subsequently, the first layer of photoresist is stripped using plasma ashing with the following parameters: O_2 = 400 sccm, N_2 = 70 sccm, at 1000 W for 15 min (figure 3(*d*)). A second photoresist layer is spin coated on the patterned oxide layer (figure 3(*e*)). This time, the 1.5 μm thick resist is exposed with the dose of 84 mJ cm^{-2} using a second photolithographic mask (separation mask) and developed for 90 s (figure 3(*f*)). This second mask is also a dark field mask with chrome everywhere except the outer ring. After the second photolithography, descum is done at the higher oxygen flow rate of 300 sccm and power of 450 W, while keeping the N_2 flow rate and the time as before.

With the combined patterns of the two masks (SiO_2 and photoresist, respectively), a DRIE of Si is performed to a target depth of about 65 μm (figure 3(*g*)) in an STS Pegasus. Then, the photoresist is stripped and the reservoir pattern in the SiO_2 is exposed (figure 3(*h*)). The second DRIE of Si is then performed to a target depth of another 60 μm (figure 3(*i*)). The etch parameters for both DRIE steps are described in detail in the next section on DRIE optimization. It should be noted here that it is the oxide layer that acts as the pattern defining mask for the DRIE steps. The resist only protects the inner reservoir of the Si master during the first dry etch. To avoid misalignment and minimize the risk of micromasking effects due to redeposition of photoresist debris during the first etch step, the outer rings in the second mask were 10 μm wider than on the first one (figure 3(*f*)). The result of the two DRIE processes is a two level structure in Si (figure 3(*j*)). After removal of the SiO_2 mask in bHF, another layer of 500 nm thick thermal SiO_2 is grown on this two-leveled Si structure and etched in bHF. This step is performed to reduce the sidewall roughness in the form of vertical striations and horizontal scallops due to the Bosch process [18].

Next, the Si master is prepared for electroplating the Ni. First, a thin release layer of around 200 nm of amorphous Si is deposited on the master using low pressure chemical vapor deposition (LPCVD) in SiH_4 at 560 °C for 1 h 20 min (figure 3(*k*)). Then 100 nm of Cr/Au are sputtered to get a conformal metal coating serving as a seed layer for electroplating. Next, 500 μm thick Ni is electroplated in a plating bath of aqueous

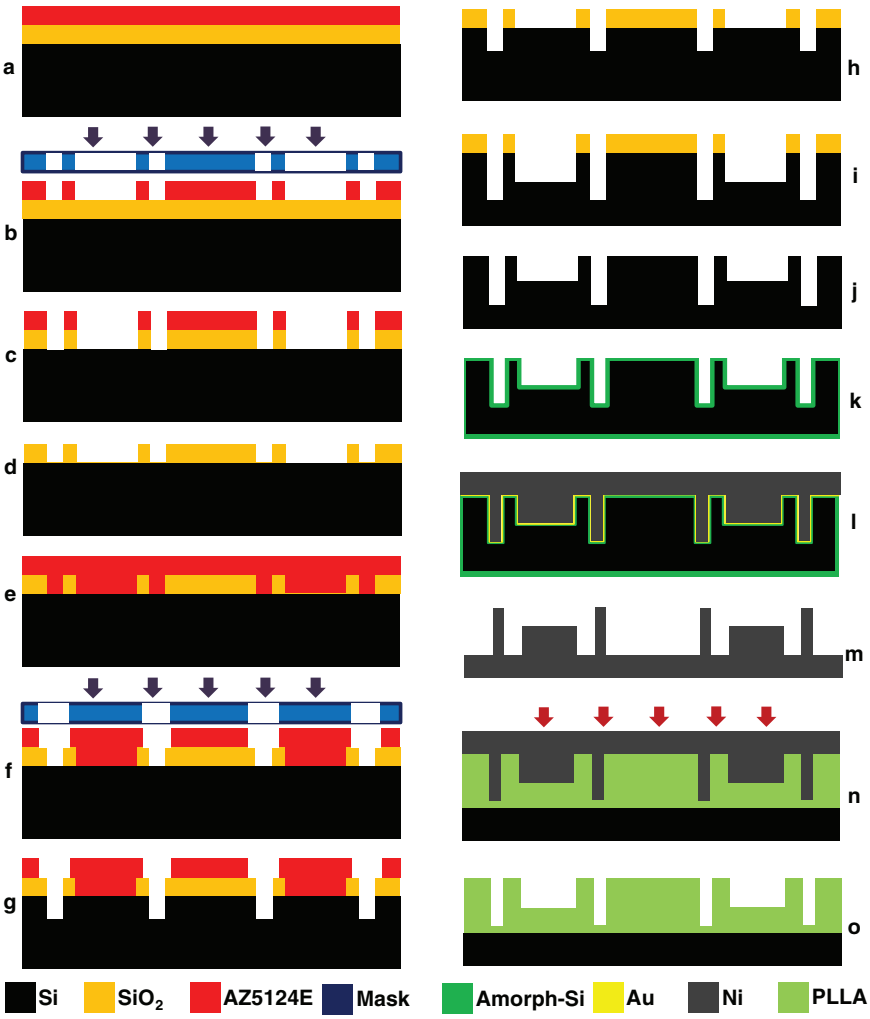

Figure 3. Process flow for the fabrication of Si master, Ni stamp and polymer replica: (*a*) spin coating of photoresist on a thermally oxidized Si wafer; (*b*) exposure of AZ5214E photoresist using base mask and development; (*c*) pattern transfer to silicon dioxide using AOE; (*d*) AZ5214E resist stripping; (*e*) spin coating of second AZ5214E photoresist layer; (*f*) exposure of AZ5214E using separation mask and development; (*g*) first DRIE etch; (*h*) AZ5214E stripping; (*i*) second DRIE etch; (*j*) oxide mask removal, sacrificial oxide growth and sacrificial oxide removal to make sidewalls smoother; (*k*) amorphous Si deposition on Si master; (*l*) Au deposition on Si master and Ni electroplating; (*m*) wet KOH Si etch to release the Ni stamp and coating with fluorocarbon; (*n*) embossing in spin coated PLLA film with the Ni stamp; (*o*) demolding to finish replication of microcontainers in PLLA.

nickel sulphamate, boric acid and sulfamic acid kept at 51 °C and pH 3.5–3.8 (figure 3(*l*)). The current is linearly increased to 0.5 A over 15 min followed by ramping to 1.5 A over an additional 15 min. The current is maintained at 1.5 A for 30 min and increased to the final value of 6.5 A over 15 min. Then the electroplating is continued for approximately 3 h until a final set-point charge of 26.8 Ah is reached. The complete process takes around 12 h to obtain 500 μm thick Ni conformably electroplated on the Si master. The Si master is then etched in 28 wt% KOH at 80 °C for 7–8 h and a released Ni stamp is obtained (figure 3(*m*)). A molecular layer of perfluorodecyltrichlorosilane (FDTS) is deposited on the Ni stamp using molecular vapor deposition (MVD) [19]. This improves the separation of the stamp and the molded polymer replica by reducing the adhesion forces between the two parts [15].

Finally, hot embossing in PLLA is performed. A 15 %wt solution of PLLA in dichloromethane (DCM) is prepared and spin coated on a Si wafer at 500 rpm at an acceleration of 500 rpm min^{-1} for 1 min. This results in a polymer film with a thickness of around 80 μm. Two layers of PLLA solution are spin coated to achieve a thickness of around 150–160 µm. The spin coated wafer is then left for 15 min to allow the solvent to evaporate. The Ni stamp is used to emboss the PLLA film at 90 °C for 15 min 1.9 MPa (figure 3(*n*)) [20]. The pressure is maintained during the cooling stage. The stack of Ni stamp and PLLA film is cooled down to 50 °C, demolding is performed and the microcontainer patterns are replicated in the PLLA (figure 3(*o*)). The entire setup is kept at atmospheric pressure.

2.3. DRIE optimization

To optimize the lithography and etching processes, test wafers were used. These wafers were Si wafers with a 1 μm thick oxide layer patterned with either the base or the separation mask. The parameters for photolithography were the same as

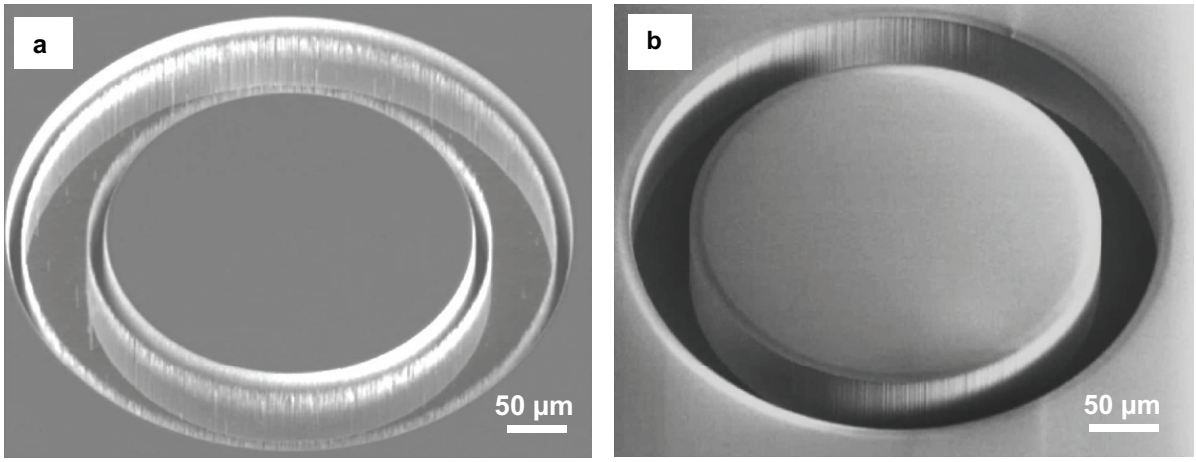

Figure 4. (*a*) Unwanted ring formation during the first DRIE step after isotropic wet etch of the oxide mask in BHF. (*b*) No unwanted ring formation during the first DRIE when dry etch is done for patterning of the oxide mask.

Table 1. Optimization of DRIE process by ramping the etch cycle time and adjusting the number of etch cycles. All the other parameters are kept constant. The duration of the reference cycle in process D is 2.4 s.

Etch cycle time (sec)		Change from reference etch cycle (%)	Number of cycles
First cycle	Final cycle		
2.4	2.64	10	230
2.4	2.52	5	270
2.4	2.46	2.5	290
2.4	2.4	0	300
2.4	2.34	−2.5	310
2.4	2.28	−5	330
2.4	2.16	−10	370
2.46	2.34	2.5 to −2.5	300
2.52	2.28	5 to −5	300
2.64	2.16	10 to −10	300

the ones described for the first lithographic step above. The test structures were used to identify the dry etch parameters that result in smooth but tapered walls, while at the same time minimizing any undercut.

The standard process (called process D), that is recommended by the manufacturer of STS Pegasus, was chosen as the starting point for optimization. The etch cycle of process D has the following parameters: SF_6 = 275 sccm, O_2 = 5 sccm, cycle time = 2.4 s, pressure = 26 mTorr, coil power = 2500 W, platen power = 35 W, temperature = 0 °C. The passivation cycle has the following parameters: C_4F_8 = 150 sccm, cycle time = 2.0 s, pressure = 20 mTorr, coil power = 2000 W, platen power = 0 W, temperature = 0 °C. Initial runs on test wafers using process D were performed and resulted in micrograss formation. Therefore process D was modified by increasing the oxygen flow rate from 5 to 15 sccm.

To optimize the sidewall tapering, the etch cycle time was ramped up and/or down from 2.4 s as detailed in table 1. While keeping all the other parameters constant except the number of cycles, the experiments were done with −10, −5, −2.5, 0, 2.5, 5, 10% change from the standard etch time of 2.4 s. After initial measurements made on the Si test wafers for the calculation of the etch rate, the number of cycles was adjusted to achieve a depth of between 110–130 μm for the separation trench. Micrograss formation had to be avoided at any cost since the surface roughness is more important for the demolding forces than the wall profile [21]. After the optimization on test wafers, the results were used for the fabrication of actual two-leveled microstructures.

3. Results and discussion

3.1. Etch mask patterning and removal

Initially, an isotropic wet etch was performed in bHF solution for 10 min to pattern the SiO_2 etch mask. During the dry etching of Si an unwanted ring was formed very close to the desired structures, as shown in figure 4(*a*). The isotropic nature of the wet etch results in a nonvertical edge of the oxide mask. It was concluded that the ring occurs due to micromasking caused by debris from the oxide layer. Hence, a dry etch was chosen for patterning the oxide layer in order to avoid these micromasking issues. This gave improved results for the test structures, as can be seen in figure 4(*b*). For photoresist stripping too, a dry etch process was preferred compared to wet stripping in acetone in order to remove all photoresist residues.

3.2. DRIE optimization

With the oxygen flow fixed at 15 sccm, the DRIE process optimization was done by ramping the etch cycle as described in table 1. The basic concept behind ramping the etch cycle time is to vary the relative etch and passivation rates [22, 23]. Alternatively, this ratio could also be changed by ramping etch and passivation gas flows [22–24]. Figure 5 shows the result of some of the optimization performed in this work. When the etch time was ramped down from 2.4 to 2.16 s (−10%), increased roughness close to the walls and formation of tall micrograss can be observed (figure 5(*a*)). When the etch cycle was kept constant at 2.4 s (0%), roughness at the bottom of the walls could be seen (figure 5(*b*)). However,

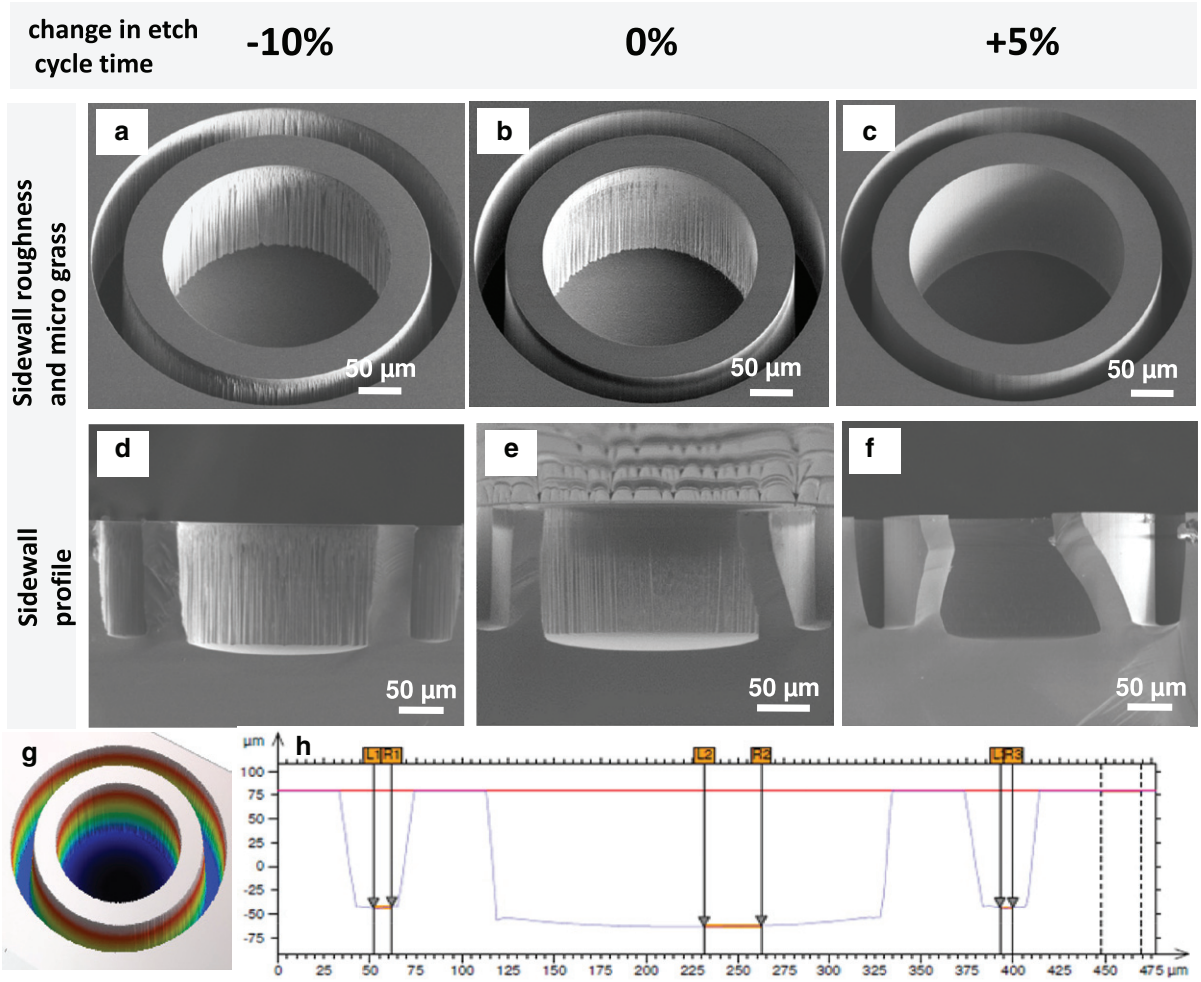

Figure 5. SEM images of 40 μm wall microcontainers with a separation trench width of 30 μm, illustrating the effect of etch cycle ramping on the surface roughness (*a*)–(*c*) and sidewall tapering (*d*)–(*f*). (*a*) and (*d*) represent −10%, (*b*) and (*e*) represent 0% and (*c*) and (*f*) represent +5% changes in etch time from standard 2.4 s. 3D optical profilometer analysis (*g*). The DRIE process was optimized to get smooth and positively tapered wall profiles as shown in the optical profilometer line scan (*h*).

when the etch cycle was ramped up from 2.4 to 2.56 s (+5%), micrograss formation could be completely avoided (figure 5(*c*)). For the change of −10% and 0% in the etch cycle, the roughness increased because of the incomplete removal of the passivation layer during the etch cycle. The absence of micrograss for 5% can be attributed to the complete removal of the passivation layer deposited in the previous passivation cycle during the etch cycle. However, ramping up (+5%) resulted in completely vertical sidewalls, a slight undercut at the top of the structure and larger scallop sizes. However, ramping down (−10%) resulted in positive tapering of sidewalls at the cost of increased surface roughness and micrograss formation (figures 5(*d*)–(*f*)).

Using these results, it was decided to ramp down the etch cycle from 2.52 to 2.28 s for 300 cycles. When ramping from 2.52 to 2.28 s, the process started with a longer etch cycle time compared to the standard process D, thereby allowing smooth wall formation (figure 5(*g*)) while the ramping down of the etch time allowed the formation of a positive profile (figure 5(*h*)). From the optical profiler measurements, it can be concluded that aspect ratio dependent etching (ARDE) occurred. The center reservoir of the Si master which has a diameter ranging from 220–280 μm etched faster than the thin separation trench with a width of 20–50 μm. This difference in etch depth was around 20 μm. Taking ARDE into account, after some corrections for etch rate, 150 cycles for each dry etch step were chosen such that separation trench depth of around 120 μm and a reservoir depth of around 80 μm could be achieved.

Finally, the dependency of the etch process on the mask material was evaluated. While keeping all the parameters constant, only the masking layer was changed. Two types of test wafers were fabricated, either with the patterned oxide layer or with the resist layer as the main masking layer. No apparent difference between the wafers was observed in SEM and it was concluded that the masking material should not have a significant impact on the microstructures for the selected process parameters.

3.3. Si master fabrication

The experiments were transferred from the test structures to the actual process with two etching steps to achieve the

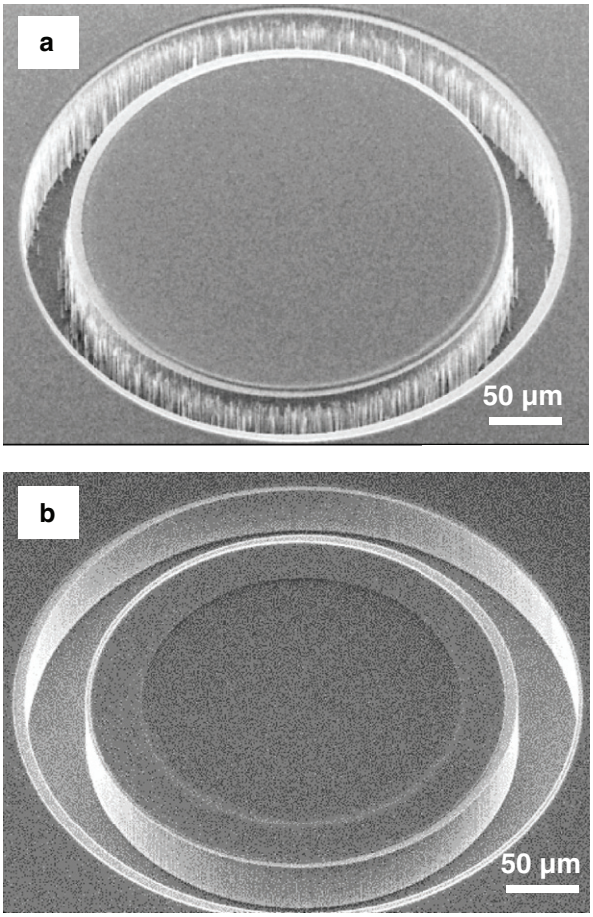

Figure 6. (*a*) Micrograss close to the walls after the first step of DRIE. (*b*) Improved structures after the first step of DRIE for the same etch parameters with modified second photolithography.

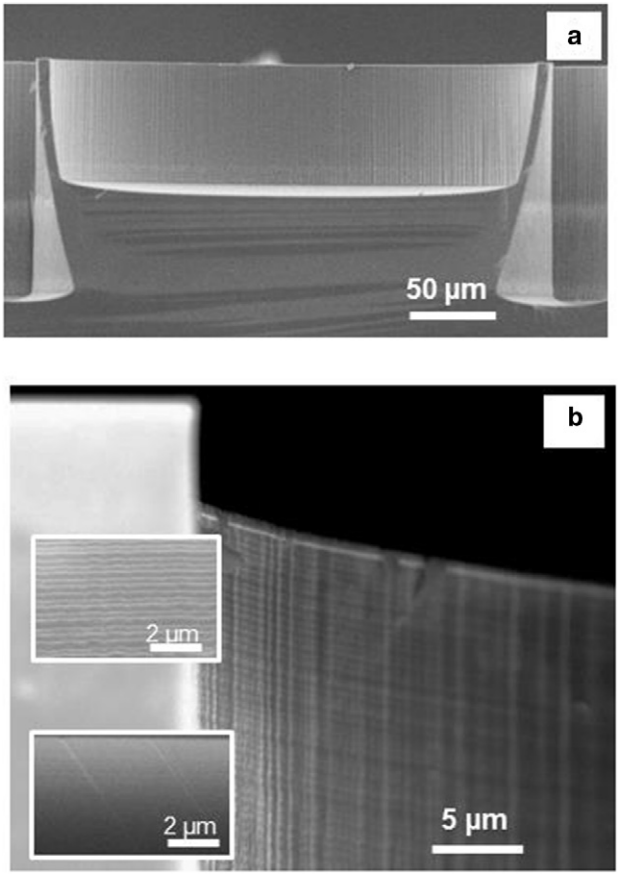

Figure 7. (*a*) SEM image showing a positive sidewall profile for the Si master with 10 μm wall thickness and 40 μm separation distance, after 300 cycles of two-step DRIE etch. (*b*) Roughness of the walls of the Si master: upper inset—without any surface treatment, and lower inset—with the oxide cleaning.

two-leveled structure. In a first run, the parameters for both photolithographic steps were kept the same with an exposure dose of 49 mJ cm^{-2} and a development step of 60 s. However, after the first DRIE step, high roughness and micrograss were seen (figure 6(*a*)), which deteriorated the structures even further during the second etch step. This roughness arises from incomplete development of the photoresist during the second photolithography step. Compared to the test structures, the second photoresist layer is spin coated on a substrate with an oxide layer with 1 μm deep trenches. Thus, when it is exposed and developed, residues are left at the edges of the trenches, which results in micromasking and increased roughness during the DRIE step. The second photolithography step was modified accordingly. The 1.5 μm thick AZ resist was exposed at a higher dose of 84 mJ cm^{-2} and developed for longer time (90 s). The descum was made harsher by increasing the oxygen flow rate (300 sccm) and power (450 W) while keeping the rest of the parameters constant. Even though more resist was sacrificed in the descum process by this measure, the remaining thickness was still sufficient to protect the reservoir of the Si master during the first DRIE step of 150 cycles. With the modified photolithography steps, the microstructures improved considerably and results identical to the test wafers could be obtained (figure 6(*b*)).

The etch cycle time was ramped from 2.52 to 2.4 s for the first 150 cycles. The photoresist was stripped and then the second etch was ramped from 2.4 to 2.28 s for the next 150 cycles. By ramping the etch cycle like this a positive taper with an angle of around 87.8° was obtained as shown in the cross section image (figure 7(*a*)). It is important that after the stripping of the photoresist, the second DRIE process starts with a passivation cycle. In the oxygen plasma both the resist and the fluorocarbon passivation on the walls of the Si structure are removed. Without an initial passivation cycle, the first etch cycle of the second DRIE step starts etching the newly exposed walls, which results in high surface roughness.

With the optimized DRIE process, without any additional surface treatment, we achieved scallops that are around 50 nm tall as shown in figure 7(*b*) (upper inset). Apart from the scallops that appear due to the Bosch etching process, vertical striations due to line edge roughness of the etch mask are visible. This effect is enhanced after the plasma etching of the oxide layer and continues to increase further during DRIE [25, 26]. It has been shown that, after the dry etching and mask oxide removal, the rough surfaces can be smoothed significantly by wet etches such as an isotropic Si etch [27]. Another interesting technique is to grow 500 nm oxide on top of the

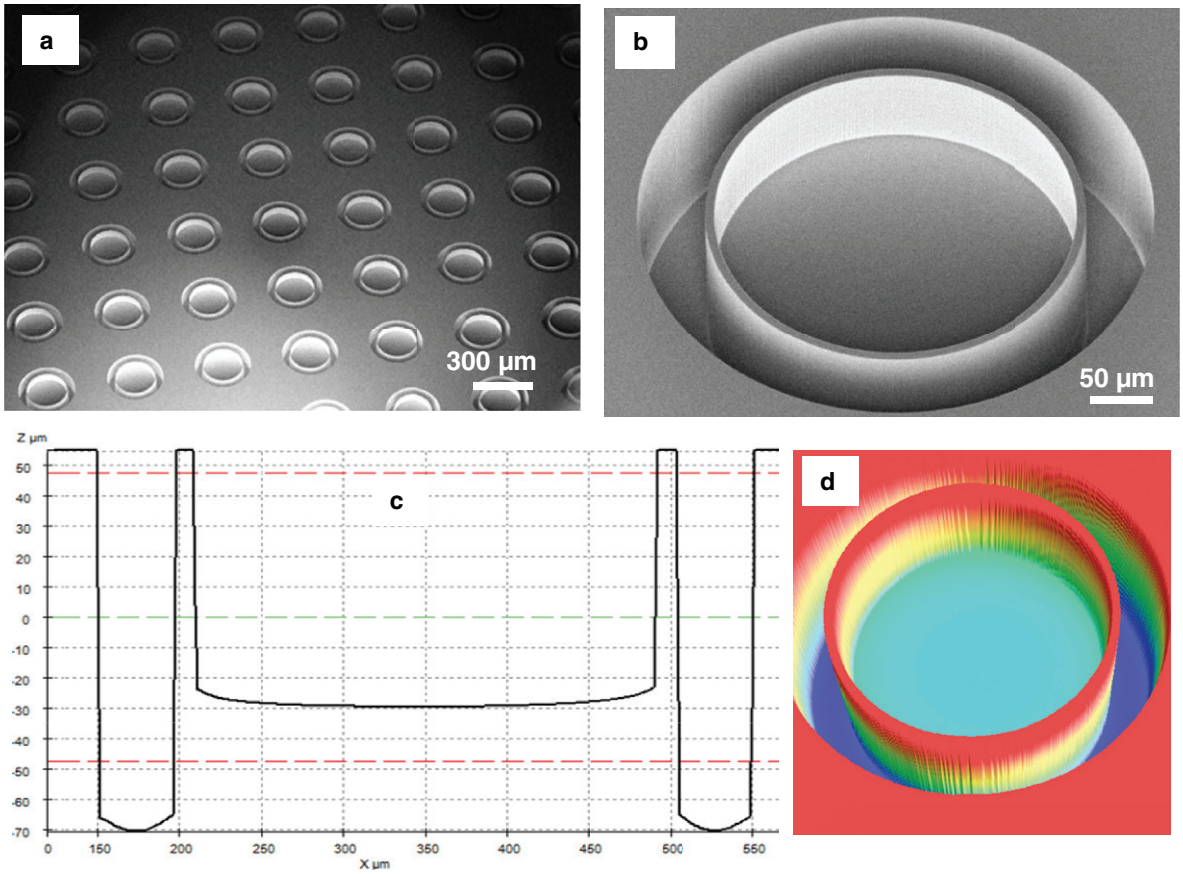

Figure 8. (*a*) Final Si master with 10 μm wide walls and 50 μm wide separation trench. (*b*) Close up view of one structure on the Si wafer. (*c*) 3D optical profilometer analysis. (*d*) Optical profilometer line scan.

Si master and then etch this sacrificial oxide. In this way, the rough corners of Si, those which have been consumed when growing the oxide layer, can be removed. In figure 7(*b*) (lower inset), it can be observed that after the sacrificial oxide growth and etching process, the sidewalls of the structure have become substantially smoother.

The final Si master is shown in figures 8(*a*) and (*b*). The etched structures have smooth walls and a high aspect ratio. Figure 8(*c*) shows the cross sectional profile obtained with a PLu Neox 3D Optical Profiler from Sensofar. The total depth of the separation trenches is measured to be 125 μm with the reservoir depth being 85 μm. Thus for a 10 μm thick wall, a high aspect ratio of close to eight is achieved.

3.4. Ni stamp fabrication

After fabrication of the Si master the Ni is electroplated. This is followed by the removal of the Si master in KOH. Since the geometry of the microcontainers is cylindrical, the Si etch stops on the {1 1 1} planes as shown in figure 9(*a*). Since alkaline solutions all have a low etch rate in {1 1 1} planes, polysilicon etch solutions (HF/H_2O + an oxidizing acid like HNO_3) were considered to remove the remaining Si at a reasonable rate. However, these wet etch solutions also etch Ni [28]. Instead, dry etching of the remaining {1 1 1} Si plane in CF_4 plasma was tried but this process left a thin layer of residues on the stamp surface, as shown in figure 9(*b*), since fluorine reacts with Ni.

Finally, an alternative approach was developed where a thin release layer was deposited on the Si master prior to the Ni electroplating. Since it was undesirable to increase the roughness of the Si surface, a 400 nm layer of LPCVD polysilicon is deposited at a very low temperature of 560 °C, where it becomes almost amorphous. The roughness of the amorphous Si layer on a standard Si wafer evaluated using ellipsometry was 2 nm. Thus, deposition of the amorphous Si release layer adds negligibly to the overall roughness of the Si master sidewalls. After the release layer deposition, deposition of a Cr/Au seed layer and then Ni electroplating proceeded as described above. During the KOH etch, the KOH attacks the amorphous Si and then the {1 1 1} residues are eroded. As a result a Ni stamp with smooth walls and positive sidewall profile is achieved as shown in figures 10(*a*)–(*b*).

3.5. Hot embossing and structure replication

As described in section 2.1, the diameter of the inner disc is varied from 220, over 240, 260, to 280 μm and the width of the outer ring structure is varied from 20, over 30, 40, to 50 μm on the Ni stamp. The effect of these variations on the etch depth on the Si master and subsequent Ni stamp and PLLA microcontainer replication has been analyzed using an optical

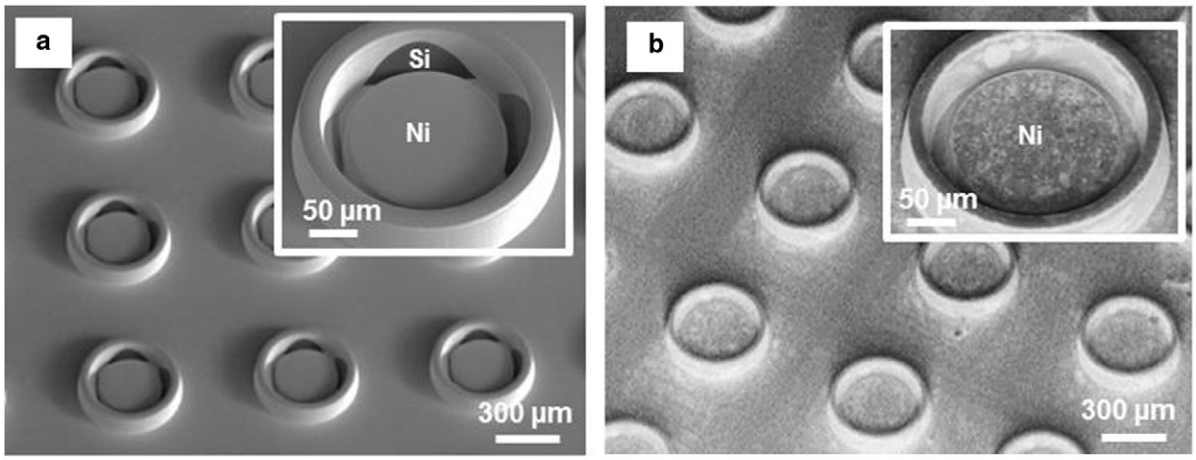

Figure 9. (*a*) SEM image showing remaining unetched Si {1 1 1} planes after electroplating Ni and attempted release in KOH. Inset: close up of one structure. (*b*) Dry etching of Si {1 1 1} planes after electroplating and KOH release. Inset: close up of one structure.

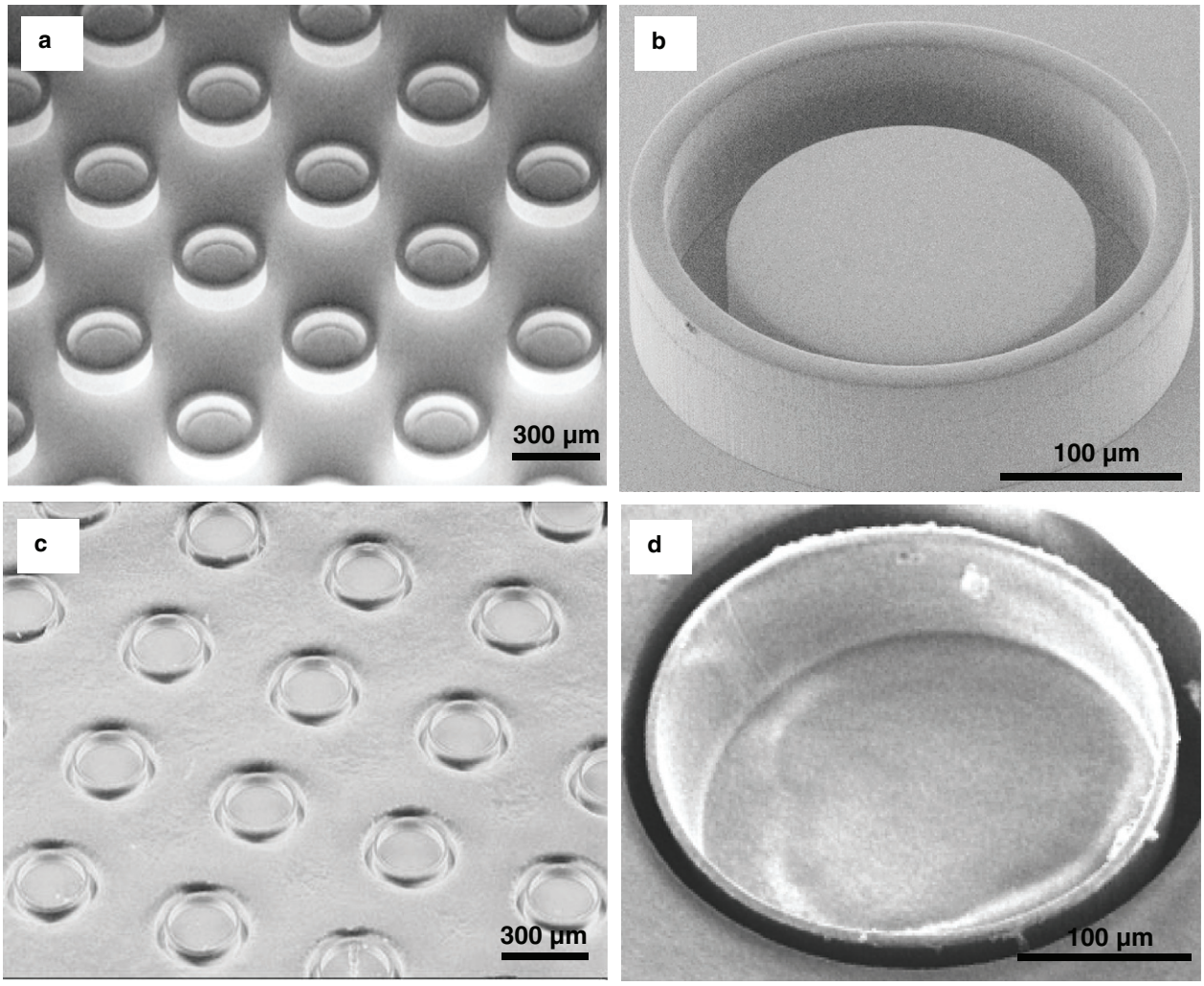

Figure 10. (*a*) SEM micrograph of final Ni stamp. (b) Close up of one structure on Ni stamp (220 μm inner disc and 30 μm separation distance). (*c*) Imprinted microcontainer in PLLA. (*d*) Close up of one microcontainer (10 μm walls and 20 μm separation distance).

profilometer. There are two dimensions we are mainly interested in: the reservoir depth in the Si master (D_{Si1}) and the PLLA (D_{PLLA1}) or the corresponding inner circle height on the stamp (H_{Ni1}), and the separation trench depth in the Si master (D_{Si2}) and PLLA (D_{PLLA2}) or the corresponding height of the outer ring on the stamp (H_{Ni2}), as depicted in figure 3. As shown in figure 11, it can be observed that there are minor variations in the total etch depth of the reservoir and separation

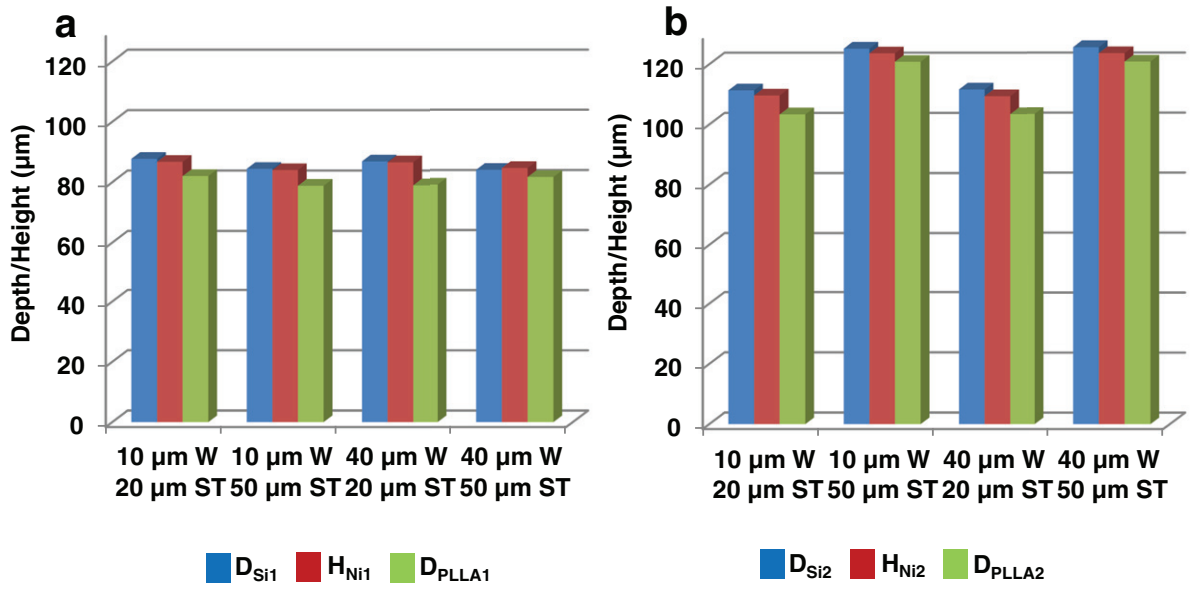

Figure 11. Measurements and comparison of the critical dimensions on Ni stamp and in Si master and PLLA using optical profiler (W = wall, ST = separation trench): (*a*) the reservoir depth in Si master (D_{Si1}) and PLLA (D_{PLLA1}) or the corresponding inner circle height on the stamp (H_{Ni1}). (*b*) The separation trench depth in Si master (D_{Si2}) and PLLA (D_{PLLA2}) or the corresponding height of the outer ring on the stamp (H_{Ni2}). The standard error is $< 1\,\mu$m for all the samples and is not shown in the graph.

trench in the Si master. The design variations of the patterns in the mask lead to the variations in etch depth of the Si master due to ARDE [29]. Since the aspect ratio for the separation trench is more than the aspect ratio for the reservoir, the differences in the depth are higher for the former. When the replication of the Ni stamp from the Si master and the PLLA microcontainer from the Ni stamp is considered (figure 10(*c*)), it can be seen that there is good replication fidelity (figure 11). We have successfully replicated all the microstructures with varying dimensions on the Ni stamp into the PLLA film. This includes fabrication of microcontainers with 10 μm wall thickness with an aspect ratio of eight (figure 10(*d*)).

4. Conclusion and outlook

We have successfully fabricated a Ni stamp with two-leveled cylindrical microstructures for hot embossing in polymers. For this purpose, we have optimized the fabrication process flow and, in particular, the deep reactive ion etch process. The standard Bosch process is optimized by ramping the etch time and modifying the oxygen flow. Finally, microstructures with the desired features: smooth walls, positive taper, minimum undercut and no lateral etch, are fabricated in Si to obtain a master. On this master, Ni is electroplated and a Ni stamp is achieved. This stamp is then molded into PLLA polymer films and good high fidelity replication of the Ni stamp is observed for trenches with a width of 20 μm and a depth of 120 μm, and for walls with a width of 10 μm and a height of 85 μm. Hence, microcontainers are successfully fabricated in a biopolymer layer. In future, the Ni stamp can be fabricated as thin shims for roll-to-roll printing in order to mass produce oral drug delivery microcontainers. The process can be easily used for various kinds of shapes, sizes and dimensions with minor changes in the process flow.

Acknowledgments

We would like to acknowledge financial support by NAMEC Villum Kann Rasmussen Centre of Excellence (65286) and by the Danish National Research Foundation's Center for Individual Nanoparticle Functionality (DNRF54). We would also like to thank the Danchip staff for their support in developing the process flow, especially Chantal Silvestre for her guidance with the optical profiler and Frederik Stöhr for his help with the DRIE process.

References

[1] Ying Z, Chan H F and Leong K W 2013 Advanced materials and processing for drug delivery: the past and the future *Adv. Drug Deliv. Rev.* **65** 104–20
[2] Matthias W 2009 *Hot Embossing: Theory and Technology of Microreplication* (Burlington, MA: William Andrew)
[3] Chirra H D, Shao L, Ciaccio N, Fox C B, Wade J M, Ma A and Desai T A 2014 Planar microdevices for enhanced *in vivo* retention and oral bioavailability of poorly permeable drugs *Adv. Healthcare Mater.* **3** 1648–54
[4] Nielsen L H, Keller S S, Gordon K C, Boisen A, Rades T and Müllertz A 2012 Spatial confinement can lead to increased stability of amorphous indomethacin *Eur. J. Pharm. Biopharm.* **81** 418–25
[5] Nagstrup J, Keller S, Almdal K and Boisen A 2011 3D microstructuring of biodegradable polymers *Microelectron. Eng.* **88** 2342–4
[6] Chen Z, Gao Y, Su R, Li C and Lin J 2003 Fabrication and characterization of poly (methyl methacrylate) microchannels by *in situ* polymerization with a novel metal template *Electrophoresis* **24** 3246–52
[7] Červenka P, Schrott W, Slouka Z, Přibyl M and Šnita D 2012 Hybrid gold–copper stamp for rapid fabrication of microchips *Microelectron. Eng.* **98** 548–51

[8] Ansari K, van Kan J A, Bettiol A A and Watt F 2006 Stamps for nanoimprint lithography fabricated by proton beam writing and nickel electroplating *J. Micromech. Microeng.* **16** 1967
[9] Becker E W, Ehrfeld W, Hagmann P, Maner A and Münchmeyer D 1986 Fabrication of microstructures with high aspect ratios and great structural heights by synchrotron radiation lithography, galvanoforming, and plastic moulding (LIGA process) *Microelectron. Eng.* **4** 35–56
[10] Chang CY, Yang S Y and Sheh J L 2006 A roller embossing process for rapid fabrication of microlens arrays on glass substrates *Microsyst. Technol.* **12** 754–9
[11] Elders J, Jansen H V, Elwenspoek M and Ehrfeld W 1995 DEEMO: a new technology for the fabrication of microstructures *Micro Electro Mechanical Systems, MEMS '95* (*Amsterdam, the Netherlands, January 29–February 2 1995*) 238–43
[12] Dentinger P M, Clift W M and Goods S H 2002 Removal of SU-8 photoresist for thick film applications *Microelectron. Eng.* **61** 993–1000
[13] Guo Y, Liu G, Xiong Y, Wang J, Huang X and Tian Y 2007 Study of hot embossing using nickel and Ni–PTFE LIGA mold inserts *J. Microelectromech. Syst.* **16** 589–97
[14] Tanzi S, Østergaard P F, Matteucci M, Christiansen T L, Cech J, Marie R and Taboryski R 2012 Fabrication of combined-scale nano-and microfluidic polymer systems using a multilevel dry etching, electroplating and molding process *J. Micromech. Microeng.* **22** 115008
[15] Park I-S, Kim J-S, Na S-H, Lim S-K, Oh Y-S and Suh S-J 2010 Fabrication of a two-step Ni stamp for blind via hole application on PWB *Microelectron. Eng.* **87** 1707–10
[16] Delaney K D, Bissacco G and Kennedy D 2012 A structured review and classification of demolding issues and proven solutions *Int. Polym. Process.* **27** 77–90
[17] Marizza P, Keller S S, Müllertz A and Boisen A 2014 Polymer-filled microcontainers for oral delivery loaded using supercritical impregnation *J. Control. Release* **173** 1–9
[18] Juan W-H and Pang S W 1996 Controlling sidewall smoothness for micromachined Si mirrors and lenses *J. Vac. Sci. Technol.* B **14** 4080–4
[19] Srinivasan U, Houston M R, Howe R T and Maboudian R 1998 Alkyltrichlorosilane-based self-assembled monolayer films for stiction reduction in silicon micromachines *J. Microelectromech. Syst.* **7** 252–60
[20] Petersen R S, Mahshid R, Andersen N K, Keller S S, Hansen H N and Boisen A 2014 Hot embossing and mechanical punching of biodegradable microcontainers for oral drug delivery *Microelectron. Eng.* **133** 104–9
[21] Kawata H, Kubo K, Watanabe Y, Sakamoto J, Yasuda M and Hirai Y 2010 Effects of mold side wall profile on demolding characteristics *Japan. J. Appl. Phys.* **49** 06GL15
[22] Chen K-S, Ayón A A, Zhang X and Spearing S M 2002 Effect of process parameters on the surface morphology and mechanical performance of silicon structures after deep reactive ion etching (DRIE) *J. Microelectromech. Syst.* **11** 264–75
[23] Wang L, Liang D, Wang Y-S and McVittie J P STSetch2 profile characterization-undercut investigation for silicon trench etching in STSetch2
[24] Wu B, Kumar A and Pamarthy S 2010 High aspect ratio silicon etch: a review *J. Appl. Phys.* **108** 051101
[25] Shin J, Han G, Ma Y, Moloni K and Cerrina F 2001 Resist line edge roughness and aerial image contrast *J. Vac. Sci. Technol.* B **19** 2890–5
[26] Constantoudis V, Kokkoris G and Gogolides E 2013 Micro/Nano lithography resist roughness plays a key role in pattern transfer *SPIE. Newsroom* doi:10.1117/2.1201303.004738
[27] Lee K K, Lim D R, Kimerling L C, Shin J and Cerrina F 2001 Fabrication of ultralow-loss Si/SiO_2 waveguides by roughness reduction *Opt. Lett.* **26** 1888–90
[28] Williams K R, Gupta K and Wasilik M 2003 Etch rates for micromachining processing-Part II *J. Microelectromech. Syst.* **12** 761–78
[29] Yeom J, Wu Y and Shannon M A 2003 Critical aspect ratio dependence in deep reactive ion etching of silicon *TRANSDUCERS, Solid-State Sensors, Actuators and Microsystems, 12th Int. Conf.* (*Boston, MA USA, 8–12 June 2003*) vol 2 pp 1631–4

Paper III

Hot punching of high-aspect-ratio 3D polymeric microstructures for drug delivery

Lab on a Chip

COMMUNICATION

View Article Online
View Journal | View Issue

Cite this: *Lab Chip*, 2015, **15**, 2576

Received 21st February 2015,
Accepted 7th May 2015

DOI: 10.1039/c5lc00372e

www.rsc.org/loc

Hot punching of high-aspect-ratio 3D polymeric microstructures for drug delivery†

Ritika S. Petersen,* Stephan S. Keller and Anja Boisen

Hot punching with two different strategies has been demonstrated as a new method of fabricating high aspect ratio 3D microstructures for drug delivery. It has been shown that this process is highly versatile with good replication fidelity and yield.

Oral drug delivery is the most preferable route of drug delivery. This is due to the ease of administration, flexibility in dosage and most importantly, patient compliance.[1] However, there are challenges with this route of delivery. These are non-specificity of the drug, degradation in the acidic environment of the stomach and low drug stability resulting in an overall low bioavailability of active ingredients.[2,3] With the recent developments in microelectromechanical systems (MEMS) technology, there has been high impetus in developing new microfabricated oral drug delivery systems (DDS) like micropatches, microreservoirs and micropore based devices.[4,5] For example, Desai *et al.* have shown in the past years, that microfabricated containers are an oral DDS that can potentially increase the bioavailability of the loaded drug.[6,7] The first of these microfabricated DDS were produced in conventional materials such as Si, poly(methyl methacrylate) (PMMA) and photoresists.[8–10] In the last years, there have been efforts to fabricate such oral drug delivery microdevices in biocompatible and biodegradable polymers like poly-L-lactic acid (PLLA), polycaprolactone (PCL), poly(lactic-co-glycolic acid) (PLGA) approved by the US Food and Drug Administration (FDA) for applications in oral drug delivery.[11,12] In order to fabricate discrete microstructures in such polymers, various fabrication techniques have been developed. DeSimone *et al.* introduced the PRINT technique which uses molding in a polymer stamp to produce microscale and sub-microscale structures.[13,14] Guan *et al.* describe a process to produce foldable hydrogels for drug delivery applications.[15]

Department of Micro- and Nanotechnology, Technical University of Denmark, Building 345B, Kongens Lyngby DK-2800, Denmark. E-mail: risi@nanotech.dtu.dk

† Electronic supplementary information (ESI) available: Experimental section on materials, device fabrication and characterization. See DOI: 10.1039/c5lc00372e

Hot embossing is a suitable technique for the fabrication of microstructures in polymers since it is a simple, low cost and scalable process with high structural replication fidelity. However, the residual layer that remains after the hot embossing process poses a challenge to produce discrete microstructures. Some methods to overcome this limitation and remove the residual layer have been introduced in the past including reactive ion etching or laser machining but these processes might affect the material properties of the biopolymer.[16,17] Kuduva-Raman-Thanumoorthy *et al.* describe a punching process after hot embossing to get discrete three-dimensional (3D) structures using a special set-up.[18] Heckele *et al.* introduced bilayer embossing with a device layer on a sacrificial layer. However, this process requires precise control of the penetration depth of the stamp in the sacrificial layer and careful selection of the device and sacrificial layers in order to avoid delamination.[19]

In this paper, we introduce hot punching as a modified hot embossing process to obtain individual biopolymer microcontainers for oral drug delivery applications. These microcontainers are 3D structures with a bottom and high aspect ratio walls forming a reservoir with a volume in the nanoliter range. The overall concept of hot punching is illustrated in Fig. 1. The process starts with the deposition of a PLLA device layer on an elastic polydimethylsiloxane (PDMS) layer (Fig. 1A1 and B1). After that, the device layer is molded by a robust Ni stamp and at the same time punched due to the presence of the underlying elastic layer (Fig. 1A2 and B2). Once the punching process is finished the microcontainers are separated from the rest of the PLLA film. Depending on the surface pretreatment of PDMS before deposition of the PLLA layer, these microstructures either remain on the underlying PDMS layer (process A, Fig. 1A3 and A4) or are transferred to a sacrificial layer such as a water soluble poly acrylic acid (PAA) layer by thermal bonding (process B, Fig. 1B3 to B7). The hot punching process has several major benefits for fabrication of discrete microstructures: i) the residual layer is penetrated during a single thermal

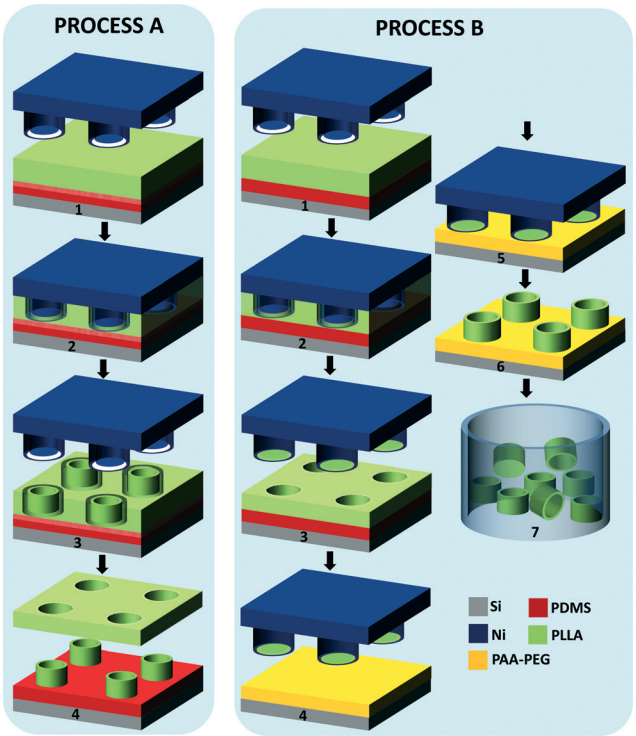

Fig. 1 Process A-Hot punching process to fabricate microcontainers on PDMS: A1. Spin coated PLLA film on ozone treated hydrophilic PDMS layer; A2. Hot embossing leading to punching of PLLA containers from the surrounding film; A3. Demolding of the stamp leaving the punched microcontainers on the PDMS layer along with the surrounding polymer film; A4. Hydrophobic recovery of PDMS layer, PLLA containers ready to be collected after peeling of interconnecting film. Process B-Hot punching process to fabricate microcontainers on a PAA–PEG sacrificial layer: B1. Spin coated PLLA film on untreated PDMS layer; B2. Hot embossing leading to punching of PLLA containers from the surrounding film; B3. Demolding of the stamp leaving the microcontainers attached to the Ni stamp; B4. Spin coating of PAA–PEG solution on Si substrate; B5. Thermal bonding of containers in Ni stamp to sacrificial PAA–PEG layer; B6. Individual microcontainers transferred on PAA–PEG layer after bonding; B7. Released microcontainers floating in water.

embossing step without formation of residues and without need of additional equipment compared to similar attempts using reactive ion etching or laser machining techniques; ii) the process is very versatile where the PDMS layer can be kept constant while the device material layer can be varied to be any thermoplastic polymer; iii) the microcontainers are obtained in ordered arrays solely defined by the stamp design and with the open side of the reservoir pointing upwards which facilitates their handling and further processing such as drug loading by inkjet printing[20] and functional layer deposition; iv) the process allows fabrication of large high aspect ratio microstructures on wafer-scale. Here, we demonstrate the fabrication of individual high aspect ratio biopolymer microcontainers with heights of 120 μm and a volume in the nanoliter range with good replication fidelity and yield.

First, a Ni stamp is fabricated with arrays of stamp units each consisting of an inner disk and an outer ring for fabrication of one individual microcontainer.[21] The inner disk and the outer ring have a height of 90 μm and 120 μm, respectively. In order to ease the demolding process and successfully replicate the microstructures, the Ni stamp (Fig. 2A) for embossing should have smooth, positively tapered sidewalls. Once the stamp is fabricated, first a 80 μm thick PDMS layer and then a 100 μm thick PLLA layer are spin coated on a Si substrate.

Since the maximum height of the structures on the Ni stamp is around 120 μm,[21] this thickness of PLLA film ensures that the Ni stamp reaches the PDMS layer during the hot punching process while at the same time it is completely filled by PLLA. The thickness of the PDMS is chosen large enough to ensure that the Ni stamp is far from being in contact with the hard Si surface beneath it.

The PLLA–PDMS layers stack is brought into contact with the Ni stamp and embossed at 90 °C.[22] During the embossing process, the PLLA polymer is above its glass transition temperature of 55–60 °C in a viscoelastic state. This viscoelastic layer lies on the elastic PDMS film. When the hard Ni stamp is brought in contact with the viscoelastic

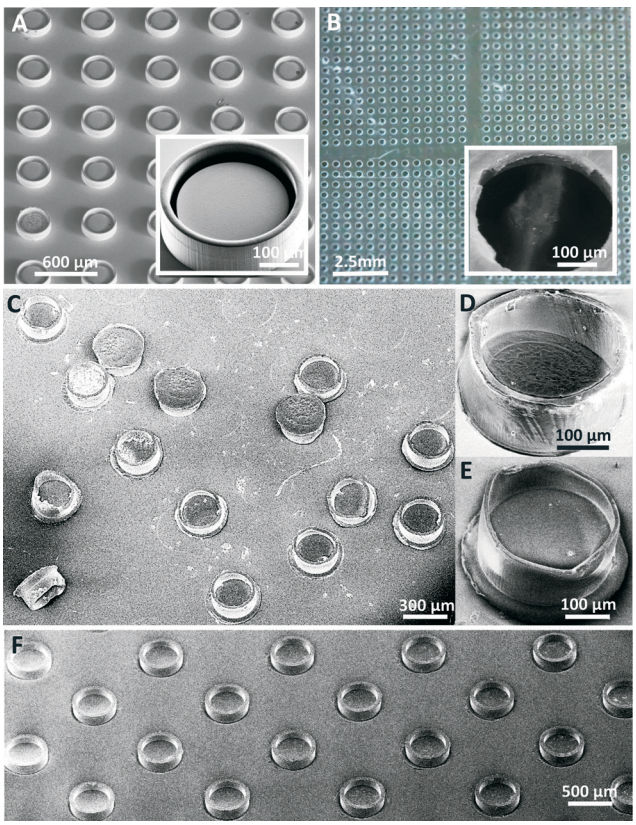

Fig. 2 A. SEM micrograph of the Ni stamp, inset: one Ni stamp unit with inner disc of diameter 260 μm, 20 μm distance between outer ring and the inner disk and outer ring width of 20 μm; B. 100% yield of hot punching; the surrounding polymer film with through holes (inset) after demolding and peeling; C. loosely attached microcontainers on the PDMS layer after two weeks of storage: D.–E. individual microcontainers with 20 μm (D) and 10 μm (E) wall thicknesses; F. PCL microcontainers on PDMS layer immediately after peeling of interconnecting PCL film after hot punching.

PLLA film the PLLA layer starts deforming under the applied compressive forces. This deformation continues into the PDMS layer too. After this, there is only a thin layer of PLLA left below the outer ring of the stamp, which is the highest feature on the stamp. This thin layer defines the residual layer in standard hot embossing. However, because of the elastic deformation of the PDMS layer in the hot punching process, this residual layer is stretched under tensile load. Once the tensile load exceeds the shear strength of the PLLA material, the residual layer is broken. Thus, the containers are separated from the rest of the PLLA layer leaving behind holes in the film (Fig. 2B). 100% yield for punching has been achieved in the sample depicted in Fig. 2B.

After the embossing process and cooling down to 50 °C, the Ni stamp is demolded from the polymer stack. Two different strategies (Fig. 1, process A and process B) can be pursued after demolding based on specific modification of the properties of the PDMS surface before deposition of the PLLA device layer. In process A, the PDMS layer is exposed to UV/ozone, immediately before spin coating of PLLA. In this case, the punched PLLA film adheres to the PDMS layer. This happens due to the low surface energy (6 mN m^{-1})[23] of the Ni stamp coated with a monolayer of perfluorodecyltrichlorosilane (FDTS) antistiction layer compared to the high surface energy (72 mN m^{-1})[24] of the ozone treated PDMS layer.

After punching, the obtained containers are stored for three days during which the PDMS layer recovers some of its hydrophobicity.[25] After three days it is possible to mechanically peel the interconnecting PLLA film from the PDMS, while the PLLA containers remain attached. After two weeks of storage the containers are only loosely attached to the PDMS as shown in Fig. 2C and can be collected by scraping. Fig. 2E and F show the microcontainers with 20 μm and 10 μm wide walls respectively. The walls are close to 120 μm high and the reservoir is 90 μm deep. It can be observed that high aspect ratios of >9 are achieved with this process. Fig. 2F shows PCL containers attached to the PDMS layer after the interconnecting film has been peeled off. This shows that the process can be extended to other polymers.

In process B, the PDMS layer is not treated with ozone before spin coating of PLLA. In this case, the punched PLLA remains attached to the stamp after demolding. The microcontainers are left in the stamp while the rest of the interconnected PLLA film with the holes is peeled off (Fig. 3A). In order to finally obtain the microcontainers, the Ni stamp with the microcontainers is thermally bonded to a sacrificial layer. Since acrylics are heavily used in adhesives and are water soluble, poly acrylic acid (PAA) is used. In order to enhance the adhesive properties of PAA and to decrease its T_g, polyethylene glycol (PEG) is added to aqueous solution of PAA. The stamp, with the PLLA containers stuck in it, is bonded to the PAA–PEG layer at 60 °C. Once the stamp is removed from the PAA–PEG layer, PLLA containers are obtained on this water soluble layer (Fig. 3B). As in process A, it can be seen in Fig. 3C and D that high aspect ratio containers can be fabricated using process B. Since the

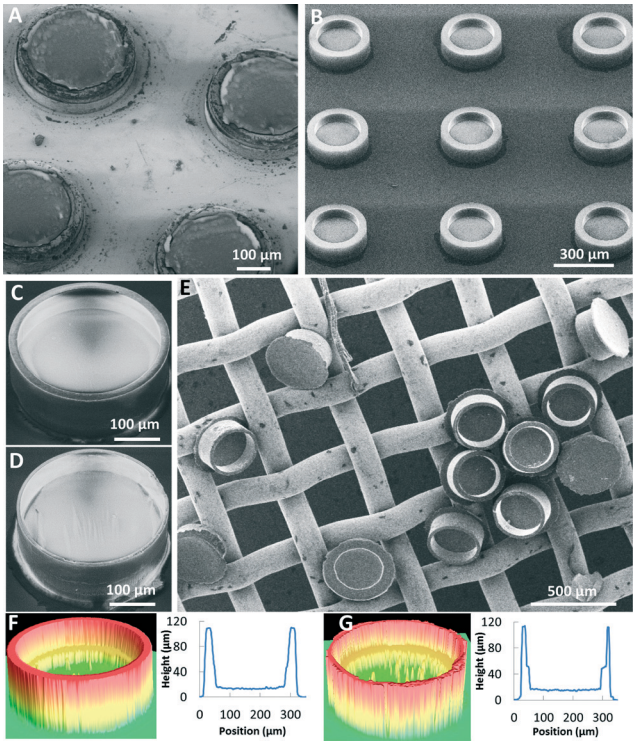

Fig. 3 A. Punched microcontainers attached to Ni stamp after demolding, B. microcontainers with 40 μm wall thicknesses bonded to the PAA–PEG sacrificial layer; C.–D. individual microcontainers with 20 μm (C) and 10 μm (D) wall thicknesses; E. microcontainers filtered through a mesh after dissolution of PAA–PEG sacrificial layer; F. height profile and 3D image of the microcontainers with 20 μm thick walls, G. height profile and 3D image of the microcontainers with 10 μm thick walls. High aspect ratio of >9 and wall heights of 120 μm are achieved.

fluorocarbon coating on the Ni stamp lowers its surface energy while PEG addition to PAA increases the surface energy of the sacrificial layer, PLLA has a higher tendency to adhere to the PAA–PEG layer. If required, the microcontainers can be separated from the Si substrate by dissolution of the PAA–PEG layer in water and further, filtering of microcontainers (Fig. 3E).

Process A and B have different advantages and drawbacks. On one hand, when the microcontainers are directly obtained on a PDMS film as in process A, the number of steps is lower than when the microcontainers are transferred on a sacrificial layer as in process B. On the other hand, microcontainers in process B remain attached to the handling substrate for a longer time. This implies that after process A, the microcontainers can only be stored for a few days during which the drug loading of the containers needs to be performed before the PDMS layer recovers its hydrophobicity and the containers detach. Process A is a dry process which means that once the containers will be loaded with drug, they will not be exposed to any kind of solvents. Compared to that, process B becomes a wet process due to the release of the containers from the substrate by dissolution of a sacrificial layer. Thus, the choice of process will depend on the final

application and the requirements for post-processing such as drug loading.

Conclusions

We have fabricated individual microcontainers in biodegradable polymer approved for oral drug delivery applications using hot punching. Hot punching is a modification of the standard embossing technique, where an elastic PDMS layer is deposited between the device PLLA layer and the hard Si substrate. We have shown that this layer allows the penetration of the residual layer and the separation of the microcontainers from the surrounding polymer film on wafer scale. We have illustrated that punched microcontainers can be obtained, either on the underlying PDMS film directly or on a sacrificial layer. Here, the sacrificial layer is a water soluble PAA layer but in principle it could be any layer with good adhesion properties to PLLA *e.g.* an adhesive tape. Both processes have good replication fidelity and give excellent yields even for structures with high aspect ratio of >9 and a height of 120 μm (Fig. 3F and G). The final microstructures are truly 3D microcontainers with 300 μm diameter and 90 μm deep reservoirs resulting in a volume of approximately 4 nL per container. This is around three orders of magnitudes more volume for drug loading in comparison to some of the other microreservoir based DDS presented in literature.[6,9,26] In future, these microcontainers will be loaded with drugs and the drug release will be characterized.

Finally, we believe that the hot punching process described here is a truly versatile and simple process which is compatible with standard hot embossing equipment and stamps. The process is not limited to fabrication of microcontainers but can be applied to other drug delivery devices or other applications like tissue engineering where fabrication of individual 3D microstructures in polymer is required. This process is suitable for high throughput production and can potentially be transferred to roll-to-roll (R2R) processing.

Acknowledgements

This research is supported by NAMEC Villum Kann Rasmussen Centre of Excellence (65286). We thank the staff at DTU Danchip for support during use of the cleanroom facilities.

Notes and references

1 S. V. Sastry, J. R. Nyshadham and J. A. Fix, *Pharm. Sci. Technol. Today*, 2000, **3**, 138.
2 M. Morishita and N. A. Peppas, *Drug Discovery Today*, 2006, **11**, 905.
3 M. Goldberg and I. Gomez-Orellana, *Nat. Rev. Drug Discovery*, 2003, **2**, 289.
4 S. Sant, S. L. Tao, O. Z. Fisher, Q. Xu, N. A. Peppas and A. Khademhosseini, *Adv. Drug Delivery Rev.*, 2012, **64**, 496.
5 C. Chiappini, E. Tasciotti, J. R. Fakhoury, D. Fine, L. Pullan, Y.-C. Wang, L. Fu, X. Liu and M. Ferrari, *ChemPhysChem*, 2010, **11**, 1029.
6 S. L. Tao and T. A. Desai, *Adv. Mater.*, 2005, **17**, 1625.
7 H. D. Chirra, L. Shao, N. Ciaccio, C. B. Fox, J. M. Wade, A. Ma and T. A. Desai, *Adv. Healthcare Mater.*, 2014, **3**, 1648.
8 J. T. Santini, M. J. Cima and R. Langer, *Nature*, 1999, **397**, 335.
9 S. L. Tao, M. W. Lubeley and T. A. Desai, *J. Controlled Release*, 2003, **88**, 215.
10 S. L. Tao, K. Popat and T. A. Desai, *Nat. Protoc.*, 2007, **1**, 3153.
11 Y. Zhang, H. F. Chan and K. W. Leong, *Adv. Drug Delivery Rev.*, 2013, **65**, 104.
12 L. Brannon-Peppas, *Int. J. Pharm.*, 1995, **116**, 1.
13 J. P. Rolland, B. W. Maynor, L. E. Euliss, A. E. Exner, G. M. Denison and J. M. DeSimone, *J. Am. Chem. Soc.*, 2005, **127**, 10096.
14 Y. J. Kelly and J. M. DeSimone, *J. Am. Chem. Soc.*, 2008, **130**, 5438.
15 J. Guan, H. He, L. J. Lee and D. J. Hansford, *Small*, 2007, **3**, 412.
16 S. J. Pearton and D. P. Norton, *Plasma Processes Polym.*, 2005, **2**, 16.
17 J. Y. Sheikh-Ahmad, *Machining of polymer composites*, Springer, New York, USA, 2009.
18 R. Kuduva-Raman-Thanumoorthy and D. Yao, *Polym. Eng. Sci.*, 2009, **49**, 1894.
19 M. Heckele and W. K. Schomburg, *J. Micromech. Microeng.*, 2004, **14**, R1.
20 P. Marizza, S. S. Keller, A. Müllertz and A. Boisen, *J. Controlled Release*, 2014, **173**, 1.
21 R. S. Petersen, S. S. Keller, O. Hansen and A. Boisen, *J. Micromech. Microeng.*, 2015, **25**, 055021.
22 R. S. Petersen, R. Mahshid, N. K. Andersen, S. S. Keller, H. N. Hansen and A. Boisen, *Microelectron. Eng.*, 2015, **133**, 104.
23 D. Janssen, R. De Palma, S. Verlaak, P. Heremans and W. Dehaen, *Thin Solid Films*, 2006, **515**, 1433.
24 K. Efimenko, W. E. Wallace and J. Genzer, *J. Colloid Interface Sci.*, 2002, **254**, 306.
25 Y. Berdichevsky, J. Khandurina, A. Guttman and Y. H. Lo, *Sens. Actuators, B*, 2004, **97**, 402.
26 A. Ahmed, C. Bonner and T. A. Desai, *J. Controlled Release*, 2002, **81**, 291.

Paper IV

Fabrication and loading of biopolymer microcontainers for oral drug delivery using hot punching

FABRICATION AND LOADING OF ORAL DRUG DELIVERY MICROCONTAINERS USING HOT PUNCHING

Ritika S. Petersen*, Mads T. Borre, Stephan S. Keller, and Anja Boisen
Department of Micro- and Nanotechnology, Technical University of Denmark

ABSTRACT

In this paper, poly-l-lactic acid (PLLA) solution is spin coated to achieve a PLLA layer of 55 µm thickness. Hot punching with a Ni stamp is optimized to fabricate microcontainers in PLLA. Process optimization of thermal bonding of the microcontainers to a poly acrylic acid (PAA) layer is performed by modifying sample preparation and varying temperature. The fabricated microcontainers are loaded by hot punching in a spin coated drug polymer film of furosemide and poly-e-caprolactone (PCL).

KEYWORDS: hot punching, hot embossing, thermal bonding, microcontainers, oral drug delivery

INTRODUCTION

Advances in microtechnology and pharmaceutical engineering led to the proposition of microcontainers as carriers for oral drug delivery. These containers are able to protect drug from degradation during transit of the gastro-intestinal tract, potentially enable one-directional drug release at the site of absorption and could thereby enhance the bioavailability of drugs [1]. It has been shown that hot embossing is a viable method for three-dimensional (3D) structuring of biopolymers [2]. However, it leads to the formation of a residual layer that connects the structures defined in the polymer. The residual layer can be removed by reactive ion etching but this is a slow, expensive process that leads to complex residues. Recently, we introduced hot punching as a new process for patterning of biopolymers [3]. Here, the hot punching process is optimized to achieve discrete 3D PLLA microcontainers with a volume of 3.3 nL with a high fabrication yield. Earlier, microcontainers have been filled with drug by micro spotting or microinjection [4]. These techniques require low viscous solutions and are time consuming. In our work, containers are filled with polymer-drug (PCL-furosemide) matrix using the same hot punching technique in a single-step in parallel manner.

EXPERIMENTAL

The process of hot punching is illustrated in Fig. 1. First, the substrate is prepared by spin coating a PLLA layer on a PDMS coated Si substrate. After that the sample is embossed with a fluorocarbon coated-Ni stamp (Fig. 1.A, Fig.2.A) for 30 min at a temperature of 105°C and a pressure of 1.9 MPa [5,6]. During the embossing, the viscoelastic PDMS underlayer presses against the stamp, the residual layer is disrupted and the microcontainers are punched out of the PLLA film. Next, the stamp and the sample are demolded. At this stage, a polymer film with through-holes is left on the Si wafer while the microcontainers remain in the stamp (Fig. 1.B, Fig. 2.B). To detach the microcontainers from the stamp, the stamp is thermally bonded to a 50 µm thick film of PAA coated on a Si wafer (Fig. 1.C). Finally the

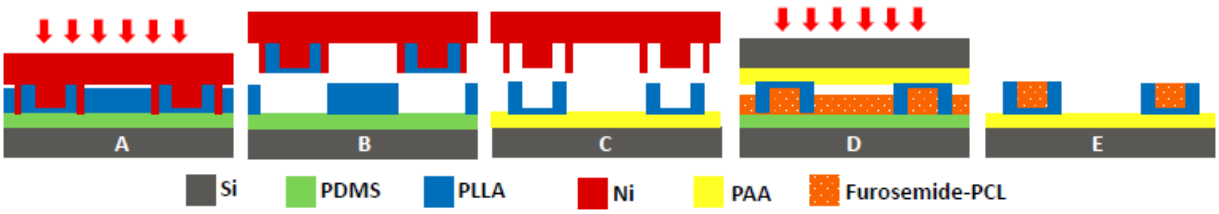

Figure 1. Hot punching for fabrication and filling of PLLA microcontainers: A. Embossing of PLLA spin coated on PDMS by Ni stamp, B. PLLA microcontainers punched out but attached to Ni stamp, C. Thermal bonding of PLLA microcontainers to PAA layer, D. Second hot punching for filling of PLLA microcontainers with PCL-Furosemide drug matrix, E. Drug loaded microcontainers.

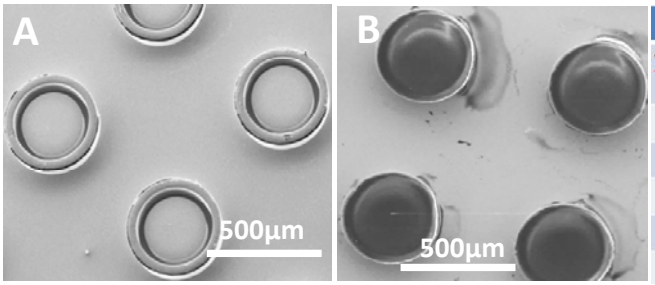

Figure 2.A. Nickel stamp, B. PLLA microcontainers punched out but attached to Ni stamp

Table 1. Optimization of Bonding

Temp (°C)	Force (KN)	Cooling Temp (°C)	Yield (%)
80	15	50	0
90	15	50	20
100	15	50	60
110	15	50	40
120	15	50	10

Table 1. Optimization of thermal bonding

containers are obtained on this water soluble PAA sacrificial layer. These biopolymer containers are further used to punch a 50 µm thick PCL-Furosemide polymer-drug matrix for 30 min at a temperature of 65 °C and a pressure of 1.9 MPa (Fig. 1.D). In this way the drug is loaded in the microcontainers in a single step (Fig. 1.E). Free-floating microcontainers are obtained by dissolution of the PAA layer in water.

RESULTS AND DISCUSSION

The flow of PLLA into the Ni stamp is considered and the required thicknesses of the PLLA film to completely fill the stamp is calculated. The dimensions of one unit on the Ni stamp are given in Fig 3.A. There are 20X20 such units with center-to-center distance of 640 µm arrayed as a square. There are 16 such squares on a wafer resulting in a total of 6400 microcontainers. Due to the distance between the individual units a local flow is assumed, where only the PLLA under each individual unit of Ni stamp is involved in the filling of the cavities. With this model (Fig. 3.B), the required PLLA thickness is calculated as 51µm. A PLLA thickness of around 55 µm is achieved by spin coating 15% wt. solution at 1000 rpm (Fig. 3.C).

Similar calculations for the local flow of the drug-polymer into the PLLA microcontainers are performed and the calculated thickness is 47 µm. However, for uniform coating of the drug polymer film, maximum thickness of 22 µm is achieved at 500 rpm for 14.6%wt. PCL-furosemide solution (Fig.3.D). Lowering the spin coating speed results in thicker but non-uniform films. In future either the concentration of the solution could be increased or multiple layers could be deposited to achieve the theoretically required thickness of the film .

For the punching of the microcontainers from the spin coated PLLA film, 100% yield is achieved at a embossing temperature of 105 ºC. To increase the yield of the thermal bonding, optimization of PAA water soluble layer preparation, thermal bonding temperature (Table 1) and time are performed. Best results are obtained when PAA solution is spin coated at 1000 rpm to a 50 µm thick PAA film and thermal bonding is conducted immediately afterwards at 100ºC for 30 min at a pressure of 1.9 MPa (Fig.4 A). If the water from the PAA layer is allowed to evaporate, it has been observed that the stiction of PAA to PLLA microcontainers has been considerably reduced. The glass transition temperature of PAA is around 100ºC and it seems that at this temperature PAA is soft enough to conform well to the PLLA attached to the Ni stamp but not too soft to get punched itself. The bonding yield achieved with these optimized parameters is around 60%.

Finally the optical images show that the containers get filled when the drug polymer matrix is punched into the fabricated PLLA microcontainers (Fig.4). The yield of this process is more than 90%. However, significant compression of the walls occurs (Fig.4.B, D and E). This could be solved by reducing the temperature and pressure applied on the microcontainers during the hot punching filling process or by increasing the thickness of the drug polymer film.

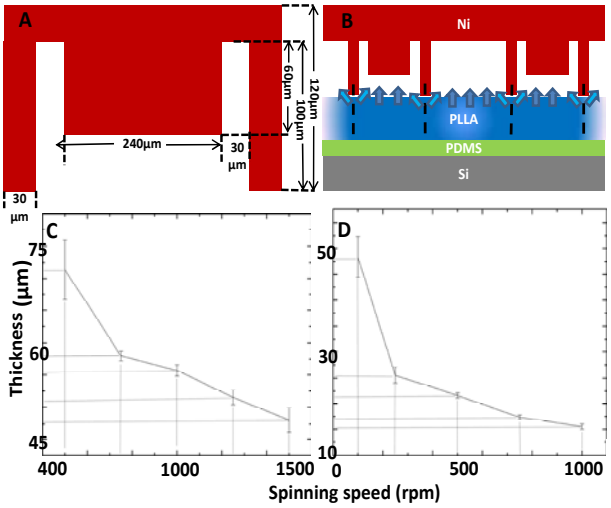

Figure 3.A. Single unit of Ni stamp, and B. Local flow of PLLA in Ni stamp; Spin curves for C. PLLA films, and D. PCL-Furosemide films

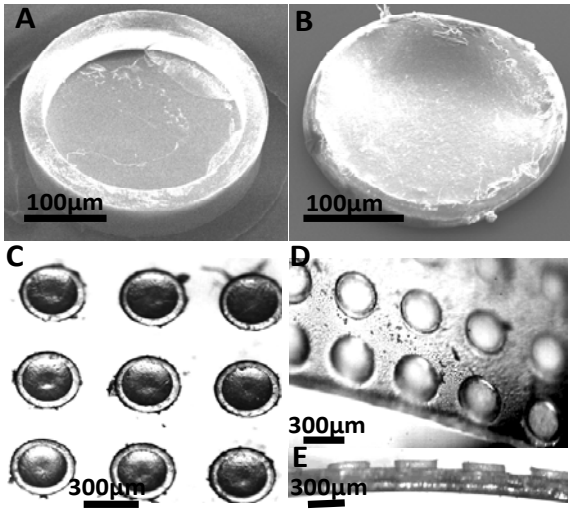

Figure 4.SEM micrographs of A. Empty, and B. Filled but compressed microcontainer, optical images of filled microcontainers- C,D, and E. top, tilted and side angles, respectively

CONCLUSION

The hot punching process described here for fabricating and filling microcontainers is a very versatile process that can be used for a range of different designs of biopolymer based oral drug delivery devices and drug types. Further optimization needs to be performed for the thermal bonding in order to get an even higher yield and for the filling technique to keep the structural integrity of the microcontainers intact.

ACKNOWLEDGEMENTS

This research was funded by Danmarks Grundforskningsfonds og Villum Fondens Center for Intelligent Drug Delivery and Sensing Using Microcontainers and Nanomechanics (IDUN)

REFERENCES

[1] Chirra, H. D., Shao, L., Ciaccio, N., Fox, C. B., Wade, J. M., Ma, A., & Desai, T. A. (2014). Planar Microdevices for Enhanced In Vivo Retention and Oral Bioavailability of Poorly Permeable Drugs. *Advanced healthcare materials*,*3*(10), 1648-1654.

[2] Nagstrup, J., Keller, S., Almdal, K., & Boisen, A. (2011). 3D microstructuring of biodegradable polymers. *Microelectronic Engineering*, *88*(8), 2342-2344.

[3] Marizza, P., Keller, S. S., & Boisen, A. (2013). Inkjet printing as a technique for filling of microwells with biocompatible polymers. *Microelectronic Engineering*, *111*, 391-395.

[4] Petersen, R. S., Keller, S. S., Hansen, O., & Boisen, A. (2015). Fabrication of Ni stamp with high aspect ratio, two-leveled, cylindrical microstructures using dry etching and electroplating. *Journal of Micromechanics and Microengineering*, *25*(5), 055021.

[5] Petersen, R. S., Keller, S. S., & Boisen, A. (2015). "Hot punching of high-aspect-ratio 3D polymeric microstructures for drug delivery." *Lab on a Chip*.

[6] Rapp, B. E., Schneider, M., & Worgull, M. (2009, April). Hot punching on an 8 inch substrate as an alternative technology to produced holes on a large scale. In *Design, Test, Integration & Packaging of MEMS/MOEMS, 2009. MEMS/MOEMS'09. Symposium on* (pp. 136-139). IEEE.

CONTACT

*Ritika Singh Petersen ; phone: +45- 45 25 63 97; risi@nanotech.dtu.dk

Paper V

Hot punching of drug-polymer matrices to load drug delivery micro-reservoirs

Hot punching of drug-polymer matrices to load drug delivery micro-reservoirs

Ritika Singh Petersen, Stephan Sylvest Keller, and Anja Boisen

Department of Micro- and Nanotechnology, Technical University of Denmark, Building 345E, DK-2800 Kongens Lyngby, Denmark

e-mail: risi@nanotech.dtu.dk

Keywords: hot punching, microcontainers, drug delivery, dissolution, Raman spectroscopy, x-ray powder diffraction

In recent times, reservoir based microdevices, which prevent the degradation of drug and allow unidirectional release, have led to enhanced bioavailability of the drug in the system. These devices have secured an important place in oral drug delivery [1, 2]. They have been conventionally fabricated in Si and photoresists like SU-8 and poly(methyl methacrylate) using standard micro-electro-mechanical systems (MEMS) fabrication technologies of photolithography and etching [3, 4]. Gradually, the focus has shifted to fabricating the reservoir based devices in biodegradable and biocompatible polymers like poly(lactic-co-glycolic acid) (PLGA), poly(ethylene glycol) dimethacrylate (PEG-DMA) and others [5]. Once these microcontainers are fabricated, loading them with drug imposes a major challenge. The loaded drug in general is embedded in a polymer matrix to tune its release properties. The polymer matrices can be hydrophobic, slow-degrading biopolymeric materials such as PLLA or PCL for sustained drug release [6]. On the other hand, they can be hydrophilic polymers or in their gel forms such as Poly Acrylic Acid (PAA) or Poly vinyl pyrrolidone (PVP) for increased drug solubility and bioavailability [7, 8]. In the past, microdevices have been loaded with drug-polymer matrices by using photolithography, microinjection and ink-jet printing [9-11]. Supercritical CO_2 has been introduced as a method to fill micro-reservoirs where

first the polymer matrix is filled in microcontainers by ink-jet printing and then the drug is loaded using supercritical CO_2 [12]. Though these techniques give good control on the amount of drug filled, they suffer from some disadvantages. Photolithography typically uses UV light which can degrade the active ingredients in a drug. Ink-jet printing cannot be performed for high molecular weight polymers and proteins due to clogging of nozzle. Supercritical CO_2 has some constraints when the micro-reservoirs are fabricated in polymers like PLLA that can themselves swell and get deformed [12]. The common limitation with all these techniques is that they are relatively slow processes. Microcontact printing has been developed as a parallel process to fill such micro-reservoirs [13]. However, this technique requires fabrication of polydimethylsiloxane (PDMS) stamp which is mechanically and chemically unfit for a large number of loading runs [14]. It also requires alignment set-up to align the stamp precisely in the micro-reservoirs [13].

Here, we introduce a high throughput, parallel process of filling micro-reservoirs in a controlled manner using hot punching technique. Microcontainers made in both polymeric material PLLA and photoresist SU-8 have been successfully loaded by furosemide (F) drug in PCL matrix using this technique. Hot punching is a combination of hot embossing and mechanical punching processes [15-17]. In hot punching, a mold is pressed into a viscoelastic polymer film, punching out the embossed microstructures from the rest of the film. In hot embossing as in Figure.1.A, the force F required to emboss a mold with a protrusion of radius R into a polymer film of initial thickness h_0 and viscosity η_0 lying on a substrate distance $h(t)$ apart from the stamp at any time t, is given by [18]:

$$F = \frac{3\pi R^4 \eta_0}{2h(t)^3}\frac{dh}{dt} \qquad 1)$$

From equation 1, it is clear that as $h(t) \rightarrow 0$, the force required for embossing a non-deformable stamp into a polymer lying on a non-deformable substrate, becomes extremely large. This in turn means that it is almost impossible to remove residual layer completely. Therefore in a typical hot

embossing process, after the microstructures are fabricated, the residual layer is removed by reactive ion etaching (RIE). However, for the application of drug loading, RIE is impractical as it would lead to the degradation of the drug lying in the drug-polymer film. To remove the residual layer, conformal contact of the mold with the sample substrate is required (i.e., $h(t) = 0$). Two conditions need to be satisfied to achieve such conformal contact: i) either the mold or the substrate is deformable, and ii) the thickness of the polymer film is high enough to fill the cavities of the mold but low enough to allow the contact of mold with the substrate.

In order to load the microcontainers, the microcontainers lying in an array on the substrate are considered as the mold (Figure.1.C.I, 1.D.I, 2.A and 2.D). This microcontainer-mold is embossed in the F-PCL film spin coated on a substrate by applying temperature and pressure. In order to emboss relatively non-deformable SU-8 microcontainers, the substrate is modified into deformable substrate by depositing PDMS film on the Si substrate before spin coating F-PCL solution (Figure.1.C.I). While embossing the PLLA microcontainers, the first condition for the conformal contact is fulfilled automatically since the microcontainer-mold in this case is made up of relatively deformable PLLA material. Thus, PLLA microcontainers can be applied for the punching of F-PCL film spin coated directly on Si without any extra PDMS layer (Figure.1.D.I).

Table 1. Dimensions of SU-8 and PLLA microcontainers

Cont-ainer	Depth of inner reservoir, H_1 (µm)	Diameter of inner reservoir, D_1 (µm)	Total height of container, H_2 (µm)	Outer diameter of container, D_2 (µm)	Center to center distance between containers, L (µm)
SU-8	60	200	100	300	450
PLLA	73	240	100	300	640

In order to fulfill the second condition for achieving conformal contact of the microcontainer-mold with the F-PCL's substrate, the required thickness of the F-PCL film is calculated. The thickness of the F-PCL film should be less than or equal to the thickness required to fill the microcontainers' reservoirs completely without leaving residual film. The various dimensions of the containers are mentioned in Table 1 and illustrated in Figure.1.B . Using mass conservation and assuming that the polymer in viscous state is an incompressible liquid, the required thickness (T_{max}) of the F-PCL films is given by:

$$T_{\max} < H_1 \left\{ 1 - \frac{\pi}{4} \left(\frac{D_2^2 - D_1^2}{L^2} \right) \right\} \quad 2)$$

Putting the values from Table 1, the calculated maximum thickness of the F-PCL film for loading SU-8 containers is 48.4 µm and PLLA microcontainers is 69.9 µm.

So far, the conformal contact between the microcontainer-mold and the F-PCL's substrate is achieved by applying the above guidelines. Once the contact is obtained, F-PCL film is punched along the walls of the microcontainers from the rest of the F-PCL film through the application of force and temperature. However, in order to load the microcontainers, it is desirable that this punched out F-PCL microstucture remain in the container reservoirs. To ensure this, the total adhesion energy between the mold and F-PCL polymer should be higher than the adhesion energy between the F-PCL polymer and its substrate. If W_{pm} and A_{pm} are the adhesion and the total contact surface area of drug-polymer to mold, respectively while W_{ps} and A_{ps} are the adhesion energy and the total contact surface area of drug-polymer to its substrate, respectively, then this condition is fulfilled when

$$A_{pm} W_{pm} > A_{ps} W_{ps} \quad 3)$$

where W_{pm} and W_{ps} are calculated from the surface energies of drug-polymer (γ_p) and mold (γ_m), and the interfacial energy between the drug-polymer and mold (γ_{pm}), and between the drug-polymer and

its substrate (γ_{ps}) by applying Young-Dupré equation and Berthelot hypothesis [19]. Taking into consideration, the cylindrical shape of the microcontainers, the above equation can also be written as:

$$\frac{W_{ps}}{W_{pm}} < \frac{2D_1H_1+D_1^2}{D_2^2} \quad 4)$$

The above mentioned condition can be fulfilled by either increasing the aspect ratio of the containers or by increasing W_{pm}. When the SU-8 container punches the F-PCL film lying on PDMS (Figure.1.C.II), W_{pm} = 69.3 mJ /m^2 and W_{ps} = 53.7 mJ /m^2 where γ_s = 20 mJ/m^2, γ_m= 30mJ/m^2 and γ_p= 40mJ/m^2 [20-22]. For the dimensions mentioned in Table.1, $W_{pm}A_{pm}$ = 4.79*10^{-6} mJ and $W_{ps}A_{ps}$ = 4.21*10^{-6} mJ. Since $W_{pm}A_{pm} > W_{ps}A_{ps}$, the punched out PCL polymer stays in the SU-8 reservoir and thus the container is loaded (Figure.1.C.III, 2.B and 2.C). The hot punching of F-PCL film by SU-8 microcontainers is performed at a temperature of 65 ºC and a pressure of 1 bar. The temperature is applied on both the plates in contact with the microcontainer-mold and the F-PCL sample. Complete filling of reservoirs is achieved by spin coating F-PCL film of around 45-50 µm thickness. This thickness is obtained by spin coating two layers of 14.7% wt. F-PCL solution prepared in fast evaporating solvents like acetone and dicholoromethane, at 400 rpm spin speed.

In order to load F-PCL in PLLA, a 21-23µm thick F-PCL film is prepared by spin coating 14.7% wt. F-PCL solution on Si substrate at 400 rpm. During hot punching, when the temperature of 75 ºC is applied to both the plate, the deformable PLLA containers lose their strutural integrity and become flat. So, the temperature is applied only to the plate in contact with F-PCL sample. After demolding, the punched out F-PCL gets attached to the PLLA microcontainers because of a very high W_{pm}. Even though in this case A_{pm} is small due to incomplete filling of the reservoir as the thickness of the spin coated F-PCL film is less than T_{max}, the adhesion of F-PCL to PLLA is high enough to compensate for this low A_{pm}. Since the glass transition temperature of PLLA generally

lies between 50-60 °C, the F-PCL polymer that is at 75 °C during hot punching, blends into the PLLA in direct contact with it [23, 24]. This results in significantly high W_{pm}, which ensures that after demolding, the punched out F-PCL structures remain in the PLLA microcontainers, thereby loading them (Figure.1.D.III, 2.E and 2.F). Optical profiler measurements show the height of the filled matrix to be 86 µm with respect to Si substrate and indicate that the PLLA containers stay structurally intact (Figure.2.G and H). High replicability and yield of > 95% are observed for the loading of both SU-8 and PLLA microcontainers.

The F-PCL matrix thus loaded in the microcontainers by applying hot punching is further characterized by performing X-ray powder diffraction (XRPD) and Raman. The furosemide release is studied by microdissolution. For the sake of simplicity, XRPD and Raman data for F-PCL loaded in PLLA microcontainers is presented here. From the XRPD and Raman data it is confirmed that both PCL and furosemide are loaded in the microcontainers. Furosemide is present in polymorph form I which is the most common and the stable of all its polymorphs due to more efficient crystal packing, higher density and the presence of sulfonamide group [25]. The spectra taken for the pure furosemide crystals show the same spectra of polymorph form I indicating that the furosemide remains in a stable form during the punching process as illustrated in Figure.3.A [25]. The sharp furosemide peaks especially at 1600 cm^{-1} and 1509 cm^{-1} in raman data and at 25º 2θ in XRPD show that Furosemide is present in semi-crystalline form (Figure.3.A and B). As can be seen from the Figure.3.C, the release profile of furosemide from PCL matrix loaded in PLLA microcontainers shows an initial fast release followed by a slow sustained release.

Hence, we demostrate here that hot punching is an effective process of loading drug-polymer matrix in micro-reservoirs. For both SU-8 and PLLA microcontainers, a high yield of loading (>95%) has been achieved. Various advantages of hot punching process for loading of micro-reservoir based oral drug delivery devices are: i) it is a versatile process that can be used to fill different

combinations of drug and polymer; ii) apart from the sample preparation, the process is a single-step, parallel process with high throughput; iii) it doesn't require any special printing or alignment tools, neither the process needs to be performed in cleanroom or under high vacuum, making it a simple process that can be scaled up, iv) it is comparatively benign towards the active components of a drug; v) it can be used for high-aspect ratio filling and in principle the leftover drug-polymer can be reused in making solution. Thus we have been able to produce an oral drug delivery device completely manufactured in biopolymeric materials and shown successful release of drug. This technique can also be used for loading hydrophilic polymers like PAA, hydrogels. etc. either as a melt or in their solution forms if the surfaces of the microcontainers are modified to match the surface energies of these polymers.

Acknowledgements

The work presented her has been funded by Danmarks Grundforskningsfonds og Villum Fondens Center for Intelligent Drug Delivery and Sensing Using Microcontainers and Nanomechanics (IDUN).

References

[1] Chien, Yie. *Novel drug delivery systems*. Informa Health Care, 1991.

[2] Lavan, David A., Terry McGuire, and Robert Langer. "Small-scale systems for in vivo drug delivery." *Nature biotechnology* 21, no. 10 (2003): 1184-1191.

[3] Shawgo, Rebecca S., Amy C. Richards Grayson, Yawen Li, and Michael J. Cima. "BioMEMS for drug delivery." *Current Opinion in Solid State and Materials Science* 6, no. 4 (2002): 329-334.

[4] Tao, Sarah L., and Tejal A. Desai. "Microfabricated drug delivery systems: from particles to pores." *Advanced drug delivery reviews* 55, no. 3 (2003): 315-328.

[5] Guan, Jingjiao, Hongyan He, L. James Lee, and Derek J. Hansford. "Fabrication of Particulate Reservoir-Containing, Capsulelike, and Self-Folding Polymer Microstructures for Drug Delivery." *Small* 3, no. 3 (2007): 412-418.

[6] Jeong, Jong-Cheol, Jaeyoung Lee, and Kilwon Cho. "Effects of crystalline microstructure on drug release behavior of poly (ε-caprolactone) microspheres."*Journal of controlled release* 92, no. 3 (2003): 249-258.

[7] Qiu, Yong, and Kinam Park. "Environment-sensitive hydrogels for drug delivery." *Advanced drug delivery reviews* 64 (2012): 49-60.

[8] Chun, Myung-Kwan, Chong-Su Cho, and Hoo-Kyun Choi. "Mucoadhesive drug carrier based on interpolymer complex of poly (vinyl pyrrolidone) and poly (acrylic acid) prepared by template polymerization." *Journal of controlled release* 81, no. 3 (2002): 327-334.

[9] Chirra, Hariharasudhan D., and Tejal A. Desai. "Multi-Reservoir Bioadhesive Microdevices for Independent Rate-Controlled Delivery of Multiple Drugs."*Small* 8, no. 24 (2012): 3839-3846.

[10] Ahmed, Aamer, Chris Bonner, and Tejal A. Desai. "Bioadhesive microdevices with multiple reservoirs: a new platform for oral drug delivery." *Journal of Controlled Release* 81, no. 3 (2002): 291-306.

[11] Kolakovic, Ruzica, Tapani Viitala, Petri Ihalainen, Natalja Genina, Jouko Peltonen, and Niklas Sandler. "Printing technologies in fabrication of drug delivery systems." *Expert opinion on drug delivery* 10, no. 12 (2013): 1711-1723.

[12] Marizza, Paolo, Stephan S. Keller, Anette Müllertz, and Anja Boisen. "Polymer-filled microcontainers for oral delivery loaded using supercritical impregnation."*Journal of Controlled Release* 173 (2014): 1-9.

[13] Lee, Hong-Pyo, and WonHyoung Ryu. "Wet microcontact printing (μCP) for micro-reservoir drug delivery systems." *Biofabrication* 5, no. 2 (2013): 025011.

[14] Mukhopadhyay, Rajendrani. "When PDMS isn't the best." *Analytical chemistry*79, no. 9 (2007): 3248-3253.

[15] Petersen, Ritika S., Stephan S. Keller, and Anja Boisen. "Hot punching of high-aspect-ratio 3D polymeric microstructures for drug delivery." *Lab on a Chip*(2015).

[16] Petersen, Ritika Singh, Rasoul Mahshid, Nis Korsgaard Andersen, Stephan Sylvest Keller, Hans Nørgaard Hansen, and Anja Boisen. "Hot embossing and mechanical punching of biodegradable microcontainers for oral drug delivery."*Microelectronic Engineering* 133 (2015): 104-109.

[17] Petersen, Ritika Singh, Stephan Sylvest Keller, Ole Hansen, and Anja Boisen. "Fabrication of Ni stamp with high aspect ratio, two-leveled, cylindrical microstructures using dry etching and electroplating." *Journal of Micromechanics and Microengineering* 25, no. 5 (2015): 055021.

[18] Torres, Clivia Marfa Sotomayor, ed. *Alternative lithography: unleashing the potentials of nanotechnology*. Springer Science & Business Media, 2012.

[19] Żenkiewicz, M. "Methods for the calculation of surface free energy of solids."*Journal of Achievements in Materials and Manufacturing Engineering* 24, no. 1 (2007): 137-145.

[20] Fuard, D., T. Tzvetkova-Chevolleau, S. Decossas, Philippe Tracqui, and P. Schiavone. "Optimization of poly-di-methyl-siloxane (PDMS) substrates for studying cellular adhesion and motility." *Microelectronic Engineering* 85, no. 5 (2008): 1289-1293.

[21] Walther, Ferdinand, Polina Davydovskaya, Stefan Zürcher, Michael Kaiser, Helmut Herberg, Alexander M. Gigler, and Robert W. Stark. "Stability of the hydrophilic behavior of oxygen plasma activated SU-8." *Journal of Micromechanics and Microengineering* 17, no. 3 (2007): 524.

[22] Cava, D., R. Gavara, J. M. Lagaron, and A. Voelkel. "Surface characterization of poly (lactic acid) and polycaprolactone by inverse gas chromatography."*Journal of Chromatography A* 1148, no. 1 (2007): 86-91.

[23] Baiardo, Massimo, Giovanna Frisoni, Mariastella Scandola, Michel Rimelen, David Lips, Kurt Ruffieux, and Erich Wintermantel. "Thermal and mechanical properties of plasticized poly (L-lactic acid)." *Journal of Applied Polymer Science* 90, no. 7 (2003): 1731-1738.

[24] Wu, Defeng, Yisheng Zhang, Ming Zhang, and Weidong Zhou. "Phase behavior and its viscoelastic response of polylactide/poly (ε-caprolactone) blend."*European Polymer Journal* 44, no. 7 (2008): 2171-2183.

[25] Babu, N. Jagadeesh, Suryanarayan Cherukuvada, Ranjit Thakuria, and Ashwini Nangia. "Conformational and synthon polymorphism in Furosemide(Lasix)."*Crystal Growth & Design* 10, no. 4 (2010): 1979-1989.

Figure.1. A. Schematic of hot embossing process where a mold is embossed in a polymer with the application of force; B. Schematic of hot punching of drug-polymer matrix by microcontainer-mold with all the features; Hot punching for loading of microcontainers with drug-polymer matrices: C. Drug-polymer loading in non-deformable SU-8 microcontainers by applying deformable substrate: 1. Fabrication of SU-8 microcontainers on fluorocarbon coating and preparation of the sample by spin coating drug-polymer solution on PDMS coated Si. 2. Hot punching drug-polymer by SU-8 microcontainer-mold, 3.Demolding of the containers with attached drug-polymer matrices punched out from rest of the film, D. Drug-polymer loading in soft PLLA microcontainers: 1. Fabrication of PLLA microcontainers bonded on water soluble PAA-PEG layer and preparation of the sample by spin coating drug-polymer solution directly on Si. 2. Hot punching drug-polymer by PLLA microcontainer-mold, 3.Demolding of the containers with attached drug-polymer matrices punched out from rest of the film, thus loading the containers.

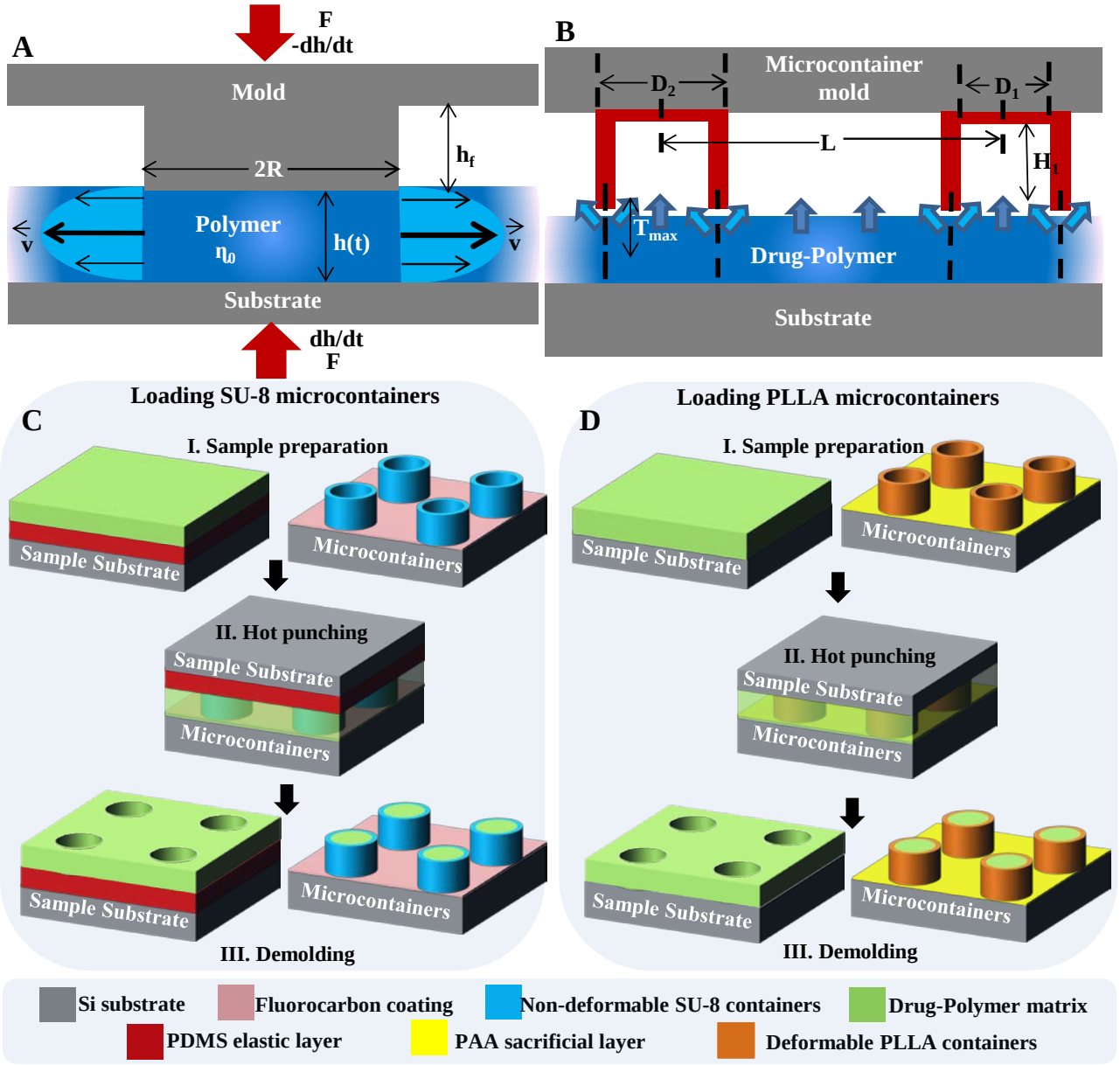
A
F
-dh/dt
Mold
2R
h_f
Polymer
η_0
h(t)
v
v
Substrate
dh/dt
F
B
Microcontainer mold
D_2
D_1
L
H_1
T_{max}
Drug-Polymer
Substrate
Loading SU-8 microcontainers
C
I. Sample preparation
Sample Substrate
Microcontainers
II. Hot punching
Sample Substrate
Microcontainers
Sample Substrate
Microcontainers
III. Demolding
Loading PLLA microcontainers
D
I. Sample preparation
Sample Substrate
Microcontainers
II. Hot punching
Sample Substrate
Microcontainers
Sample Substrate
Microcontainers
III. Demolding
Si substrate
Fluorocarbon coating
Non-deformable SU-8 containers
Drug-Polymer matrix
PDMS elastic layer
PAA sacrificial layer
Deformable PLLA containers

Figure.2 SEM micrographs of: A. Empty PLLA containers B. F-PCL loading in PLLA microcontainers using optimized parameters, C. closeup; D.Empty SU-8 containers B. F-PCL loading in SU-8 microcontainers, C. closeup; Optical profiler measurements of G. empty and H. loaded PLLA microcontainers along with the 3D images.

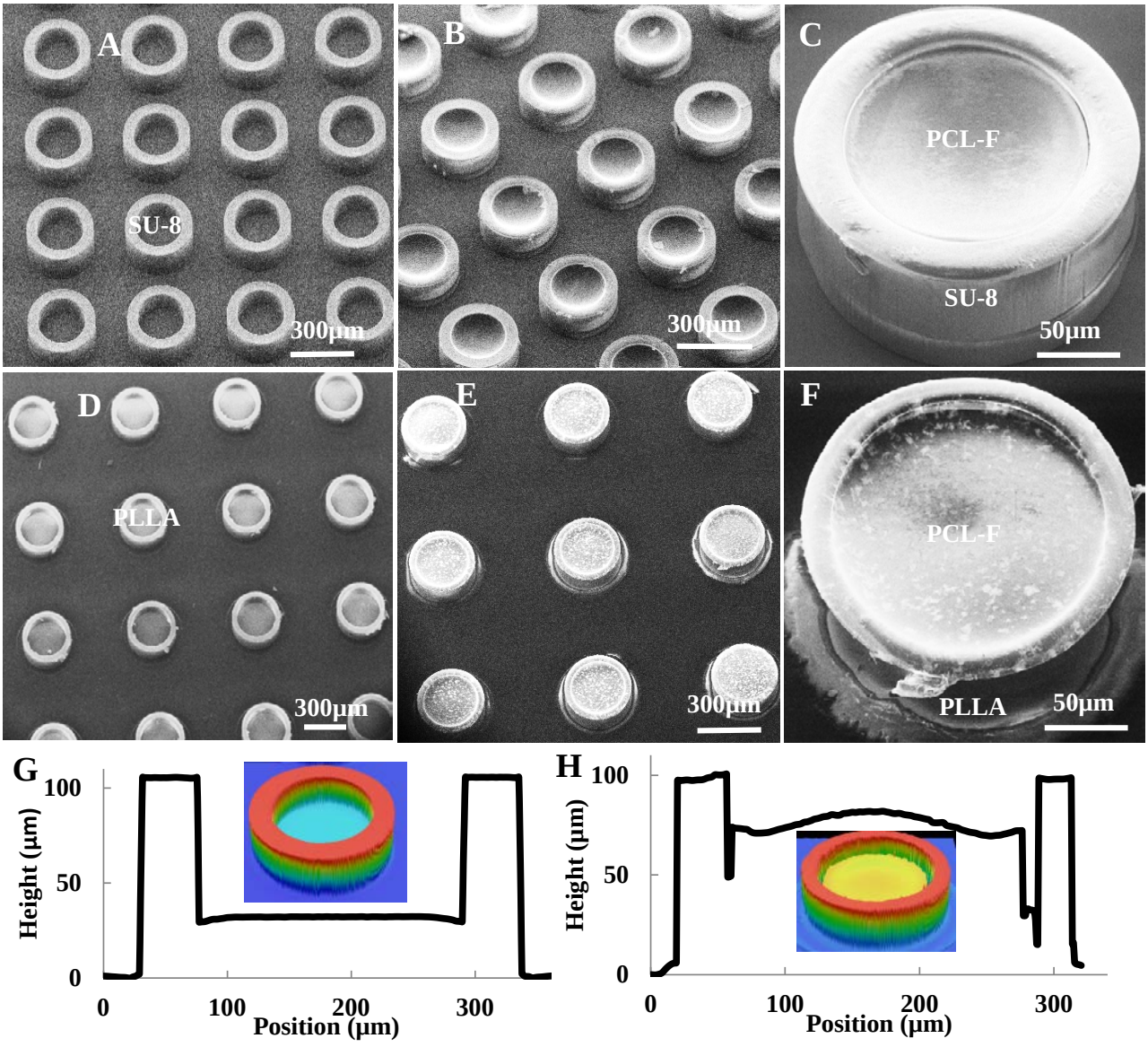

Figure. 3. A. Raman Spectra B. X-ray diffractometry of F-PCL matrix loaded in PLLA microcontainers, only PCL polymer loaded in PLLA microcontainers and pure crystalline powder. C. Dissolution release of Furosemide from PCL matrix**.**

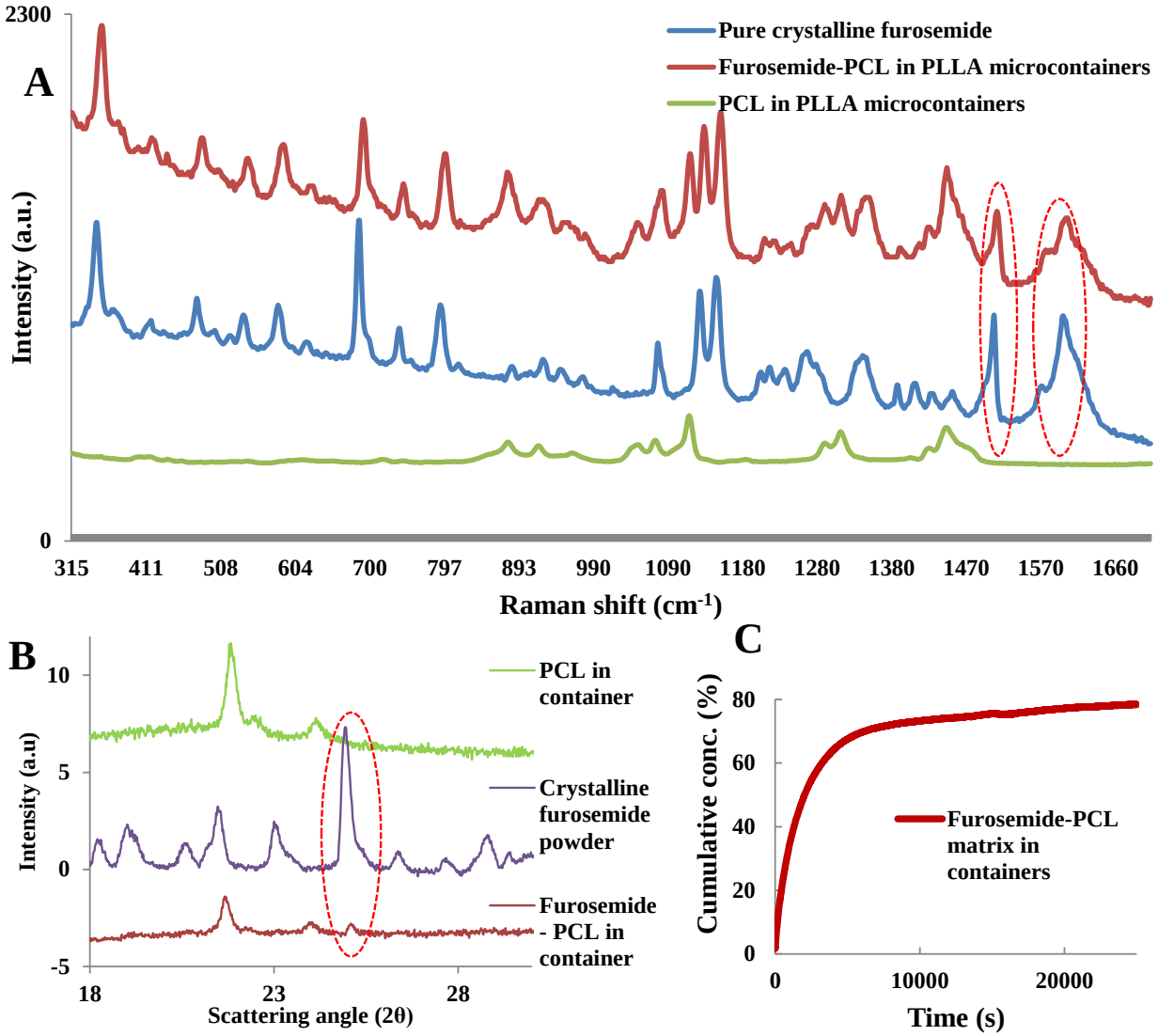

Patent

Method for manufacturing carrier containing e.g. proteins for human during oral drug delivery operation for food and drug administration application in pharmaceutical industry, involves providing active ingredient to core layer

Method for manufacturing carrier containing e.g. proteins for human during oral drug delivery operation for food and drug administration application in pharmaceutical industry, involves providing active ingredient to core layer

Research › Patent – Annual report year: 2015

Inventor: Nagstrup, Johan
Nanoprobes, Department of Micro- and Nanotechnology, Technical University of Denmark

Inventor: Keller, Stephan Sylvest
Biomaterial Microsystems, Department of Micro- and Nanotechnology, Technical University of Denmark, Ørsteds Plads, 2800, Kgs. Lyngby, Denmark
Email: stephan.keller@nanotech.dtu.dk

Inventor: Boisen, Anja
Nanoprobes, Department of Micro- and Nanotechnology, Technical University of Denmark, Ørsteds Plads, 2800, Kgs. Lyngby, Denmark
Email: anja.boisen@nanotech.dtu.dk

Inventor: Petersen, Ritika Singh
Nanoprobes, Department of Micro- and Nanotechnology, Technical University of Denmark, Ørsteds Plads, 2800, Kgs. Lyngby, Denmark
Email: risi@nanotech.dtu.dk

By the same authors

Angle resolved characterization …
Journal article – Annual report y…

Degradation studies of spray co…
Poster – Annual report year: 20…

Exploring Plasmonic Resonance…
Conference abstract in proceedi…

Fabrication of Ni stamp with hig…
Journal article – Annual report y…

Hot embossing and mechanical …
Journal article – Annual report y…

NOVELTY - The method involves preparing a multi-layered film comprising a core layer and a barrier layer, where the core layer comprises active ingredient. The multi-layered film is subjected to a hot embossing step using an embossing stamp including protrusions that allows for generation of the micro-containers containing an active ingredient or containing a core layer that is configured to accept the active ingredient such that the barrier layer partially encloses the core layer. The active ingredient is provided to the core layer when the core layer is configured to accept the active ingredient.

USE - Method for manufacturing a multi-layered micro-container i.e. carrier, containing an active ingredient e.g. small organic molecules, proteins, peptides, vitamins, antibodies, antibody fragments, vaccines, RNA, DNA and antibiotics, for a patient e.g. human and animal, during an oral drug delivery operation for a food and drug administration (FDA) application in a pharmaceutical industry.

ADVANTAGE - The method enables allowing an individual micro-structure stuck in an embossing stamp to be demolded under the conditions such that demolding operation is done by treating elastically or plastically deformable layer to increase stiction of the release layer. The method enables manufacturing the micro-container including an outer diameter of 200-500 pm and a height of 2-70 pm such that wall thickness is larger than 5 m to increase geometrical stability and reduce buckling. The method enables manufacturing a multi-layered micro-container to enable unidirectional release at a site of absorption, thus increasing bioavailability of drugs.

DETAILED DESCRIPTION - The barrier layer is made out of polycaprolactone (PCL), polylactic acid (PLA), polyglycolic acid (PGA), hydroxypropylmethyl cellulose (HPMC), polymethacrylate (PMMA), Eudragits Poly-methacylic acid-co-methyl methacrylate, ethyl cellulose (EC), polyvinyl alcohol (PVA), polyvinylpyrollidone (PVP), polyethylene glycol (PEG), polyethylene glycol methacrylate (PEGMA), polyethylene glycol dimethacrylate (PEGDMA), poly-lactic-co-glycolic acid (PGLA), polyacrylic acid (PAA) and copolymer. An INDEPENDENT CLAIM is also included for a micro-container.

Original language	English
Patent number	WO2015028670-A2
Country	Denmark
State	Published - 2015

Bibliography

[1] Sastry, Srikonda Venkateswara, Janaki Ram Nyshadham, and Joseph A. Fix. "Recent technological advances in oral drug delivery–a review." *Pharmaceutical science & technology today* 3, no. 4 (2000): 138-145.

[2] Fox, Cade B., Jean Kim, Long V. Le, Cameron L. Nemeth, Hariharasudhan D. Chirra, and Tejal A. Desai. "Micro/nanofabricated Platforms for Oral Drug Delivery." *Journal of Controlled Release* (2015).

[3] Hamman, Josias H., Gill M. Enslin, and Awie F. Kotzé. "Oral delivery of peptide drugs." *BioDrugs* 19, no. 3 (2005): 165-177.

[4] Calcagno, Anna Maria, and Teruna J. Siahaan. "Physiological, biochemical, and chemical barriers to oral drug delivery." *Drug Delivery: Principles and Applications* (2005): 15-27.

[5] Müller, Rainer H., Karsten MaÈder, and Sven Gohla. "Solid lipid nanoparticles (SLN) for controlled drug delivery–a review of the state of the art." *European journal of pharmaceutics and biopharmaceutics* 50, no. 1 (2000): 161-177.

[6] Tao, Sarah L., and Tejal A. Desai. "Microfabricated drug delivery systems: from particles to pores." *Advanced drug delivery reviews* 55, no. 3 (2003): 315-328.

[7] Ahmed, Aamer, Chris Bonner, and Tejal A. Desai. "Bioadhesive microdevices with multiple reservoirs: a new platform for oral drug delivery." *Journal of Controlled Release* 81, no. 3 (2002): 291-306.

[8] Keller, Stephan Sylvest, Filippo Giacomo Bosco, and Anja Boisen. "Ferromagnetic shadow mask for spray coating of polymer patterns."*Microelectronic Engineering* 110 (2013): 427-431.

[9] Ainslie, Kristy M., Rachel D. Lowe, Tristan T. Beaudette, Lamar Petty, Eric M. Bachelder, and Tejal A. Desai. "Microfabricated Devices for Enhanced Bioadhesive Drug Delivery: Attachment to and Small-Molecule Release Through a Cell Monolayer Under Flow." *Small* 5, no. 24 (2009): 2857-2863.

[10] Tao, Sarah L., and Tejal A. Desai. "Micromachined devices: the impact of controlled geometry from cell-targeting to bioavailability." *Journal of controlled release* 109, no. 1 (2005): 127-138.

[11] Han, Chao, and Binghe Wang. "Factors that impact the developability of drug candidates: an overview." *Chapter* 1 (2005): 1-5.

[12] Ahmed, Aamer, Chris Bonner, and Tejal A. Desai. "Bioadhesive microdevices for drug delivery: a feasibility study." *Biomedical Microdevices* 3, no. 2 (2001): 89-96.

[13] Lavan, David A., Terry McGuire, and Robert Langer. "Small-scale systems for in vivo drug delivery." *Nature biotechnology* 21, no. 10 (2003): 1184-1191.

[14] Zhang, Ying, Hon Fai Chan, and Kam W. Leong. "Advanced materials and processing for drug delivery: the past and the future." *Advanced drug delivery reviews* 65, no. 1 (2013): 104-120.

[15] Ziaie, Babak, Antonio Baldi, Ming Lei, Yuandong Gu, and Ronald A. Siegel. "Hard and soft micromachining for BioMEMS: review of techniques and examples of applications in microfluidics and drug delivery." *Advanced drug delivery reviews* 56, no. 2 (2004): 145-172.

[16] Langer, Robert, and Nicholas A. Peppas. "Advances in biomaterials, drug delivery, and bionanotechnology." *AIChE Journal* 49, no. 12 (2003): 2990-3006.

[17] Tsang, Valerie Liu, and Sangeeta N. Bhatia. "Three-dimensional tissue fabrication." *Advanced drug delivery reviews* 56, no. 11 (2004): 1635-1647.

[18] Rötting, O., W. Röpke, H. Becker, and C. Gärtner. "Polymer microfabrication technologies." *Microsystem Technologies* 8, no. 1 (2002): 32-36.

[19] Ahn, Se Hyun, and L. Jay Guo. "Large-area roll-to-roll and roll-to-plate nanoimprint lithography: a step toward high-throughput application of continuous nanoimprinting." ACS nano 3, no. 8 (2009): 2304-2310.

[20] Scheer, H-C., and H. Schulz. "A contribution to the flow behaviour of thin polymer films during hot embossing lithography." *Microelectronic Engineering*56, no. 3 (2001): 311-332.

[21] Pearton, Stephen J., and David P. Norton. "Dry etching of electronic oxides, polymers, and semiconductors." *Plasma Processes and Polymers* 2, no. 1 (2005): 16-37.

[22] Sheikh-Ahmad, Jamal Y. *Machining of polymer composites*. New York: Springer, 2009.

[23] Tao, Sarah L., and Tejal A. Desai. "Microfabrication of multilayer, asymmetric, polymeric devices for drug delivery." *Advanced Materials* 17, no. 13 (2005): 1625-1630.

[24] Martin, Frank J., and Carl Grove. "Microfabricated drug delivery systems: concepts to improve clinical benefit." *Biomedical Microdevices* 3, no. 2 (2001): 97-108.

[25] Sant, Shilpa, Sarah L. Tao, Omar Z. Fisher, Qiaobing Xu, Nicholas A. Peppas, and Ali Khademhosseini. "Microfabrication technologies for oral drug delivery."*Advanced drug delivery reviews* 64, no. 6 (2012): 496-507.

[26] Ainslie, Kristy M., and Tejal A. Desai. "Microtechnologies for drug delivery." In *Long Acting Injections and Implants*, pp. 359-381. Springer US, 2012.

[27] Chirra, Hariharasudhan D., and Tejal A. Desai. "Multi-Reservoir Bioadhesive Microdevices for Independent Rate-Controlled Delivery of Multiple Drugs."*Small* 8, no. 24 (2012): 3839-3846.

[28] Guan, Jingjiao, Hongyan He, L. James Lee, and Derek J. Hansford. "Fabrication of Particulate Reservoir-Containing, Capsulelike, and Self-Folding Polymer Microstructures for Drug Delivery." *Small* 3, no. 3 (2007): 412-418.

[29] Rolland, Jason P., Benjamin W. Maynor, Larken E. Euliss, Ansley E. Exner, Ginger M. Denison, and Joseph M. DeSimone. "Direct fabrication and harvesting of monodisperse, shape-specific nanobiomaterials." *Journal of the American Chemical Society* 127, no. 28 (2005): 10096-10100.

[30] Kelly, Jennifer Y., and Joseph M. DeSimone. "Shape-specific, monodisperse nano-molding of protein particles." *Journal of the American Chemical Society*130, no. 16 (2008): 5438-5439.

[31] Gratton, Stephanie EA, Patrick D. Pohlhaus, Jin Lee, Ji Guo, Moo J. Cho, and Joseph M. DeSimone. "Nanofabricated particles for engineered drug therapies: A preliminary biodistribution study of PRINT™ nanoparticles." *Journal of Controlled Release* 121, no. 1 (2007): 10-18.

[32] Garcia, Andres, Peter Mack, Stuart Williams, Catherine Fromen, Tammy Shen, Janet Tully, Jonathan Pillai *et al*. "Microfabricated engineered particle systems for respiratory drug delivery and other pharmaceutical applications." Journal of drug delivery (2012).

[33] Gratton, Stephanie EA, Stuart S. Williams, Mary E. Napier, Patrick D. Pohlhaus, Zhilian Zhou, Kenton B. Wiles, Benjamin W. Maynor *et al*. "The pursuit of a scalable nanofabrication platform for use in material and life science applications." *Accounts of chemical research* 41, no. 12 (2008): 1685-1695.

[34] Randall, Christina L., Timothy G. Leong, Noy Bassik, and David H. Gracias. "3D lithographically fabricated nanoliter containers for drug delivery." *Advanced drug delivery reviews* 59, no. 15 (2007): 1547-1561.

[35] Azam, Anum, Kate E. Laflin, Mustapha Jamal, Rohan Fernandes, and David H. Gracias. "Self-folding micropatterned polymeric containers." *Biomedical microdevices* 13, no. 1 (2011): 51-58.

[36] Whitesides, George M., Emanuele Ostuni, Shuichi Takayama, Xingyu Jiang, and Donald E. Ingber. "Soft lithography in biology and biochemistry." *Annual review of biomedical engineering* 3, no. 1 (2001): 335-373.

[37] Xia, Younan, and George M. Whitesides. "Soft lithography." *Annual review of materials science* 28, no. 1 (1998): 153-184.

[38] Ho, Dominic, Jianli Zou, Bogdan Zdyrko, K. Swaminathan Iyer, and Igor Luzinov. "Capillary force lithography: the versatility of this facile approach in developing nanoscale applications." *Nanoscale* 7, no. 2 (2015): 401-414.

[39] Becker, Holger, and Ulf Heim. "Hot embossing as a method for the fabrication of polymer high aspect ratio structures." *Sensors and Actuators A: Physical*83, no. 1 (2000): 130-135.

[40] Chen, Zhifeng, Yunhua Gao, Rongguo Su, Chengwu Li, and Jinming Lin. "Fabrication and characterization of poly (methyl methacrylate) microchannels by in situ polymerization with a novel metal template." *Electrophoresis* 24, no. 18 (2003): 3246-3252.

[41] Červenka, Petr, Walter Schrott, Zdeněk Slouka, Michal Přibyl, and Dalimil Šnita. "Hybrid gold–copper stamp for rapid fabrication of microchips."Microelectronic Engineering 98 (2012): 548-551.

[42] Ansari, Kambiz, Jeroen Anton van Kan, Andrew Anthony Bettiol, and Frank Watt. "Stamps for nanoimprint lithography fabricated by proton beam writing and nickel electroplating." Journal of Micromechanics and Microengineering 16, no. 10 (2006): 1967.

[43] Kuduva-Raman-Thanumoorthy, Ramasubramani, and Donggang Yao. "Hot embossing of discrete microparts." *Polymer Engineering & Science* 49, no. 10 (2009): 1894-1901.

[44] Heckele, M., and W. K. Schomburg. "Review on micro molding of thermoplastic polymers." *Journal of Micromechanics and Microengineering* 14, no. 3 (2004): R1.

[45] Buyukserin, Fatih, Mukti Aryal, Jinming Gao, and Wenchuang Hu. "Fabrication of polymeric nanorods using bilayer nanoimprint lithography." *Small* 5, no. 14 (2009): 1632-1636.

[46] Chang, C. Y., Sen Yeu Yang, and J. L. Sheh. "A roller embossing process for rapid fabrication of microlens arrays on glass substrates." Microsystem technologies 12, no. 8 (2006): 754-759.

[47] Becker, EoWo, Wo Ehrfeld, Po Hagmann, A. Maner, and D. Münchmeyer. "Fabrication of microstructures with high aspect ratios and great structural heights by synchrotron radiation lithography, galvanoforming, and plastic moulding (LIGA process)." Microelectronic engineering 4, no. 1 (1986): 35-56.

[48] Elders, J., H. V. Jansen, M. Elwenspoek, and W. Ehrfeld. "DEEMO: a new technology for the fabrication of microstructures." (1995): 238-243.

[49] Dentinger, Paul M., W. Miles Clift, and Steven H. Goods. "Removal of SU-8 photoresist for thick film applications." Microelectronic Engineering 61 (2002): 993-1000.

[50] Guo, Yuhua, Gang Liu, Ying Xiong, Jun Wang, Xinlong Huang, and Yangchao Tian. "Study of Hot Embossing Using Nickel and Ni–PTFE LIGA Mold Inserts."Microelectromechanical Systems, Journal of 16, no. 3 (2007): 589-597.

[51] Tanzi, Simone, Peter Friis Østergaard, Marco Matteucci, Thomas Lehrmann Christiansen, Jiri Cech, Rodolphe Marie, and Rafael Taboryski. "Fabrication of combined-scale nano-and microfluidic polymer systems using a multilevel dry etching, electroplating and molding process." Journal of Micromechanics and Microengineering 22, no. 11 (2012): 115008.

[52] Park, In-Soo, Jin-Soo Kim, Seong-Hun Na, Seung-Kyu Lim, Young-Soo Oh, and Su-Jeong Suh. "Fabrication of a two-step Ni stamp for blind via hole application on PWB." Microelectronic Engineering 87, no. 9 (2010): 1707-1710

[53] Nagstrup, Johan, Anja Boisen, and Stephan Sylvest Keller. "Micro fabrication of biodegradable polymer drug delivery devices." *Technical University of Denmark* (2012).

[54] Dash, Tapan K., and V. Badireenath Konkimalla. "Poly-ϵ-caprolactone based formulations for drug delivery and tissue engineering: A review." *Journal of Controlled Release* 158, no. 1 (2012): 15-33.

[55] Anders, Reinhold, and Hans P. Merkle. "Evaluation of laminated muco-adhesive patches for buccal drug delivery." International Journal of Pharmaceutics 49, no. 3 (1989): 231-240.

[56] Breitenbach, Jörg. "Melt extrusion: from process to drug delivery technology."*European Journal of Pharmaceutics and Biopharmaceutics* 54, no. 2 (2002): 107-117.

[57] Konno, Hajime, and Lynne S. Taylor. "Influence of different polymers on the crystallization tendency of molecularly dispersed amorphous felodipine."*Journal of pharmaceutical sciences* 95, no. 12 (2006): 2692-2705.

[58] Prausnitz, Mark R., and Robert Langer. "Transdermal drug delivery." *Nature biotechnology* 26, no. 11 (2008): 1261-1268.

[59] Nafee, N. A.; Boraie, M.; Ismail, F. A.; Mortada, L. M. Design and characterization of mucoadhesive buccal patches containing cetylpyridinium chloride. Acta Pharm. 2003, 53 (3), 199−212.

[60] James, I. G.; O'Brien, C. M.; McDonald, C. J. A randomized, double-blind, double-dummy comparison of the efficacy and tolerability of low-dose transdermal buprenorphine (BuTrans Seven-Day Patches) with buprenorphine sublingual tablets (Temgesic) in patients with osteoarthritis pain. J. Pain Symptom Manag. 2010, 40 (2), 266−278.

[61] Tao, Sarah L., and Tejal A. Desai. "Gastrointestinal patch systems for oral drug delivery." *Drug discovery today* 10, no. 13 (2005): 909-915.

[62] Kellner, Thomas, Heike MA Ehmann, Simone Schrank, Birgit Kunert, Andreas Zimmer, Eva Roblegg, and Oliver Werzer. "Crystallographic Textures and Morphologies of Solution Cast Ibuprofen Composite Films at Solid Surfaces."*Molecular pharmaceutics* 11, no. 11 (2014): 4084-4091.

[63] Marizza, Paolo, Stephan Sylvest Keller, and Anja Boisen. "Inkjet printing as a technique for filling of micro-wells with biocompatible polymers."*Microelectronic Engineering* 111 (2013): 391-395.

[64] Nielsen, Line Hagner, Johan Nagstrup, Sarah Gordon, Stephan Sylvest Keller, Jesper Østergaard, Thomas Rades, Anette Müllertz, and Anja Boisen. "pH-triggered drug release from biodegradable microwells for oral drug delivery."*Biomedical microdevices* 17, no. 3 (2015): 1-7.

[65] Marizza, Paolo, Stephan S. Keller, Anette Müllertz, and Anja Boisen. "Polymer-filled microcontainers for oral delivery loaded using supercritical impregnation."*Journal of Controlled Release* 173 (2014): 1-9.

[66] Uskokovic, Vuk, Kunwoo Lee, Phin Peng Lee, Kathleen E. Fischer, and Tejal A. Desai. "Shape effect in the design of nanowire-coated microparticles as transepithelial drug delivery devices." *ACS nano* 6, no. 9 (2012): 7832-7841.

[67] Delamarche, Emmanuel. "Microcontact printing of proteins." *Protein Science Encyclopedia* (2000).

[68] Lorenz, Hubert, M. Despont, N. Fahrni, N. LaBianca, Philippe Renaud, and P. Vettiger. "SU-8: a low-cost negative resist for MEMS." *Journal of Micromechanics and Microengineering* 7, no. 3 (1997): 121.

[69] del Campo, Aránzazu, and Christian Greiner. "SU-8: a photoresist for high-aspect-ratio and 3D submicron lithography." *Journal of Micromechanics and Microengineering* 17, no. 6 (2007): R81.

[70] Lorenz, Hubert, M. Despont, N. Fahrni, J. Brugger, P. Vettiger, and Philippe Renaud. "High-aspect-ratio, ultrathick, negative-tone near-UV photoresist and its applications for MEMS." *Sensors and Actuators A: Physical* 64, no. 1 (1998): 33-39.

[71] Voskerician, Gabriela, Matthew S. Shive, Rebecca S. Shawgo, Horst Von Recum, James M. Anderson, Michael J. Cima, and Robert Langer. "Biocompatibility and biofouling of MEMS drug delivery devices." *Biomaterials*24, no. 11 (2003): 1959-1967.

[72] Chang, Chia-Jung, Chung-Shi Yang, Li-Hua Lan, Pen-Cheng Wang, and Fan-Gang Tseng. "Fabrication of a SU-8-based polymer-enclosed channel with a penetrating UV/ozone-modified interior surface for electrokinetic separation of proteins." *Journal of Micromechanics and Microengineering* 20, no. 11 (2010): 115031.

[73] Walther, Ferdinand, Polina Davydovskaya, Stefan Zürcher, Michael Kaiser, Helmut Herberg, Alexander M. Gigler, and Robert W. Stark. "Stability of the hydrophilic behavior of oxygen plasma activated SU-8." *Journal of Micromechanics and Microengineering* 17, no. 3 (2007): 524.

[74] Jo, Byung-Ho, Linda M. Van Lerberghe, Kathleen M. Motsegood, and David J. Beebe. "Three-dimensional micro-channel fabrication in polydimethylsiloxane (PDMS) elastomer." *Microelectromechanical Systems, Journal of* 9, no. 1 (2000): 76-81.

[75] Brittain, Scott, Kateri Paul, Xiao-Mei Zhao, and George Whitesides. "Soft lithography and microfabrication." *Physics World* 11, no. 5 (1998): 31-36.

[76] Toepke, Michael W., and David J. Beebe. "PDMS absorption of small molecules and consequences in microfluidic applications." *Lab Chip* 6, no. 12 (2006): 1484-1486.

[77] Mukhopadhyay, Rajendrani. "When PDMS isn't the best." *Analytical chemistry*79, no. 9 (2007): 3248-3253.

[78] Odom, Teri W., J. Christopher Love, Daniel B. Wolfe, Kateri E. Paul, and George M. Whitesides. "Improved pattern transfer in soft lithography using composite stamps." *Langmuir* 18, no. 13 (2002): 5314-5320.

[79] Schmid, H., and B. Michel. "Siloxane polymers for high-resolution, high-accuracy soft lithography." *Macromolecules* 33, no. 8 (2000): 3042-3049.

[80] Boutevin, Bernard, Francine Guida-Pietrasanta, and Amédée Ratsimihety. "Synthesis of photocrosslinkable fluorinated polydimethylsiloxanes: direct introduction of acrylic pendant groups via hydrosilylation." *Journal of Polymer Science Part A: Polymer Chemistry* 38, no. 20 (2000): 3722-3728.

[81] Cong, Hailin, and Tingrui Pan. "Photopatternable conductive PDMS materials for microfabrication." *Advanced Functional Materials* 18, no. 13 (2008): 1912-1921.

[82] Petersen, Ritika S., Stephan S. Keller, and Anja Boisen. "Hot punching of high-aspect-ratio 3D polymeric microstructures for drug delivery." *Lab on a Chip*(2015).

[83] Zhou, Jinwen, Amanda Vera Ellis, and Nicolas Hans Voelcker. "Recent developments in PDMS surface modification for microfluidic devices."*Electrophoresis* 31, no. 1 (2010): 2-16.

[84] Efimenko, Kirill, William E. Wallace, and Jan Genzer. "Surface modification of Sylgard-184 poly (dimethyl siloxane) networks by ultraviolet and ultraviolet/ozone treatment." *Journal of colloid and interface science* 254, no. 2 (2002): 306-315.

[85] Oláh, Attila, Henrik Hillborg, and G. Julius Vancso. "Hydrophobic recovery of UV/ozone treated poly (dimethylsiloxane): adhesion studies by contact mechanics and mechanism of surface modification." *Applied Surface Science*239, no. 3 (2005): 410-423.

[86] Shalaby, Shalaby W., Charles L. McCormick, and George B. Butler. *Water-soluble polymers: synthesis, solution properties, and applications*. American Chemical Society, 1991.

[87] Williams, Peter A., ed. *Handbook of industrial water soluble polymers*. John Wiley & Sons, 2008.

[88] Park, Haesun, and Joseph R. Robinson. "Mechanisms of mucoadhesion of poly (acrylic acid) hydrogels." *Pharmaceutical research* 4, no. 6 (1987): 457-464.

[89] Lele, B. S., and A. S. Hoffman. "Mucoadhesive drug carriers based on complexes of poly (acrylic acid) and PEGylated drugs having hydrolysable PEG–anhydride–drug linkages." *Journal of controlled release* 69, no. 2 (2000): 237-248.

[90] Gudeman, Linda F., and Nikolaos A. Peppas. "pH-sensitive membranes from poly (vinyl alcohol)/poly (acrylic acid) interpenetrating networks." *Journal of membrane science* 107, no. 3 (1995): 239-248.

[91] Linder, Vincent, Byron D. Gates, Declan Ryan, Babak A. Parviz, and George M. Whitesides. "Water-Soluble Sacrificial Layers for Surface Micromachining."*small* 1, no. 7 (2005): 730-736.

[92] Mahdavinia, G. R., A. Pourjavadi, H. Hosseinzadeh, and M. J. Zohuriaan. "Modified chitosan 4. Superabsorbent hydrogels from poly (acrylic acid-co-acrylamide) grafted chitosan with salt-and pH-responsiveness properties."*European Polymer Journal* 40, no. 7 (2004): 1399-1407.

[93] http://www.microchem.com/pdf/SU-82000DataSheet2025thru2075Ver4.pdf

[94] Ishimuro, Y., and K. Ueberreiter. "The surface tension of poly (acrylic acid) in aqueous solution." *Colloid and Polymer Science* 258, no. 8 (1980): 928-931.

[95] http://www.sigmaaldrich.com/catalog/product/aldrich/323667?lang=en&region=DK

[96] Garlotta, Donald. "A literature review of poly (lactic acid)." *Journal of Polymers and the Environment* 9, no. 2 (2001): 63-84.

[97] Auras, Rafael A., Loong-Tak Lim, Susan EM Selke, and Hideto Tsuji, eds. *Poly (lactic acid): synthesis, structures, properties, processing, and applications*. Vol. 10. John Wiley & Sons, 2011.

[98] Giordano, Russell A., Benjamin M. Wu, Scott W. Borland, Linda G. Cima, Emanuel M. Sachs, and Michael J. Cima. "Mechanical properties of dense polylactic acid structures fabricated by three dimensional printing." *Journal of Biomaterials Science, Polymer Edition* 8, no. 1 (1997): 63-75.

[99] Lim, L-T., R. Auras, and M1 Rubino. "Processing technologies for poly (lactic acid)." *Progress in polymer science* 33, no. 8 (2008): 820-852.

[100] Lunt, James. "Large-scale production, properties and commercial applications of polylactic acid polymers." *Polymer degradation and stability* 59, no. 1 (1998): 145-152.

[101] Bose, Sanjukta, Stephan S. Keller, Anja Boisen, and Kristoffer Almdal. "Microcantilever sensors for fast analysis of enzymatic degradation of poly (d, l-lactide)." *Polymer Degradation and Stability* 119 (2015): 1-8.

[102] Rasal, Rahul M., Amol V. Janorkar, and Douglas E. Hirt. "Poly (lactic acid) modifications." *Progress in polymer science* 35, no. 3 (2010): 338-356.

[103] Koo, Gwang-Hoe, and Jinho Jang. "Surface modification of poly (lactic acid) by UV/Ozone irradiation." *Fibers and Polymers* 9, no. 6 (2008): 674-678.

[104] Cava, D., R. Gavara, J. M. Lagaron, and A. Voelkel. "Surface characterization of poly (lactic acid) and polycaprolactone by inverse gas chromatography."*Journal of Chromatography A* 1148, no. 1 (2007): 86-91.

[105] Woodruff, Maria Ann, and Dietmar Werner Hutmacher. "The return of a forgotten polymer—polycaprolactone in the 21st century." *Progress in Polymer Science* 35, no. 10 (2010): 1217-1256.

[106] Granero, G. E., M. R. Longhi, M. J. Mora, H. E. Junginger, K. K. Midha, V. P. Shah, S. Stavchansky, J. B. Dressman, and D. M. Barends. "Biowaiver monographs for immediate release solid oral dosage forms: Furosemide."*Journal of pharmaceutical sciences* 99, no. 6 (2010): 2544-2556.

[107] Dahan, Arik, Jonathan M. Miller, and Gordon L. Amidon. "Prediction of solubility and permeability class membership: provisional BCS classification of the world's top oral drugs." *The AAPS journal* 11, no. 4 (2009): 740-746.

[108] Kaminska, E., K. Adrjanowicz, K. Kaminski, P. Wlodarczyk, L. Hawelek, K. Kolodziejczyk, M. Tarnacka et al. "A new way of stabilization of furosemide upon cryogenic grinding by using acylated saccharides matrices. The role of hydrogen bonds in decomposition mechanism." *Molecular pharmaceutics* 10, no. 5 (2013): 1824-1835.

[109] Santus, Giancarlo, Giuseppe Bottoni, and Caterina Lazzarini. "Controlled-release mucoadhesive pharmaceutical composition for the oral administration of furosemide." U.S. Patent 5,571,533, issued November 5, 1996.

[110] Babu, N. Jagadeesh, Suryanarayan Cherukuvada, Ranjit Thakuria, and Ashwini Nangia. "Conformational and synthon polymorphism in furosemide (Lasix)."*Crystal Growth & Design* 10, no. 4 (2010): 1979-1989.

[111] Matsuda, Yoshihisa, and Etsuko Tatsumi. "Physicochemical characterization of furosemide modifications." *International journal of pharmaceutics* 60, no. 1 (1990): 11-26.

[112] Teófilo Vasconcelos, Bruno Sarmento, Paulo Costa, Solid dispersions as strategy to improve oral bioavailability of poor water soluble drugs, Drug Discovery Today, Volume 12, Issues 23–24, December 2007, Pages 1068-1075, ISSN 1359-6446, 10.1016/j.drudis.2007.09.005.

[113] Nielsen, Line Hagner, Sarah Gordon, Jari Pekka Pajander, Jesper Østergaard, Thomas Rades, and Anette Müllertz. "Biorelevant characterisation of amorphous furosemide salt exhibits conversion to a furosemide hydrate during dissolution." *International journal of pharmaceutics* 457, no. 1 (2013): 14-24.

[114] Cowley, John Maxwell. *Diffraction physics*. Elsevier, 1995.

[115] Goldstein, Joseph, Dale E. Newbury, Patrick Echlin, David C. Joy, Alton D. Romig Jr, Charles E. Lyman, Charles Fiori, and Eric Lifshin. *Scanning electron microscopy and X-ray microanalysis: a text for biologists, materials scientists, and geologists*. Springer Science & Business Media, 2012.

[116] Stokes, Debbie. *Principles and practice of variable pressure: Environmental scanning electron microscopy (VP-ESEM)*. John Wiley & Sons, 2008.

[117] Conroy, Mike, and Joe Armstrong. "A comparison of surface metrology techniques." In *Journal of Physics: Conference Series*, vol. 13, no. 1, p. 458. IOP Publishing, 2005.Larkin, Peter. *Infrared and Raman spectroscopy; principles and spectral interpretation*. Elsevier, 2011.

[118] Mozer, Wayne. "Optical Profiling Outperforms Confocal Microscopy." *Veeco apps note (2003)* (2002).

[119] Storey, Richard A., and Ingvar Ymén, eds. *Solid state characterization of pharmaceuticals*. John Wiley & Sons, 2011.

[120] Smith, Ewen, and Geoffrey Dent. *Modern Raman spectroscopy: a practical approach*. John Wiley & Sons, 2013.

[121] Larkin, Peter. *Infrared and Raman spectroscopy; principles and spectral interpretation*. Elsevier, 2011.

[122] Höhne, Günther, Wolfgang Hemminger, and H-J. Flammersheim. *Differential scanning calorimetry*. Springer Science & Business Media, 2003.

[123] Dressman, Jennifer B., Gordon L. Amidon, Christos Reppas, and Vinod P. Shah. "Dissolution testing as a prognostic tool for oral drug absorption: immediate release dosage forms." *Pharmaceutical research* 15, no. 1 (1998): 11-22.

[124] Cohen, Jordan L., Barbara B. Hubert, Lewis J. Leeson, Christopher T. Rhodes, Joseph R. Robinson, Theodore J. Roseman, and Eli Shefter. "The development of USP dissolution and drug release standards." *Pharmaceutical research* 7, no. 10 (1990): 983-987.

[125] Lu, Xujin, Ruben Lozano, and Pankaj Shah. "In situ dissolution testing using different UV fiber optic probes and instruments." *Dissolution Technologies* 10, no. 4 (2003): 6-16.

[126] Avdeef, Alex, and Oksana Tsinman. "Miniaturized rotating disk intrinsic dissolution rate measurement: effects of buffer capacity in comparisons to traditional Wood's apparatus." *Pharmaceutical research* 25, no. 11 (2008): 2613-2627.

[127] Wunderlich, Martin, Terry Way, and J. Dressman. "Practical considerations when using fiber optics for dissolution testing." *Dissolution Technologies* 10, no. 4 (2003): 17-19.

[128] Emslie, Alfred G., Francis T. Bonner, and Leslie G. Peck. "Flow of a viscous liquid on a rotating disk." *Journal of Applied Physics* 29, no. 5 (1958): 858-862.

[129] Meyerhofer, Dietrich. "Characteristics of resist films produced by spinning."*Journal of Applied Physics* 49, no. 7 (1978): 3993-3997.

[130] Daughton, W. J., and F. L. Givens. "An Investigation of the Thickness Variation of Spun-on Thin Films Commonly Associated with the Semiconductor Industry." *Journal of The Electrochemical Society* 129, no. 1 (1982): 173-179.

[131] Torres, Clivia Marfa Sotomayor, ed. *Alternative lithography: unleashing the potentials of nanotechnology*. Springer Science & Business Media, 2012.

[132] Worgull, Matthias. *Hot embossing: theory and technology of microreplication*. William Andrew, 2009.

[133] Heyderman, L. J., H. Schift, C. David, J. Gobrecht, and T. Schweizer. "Flow behaviour of thin polymer films used for hot embossing lithography."*Microelectronic Engineering* 54, no. 3 (2000): 229-245.

[134] Delaney, K. D., G. Bissacco, and D. Kennedy. "A structured review and classification of demolding issues and proven solutions." *International Polymer Processing* 27, no. 1 (2012): 77-90.

[135] Guo, Yuhua, Gang Liu, Xuelin Zhu, and Yangchao Tian. "Analysis of the demolding forces during hot embossing." *Microsystem technologies* 13, no. 5-6 (2007): 411-415.

[136] Franssila, S. (2010) Deep Reactive Ion Etching, in Introduction to Microfabrication, Second Edition, John Wiley & Sons, Ltd, Chichester, UK

[137] http://www-inst.eecs.berkeley.edu/~ee143/fa10/lectures/Lec_15.pdf

[138] Jansen, H. V., M. J. De Boer, S. Unnikrishnan, M. C. Louwerse, and M. C. Elwenspoek. "Black silicon method X: a review on high speed and selective plasma etching of silicon with profile control: an in-depth comparison between Bosch and cryostat DRIE processes as a roadmap to next generation equipment." *Journal of Micromechanics and Microengineering* 19, no. 3 (2009): 033001.

[139] Li, R., Y. Lamy, W. F. A. Besling, F. Roozeboom, and P. M. Sarro. "Continuous deep reactive ion etching of tapered via holes for three-dimensional integration." *Journal of Micromechanics and Microengineering* 18, no. 12 (2008): 125023.

[140] Dixit, Pradeep, Sami Vähänen, Jaakko Salonen, and Philippe Monnoyer. "Effect of Process Gases on Fabricating Tapered Through-Silicon vias by Continuous SF6/O2/Ar Plasma Etching." *ECS Journal of Solid State Science and Technology* 1, no. 3 (2012): P107-P116.

[141] Wu, Banqiu, Ajay Kumar, and Sharma Pamarthy. "High aspect ratio silicon etch: a review." *Journal of applied physics* 108, no. 5 (2010): 051101.

[142] Chen, Kuo-Shen, Arturo Ayón, Xin Zhang, and S. Mark Spearing. "Effect of process parameters on the surface morphology and mechanical performance of silicon structures after deep reactive ion etching (DRIE)."*Microelectromechanical Systems, Journal of* 11, no. 3 (2002): 264-275.

[143] file:///C:/Users/risi/Downloads/STS_ASE_DRIE_Trends.pdf

[144] Nagarajan, Ranganathan, Krishnamachar Prasad, Liao Ebin, and Balasubramanian Narayanan. "Development of dual-etch via tapering process for through-silicon interconnection." *Sensors and Actuators A: Physical* 139, no. 1 (2007): 323-329.

[145] Joo, Byung-Yun, Sung-Han Rhim, and Soo-Ik Oh. "Micro-hole fabrication by mechanical punching process." *Journal of Materials Processing Technology*170, no. 3 (2005): 593-601.

[146] Theis, Henry Ericsson. *Handbook of Metalforming Processes*. CRC Press, 1999.

[147] Yoon, Hyunsik, Tae-il Kim, Sejin Choi, Kahp Y. Suh, M. Joon Kim, and Hong H. Lee. "Capillary force lithography with impermeable molds." *Applied physics letters* 88, no. 25 (2006): 254104.

[148] Van Oss, Carel J., Manoj K. Chaudhury, and Robert J. Good. "Interfacial Lifshitz-van der Waals and polar interactions in macroscopic systems."*Chemical Reviews* 88, no. 6 (1988): 927-941.

[149] http://web.mit.edu/nnf/education/wettability/summerreading-2005short.pdf

[150] Żenkiewicz, M. "Methods for the calculation of surface free energy of solids."*Journal of Achievements in Materials and Manufacturing Engineering* 24, no. 1 (2007): 137-145.

[151] Janssen, Dimitri, Randy De Palma, Stijn Verlaak, Paul Heremans, and Wim Dehaen. "Static solvent contact angle measurements, surface free energy and wettability determination of various self-assembled monolayers on silicon dioxide." *Thin Solid Films* 515, no. 4 (2006): 1433-1438.

[152] Yoon, Hyunsik, Sung Hoon Lee, Seung Hyun Sung, Kahp Y. Suh, and Kookheon Char. "Mold design rules for residual layer-free patterning in thermal imprint lithography." *Langmuir* 27, no. 12 (2011): 7944-7948.

[153] Cole, D. J. "Surface chemistry and adhesive properties of oxidised Si surfaces." PhD diss., University of Cambridge, 2008.

[154] Martinez, Nelson. "Wettability of silicon, silicon dioxide, and organosilicate glass." PhD diss., University of North Texas, 2009.

[155] Kim, Bongsoo, Minwoo Park, Youn Sang Kim, and Unyong Jeong. "Thermal Expansion and Contraction of an Elastomer Stamp Causes Position-Dependent Polymer Patterns in Capillary Force Lithography." *ACS applied materials & interfaces* 3, no. 12 (2011): 4695-4702.

[156] Crank, John. *The mathematics of diffusion*. Oxford university press, 1979.

[157] Siepmann, J., and F. Siepmann. "Mathematical modeling of drug delivery."*International journal of pharmaceutics* 364, no. 2 (2008): 328-343.

[158] Siepmann, Juergen, and Florence Siepmann. "Modeling of diffusion controlled drug delivery." *Journal of Controlled Release* 161, no. 2 (2012): 351-362.

[159] Alfrey, Turner, E. F. Gurnee, and W. G. Lloyd. "Diffusion in glassy polymers." In *Journal of Polymer Science Part C: Polymer Symposia*, vol. 12, no. 1, pp. 249-261. Wiley Subscription Services, Inc., A Wiley Company, 1966.

[160] Ritger, Philip L., and Nikolaos A. Peppas. "A simple equation for description of solute release I. Fickian and non-Fickian release from non-swellable devices in the form of slabs, spheres, cylinders or discs." *Journal of controlled release* 5, no. 1 (1987): 23-36.

[161] Ritger, Philip L., and Nikolaos A. Peppas. "A simple equation for description of solute release II. Fickian and anomalous release from swellable devices."*Journal of controlled release* 5, no. 1 (1987): 37-42.

[162] De Kee, D., Q. Liu, and J. Hinestroza. "Viscoelastic (Non-Fickian) Diffusion."*The Canadian Journal of Chemical Engineering* 83, no. 6 (2005): 913-929.

[163] Kosmidis, Kosmas, Eleni Rinaki, Panos Argyrakis, and Panos Macheras. "Analysis of Case II drug transport with radial and axial release from cylinders."*International journal of pharmaceutics* 254, no. 2 (2003): 183-188.

[164] Huang, Xiao, and Christopher S. Brazel. "On the importance and mechanisms of burst release in matrix-controlled drug delivery systems." *Journal of controlled release* 73, no. 2 (2001): 121-136.

[165] Heyderman, L. J., H. Schift, C. David, J. Gobrecht, and T. Schweizer. "Flow behaviour of thin polymer films used for hot embossing lithography."*Microelectronic Engineering* 54, no. 3 (2000): 229-245.

APPENDIX 1

MATLAB CODES

1.1 MATLAB code for least square fitting of spin coating curves

```
function y = Lsqcurvefit_example_function(fun_coef, x)

A=fun_coef(1);
B=fun_coef(2);
y = A.*x.^(-2/3)+B;
```

```
clear all;
close all;
format compact;

% Fit to the function y=A*x^(-2/3)+B

if false
    % Generate "measurement" data
    A=10000;
    B=100;
    x=[400 500 600 700 800 1000]; % example numbers
    y=A.*x.^(-2/3)+B+randn(1,length(x))*10;
    clear('A','B');
else
    % Real measurements
    x=[500 1000 1500 2000 2500];
    y=[75.2 58.5 50.8 47.9 40.5];
end

guess=[200; 200]; % Initial guess on coefficients A and B

options = optimset ('TolX', 1e-18,'TolFun' ,1e-18, 'MaxFunEvals' ,400000, ...
    'MaxIter' ,200000, 'Display','off');

Coefficients1 = lsqcurvefit(@Lsqcurvefit_example_function ...
    ,guess,x,y); % fit without lower og upper boundaries

A=Coefficients1(1)
B=Coefficients1(2)

plot(x,y,'*')
hold on
x_fit=min(x)*0.9:(max(x)-min(x))/100:max(x)*1.1;
y_fit=Lsqcurvefit_example_function([A;B],x_fit);
plot(x_fit,y_fit);


%
% Coefficients2 = lsqcurvefit(@Lsqcurvefit_example_function ...
%     ,guess,x,y,[1e-3; 1e-3],[100000; 100000]); ...
%     % fit med lower og upper boundaries
%
% A=Coefficients2(1)
```

```
% B=Coefficients2(2)
```

1.2 MATLAB code of the interfacial energy, surface contact area and total adhesion energy calculations done for the fabrication of microcontainers:

```
clear all;
close all;
 % loading of microcontainer
prompt = 'What is dm ';
dm=input(prompt)
prompt = 'What is separation distance ';
sp=input(prompt)
rm=dm/2
rs2=rm+(sp/2)
rs=rm+sp
prompt = 'What is hsep';
hm=input(prompt)
prompt = 'What is hres';
hm2=input(prompt)
prompt = 'What is rm2';
rm2=input(prompt)
Hmin=((pi*(rm^2)*hm)-(pi*(rm2^2)*hm2))/(pi*(rs2^2))
prompt = 'What is ys ';
ys=input(prompt)
prompt = 'What is yp ';
yp=input(prompt)
prompt = 'What is ym ';
ym=input(prompt)
Wpm=yp+ym-(((yp^(1/2))- (ym^(1/2)))^2)
Wps=yp+ys-(((ys^(1/2))- (yp^(1/2)))^2)
Aps=pi*(rs^2)
Apm=pi*(rm2^2)+ 2*pi*rm2*hm2 +2*pi*rm*hm
Tadhm= Wpm*Apm
Tadhs= Wps*Aps
```

1.3 MATLAB code of the the interfacial energy, surface contact area and total adhesion energy calculations done for the loading of microcontainers:

```
clear all;
close all;
 % loading of microcontainer
 prompt = 'What is ds ';
ds=input(prompt)
rs=ds/2
prompt = 'What is wall thickness ';
wt=input(prompt)
rs2=(ds/2)-(wt/2)
prompt = 'What is dm ';
dm=input(prompt)
rm=dm/2
prompt = 'What is hm';
hm=input(prompt)
Hmin=(pi*(rm^2)*hm)/(pi*(rs2^2))
prompt = 'What is ys ';
ys=input(prompt)
prompt = 'What is yp ';
```

```
yp=input(prompt)
prompt = 'What is ym ';
ym=input(prompt)
Wpm=yp+ym-(((yp^(1/2))- (ym^(1/2)))^2)
Wps=yp+ys-(((ys^(1/2))- (yp^(1/2)))^2)
Aps=pi*(rs^2)
Apm=pi*(rm^2)+ 2*pi*rm*hm
Tadhm= Wpm*Apm
Tadhs= Wps*Aps
```

APPENDIX 2

SPIN CURVES

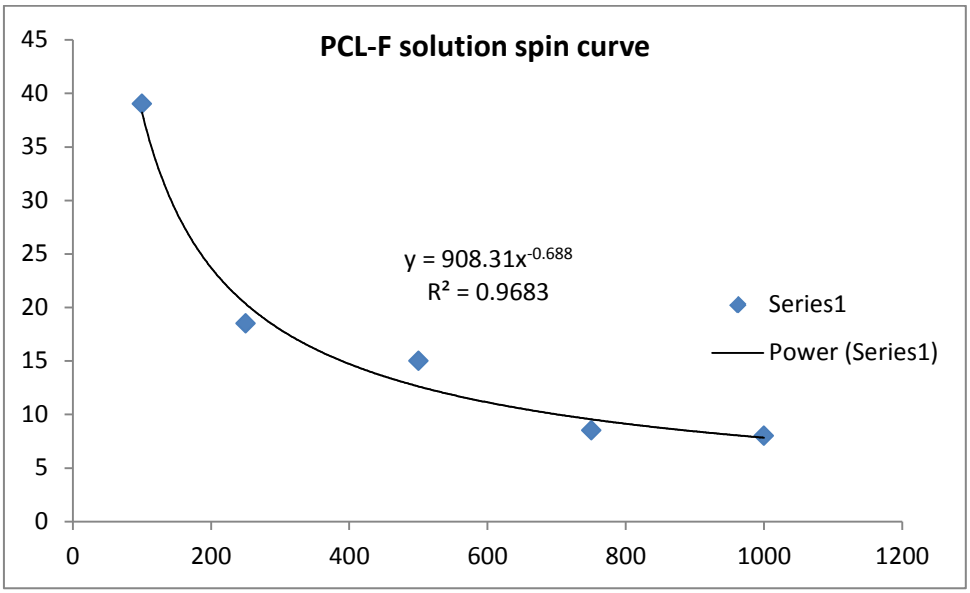

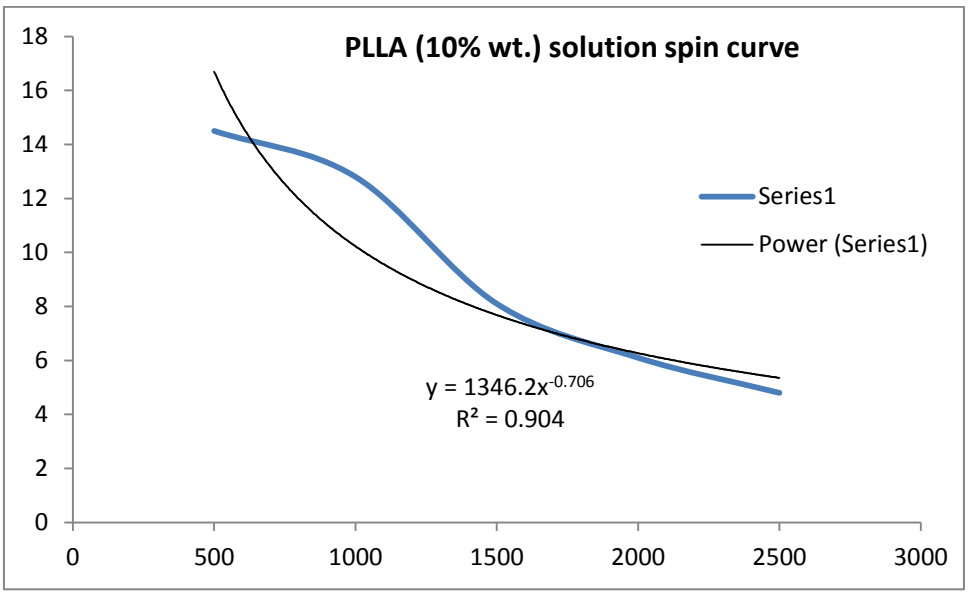

The measured values are fitted to a trendline provided by microscoft excel program.

APPENDIX 3

ADDITIONAL SEM MICROGRAPHS

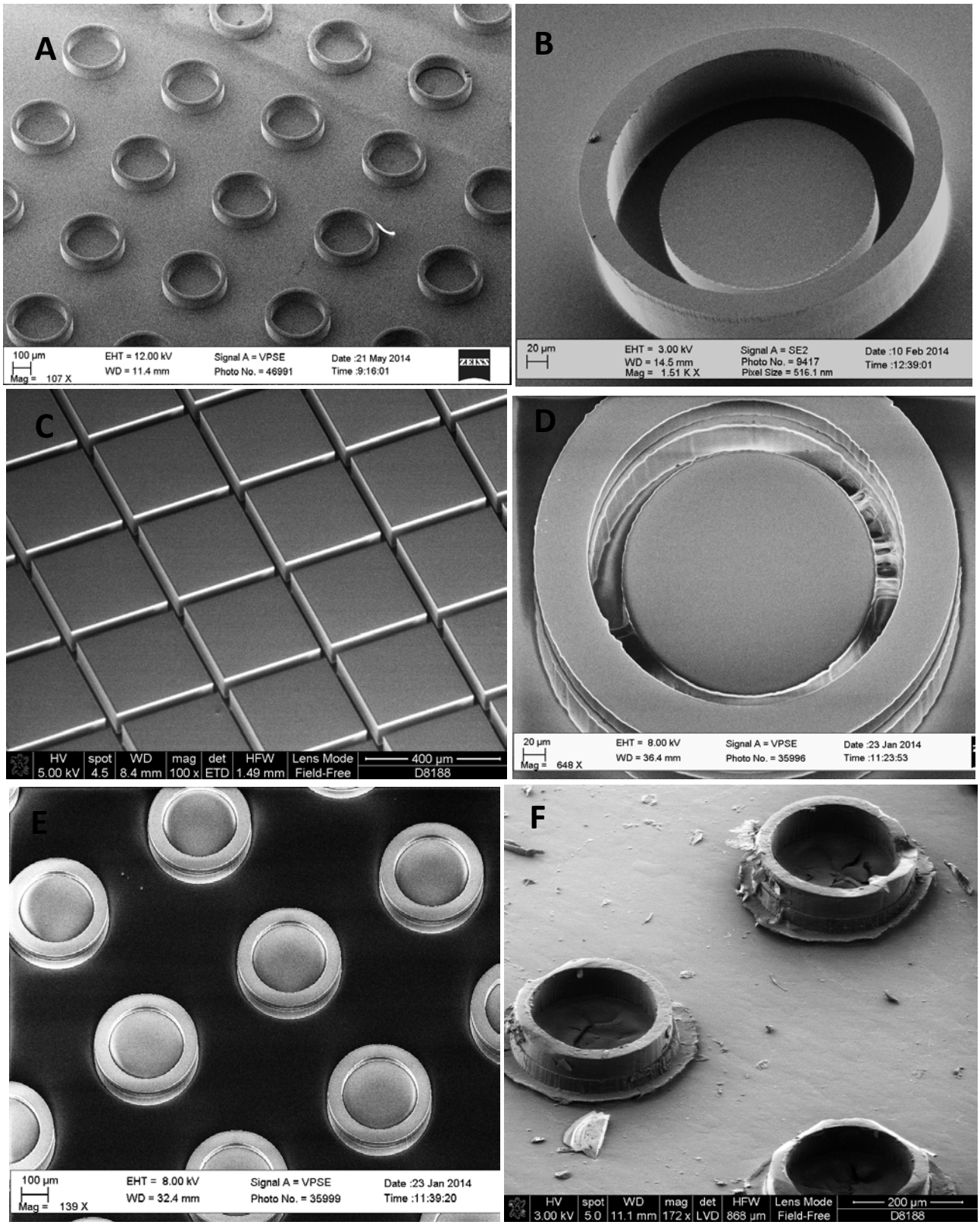

SEM micrographs of: A. Ni stamp fabricated for obtaining circular micropatches using hot punching, B. Stamp fabrication in Si for microcontainers fabrication, C. Si master for the electroplating of Ni for obtaining square shaped micropatches, D and E. Unsucessful attempts of fabricating SU-8 stamps for fabrication of microcontainers, F. old microcontainers bonded on a tape from Ni stamp after hot punching process.

APPENDIX 4

SIMPRINT SIMULATIONS

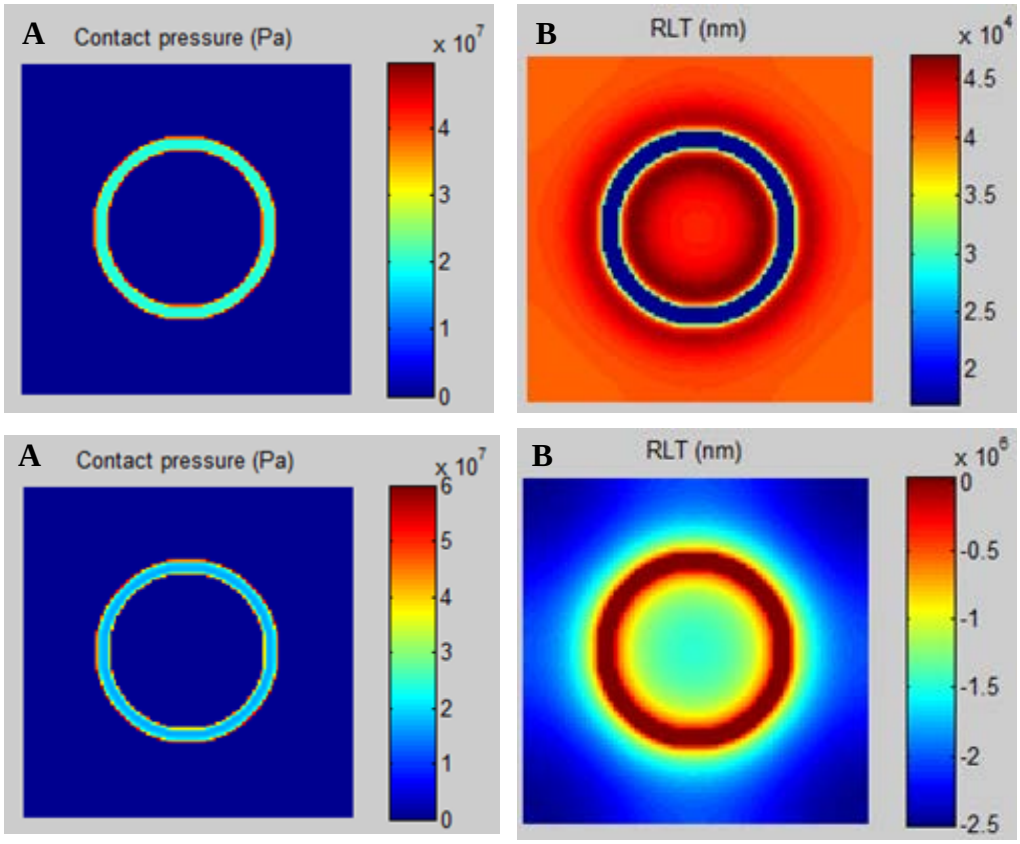

This figure shows some of the simulation attempts using SIMPRINT software. The first row shows the simulation of Ni stamp embossing in PMMA (high molecular weight) polymer spin coated on Si substrate. The second row shows the simulation of Ni stamp embossing in PMMA polymer spin coated on PDMS substrate. The second simulation threw error stating “Residual layer in negative.” Though there was an error, it is still interesting to see that for the PMMA on PDMS stamp, the residual layer under the highest feature (separation distance) on the Ni stamp is calculated as zero. On the other hand, the calculated residual layer for PMMA on Si substrate, embossed by the same Ni stamp, is a non-zero positive value.

APPENDIX 5

PROCESS FLOW FOR FABRICATION OF SU-8 MICROCONTAINERS

(developed and optimized by Stephan Sylvest Keller)

These process flows have been used for the fabrication of SU-8 microcontainers for loading purposes on fluorocarbon coated Si substrate (top) or on a water soluble sacrificial PAA layer for containers release.

Project:		**Fabrication of SU-8 microcontainers**				
Operator:		**Stephan**				
Substrates:		**Silicon <100>, 100mm, 525µm, single side**				
Goal:		**SU-8 microcontainers with 300µm external diameter for Milad/Line**				
Step Nº	Description	Equipment	Program/Parameters	Target	Actual	Remarks
1	WAFER PREPARATION					
1.1	Stock out					10 wafers
2	SU-8 FIRST LAYER SPINNING					
2.1	SU-8 spin-coating	Z3/KS Spinner	1000rpm, 30s, 200rpm/s; 3000 rpm, 120s, 400rpm/s	34 µm		SU-8 2075; 6s; 42psi; Gyrset
2.2a	SU-8 soft-bake	Z3/Hotplate1	2h, 50ºC, 2ºC/min			5 wafers
2.2b	SU-8 soft-bake	Z3/Hotplate2	2h, 50ºC, 2ºC/min			5 wafers
3	SU-8 FIRST LAYER PHOTOLITHOGRAPHY					
3.1	SU-8 exposure	Z3/KS Aligner	2x250 mJ/cm2; soft contact			Mask bottom - 300um
3.2a	Post-exposure bake	Z3/Hotplate1	6h, 50ºC, 2ºC/min			5 wafers
3.2b	Post-exposure bake	Z3/Hotplate2	6h, 50ºC, 2ºC/min			5 wafers
4	SU-8 SECOND LAYER SPINNING					
4.1	SU-8 spin-coating	Z3/KS Spinner	500rpm, 30s, 100rpm/s; 1500 rpm, 60s, 200rpm/s	250 µm		SU-8 2150; 40s; 42psi; Gyrset
4.2a	SU-8 soft-bake	Z3/Hotplate1	10h, 50ºC, 2ºC/min			300um
4.2b	SU-8 soft-bake	Z3/Hotplate2	10h, 50ºC, 2ºC/min			varia
5	SU-8 SECOND LAYER PHOTOLITHOGRAPHY					
5.1	SU-8 exposure	Z3/KS Aligner	2x250mJ/cm2, sub 900µm, al 100µm, exp 50µm			GlobalWEC, Prox; Mask 300um
5.2a	Post-exposure bake	Z3/Hotplate1	10h, 50ºC, 2ºC/min			5 wafers
5.2b	Post-exposure bake	Z3/Hotplate2	10h, 50ºC, 2ºC/min			5 wafers
5.3	SU-8 development	Z3/Developer	20min FIRST, 20min FINAL			PGMEA
5.4	Rinse	Z3/Developer	Isopropanol, Air			

Project:		**Fabrication of SU-8 microcontainers on PAA release layer**				
Operator:		**Stephan**				
Last revision:		**02-24-2012**				
Substrates:		**Silicon <100>, 100mm, 525µm, single side**				
Goal:		**Partial underetch of microcontainers to allow spray-coating**				
Step Nº	Description	Equipment	Program/Parameters	Target	Actual	Remarks
1	WAFER PREPARATION					
1.1	Stock out					
1.2a	PAA spin-coating	Z3/Manual spinne	500rpm, 60s, xrpm/s			A
1.2b	PAA spin-coating	Z3/Manual spinne	1000rpm, 60s, xrpm/s			B
1.3	PAA bake	Z3/Fumehood	10min, 80ºC			
2	SU-8 FIRST LAYER SPINNING					
2.1	SU-8 spin-coating	Z3/KS Spinner	1000rpm, 30s, 200rpm/s; 3000 rpm, 120s, 400rpm/s	34 µm		SU-8 2075; 6s; 42psi; Gyrset
2.2	SU-8 soft-bake	Z3/Hotplate1	2h, 50ºC, 2ºC/min			
3	SU-8 FIRST LAYER PHOTOLITHOGRAPHY					
3.1	SU-8 exposure	Z3/KS Aligner	2x250 mJ/cm2; soft contact			Mask bottom - 300um
3.2	Post-exposure bake	Z3/Hotplate1	6h, 50ºC, 2ºC/min			
4	SU-8 SECOND LAYER SPINNING					
4.1	SU-8 spin-coating	Z3/KS Spinner	300rpm, 30s, 100rpm/s; 600 rpm, 60s, 100rpm/s	200 µm		SU-8 2075; 8s; 42psi; Gyrset
4.2	SU-8 soft-bake	Z3/Hotplate2	10h, 50ºC, 2ºC/min			300um
5	SU-8 SECOND LAYER PHOTOLITHOGRAPHY					
5.1a	SU-8 exposure	Z3/KS Aligner	1x500mJ/cm2, sub 900µm, al 100µm, exp 50µm		B	GlobalWEC, Prox; Mask 300um
5.1b	SU-8 exposure	Z3/KS Aligner	1x1000mJ/cm2, sub 900µm, al 150µm, exp 150µm		A	GlobalWEC, Prox; Mask 300um
5.2b	Post-exposure bake	Z3/Hotplate2	10h, 50ºC, 2ºC/min			
5.3	SU-8 development	Z3/Developer	20min FIRST, 20min FINAL			PGMEA
5.4	Rinse	Z3/Developer	Isopropanol, Air			
5.5	Thickness	Z9/Dektak				
5.6	SEM inspection	SEM-FEI				
6	RELEASE					
6.1	Residual layer etch	Z2/ASE	SU8.set (50sccm O2, 5sccm SF6, 800W, 15W, 94.5%APC, 20m		A	
6.2	Release	Z3/Fumehood	H2O, 1min			
6.3	Residual layer etch	Z2/ASE	SU8.set (50sccm O2, 5sccm SF6, 800W, 15W, 94.5%APC, 20m		B	

Published by:
DTU Nanotech
Department of Micro- and Nanotechnology
Technical University of Denmark
Ørsteds Plads, building 345B
DK-2800 Kgs. Lyngby